DTU

Low temperature heating and high temperature cooling systems using Phase Change Materials

Eleftherios Bourdakis

Low temperature heating and high temperature cooling systems using Phase Change Materials for new buildings and energy renovation of existing buildings

Eleftherios Bourdakis

PhD dissertation

July 2018

DTU Civil Engineering

Department of Civil Engineering

Title: Low temperature heating and high temperature cooling systems using Phase Change Materials for new buildings and energy renovation of existing buildings

Period: 1st October 2014 – 31st of July 2018

Institute: International Centre for Indoor Environment and Energy (ICIEE), Department of Civil Engineering, Technical University of Denmark (DTU)
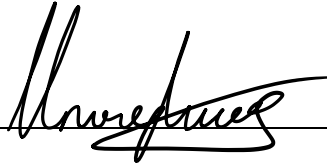
PhD Student: Eleftherios Bourdakis

Supervisor: Professor Bjarne W. Olesen

Declaration

I hereby declare that this thesis was written by myself entirely. All sources and materials I have used are hereby enclosed. The thesis has not been submitted further in this form or any other form and has not been used to obtain any other equivalent qualifications at any other organisation/institute.

Eleftherios Bourdakis

31st July 2018

Kongens Lyngby, Denmark

Acknowledgements

I would like to express my gratitude to my supervisor Bjarne W. Olesen for giving me the opportunity to become a part of his team and work on this very interesting project. His continuous guidance and feedback throughout these years are very much appreciated. Furthermore, his successful career full of achievements acted as a motivation force driving me forward and encouraging me to work harder.

I would like to thank my advisors Fred Baumann and Stefano Schiavon from the University of California, Berkeley for inviting me to their department as a visiting scholar. I would also like to thank my friends there for making these six months an unforgettable experience.

I would also like to express my warm thanks to all the ICIEE colleagues but mainly to two vital members of the Centre. None of the experiments would be accomplished without Nico H. Ziersen assisting in setting up the chambers and installing the required equipment, while our great secretary Snjezana Skocajic was always there for me able to solve any bureaucratic problem would occur.

I would like to express my sincere gratitude to my co-authors for their contribution in accomplishing all the experimental and numerical research and publications that consist a part of this PhD dissertation.

I would also like to thank Panagiota, Kyriaki, Mariya, Ongun, Emilie, Barbora, Luca and Thibault for making every day at ICIEE fun and pleasant. I could not ask for better colleagues.

Finally, I would like to thank my friends and family for their continuous support all these years. Last but definitely not least, I would like to thank Adelaida. The past three years and especially the last six months, she has been more than supportive. I would not be able to make it without her encouragement and faith in me.

Abstract

Residential and commercial buildings are accountable for approximately 40% of the energy use in the European Union (EU), and two-thirds of this energy is used for space heating. Nevertheless, the demand for cooling is expected to rise, due to global warming, increased comfort requirements (e.g. all cars have air-conditioning nowadays), increased internal loads, better insulated and airtight buildings keeping the internal loads inside, resulting in temperature increase. The EU has recently set updated targets for energy use reduction by the year 2030, while it recognises the importance of the construction sector in achieving these targets and especially the importance of addressing the issues related to the existing building stock, as this was underlined in the amended version of the Directive on Energy Performance of Buildings.

The aim of the present dissertation is to examine the potential of incorporating active ceiling panels containing Phase Change Material (PCM) in office buildings, using both numerical and experimental means. The main objectives of the projects were to examine experimentally the possibility of combining PVT panels to produce cold water through the process of nocturnal radiative cooling with PCM ceiling panels for space cooling and to create and validate a model of the aforementioned system in TRNSYS to conduct parametric studies and optimise it without being affected by the contingency of the outdoor weather conditions.

The most important findings of the research conducted for this dissertation are summarised below.

People who had higher metabolic rate than sedentary activity due to walking to work, were accessible to lower temperature than what suggested by the European Standard EN 15251 at the beginning of the occupancy period. That would enable higher utilisation of nighttime ventilation for cooling office buildings passively.

Fanger's thermal comfort model is applicable also in cases with non-steady conditions, although it was developed using data from experiments conducted under steady-state conditions.

Active ceiling panels containing PCM are an efficient method for providing an acceptable thermal environment. Furthermore, nocturnal radiative cooling process can reduce the energy use of the refrigerant equipment substantially and combined with

the electricity produced by the PVT during daytime, it can result in a surplus of electricity, if the weather conditions are in favour.

Nocturnal radiative cooling was beneficial in all locations simulated, although the performance varied significantly among the different locations. The higher the latitude, the higher the effectiveness of the nocturnal radiative cooling, due to the lower negative impact from convection. On the other hand, the lower the latitude, the better the thermal environment provided by the active ceiling panels containing PCM, due to the more vertical position of the sun.

A correct design of passive PCM panels can result in substantial energy savings, but a wrong design can result in increasing the energy use of the building to maintain the desired thermal environment. A thorough investigation about the appropriate materials and panel parameters (PCM surface area, panel thicknessn etc.) should precede the panel construction.

Although PCM tiles add additional thermal mass and contribute in reducing the energy use of the HVAC equipment, they cannot stand alone as a cooling system and should only be considered as a secondary system supplementing the main system, either all-air or radiant system.

In case of active PCM panels, to ensure the full discharge of the PCM, the pipes should be embedded in the PCM layer to take advantage of the better contact between PCM and the cooling medium.

For passive PCM panels the ideal thickness was 20 mm, while for active PCM panels 30 mm. That would result in significantly higher thermal mass in the case of incorporating active PCM panels compared to passive panels.

Active ceiling panels containing PCM and PVT panels are two technologies that can greatly contribute in achieving the targets for reduction of the energy use in the construction sector and realise a decarbonised building stock, and at the same provide the desired thermal environment. PCM tiles require further investigation before they can be considered a potential option for providing an acceptable thermal environment.

Resumé

Bolig- og erhvervsbygninger er ansvarlige for ca. 40% af energiforbruget i EU, og to tredjedele af denne energi bruges til rumopvarmning. Efterspørgslen efter køling forventes dog at stige som følge af global opvarmning, øgede komfortbehov (f.eks. alle biler har aircondition i dag), øgede interne belastninger, bedre isolerede og lufttætte bygninger, der i mindre grad vil miste varmen (afkøles) om natten, hvilket ofte resulterer i for høje rumtemperaturer. EU har for nylig opstillet opdaterede mål for reduktion af energiforbruget inden år 2030, mens det anerkender byggesektorens betydning for at nå disse mål og især vigtigheden af at løse problemerne med energirenovering af den eksisterende boligmasse.

Formålet med den foreliggende afhandling er at undersøge både med numeriske og eksperimentelle metoder mulighederne for at anvende loftskølingspaneler indeholdende faseskiftende materialer (PCM) i en kontorbygning. Hovedformålene med projektet er at eksperimentelt undersøge muligheden for at kombinere PVT-paneler til at nedkøle vandet i panelerne ved varmetab om natten gennem strålingstab til himlen og konvektivt tab til luften. med PCM-loftspaneler til rumkøling og at udvikle og validere en numerisk model af det førnævnte system i TRNSYS for at udføre parametrisk undersøgelser og optimere det under forskellige udendørs vejrforhold.

De vigtigste resultater fra dette projekt er opsummeret nedenfor.

Personer, der har lidt højere aktivitet end stillesiddende på vej til arbejde, accepterer en lavere rumtemperatur om morgenen i forhold til hvad, der bliver foreslået i den europæiske standard EN 15251. Det muliggør en højere udnyttelse af natventilation til køling af kontorbygninger passivt. Denne undersøgelse med forsøgspersoner viste også at Fangers termiske komfortmodel (PMV-PPD) er også anvendelig i situationer med varierende rumtemperaturer, selv om modellen blev udviklet baseret på eksperimenter med næsten konstante betingelser.

Loftskølepaneler indeholdende PCM er en effektiv metode til at tilvejebringe et acceptabelt termisk indeklima. Endvidere kan den natlige strålingskøleproces reducere energiforbruget til køling og kombineret med den elektricitet, der produceres af PVT om dagen, kan resultere i overskud af elektricitet afhængigt af vejrforholdene.

Strålingskøling om natten var anvendelig på alle geografiske lokaliteter, selv om effektiviteten varierede betydeligt mellem de forskellige steder. Jo højere mod nord, jo

højere effektiviteten af den natlige afkøling på grund af den mindre negative konvektive påvirkning fra høje lufttemperaturer om natten. På den anden side jo længere sydpå, desto bedre er det termiske indeklima, der leveres af de aktive loftskøleplader, der indeholder PCM, på grund af solens mere vertikale position.

Et korrekt design af passive PCM paneler kan resultere i betydelige energibesparelser, men et forkert design kan resultere i at øge bygningens energiforbrug for at opretholde det ønskede termiske indeklima. En grundig undersøgelse af de relevante materialer og panelparametre (PCM overfladeareal, paneltykkelse mv.) Bør gå forud for panelkonstruktionen.

Selv om PCM-plader tilføjer ekstra termisk masse og bidrager til at reducere energiforbruget af HVAC-udstyret, kan de ikke stå alene som et kølesystem og bør kun betragtes som et sekundært system, der suppleres af luftkonditionerings eller strålingskølesystem.

I tilfælde af aktive PCM kølepaneler, skal rørene være indlejret i PCM laget for at udnytte den bedre kontakt mellem PCM og kølemediet, for at sikre fuld udnyttelse af PCM,

For passive PCM paneler er den ideelle tykkelse 20 mm, mens for aktive PCM paneler 30 mm er optimalt. Det ville resultere i væsentligt højere termisk masse ved brug af 30mm aktive PCM paneler sammenlignet med 20 mm passive paneler.

Aktive loftskølepaneler, der indeholder PCM er sammen med PVT-paneler to teknologier, som i høj grad kan bidrage til at nå målene for reduktion af energiforbruget i byggesektoren og reducere CO_2 emissionen ved samtidig at opretholde det ønskede termiske indeklima. PCM-kølepaneler kræver dog yderligere undersøgelse, før de kan betragtes som en potentiel mulighed for at tilvejebringe et acceptabelt termisk indeklima.

Table of Contents

List of figures

List of tables

Abbreviations

ASHRAE	American Society of Heating, Refrigeration and Air-conditioning Engineers
AWHP	Air-to-Water Heat Pump
BMI	Body Mass Index
CAV	Constant Air Volume
CEN	European Committee for Standardization
COP	Coefficient of Performance
CWT	Cold Water Tank
DG ENER	Directorate General for Energy
DHW	Domestic Hot Water
DPV	Ductless Personalised Ventilation
DTU	Technical University of Denmark
EC	European Commission
EED	Directive on Energy Efficiency
EER	Energy Efficiency Ratio
EGA	Equivalent Glazing Area
EPBD	Directive on Energy Performance of Buildings
ESS	Embedded Surface System
EU	European Union
HRE	Heat Roadmap Europe
HVAC	Heating, Ventilation and Air-Conditioning
HWT	Hot Water Tank
ICIEE	International Centre for Indoor Environment and Energy
IEQ	Indoor Environment Quality
ISO	International Standardisation Organisation
IWEC	International Weather for Energy Calculations
LHS	Latent Heat Storage
PCM	Phase Change Material
PCTR	Phase Change Temperature Range
PEG	Poly-Ethylene Glycol
PMV	Predicted Mean Vote
PPD	Predicted Percentage of Dissatisfied

PV   PhotoVoltaic

PVT   PhotoVoltaic Thermal

RCP   Radiant Ceiling Panel

RMSE   Root Mean Square Errors

SBS   Sick Building Syndrome

SHGC   Solar Heat Gains Coefficient

SHS   Sensible Heat Storage

TABS   Thermally Active Building System

TRNSYS   TRaNsient SYstem Simulation tool

UN   United Nations

UNEP   United Nations Environment Programme

Nomenclature

A	Surface area
a	Coefficient defining the Convective heat exchange coefficient
b	Coefficient defining the Convective heat exchange coefficient
C_p	Specific heat capacity
$C_{p,eff,peak}$	Peak effective heat capacity
$C_{p,sens}$	Sensible heat capacity
d	Panel thickness
ENS	Energy Savings
h_{conv}	Convective heat exchange coefficient
HG	Heat Gains
n	Fraction of sky covered by opaque clouds, $0 \leq n \leq 1$
P_{cond}	Conductive heat on the panel surface
P_{conv}	Convective heat on the panel surface
P_{rad}	Radiative heat on the panel surface
$P_{surface}$	Total heat on the panel surface
$Q_{surface}$	Heat flux on the panel surface
T_a	Outdoor air temperature
T_{CWT}	Water temperature in the middle of the CWT
T_{dew}	Dew point temperature
T_{HWT}	Water temperature in the middle of the HWT
$T_{m,s}$	Melting/solidifying point
$T_{operative}$	Operative temperature
T_{pc}	Phase change temperature
T_{PVT}	Water temperature exiting the PVT panels
T_{rad}	Mean surface temperature of the collector
T_{sky}	Sky temperature
$T_{surface}$	Panel surface temperature
v	Air speed on the collector surface

Z_c	height of the cloud's base
Z_*	Reference value set to 8.2 km
ε_c	Hemispherical cloud emissivity
ε_r	Emissivity of the collector's surface
ε_{sky}	Emissivity of the sky
ε_0	Emissivity of clear sky
σ	Stephan-Boltzmann constant

List of publications

The following list includes the list of journal and conference papers produced by the author in the context of this PhD thesis.

Journal publications

1. **Bourdakis E.**, Péan T. Q., Gennari L., & Olesen B. W. (2016). Daytime space cooling with phase change material ceiling panels discharged using rooftop photovoltaic/thermal panels and nighttime ventilation. Science and Technology for the Built Environment, 4731(June), 1–9. https://doi.org/10.1080/23744731.2016.1181511

2. **Bourdakis E.**, Simone A., & Olesen B.W. (2018). An experimental study of the effect of different starting room temperatures on occupant comfort in Danish summer weather. Building and Environment. https://doi.org/10.1016/j.buildenv.2018.03.046

3. **Bourdakis E.**, Gkoufas N.A., & Olesen B.W. (2018). Simulation study for the design of radiant ceiling panels containing phase change material. Submitted at Applied Thermal Engineering

4. Eilersen E.C.R., Krintel C.H., **Bourdakis E.**, Kazanci O.B., Olesen B.W. (2018). Development of a simplified method for designing office buildings with a PCM-enhanced suspended ceiling. Submitted at Science and Technology for the Built Environment

Conference publications

5. **Bourdakis E.**, Grossule F., & Olesen B. W. (2015). Night time cooling by ventilation or night sky radiation combined with in-room radiant cooling panels including Phase Change Materials. Presented at AIVC 2015

6. **Bourdakis E.**, Kazanci O. B., Grossule F., & Olesen B. W. (2016). Simulation Study of Discharging PCM Ceiling Panels through Night-time Radiative Cooling. Presented at ASHRAE Annual Conference 2016

7. **Bourdakis E.**, Peán Q. T., Gennari L., & Olesen B. W. (2016). Experimental study of discharging PCM ceiling panels through nocturnal radiative cooling. Presented at IACVEQ 2016

8. **Bourdakis E.**, Kazanci O. B., Peán Q. T., & Olesen B. W. (2016). Parametric analysis of the control of solar panels for nocturnal radiative cooling coupled with in room PCM ceiling panels. Presented at ASHRAE Winter Conference 2017

List of publication that are not included in the dissertation

The following publications were produced during these PhD studies, but were **not** the main focus of it. Hence, they are **not** attached at the end of the dissertation.

Journal publications

a) Herasaki A., **Bourdakis E.**, Ploskic A., & Holmberg S. (2015). Experimental study of energy performance in low-temperature hydronic heating systems. Energy and Buildings, 109, 108–114. https://doi.org/10.1016/j.enbuild.2015.09.064

b) Jin Q., Simone A., Olesen B.W., Holmberg S.K.M. & **Bourdakis E.** (2016): Laboratory study of subjective perceptions to low temperature heating systems with exhaust ventilation in Nordic countries, Science and Technology for the Built Environment, https://doi.org/10.1080/23744731.2017.1251266

c) Pantelic J., Schiavon S., Ning B., **Bourdakis E.**, Raftery P., Bauman F. (2018): Full scale laboratory experiment on the cooling capacity of a radiant floor system. Energy and Buildings, https://doi.org/10.1016/j.enbuild.2018.03.002

Conference Publications

d) Peán Q. T., Gennari L., Kazanci O. B., **Bourdakis E.**, & Olesen B. W. (2016). Influence of the environmental parameters on nocturnal radiative cooling capacity of solar collectors. Presented at Klima 2016

e) **Bourdakis E.**, Bauman F., Schiavon S., Raftery P., & Olesen B. W. (2017). Cooling load calculations of radiant and all-air systems for commercial buildings. Presented at Building Simulations 2017

f) Flemming Nielsen L., **Bourdakis E.**, Kazanci O. B., & Olesen B. W. (2016). The Influence of a Radiant Panel System with Integrated Phase Change Material on Energy Use and Thermal Indoor Environment. Presented at ASHRAE Winter Conference 2018

g) Farhan H., Stefansen C., **Bourdakis E.**, Kazanci O. B., & Olesen B. W. (2016). Simulation Study of Active Ceilings with Phase Change Material in Office Buildings for Different National Building Regulations. Presented at ASHRAE Winter Conference 2018

h) Stefansen C., Farhan H., **Bourdakis E.**, Kazanci O. B., & Olesen B. W. (2016). Simulation Study of Performance of Active Ceilings with Phase Change Material in Office Buildings Under Extreme Climate Conditions. Presented at ASHRAE Winter Conference 2018

1 Introduction

The built environment (residential and commercial) is responsible for approximately 40% of the energy use in the European Union (EU), and two-thirds of this energy is used for space heating [1]. Reducing the energy of the built environment is an issue of outmost importance, due to the global aim of reducing the greenhouse gas emissions, as reflected in the recent Paris Agreement [2].

In the EU about half of the final energy demand is used for heating and cooling purposes, of which 96% is heating [1]. Cooling accounts for only 2% of the EU's final energy demand, but this figure might increase as temperatures rise due to climate change [1]. Furthermore, the demand for cooling is expected to rise, due to increased comfort requirements (e.g. nowadays all cars have air-conditioning), increased internal load and better insulated and airtight buildings keeping the internal loads inside, resulting in temperature increase. In line with their energy use, the built environment and industry are a significant contributor to CO_2 emissions in the EU, responsible for 27% of the CO_2 emissions in 2015.[1] Renewables account for a relatively small share of the heating and cooling demand, in 2016 only 19% of the energy required came from renewable energy sources, the remainder of the heat was produced from fossil fuels.[2] According to DG ENER, new buildings, following the latest Directives on Energy Performance of Buildings (EPBD) and Energy Efficiency (EED), consume approximately 3 to 5 litres of heating oil per m² per year, while older building (usually with inefficient heating systems and a lack of insulation) require on average 25 litres per m² per year and can reach up to 60 litres [3]. Currently, the EU is heavily dependent on oil and natural gas imports for its energy and heating supply. Heating and cooling accounts for 68% of the gas imports [4]. Thus, by reducing the energy use in the built environment, the EU will become less dependent on third countries and less vulnerable to unpredicted increases in fuel prices.

Energy poverty is the inability to afford adequate heating, cooling, lighting and the electricity to power appliances. Although energy poverty is an issue mostly associated with sub-Saharan and some Asian countries, it is also present in developed countries. According to DG ENER, more than 50 million households in the EU are struggling to attain adequate warmth, pay their utility bills on time and live in homes free of damp

---

[1] https://ec.europa.eu/energy/en/data-analysis/country
[2] http://ec.europa.eu/eurostat/web/energy/data/shares

and mold [5]. Continuous exposure to unpleasant indoor conditions can cause illnesses which translate into increased lost man-hours due to sick leave and an increase in public healthcare expenditure.

The performance of heating and cooling systems not only affects the energy use of the building, but also the wellbeing of the occupants, by providing the desired indoor environment and especially thermal comfort. Thermal comfort is the condition of mind that expresses satisfaction with the thermal environment [6]. International and European standards define temperature ranges for different types of buildings and climatic conditions [7], [8]. Inadequate heating and cooling systems fail to provide the required temperature in the buildings resulting in lack of heat in winter and overheating in summer. This results in increased levels of thermal discomfort which is associated with low productivity in educational and office working environments [9], [10]. Furthermore, studies have shown that increased thermal discomfort can also cause distraction, generate complaints and increase the intensity of Sick Building Syndrome (SBS) symptoms [11], [12]. SBS symptoms include headache, nose irritation (stuffy, running), irritated throat, fatigue, dry eyes, difficulty in concentrating, a lack of alertness etc.

Buildings have a lifespan of several decades, and therefore actions taken now will have an impact on their performance and CO_2 emissions over a long period. According to the United Nations Environment Programme (UNEP), the majority of the buildings that will exist by the year 2050 in the developed countries have already been built [13]. Therefore, the EU targets - in terms of reduction of energy use, decarbonisation of the heating and cooling sector, eliminating energy poverty in the EU and becoming less dependent on fossil fuel imports - can only be achieved if very large changes are implemented in existing buildings.

1.1 Hypothesis and objectives

The main hypothesis addressed in this PhD dissertation is that embedding Phase Change Material (PCM) in radiant ceiling panels can be an energy efficient system for space cooling and at the same time provide an acceptable thermal environment in office buildings in general and especially for energy retrofitting existing buildings. This hypothesis was answered through five objectives which were examined during these PhD studies.

- The first objective was to examine whether office workers prefer in the morning room temperature below the comfort range for sedentary activity, due to elevated metabolic rate, increased by commuting to work on foot.

- The second objective was to examine experimentally the possibility of combining PVT panels to produce cold water through the process of nocturnal radiative cooling with PCM ceiling panels for space cooling. The combination was evaluated both in terms of thermal environment provided and energy use required for its operation.

- The third objective was to create and validate a model of the aforementioned system in TRNSYS to conduct parametric studies and optimise it without being affected by the contingency of the outdoor weather conditions.

- The fourth objective was to create a simplified method for calculating the potential energy savings from implementing ceiling panels containing PCM in office buildings.

- The fifth objective was to design a new type of radiant ceiling panels containing PCM.

1.2 Outline of the dissertation

This dissertation consists of both numerical simulations and experimental parts. The experimental part took place in the facilities of the International Centre for Indoor Environment and Energy (ICIEE), located at the campus of the Technical University of Denmark (DTU), at Kongens Lyngby, Denmark.

The work in this dissertation can be divided as follows:

- Thermal comfort in office buildings during the cooling period

- Experimental investigation of the combination of phase change material (PCM) for space cooling and PVT panels to produce cold water

- Validation of a TRNSYS model and dynamic simulations

- Investigation of a new design of PCM ceiling panels through simulations and experiments

Chapter 2 summarises the background theory of PCMs, nocturnal radiative cooling and indoor environment requirements based on the corresponding European Standard. **Chapter 3** presents the results of the human subject experiment on thermal comfort in office buildings during the cooling period. **Chapter 4** presents the results of the experimental and numerical investigation of the combination PVT panels to produce cold water through the process of nocturnal radiative cooling with PCM ceiling panels for space cooling. **Chapter 5** presents the results of a TRNSYS model created to develop a simplified method for estimating the performance of ceiling panels containing PCM. **Chapter 7** presents the numerical and experimental results of the development a new radiant ceiling panel containing PCM. **Chapter 7** summarises the overall conclusions of this PhD dissertation, while **Chapter 8** lists proposals for further investigation.

2 Background

This chapter presents the most important background theory about radiant heating and cooling systems, phase change materials (PCMs), nocturnal radiative cooling and thermal comfort.

2.1 Thermally Activated Building Systems (TABS)

There are three types of radiant heating and cooling systems, thermal activated building systems (TABS), embedded surface systems (ESS) and radiant ceiling panels (RCPs). TABS integrate the building structure in the heating and cooling systems of a building, by embedding pipes in the concrete slab [14]. Compared to TABS, in ESS the active layer is separated by the main core of the slab with an insulation layer, while radiant panels are panels with integrated pipes suspended under the ceiling. [15]. Figure 2-1 shows a cross-section of TABS with and without sound insulation.
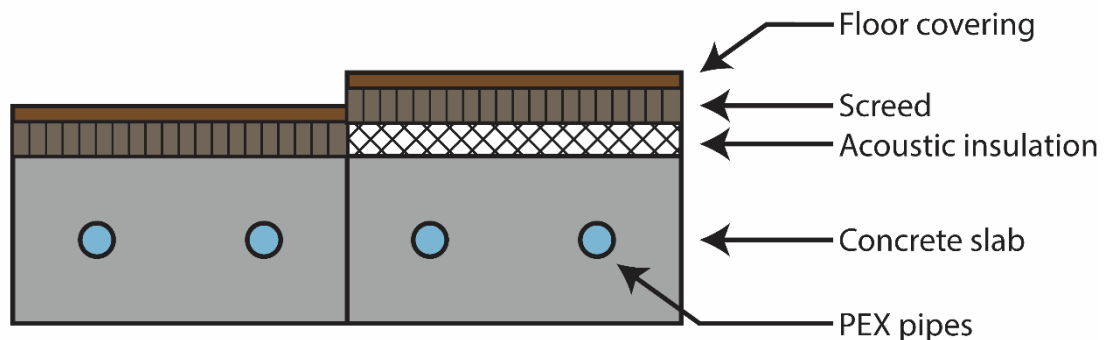
Figure 2-1: Cross-section of a thermally active building system TABS) with sound insulation (right) and without (left) [15]

TABS can utilise the thermal mass of the building by storing energy during nighttime and releasing it during the occupancy period. In that way, part of the cooling load is shifted to nighttime resulting in lower peak cooling demand [15], [16]. During nighttime several countries have lower electricity tariffs which means lower operation cost for pumps and cooling equipment compared to a system operating during the occupancy period [15], [17]. In addition to that, the temperature of the water circulating in the pipes is closer to the room temperature and the outdoor air has a lower temperature compared to daytime, which results in higher efficiency for cooling equipment such as air-to-water heat pumps (AWHP) [15], [18].

Apart from benefits in energy use, TABS are also providing a better thermal environment compared to all-air systems [19]. The reduction of the air component of the heating, ventilation and air-conditioning (HVAC) system results in reduction in the risk of draught and noise originating from the ventilation system [20]. Furthermore, they provide a more uniform thermal environment due to the large active surface [21]. Nevertheless, despite all the advantages of the use of TABS their implementation in an existing construction is challenging or even impossible, from a structural point of view.

2.2 Phase Change Materials (PCMs)

Phase Change Materials (PCMs) are chemical substances that store large amounts of energy when they melt (charging process) and release it when they solidify (discharging process). The phase change occurs when the temperature of the PCM is within a temperature range (phase change temperature range) which is around a temperature called melting or solidifying point depending on the process that is taking place. During the phase change process PCMs are storying or releasing large amounts of energy. Thus, PCMs are classified as latent heat storage (LHS) materials. Latent heat storage depends on the material's phase change enthalpy to store energy within the phase change temperature range, resulting in higher energy density than sensible heat storage (SHS) [22].

There are three different methods for incorporating PCM in construction elements [23]. Firstly, PCM can be implemented through impregnation or immersion, e.g. in a concrete-PCM mixture, but in that case, there is a high risk of leakage [24]. Marco-encapsulation is the technique in which the PCM is contained in a form of package, e.g. tubes, panels, etc. [25]. Although leakage issue is solved with macro-encapsulation, the heat transfer coefficient is reduced significantly, which may result in partial solidification during the discharging process [26]. In micro-encapsulation, PCM is contained in very small spheres with a diameter in the range of 0.05 µm to 5000 µm [27]. Figure 2-2 shows the different types of micro-encapsulation.
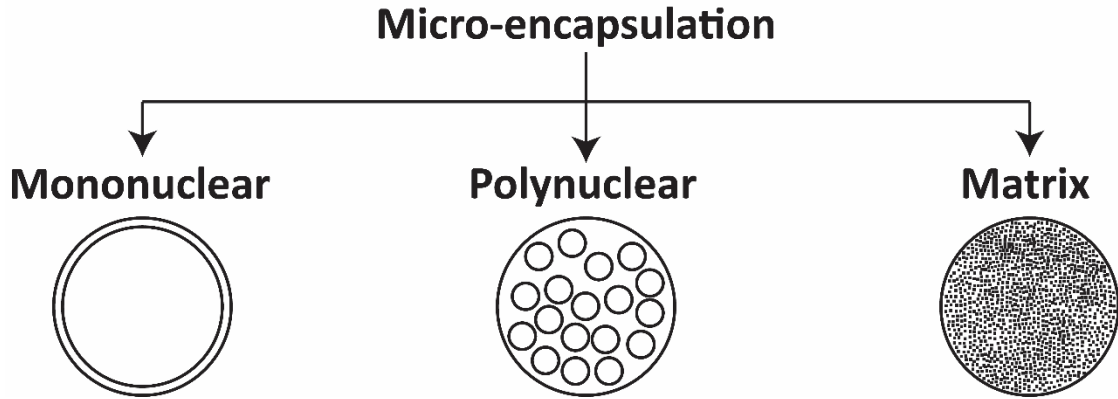
Figure 2-2: Types of micro-encapsulation [28]

2.2.1 Thermal properties of the PCMs

Due to the chemical complexity of PCMs, several parameters require to been taken into consideration when selecting the appropriate material for an application. Table 2-1 shows the key design parameters for a PCM selection.

Table 2-1: Key design properties for a PCM [29]–[31]

Thermal	Physical	Chemical	Kinetic	Other
High heat of fusion	Low vapour pressure	Non-corrosive	No super-cooling	Low cost
High specific heat capacity	Small volumetric change during phase change	Non-toxic	No sub-cooling	Abundant
High thermal conductivity	High density	Non-flammable	High nucleating rate	
Appropriate phase change temperature range	High phase stability	Compatible with container material	High crystallisation rate	
		Long term chemical cycling stability	No phase segregation	

Figure 2-3 shows the evolution of the heat capacity (C_p) of the PCM as the temperature of the PCM changes. Suppose the material is at a temperature lower than the melting point T_m. As the temperature increase, the heat capacity increases slightly. Once the temperature of the material is within the phase change temperature range (PCTR), the C_p increases substantially. During the phase change, the rate of change of the temperature drops and once it reaches the melting point, C_p reaches its peak value, namely $C_{p,eff,peak}$. Once the material is fully melted, the material behaves as a

7

conventional material, the temperature rate of change increases again, and the C_p drops back to the value similar to the one it has when it was fully melted.
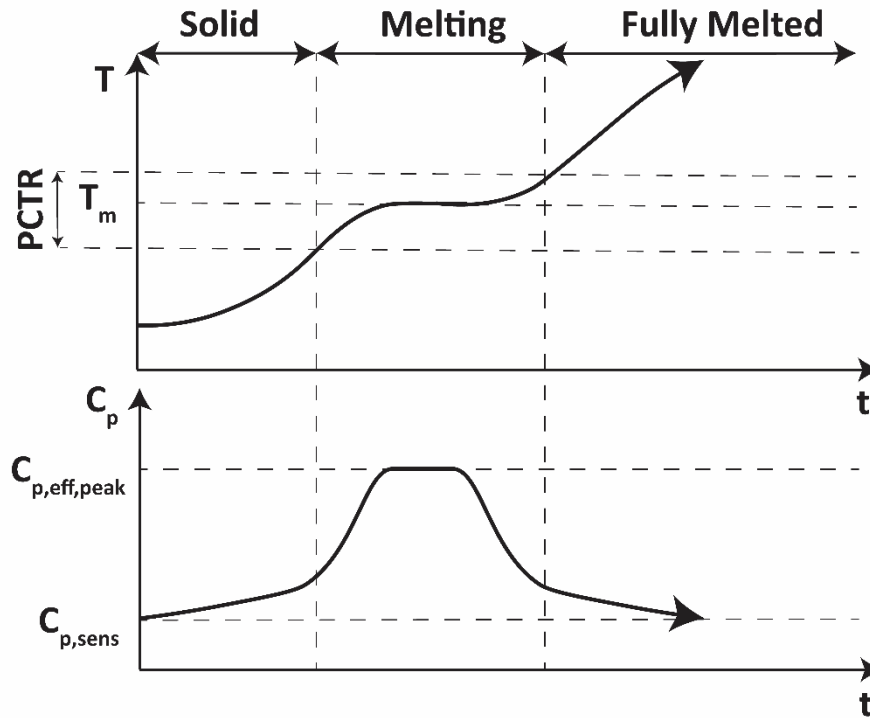
Figure 2-3: Correlation of temperature and thermal capacity during the melting process

Figure 2-4 shows a comparison of the heat stored by a conventional building material and a PCM. When the temperature of the material is below the melting point, the heat stored is comparable in the two materials. Once the PCM starts to melt it continues to store energy but its temperature changes only slightly, until it is fully melted. Once it is fully melted it starts behaving as conventional material again. On the other hand, a conventional building material absorbs heat at a linear rate compared to its temperature. For a certain temperature T_1 higher than the PCTR of the PCM, the PCM has stored significantly more heat than the conventional building material, as shown by the red line in Figure 2-4.
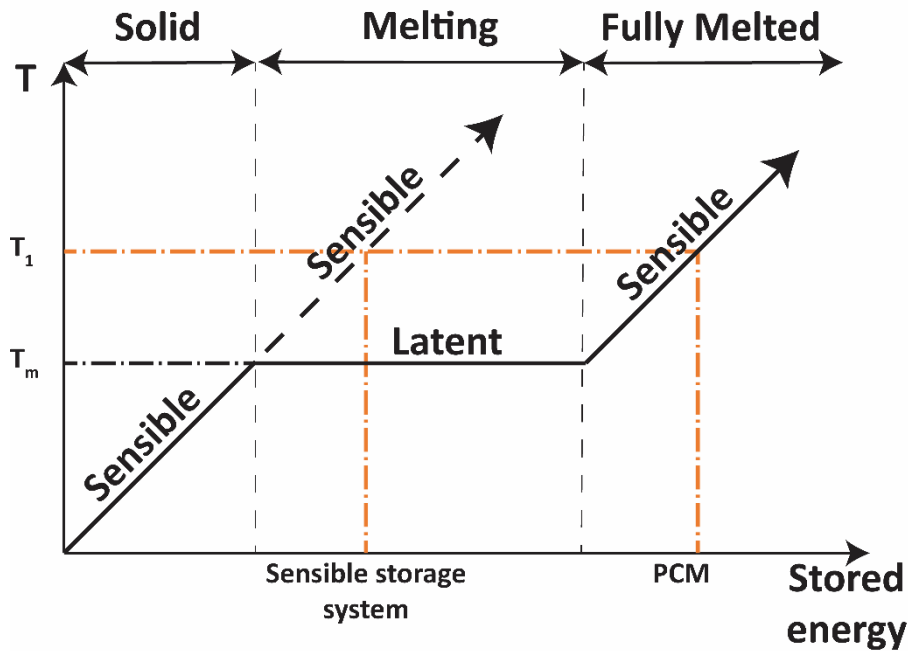
Figure 2-4: Heat storage comparison between a sensible and latent heat storage system

Heat of fusion is the change in the enthalpy of the material that takes places when it absorbs heat changes state from solid to liquid. The higher the heat of fusion is, the higher the heat the PCM will require to absorb to melt completely. Ideally, the PCM should melt congruently, namely the material should melt completely, so that both the solid and liquid phases are homogeneous [32].

2.2.2 PCM types

There are several types of PCM that are utilised in different industrial sectors and they are divided in three main categories, organic, inorganic and eutectic PCMs. Organic PCMs include paraffins, fatty acids, polyethylene glycols (PEG) and sugar alcohols, while inorganic PCMs are mainly salt hydrates [33].

Paraffins have high heat of fusion, narrow phase change temperature range, good melting congruency, low vapour pressure, no super-cooling occurs and are non-toxic [30], [34]–[39]. Their biggest drawbacks are their high volumetric change during the phase change, flammability, low thermal conductivity and heat storage capacity per unit volume [23], [30], [38], [40], [41]. Fatty acids have good melting congruency, low vapour pressure, are chemically stable, non-toxic and they can be produced sustainably by utilising plant and animal waste [39], [42]–[44]. On the other hand, they

9

have lower heat of fusion than paraffins, they are slightly corrosive, super-cooling occurs and they have a strong odour [38], [44], [45]. PEGs have high heat of fusion, they are non-toxic and chemically stable, they have a congruent melting and no super-cooling occurs [46]–[48]. Nevertheless, they are expensive, and they have low heat storage capacity per unit volume and low conductivity [48]. Sugar alcohols have the highest heat of fusion among the organic PCMs but their melting temperature of 90 – 200°C makes them inappropriate for building envelope applications [38], [49].

Salt hydrates have high latent heat capacity are abundant at low cost, are non-toxic, non-flammable and have a higher heat of fusion than organic PCMs [31], [50], [51]. On the other hand, corrosion occurs when they are combined with metals, they are subject to volumetric change and super-cooling and they have incongruent melting [37], [38], [50], [52]–[54]. Metal PCMs have high thermal conductivity and heat of fusion per unit volume, but their melting point is too high to be applicable in building elements and they are too heavy [38], [55].

Eutectic PCMs are chemical mixtures of multiple PCMs, which results in a melting point lower than that of each component separately [56]. Eutectic PCM have higher phase change enthalpy compared to paraffin and salt hydrates and high durability, can easily be impregnated in porous materials and have adjustable melting point based on their components' composition, but this results in low information on their thermophysical properties as they differ depending on the concentration of each component [22], [41], [55], [57]–[59]. Table 2-2 summarises the different PCM categories with their advantages and disadvantages.

Table 2-2: Advantages and disadvantages of PCM subcategories

PCM category	PCM subcategory	Advantages	Disadvantages
Organic	Paraffins	+ high heat of fusion + narrow temperature range + good melting congruency + no super-cooling + non-toxic + low vapour pressure	− High volume change − flammability − low heat storage capacity per unit volume − low thermal conductivity
	Fatty acids	+ good melting congruency + chemically stable + non-toxic + can be produced sustainably + low vapour pressure	− lower heat of fusion than paraffins − slightly corrosive − super-cooling − some have a strong odour which makes them inapplicable for building applications
	polyethylene glycols (PEG)	+ high heat of fusion + non-toxic + chemically stable + congruent melting + no super-cooling occurs	− high cost − low heat storage capacity per unit volume − Low thermal conductivity
	sugar alcohols	+ highest heat of fusion among the organic PCMs	− Inappropriate for indoor environment applications due to high melting temperature point (100°C – 200°C)
Inorganic	salt hydrates	+ low cost + narrow melting range + non-flammable + high latent heat of fusion	− corrosion when combined with metals − subject to volumetric change − subject to super-cooling − incongruent melting
	metals	+ high heat of fusion per unit volume + high thermal conductivity	− very high melting point for building applications − high weight
Eutectic	chemical mixtures of multiple PCMs	+ higher phase change enthalpy compared to paraffin and salt hydrate PCMs + adjustable melting point depending on the components composition + long-term durability + easy impregnation in porous materials	− low information on thermophysical properties − incongruent melting

2.2.3 Applications in the built environment

The performance of PCM integrated in construction components in terms of thermal comfort provided and energy savings both in passive and active systems, has been investigated thoroughly. In passive systems no refrigerant cycle is incorporated, e.g. PCM impregnated in concrete or incorporated in gypsum panels. In these systems, PCM gets discharged using methods such as nighttime ventilation, and therefore the performance of PCM depends heavily on the outdoor conditions. On the other hand, in active system PCM gets discharged by circulating either air or water which has been cooled down using refrigeration equipment, e.g. chillers or air-to-water heat pumps (AWHP). Since in active systems there is higher control of the temperature of the refrigerant fluid, discharging the PCM is unaffected by the outdoor weather conditions.

Stovall and Tomlinson (1995) simulated passive wallboard with different PCM volume content, varying from 0% to 27% and they concluded that the PCM did not improve occupant comfort with traditional thermostat control, but improved the heat load management [60]. Athienitis et al. (1997) investigated both experimentally and numerically the thermal performance of a passive solar test-room with PCM and found that the integration of PCM reduced the maximum air room temperature by approximately 4°C during daytime [61]. Banu et al. (1998) proved that differential scanning calorimetry is adequately accurate at predicting the performance of a full-scale installation of PCM wallboards and therefore large scale tests can be avoided [62]. Vakilaltojjar and Saman (2001) impregnated PCM in thin flat containers which had a gap in between so that air can flow. They found that although the performance of the construction would benefit by making the PCM slabs thinner, that would results in higher pressure drop across the storage system [63]. Koschenz and Lehmann (2004) designed and tested an active ceiling panel containing PCM. they concluded that 50 mm of mixture of micro-encapsulated PCM and gypsum was adequate to maintain a comfortable temperature in an office room [64]. Takeda et al. (2004) developed a similar system and tested it under eight Japanese climates numerically. Their results showed a reduction in the ventilation load by 42.8% - 62.8% and that the reduction depended more on the daily temperature range rather the average daily temperature [65]. Saman et al. (2005) examined numerically, the thermal performance of a PCM thermal storage unit for a roof integrated solar heating system and found that a higher inlet air temperature increased the heat transfer rates and decreased the

melting period [66]. Schossig et al. (2005) investigated the performance of micro-encapsulated PCM integrated in construction materials both numerically and experimentally. Their major findings were that PCM resulted in narrower temperature fluctuations, reduction in cooling demand and increase in thermal comfort in lightweight buildings [26]. Cabeza et al. (2007) installed microencapsulated PCM in concrete walls in a cubicle and compared with a cubicle with conventional concrete. Their results showed that the cubicle with the PCM had narrower daily temperature fluctuation than the cubicle with the concrete [67]. In an numerical study, Artmann (2009) found that 15 mm thick gypsum plaster board with 20% of PCM had a similar effect to diurnal heat storage capacity with 50 mm of concrete, while 15 mm thick gypsum plaster board with 40% of PCM had a similar effect with 100 mm of concrete [68].The performance of integrating PCM passively in walls in eight Australian cities was investigated in a numerical study and was found that although PCM was reducing the energy use of the building independent of the climate conditions, the performance varied and PCM with different melting point had different performance depending on the climate conditions [69]. Lopez et al. (2013) developed a numerical model which was validated experimentally to test and optimise the performance of a PCM to air heat exchanger [70]. Mandilaras et al. (2013) installed gypsum plasterboards containing PCM in a two-storey family house located in Midwest Greece. They found that the thermal mass of the building was enhanced during late spring, early summer and autumn [71]. Alvarez et al. (2013) simulated the integration of PCM for natural cooling of buildings, using seven different buildings models and concluded that placing the PCM in the core of mechanically ventilated air layers resulted in a significant increase of the convective heat transfer coefficients [72]. Ascione et al. (2014) investigated the effect of integrating PCM on the exterior building envelope in five Mediterranean cities during the cooling season, and concluded that the ideal PCM panel thickness was 30 mm and it was most beneficial for semi-arid climate [73]. Bastani et al. (2014) developed a tool to estimate the required thickness of a PCM wallboard which needs to be charged during the off-peak [74]. Bruno et al. (2014) conducted a numerical study to test the performance of a PCM system coupled to an inverter chiller cooling system and found that in some cases, although up to 85% of the energy use could be sifted to off-peak period the energy use was increased by 7.6% [75]. Biswas and Abhari (2014) conducted a side by side comparison between a test-room with PCM-enhanced cellulose insulation and a test-room with pure cellulose

insulation and used the extracted data to validate a simulation model. Their simulations showed that incorporating PCM only in the inner section of an exterior wall can achieve better thermal comfort and at lower cost, compared to adding PCM to the entire wall cavity [76]. Atkin and Farid (2015) examined the effect of PCM infused graphite and aluminium find on the efficiency of photovoltaic (PV) cells. They found that infusing PCM in graphite increased significantly the efficiency of PV cells compared to pure PCM [77]. Borderon et al. (2015) tested the incorporation of PCM in the heat exchanger of the ventilation system in four different French climates numerically, and found that the thermal comfort was significantly improved in all four climates examined [78]. Barzin et al. (2015) examined experimentally the performance of nighttime ventilation for discharging the PCM impregnated in gypsum boards and found that the PCM-gypsum boards results in 73% savings in electricity compared to conventional gypsum boards [79]. In another study, Alam et al. (2017) compared the performance of passive and free cooling PCM in a residential building in Melbourne, Australia, experimentally and numerically. They found that the free cooling application was more effective in reducing the indoor air temperature than the passive method [80]. Different control strategies for discharging PCM wallboards were evaluated numerically. It was found that by setting the room temperature lower and upper limits close to melting and solidifying points results in higher latent heat capacity of the PCM being utilised [81].

2.2.4 Barriers to broad PCM utilisation

As mentioned in Chapter 2.2.2, PCMs vary significantly and the different categories have different advantages and disadvantages. Therefore, there is no ideal solution applicable to all problems, and for each application a thorough investigation is required in advance to identify the best possible materials.

For the same application, different materials require different adjustments in the design. If PCM is impregnated, there might be leakage issue. To solve that issue a container is required. If the container is metallic, inorganic PCM will cause corrosion so should either be avoided, or a membrane should be installed between, to prevent the PCM from contacting the metal surface. But in that case, the membrane will reduce the thermal conductivity. If organic PCM is preferred instead, due to its flammability special design is required to comply with building fire safety Standards [82]–[84].

Due to the complex chemical behavior of PCMs, the number of reliable building simulation tools that can predict the behavior of PCMS is limited. This reduces the possibilities of further investigation of PCMs by researchers and discourages engineers and contractors to incorporate such a material in their project.

Most PCMs have a high acquisition cost as a raw material and combined with the adjustments in the designed required to solve the problems of the nature of the PCMs (leakage, corrosion, flammability, etc.) the investment cost is increased substantially. In combination with the inability to predict the performance of the PCM in advance, it is an investment with a high feasibility risk.

2.3 Nocturnal radiative cooling

Buildings have the possibility of utilising the ground and the outdoor air as heat sinks to release the excess heat, using ground source heat exchangers and exhaust ventilation, respectively. The sky is another heat sink which is not broadly utilised so far. The earth is continuously exchanging longwave radiation with the sky. During nighttime, the effective temperature of the sky is lower than the surfaces on earth and longwave radiation is released from the earth surface towards the sky. That process is called radiative cooling. The same process is taking place also during daytime, but in that case, the radiation coming from the sun is inserted in the equilibrium and the overall outcome is positive, namely, more energy absorbed by the earth surface than released by it. By circulating water in solar collectors during nighttime, they could be exploited to release heat towards the sky and get back water with lower temperature.

2.3.1 Theory and properties of nocturnal radiative cooling

Meir et al. (2002) described the theoretical part of the process of nocturnal radiative cooling [85]. The heat gain or loss from a horizontal surface are the sum of the convective, radiative and conductive heat exchange, as shown in Equation (2-1).

$$P_{surface} = P_{conv} + P_{rad} + P_{cond}$$

(2-1)

At the surface of a solar collector the conductive heat transfer can be safely considered negligible. Then, Equation (2-1) is expressed as below

$$P_{surface} = P_{conv} + P_{rad}$$

The convective heat transfer is describe by Equation (2-3),

$$P_{conv} = h_{conv} \cdot A \cdot (T_{rad} - T_a)$$

where

h_{conv} is the convective heat exchange coefficient,

A is the surface area,

T_{rad} is the mean surface temperature of the collector

and T_a is the outdoor air temperature.

The convective heat exchange coefficient depends linearly from the wind speed on the surface of the solar collector, as shown in Equation (2-4).

$$h_{conv} = a \cdot v + b$$

v is the speed of the air on the collector's surface, while a and b are coefficients with varying values, based on the literature [85]–[87]. The radiative heat transfer is expressed by Stefan-Boltzmann law describing the power radiated by a black body, shown in Equation (2-5),

$$P_{rad} = A \cdot \sigma \cdot \varepsilon_r \cdot (T_{rad}^4 - T_{sky}^4)$$

where

σ is the Stephan-Boltzmann constant,

ε_r is the emissivity of the collector's surface

and T_{sky} is the sky temperature, a fictive parameter, which is the equivalent temperature of the sky assumed as a black body [88]. T_{sky} is described by Equation (2-4).

$$T_{sky} = \varepsilon_{sky}^{1/4} \cdot T_a \qquad \text{(2-6)}$$

where ε_{sky} is the emissivity of the sky. ε_{sky} depends on the weather conditions, namely the outdoor air and dew point temperature, the fraction of sky being covered by clouds, the cloud emittance, the temperature different between surface and the base of the clouds and the height of the base of the clouds. ε_{sky} is given by Equation (2-7) [88],

$$\varepsilon_{sky} = \varepsilon_0 + (1 - \varepsilon_0) \cdot \varepsilon_c \cdot n \cdot e^{-Z_c/Z_*} \qquad \text{(2-7)}$$

where ε_0 is the emissivity of clear sky,

ε_c is the hemispherical cloud emissivity, calculated as following:

- $\varepsilon_c \approx 1$ for $Z_c < 4\ km$

- $\varepsilon_c = 0.74 -\ 0.084 \cdot (Z_c - 4)$ for $4 < Z_c < 11\ km$

- $\varepsilon_c = 0.15$ for $Z_c > 11\ km$

Z_c is the height of the cloud's base,

Z_* is a reference value set to 8.2 km,

n is the fraction of sky covered by opaque clouds, $0 \leq n \leq 1$.

ε_0 is calculated using Equation

$$\varepsilon_0 = 0.71 + 0.0056 \cdot T_{dew} + 0.000073 \cdot T_{dew}^2 \qquad \text{(2-8)}$$

Where T_{dew} is the dew point temperature of the outdoor air.

2.3.2 Applications in the built environment

Cold water produced through the process of nocturnal radiative cooling can be circulated in radiant systems or PCM panels to condition the room temperature and discharge the PCM. As mentioned earlier, only limited case of applications of nocturnal radiative cooling in the built environment were identified.

Erell and Etzion (2000) developed and validated an analytical model to describe the operation of nocturnal radiative cooling and concluded that the metal fins used in typical flat plate collectors are less efficient for cooling applications [89]. Meir et al. (2002) tested a polymer-based radiative cooling system experimentally and numerically. They found that even when the outdoor conditions were not in favor of producing cold water, nocturnal radiative cooling was covering a significant fraction of the cooling demand [85]. Eicker and Dalibard (2011) reported the performance of the PVT panels used in the Solar Decathlon Europe 2010 competition by the team of the University of Applied Science in Stuttgart, Germany. Their PVT panels provided on average a cooling power of 41 W/m² during nighttime, tested in Madrid, Spain [90]. Hosseinzadeh and Taherian (2012) assessed both numerically and experimentally the performance of a flat plate solar collector installed in Babol, Iran, in terms of nocturnal radiative cooling. The water temperature difference between the inlet and outlet of the solar collectors was approximately 7 – 8°C, while the cooling power varied between 23 W/m² and 52 W/m² [91]. Similar cooling power (50 W/m²) was measured by Anderson et al. (2013), who examined theoretically and experimentally the performance of an unglazed solar collector in nighttime radiative cooling [92]. Péan et al. (2015) tested experimentally the performance of three PVT panels and an unglazed solar collector. In that case the cooling power reached 75 W/m², while the COP of the system varied between 19 and 59 [93].

Only a few cases where nocturnal radiative cooling was utilised to discharge PCM integrated in the construction were identified in the literature. Fiorentini et al. (2015) developed a simulation model based on a project house of a Solar Decathlon China 2013 competition which combined PVT panels with PCM integrated on the ceiling ventilation system [94]. Lin et al. (2014) tested numerically that model, and concluded that the combination of PVT and PCM provided significantly better thermal environment than the reference case and the case with only PCM [95].

2.4 Indoor environment

Nowadays, most people spend most of their life indoors, either at home or their working place, especially in urban areas. It is therefore essential to ensure the best possible indoor environment quality (IEQ) for building occupants. Indoor environment includes the thermal environment, air quality, relative humidity, lighting and noise levels.

2.4.1 European standard EN-15251 guidelines about thermal environment

The European Committee for Standardization (CEN) published in 2007 the Standard EN 125251 which provides the guidelines for all parameters related to IEQ [7]. For each parameter, the Standards defines a range or a value for different categories. The criteria for the thermal environment are in accordance with the thermal comfort indices predicted mean vote (PMV) and predicted percentage of dissatisfied (PPD) and should comply with the Articles 4, 6, 8 and 9 of the Directive on the Energy Performance of Buildings (EPBD) [96].

Table 2-3: Description of each category of Standard EN 15251 [7]

Category	Explanation
I	High level of expectation and is recommendned for spaces, occupied by very sensitive and fragile persons with special requirements like handicapped, sick, very young children and elderly persons
II	Normal level of expectation and should be used for new buildings and renovations
III	An acceptable, moderate level of expectation and may be used for existing buildings
IV	Values outside the criteria for the above categories. This category should only be accepted for a limited part of the year

Table 2-4 shows the recommended values and ranges for PPD and PMV, respectively, for each category of EN 15251. The PVM-PPD index takes into consideration the effect of all six thermal parameters, namely, clothing value, activity level, air temperature, mean radiant temperature, air velocity and relative humidity.

Table 2-4: Recommended categories for design of mechanical heated and cooled buildings [7]

Category	Thermal state of the body as a whole	
	PPD, %	PMV
I	<6	-0.2 < PMV < +0.2
II	<10	-0.5 < PMV < +0.5
III	<15	-0.7 < PMV < +0.7
IV	>15	PMV < -0.7 or +0.7<PMV

Furthermore, assuming specific values for the metabolic rate and the clothing value, Standard EN 15251 defines design values and temperature ranges for different building or space types. Table 2-5 and Table 2-6 show examples of design values of the indoor temperature and temperature range for energy calculations for office building types of space. It should be stated that although in Standard EN 15251 there is a seasonal effect on both the adaptive model and the PMV-PPD approach mainly due to change in clothing level from winter to summer, the effect of a change in metabolic rate (activity level) during the day on the acceptable room temperature has not been thoroughly studied.

Table 2-5: Examples of recommended design values of the indoor temperature for design buildings and HVAC systems for office types of spaces[7]

Type of building/space	Category	Operative temperature, °C	
		Minimum for heating ~ 1.0 clo	Maximum for cooling ~ 0.5 clo
Single office (cellular office) sedentary ~ 1.2 met	I	21.0	25.5
	II	20.0	26.0
	III	19.0	27.0
Landscaped office (open plan office) sedentary ~ 1.2 met	I	21.0	25.5
	II	20.0	26.0
	III	19.0	27.0
Conference room sedentary ~ 1.2 met	I	21.0	25.5
	II	20.0	26.0
	III	19.0	27.0

Table 2-6: Temperature range for hourly calculation of cooling and heating energy for office types of space[7]

Type of building/space	Category	Temperature range for heating, °C ~ 1.0 clo	Temperature range for cooling, °C ~ 0.5 clo
Offices and	I	21.0 – 23.0	23.5 – 25.5
spaces with similar	II	20.0 – 24.0	23.0 – 26.0
activity			
sedentary ~ 1.2	III	19.0 – 25.0	22.0 – 27.0
met			

2.4.2 Thermal comfort

Although Standard EN 15251 defines specific design values for operative temperature, steady-state conditions are rarely observed, due to fluctuations in solar heat gains and occupancy level. Especially in modern large office buildings, occupancy is a very dynamic factor, with most of the employees not being assigned a specific office or desk, but rather sit in different desks depending on their current task, meeting or having the possibility to work from distance. Furthermore, the operation of radiant systems such as TABS or active PCM panels is based on temperature drifts, rather than a constant setpoint value as in the case of an all-air system [97]. ASHRAE Standard 55 defines specific limits for temperature drifts and ramps (Table 5.3.5.3) [8]. Nevertheless, most of the human subject experiments examining thermal comfort, have been either been conducted under steady-state conditions and in a thermally uniform environment, or in a non-uniform but constant thermal environment. Only a few studies have been conducted under transient or non-steady uniform conditions.

Arens et al. (2006) exposed subjects to a uniform environment and the subjects reported their local and overall thermal sensation and comfort, and was found that overall sensation and comfort followed the warmest local sensation in warm environments and the coldest in cool environments [98]. Melikov et al. (2007) conducted a human subject experiment where 30 subjects were sitting in a room ventilated by a chilled beam having a room air temperature of 24°C constantly. When the heat load were increased from 30 W/m² to 70 W/m² the percentage of subjects dissatisfied increased substantially [99]. Dalewski et al. (2014) assessed the

performance of ductless personalised ventilation (DPV) in conjunction with displacement ventilation in a human subject experiment with 30 subjects. It was found that the use of DPV improved perceived air quality and thermal comfort compared to displacement ventilation alone [100]. In another study, the responses of 24 subjects exposed to a personalised ventilation combined with chilled ceiling were compared with their corresponding responses from being exposed to mixing ventilation with chilled ceiling. It was found that the combination of personalised ventilation with chilled ceiling resulted in thermal sensation closer to neutral than compared to mixing ventilation combined with chilled ceiling [101]. Arghand et al. (2016) reported the responses of 24 subjects exposed to localised chilled beam and mixing ventilation, both combined with chilled ceiling. In the case of the combination of localised chilled beam with chilled ceiling the subjects reported better both local and overall thermal sensation acceptability [102]. Jin et al. (2017) exposed 24 subjects to three heating systems, conventional radiator, ventilative radiator and floor heating. Both ventilative radiator and floor heating provided a better thermal environment than the conventional radiator [103]. In another study the thermal environment in an office room provided by chilled beam, chilled beam with radiant panels, chilled ceiling with mixing ventilation and desk partition-mounted local radiant ceiling panels with mixing ventilation was compared. It was found that the differences in the thermal conditions achieved with the four systems tested were insignificant [104].

Zhang et al. (2010) reported the results from 109 human tests that were performed under non-uniform and transient conditions and developed predictive models of local and overall thermal sensation and comfort [105]. Human subjects were exposed to partial- and whole-body heating and cooling and it was found that hand and finger temperatures fluctuated significantly when the body was near a neutral thermal state, and the core temperature increased in response to skin cooling and decreased in response to skin heating [106]. In another study, Zhang et al. (2010) developed a model for predicting the local thermal sensation, local comfort of different parts of the human body and the whole-body thermal sensation and comfort responses [107]–[109]. Arens et al. (2006) reported the responses from human subjects exposed to sequences of partial-body cooling and warming over of period of three hours. It was found that the whole body experienced a step-change the thermal sensation and

comfort reported were closer to neutral than when local body parts were cooled or warmed [110].

Sedentary unclothed men reported their thermal sensation under transient condition and it was found that when the temperature was increasing, the rate of rise of skin temperature caused a sensation that reduced the discomfort caused by the lower skin temperature [111]. In another study, 52 subjects reported their thermal sensation under different temperature ramps and linear relationship between mean thermal sensation and operative temperature was observed [12]. Griffiths and McIntyre (1974) examined steady state and 3 levels of both increasing and decreasing temperature ramps, and developed a method for predicting the level of dissatisfaction produced by temperature changes [112]. McIntyre and Gonzalez (1976) examined the impact of clothing insulation and activity level on men's thermal sensitivity during rapid temperature drops in a human subject experiment with 20 subjects. They concluded that for resting subjects, thermal sensitivity was not affected by season or clothing insulation [113]. Hensen (1990) conducted a literature review study on thermal comfort in transient conditions and concluded that ramps between 0.5 K/h and 1.5 K/h do not impact the range of the comfort zone [114]. Goto et al. (2006) investigated the impact of different activity intensity and duration on thermal sensation and concluded that participants' thermal sensation was more sensitive to changes in core temperature caused by a reduction in activity than by increased activity [115].

Since the operation of radiant systems is based on temperature drifts, it is important that drift to take place within the comfort range as this is suggested by the standards (e.g. 23-26°C for Category II of Standard EN 15251 [7]). Otherwise, it will result in overheating in the afternoon. If temperatures lower than the lower limit of the comfort range were acceptable at the beginning of the occupancy period (e.g. 20°C or 21°C), it would extend the range of the temperature drift, minimising the risk of overheating in the afternoon. Furthermore, until the room temperature reaches the comfort range, no active system would be required, as the temperature would increase due to solar heat gains and the internal heat sources. Thus, the operation time of the HVAC equipment would be reduced, resulting in energy savings.

3 Correlation of increased metabolic rate with the thermal comfort at the beginning of occupancy period of office buildings during the cooling period

This chapter summarises the findings from a human subject experiment carried out during the period April – May 2015 at the facilities of ICIEE. These findings address the first objective of the PhD dissertation and has been based on Paper 2. Details can be found in this publication.

3.1 The effect of different starting room temperature on occupant comfort in Danish summer weather

Findings of this study have been published in the Building and Environment journal:

Bourdakis E., Simone A., & Olesen B.W. (2018). An experimental study of the effect of different starting room temperatures on occupant comfort in Danish summer weather. Building and Environment, https://doi.org/10.1016/j.buildenv.2018.03.046

As office workers will usually have a slightly elevated metabolic rate when arriving at work, they may prefer at the beginning of the occupancy period a room temperature below the comfort range for sedentary activity, as this is defined by the European Standard 15251 [7]. The existing European and international standards take into consideration a seasonal effect on both the adaptive and the PMV-PPD models either through changes in the clothing level from winter to summer and vise-versa or by changing outside temperatures [7], [8]. So far, the impact of a change in the activity level (metabolic rate) on the acceptable room temperature has not been investigated thoroughly. Most people will have an increased activity level (higher than sedentary) when arriving at work. This may result in a warmth sensation when entering an office where the room temperature is designed for sedentary activity level. A slightly lower temperature than the current comfort range at the beginning of the occupancy period may increase the comfort sensation of the occupants and enable the possibility of exploiting night-cooling.

3.1.1 Method

The experiment was carried out in the climatic chambers of the ICIEE at DTU in the period mid of April to beginning of May. At first, 30 DTU students were recruited and split randomly to groups of five. They were from 22 to 27 years old, they were all healthy and physically fit and they had a normal Body Mass Index (BMI). The participants were requested to wear light summer clothing, and this resulted in an effective clo-value of 0.5 when taking into consideration the insulation of an office chair [8]. Each subject participated in four different sessions and in each session only once. To minimise possible bias caused by the order of exposure, the four sessions were spread randomly during the three weeks of the experiment, and it was ensured that no participant would come twice on the same day or on consecutive days. Each session consisted of two phases: the commute phase, which simulated commuting to work on foot, and the office phase. The first part of the experiment was conducted in a HVAC controlled office room, where the temperature was maintained constant at 18°C. This is the average outdoor air temperature for Northern European summer weather conditions at the typical working day commuting time, namely from 07:00 to 09:00. For this commute session, three treadmills and two steps were installed on which the subjects exercised for 15 min at an average activity level of 1.5 met. For all participants to have comparable activity level, the subjects switched positions so that they exercised for a total of 9 min on the treadmill and 6 min on the steps. The climatic chamber where the second phase took place was furnished to represent a five-person landscape office. After the commuting session, the participants walked directly into the conditioned office room and sat down at their assigned desk (second experimental session).

Table 3-1: Temperature schedule for the four sessions

Time of temperature change	00:00	00:30	01:00	01:30	02:00	02:30	03:00
Case 1	18.5°C	20°C	21.5°C	23°C	24.5°C	24.5°C	
Case 2	20°C	21.5°C	23°C	24.5°C	26°C	27.5°C	27.5°C
Case 3	21.5°C	23°C	24.5°C	26°C	26°C		
Case 4	23°C	24.5°C	26°C	27.5°C	27.5°C		

3.1.2 Results

Figure 3-1 shows the whole-body thermal sensation as a function of the room operative temperature, while the whiskers show the standard deviation. The shaded area is the comfort zone. When the starting temperature was 18.5°C, the subject felt the closest to neutral when they entered the climate chamber, compared to the other three cases. After 30 minutes, in the second questionnaire of Case 1 the subjects reported feeling slightly cool, as the effect of exercising quickly decreased.
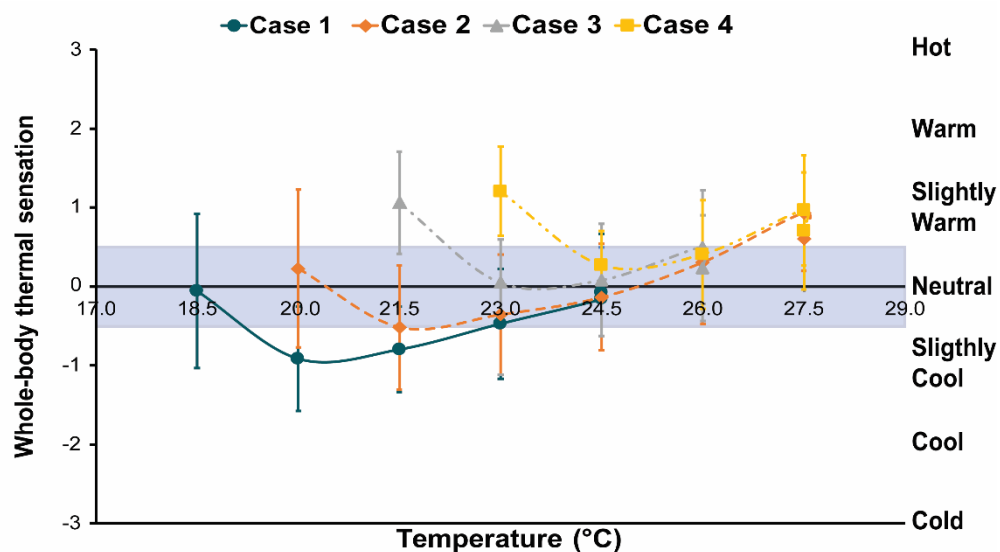
Figure 3-1: Whole-body thermal sensation as a function of the room air temperature. Whiskers show the standard deviation for each questionnaire. The shaded area shows the comfort zone

Figure 3-2 shows the percentage of the subjects dissatisfied with the thermal environment as a function of the mean thermal sensation. The black line shows the predicted percentage dissatisfied (PPD) curve originating from Fanger's model [116]. Although the conditions in this experiment were transient (temperature ramp of 1.5K/0.5h), the results in the neutral zone (whole-body thermal sensation of ±0.5) follow Fanger's model quite satisfactorily, although it was developed from data obtained in steady-state studies. Kolarik et al. (2009) made a similar observation in their study. These are strong indications that Fanger's model has a broader range of application, rather than just steady-state conditions.
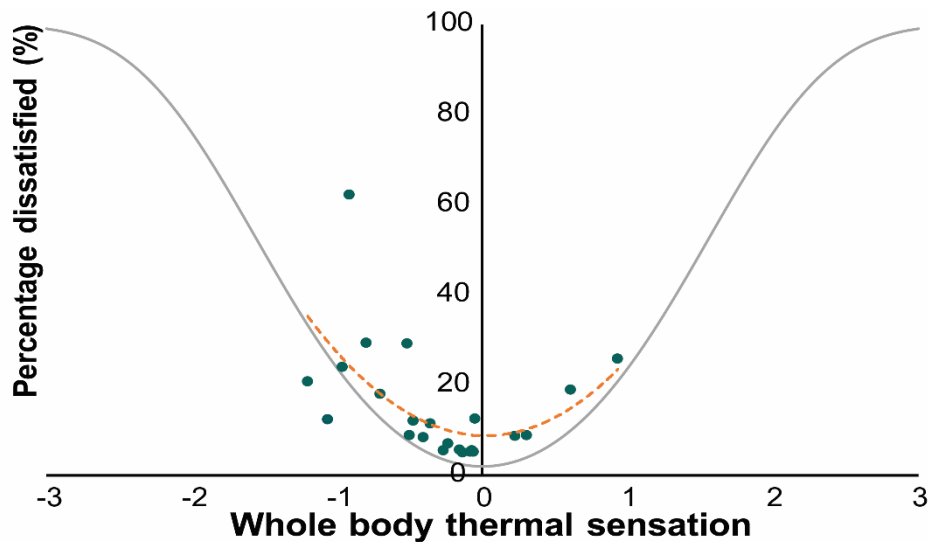
Figure 3-2: Combined results of percentage of subjects dissatisfied with the thermal environment

3.1.3 Main findings and conclusions

1. No significant differences were observed between the subjective responses of male and female participants

2. Due to the increased metabolic rate from walking, lower room temperature than what suggested by EN Standard 15251 [7] were reported as acceptable at the beginning of the occupancy period.

3. The impact of the physical exercise had disappeared after approximately 30 min

4. Although the conditions in this experiment were transient (an increasing temperature ramp of 1.5K/0.5 h), the results in the neutral zone followed Fanger's model quite closely, although his model was developed from data obtained in steady-state exposures

5. In countries where most people commute on foot or by bike, the room temperature at the beginning of the occupancy period could be 20°C–21.5°C, namely lower than EN Standard 15251 suggests. It should then increase steadily at a rate of 1.5K/0.5 h to reach the comfort range of 23°C–26°C.

4 The combination of phase change material (PCM) for space cooling and PVT for exploiting nocturnal radiative cooling

This chapter summarises the findings from the studies carried to investigate the potential of coupling radiant ceiling panels containing PCM for space cooling, with PVT panels for exploiting the principle of nocturnal radiative cooling to produce cold water circulated in the PCM panels. These findings address the second and third objectives of the PhD dissertation and has been based on Paper 1, 5 6, 7 and 8. Detailed information in the experimental method, the simulation models and further results can be found in these publications.

4.1 Daytime space cooling with phase change material ceiling panels discharged using rooftop photovoltaic thermal panels and nighttime ventilation

Findings of this study have been published in the Science and Technology for the Built Environment journal and the proceedings of the IAQVEC 2016 conference:

Bourdakis E., Péan T. Q., Gennari L., & Olesen B. W. (2016). Daytime space cooling with phase change material ceiling panels discharged using rooftop photovoltaic/thermal panels and nighttime ventilation. Science and Technology for the Built Environment, 4731(June), 1–9. https://doi.org/10.1080/23744731.2016.1181511

Bourdakis E., Peán Q. T., Gennari L., & Olesen B. W. (2016). Experimental study of discharging PCM ceiling panels through nocturnal radiative cooling. Presented at IACVEQ 2016

Thermally active building systems (TABS) have the potential of reducing the energy required for the operation of HVAC systems. Their high thermal mass results in the distribution of cooling over a longer period of time which leads to lower peaks of cooling/heating demand [15]. Although TABS seem to be a promising solution for new constructions, they are not always applicable to renovation projects, as it is technically challenging to include a new 150 mm concrete slab in existing buildings. This

drawback could be solved by installing radiant ceiling panels containing PCM, since they have the thickness of a lightweight construction, but their effective thermal mass is comparable to that of a heavyweight building element.

4.1.1 Method

The experiment took place in a climate chamber with floor area of 22.7 m² and height of 3 m. At 2.5 m above the floor, the radiant ceiling panels containing the PCM panels were installed as a suspended ceiling and each panel contained 6 kg of PCM. The plenum that was formed between the suspended ceiling and the chamber's roof was used to supply fresh air inside the room. The PCM used was microencapsulated paraffin with a melting point of 23°C and a latent heat capacity of 110 kJ/kg. The PCM panels had embedded Alu-PEX pipes for circulating cold water. Figure 4-1 shows the construction of the PCM panels used in the experiment.
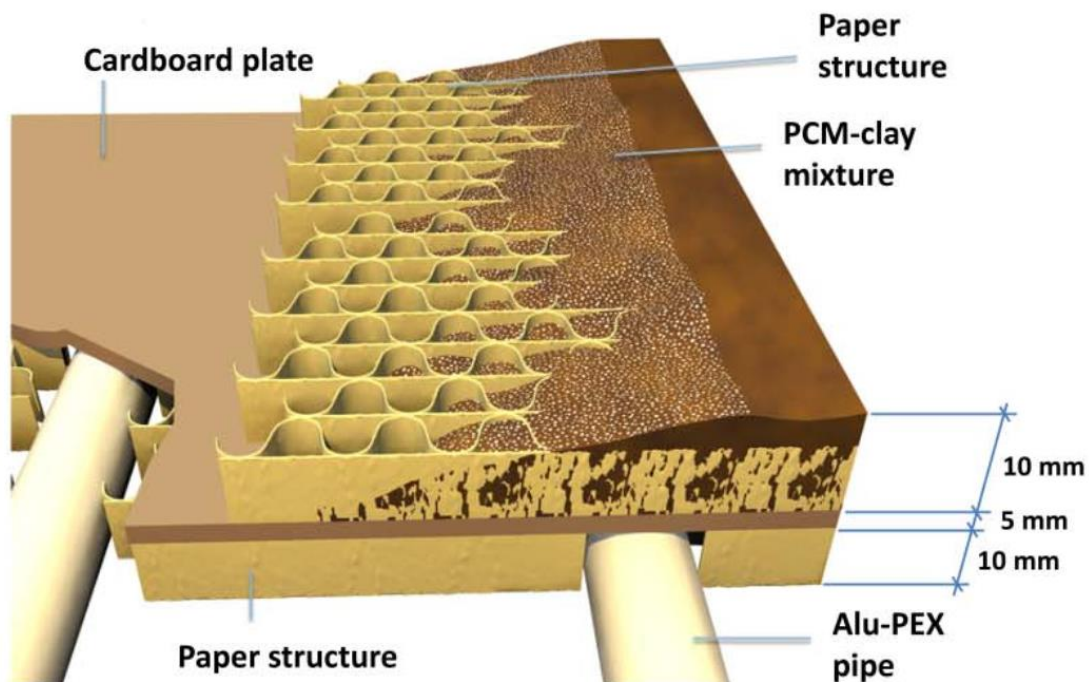
Figure 4-1: Construction of the PCM-clay panels with layer thickness[117]

The chamber interior was arranged to represent a two-person office, using heat dummies, and the total sensible heat gains were 23.8 W/m². The chamber was not directly exposed to sunlight; thus, an electrical heating wall panel was used to simulate

the solar heat gains of a window facing south. The air supply temperature was varying from 18°C to 20°C, while the ventilation flow rate was set to 30 l/s, which is the minimum airflow rate required to provide fresh air and removing latent heat gains and pollutants for an office with the size of the climate chamber having two occupants [7]. The internal heat sources and the ventilation were activated from 9:00 to 17:00. Three polycrystalline PVT panels were installed on the roof of the building. The PVT panels were connected through a plate heat exchanger with two storage tanks (Figure 4-2). One tank was used to store hot water (HWT) while in the second one, cold water was stored (CWT). The direction of the water after the heat exchanger toward the tanks was determined automatically based on the following conditions:

$$T_{PVT} - T_{HWT} > 1\ K \qquad\qquad (4\text{-}1)$$

$$T_{CWT} - T_{PVT} > 1\ K \qquad\qquad (4\text{-}2)$$

where

- T_{PVT} is the water temperature exiting the PVT panels,

- T_{HWT} is the water temperature in the middle of the HWT,

- T_{CWT} is the water temperature in the middle of the CWT.

If neither of the two conditions was met, then the pump between the heat exchanger and the tanks was switched off. The CWT had two internal spiral heat exchangers; the upper one was connected to the plate heat exchanger, while the lower one was connected to the main chiller of the laboratory facilities (Figure 4-2).
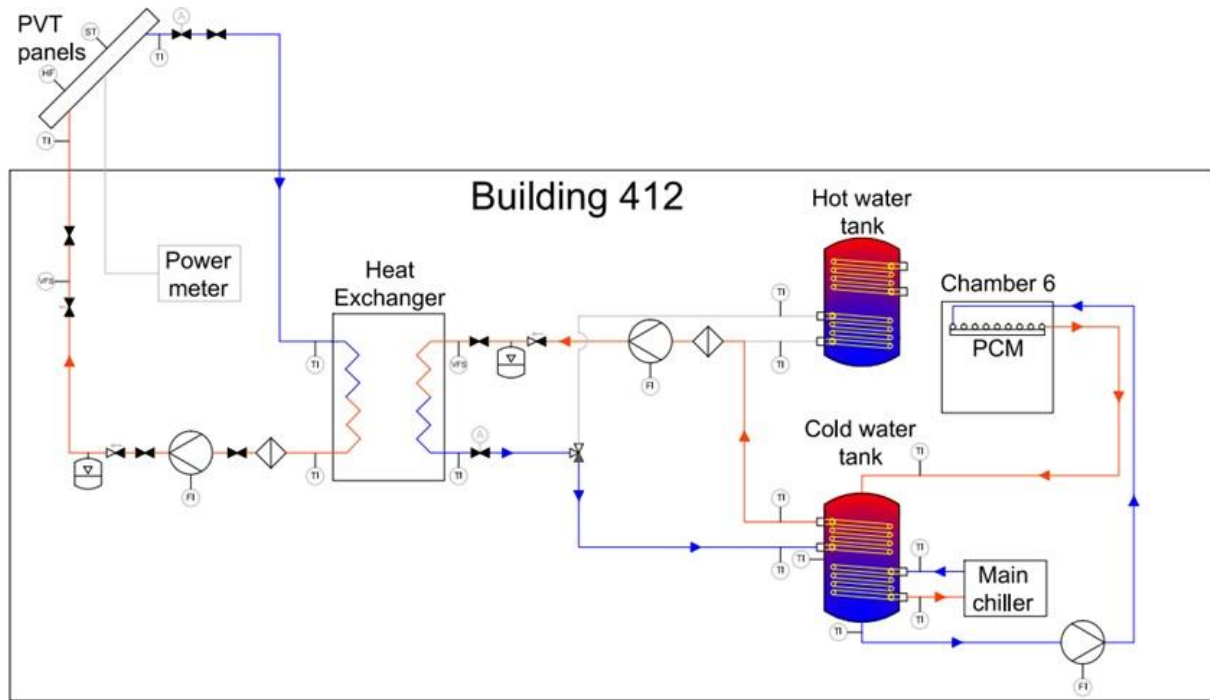
Figure 4-2: Schematic drawing of the hydronic system

The main chiller was used as an auxiliary system for providing cold water whenever the production from nighttime radiative cooling was not sufficient. The water from the bottom of the CWT was circulated to the PCM panels and from there it was returned to the top of the CWT. The water flow rate was 210 kg/h and the circulation of the water was started at 5:00 and continued until 9:00, provided that the following conditions were met:

- The average lower surface temperature of the PCM panels was above 21°C,

- The operative temperature of the room was above 21°C,

- The temperature of the water in the middle of the CWT was below 20°C.

That time of the day was selected so that nocturnal radiative cooling will have reduced the temperature of the water stored in the CWT and there was still adequate time to discharge the PCM panels. During the occupancy period, the water circulation to the PCM panels was activated automatically if the temperature at the middle of the CWT was below 20°C and the operative temperature of the room was above 25.5°C. Table 4-1 show the configurations examined. Each experimental case lasted five days and the experiment took place from July to September 2015.

Table 4-1: Cases examined

Case	Nighttime ventilation	Improved air mixing	Operation of embedded water system during nighttime
1	No	No	Yes
2	No	Yes	Yes
3	30 l/s at 18°C – 20°C	Yes	Yes
4	30 l/s at 18°C – 20°C	No	Yes
5	30 l/s at 18°C – 20°C	No	No

4.1.2 Results

Figure 4-3 shows the operative temperature for five experimental cases examined. The grey shaded areas illustrate the occupancy period, while the three pairs of horizontal dashed lines show the lower and upper limits of the Categories I (23.5 – 25.5°C), II (23 – 26°C) and III (22 – 27°C) of Standard EN 15251 [7].
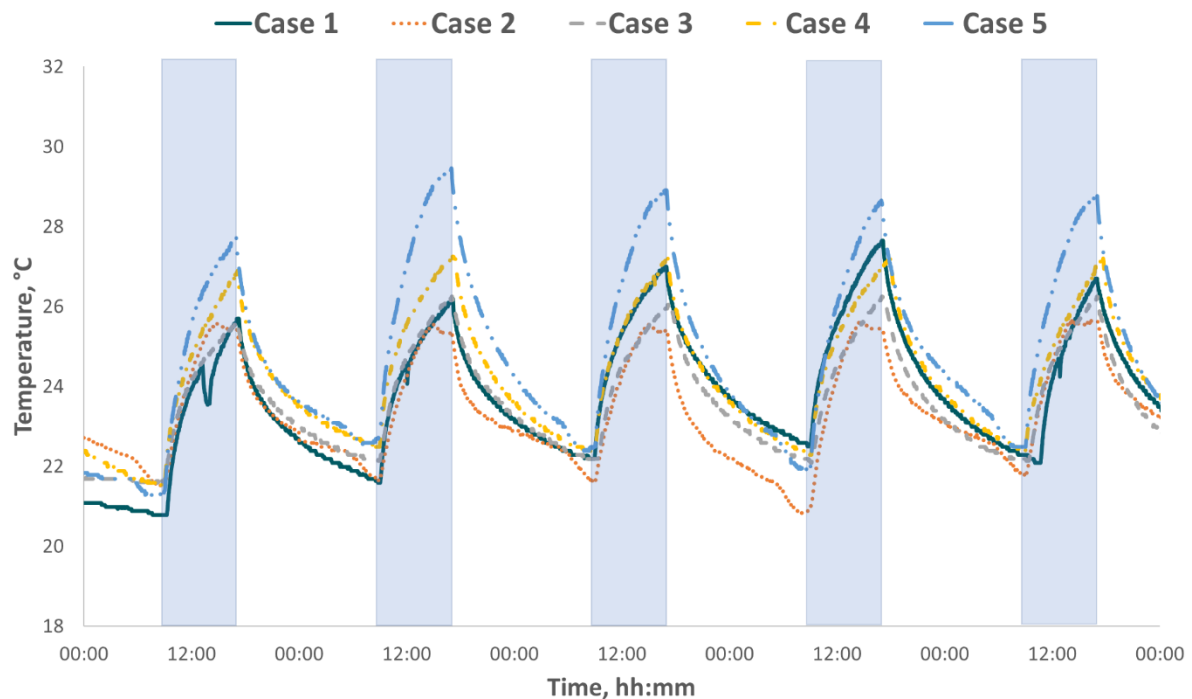
Figure 4-3: Operative temperature. The shaded areas show the occupancy period

Case 3 had the highest percentage of occupancy period within the range of Category III, while case 5 failed to provide an acceptable thermal environment (only 50% of the occupancy period was within the range of Category III). That shows that the quantity

of the PCM was not enough to store the sensible heat emitted during the occupancy period, resulting in overheating, and at the same time, the air flow rate during the night was insufficient for discharging the PCM.

Figure 4-4 shows the temperature in the middle of the hot water tank (HWT) during the period 10-14 of August 2015, in correlation with the solar radiation on the PVT surface during the same period. The temperature in the middle of the HWT reached 54°C which makes it suitable for domestic hot water (DHW) use. Nevertheless, since the water in the HWT was not utilised, the temperature in the tank was dropping only due to heat losses. That resulted in the linear temperature drop observed between the 1st and the 3rd day in Figure 4-4. Due to the high temperature in the HWT, during that period, Condition (4-1) was not fulfilled, resulting in an underestimation of the performance of the PVT panels in terms of producing DHW.
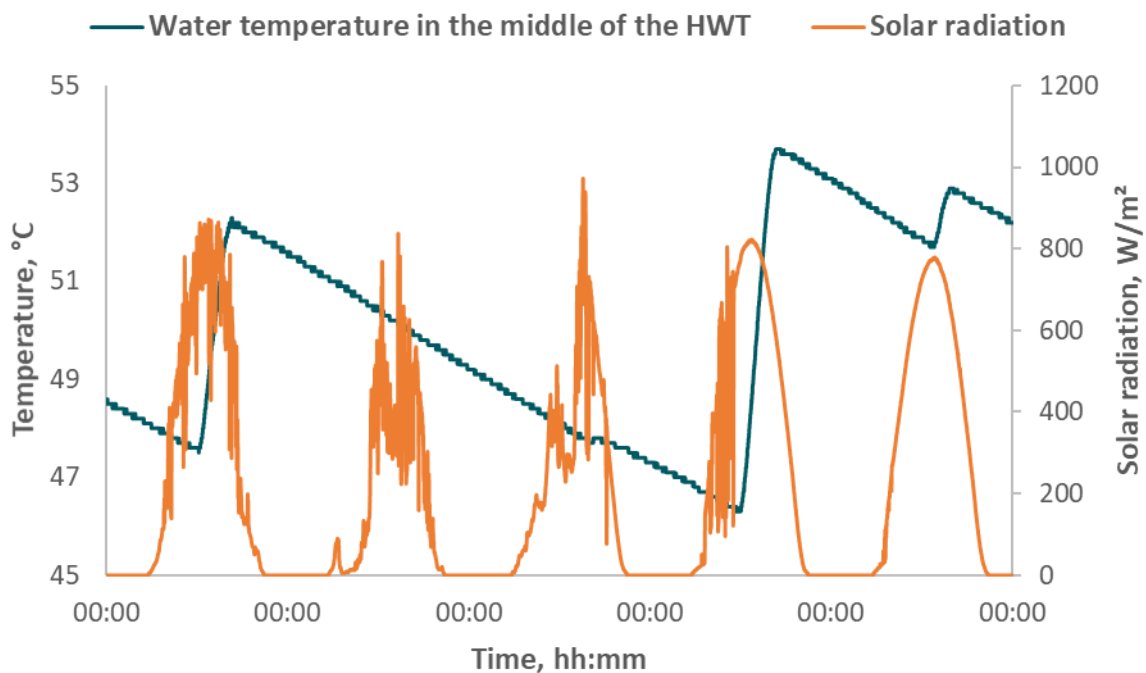
Figure 4-4: Correlation between solar radiation and temperature in the middle of the hot water tank (HWT) during the period 10-14 of August 2015

Figure 4-5 shows the electrical energy produced by the PVT panels and the energy use of the chamber, split in energy use by the office equipment, the water pumps, the

ventilation and the chiller. Case 2 was the only one were the electricity produced by the PVT panels was adequate to supply the whole demand of the chamber, due to the low energy use of the water chiller. The chiller was hardly used due to the outdoor conditions which were in favour of exploiting nocturnal radiative cooling. Case 3 had the higher electricity production. Nevertheless, this was not sufficient to cover the demand due to the high energy use of the chiller.
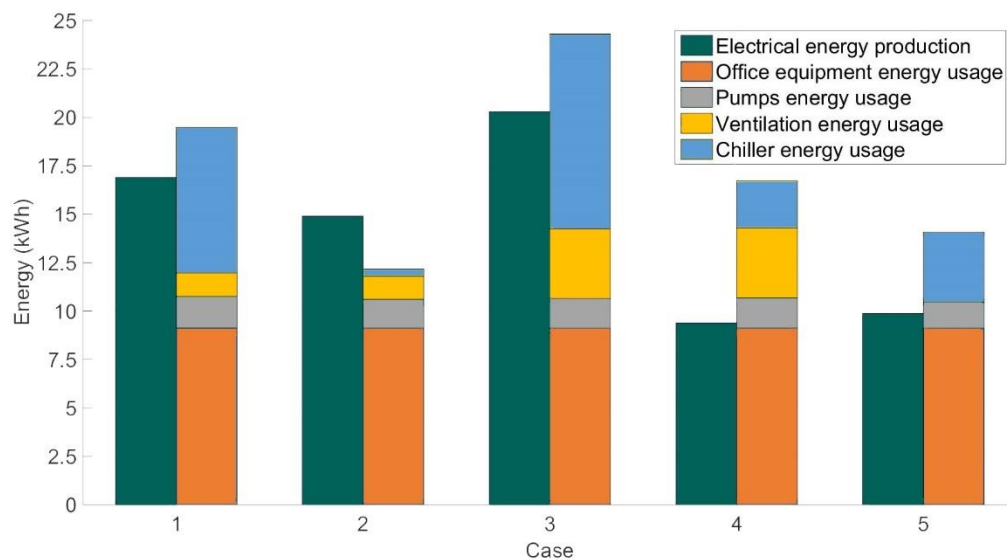
Figure 4-5: Comparison of electricity production and energy use for each experimental case

The variation of the solar radiation shown in Figure 4-6, affected the heating power output of the PVTs and making it impossible to conclude which flow rate in the solar loop is the most effective for water heating.
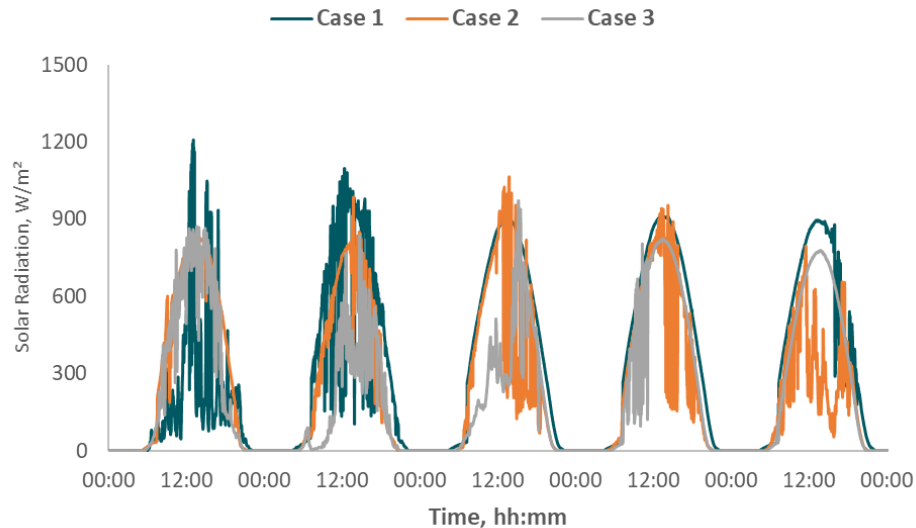
Figure 4-6: Solar radiation over time

4.1.3 Main findings and conclusions

1. The PCM ceiling panels provided an acceptable thermal environment in the office room when the embedded pipes were in use.

2. The location of the PCM compared to the heat gain sources affects significantly the performance of the PCM. Therefore, special attention has to be given when designing a cooling system which includes PCM.

3. The tested air flow rate proved insufficient when only nighttime ventilation was used as discharging method.

4. Out of the three examined flow rates in the PCM loop, the highest one provided the best thermal environment in the chamber.

5. The variations in the weather conditions between the three cases cannot lead to a safe conclusion whether the measured differences in the heating and cooling power of the PVTs can be attributed to the different flow rate in the solar loop or the weather conditions.

6. PVT panels proved to be an efficient solution to produce electrical energy and heating and cooling water for domestic hot water and space cooling respectively, contributing to the spread of nZEBs.

7. Although the PVT panels performed satisfactorily, their performance cannot be accurately predicted due to variation in the weather conditions to which they were exposed.

4.2 Development and validation of a TRNSYS model

Finding of this study have been published in the proceedings of the AIVC 2015 conference, ASHRAE Annual Meeting 2016 and ASHRAE Winter Meeting 2017:

Bourdakis E., Grossule F., & Olesen B. W. (2016). Night time cooling by ventilation or night sky radiation combined with in-room radiant cooling panels including Phase Change Materials. Presented at AIVC 2015

Bourdakis E., Kazanci O. B., Grossule F., & Olesen B. W. (2016). Simulation Study of Discharging PCM Ceiling Panels through Night-time Radiative Cooling. Presented at ASHRAE Annual Conference 2016

Bourdakis E., Kazanci O. B., Peán Q. T., & Olesen B. W. (2016). Parametric analysis of the control of solar panels for nocturnal radiative cooling coupled with in room PCM ceiling panels. Presented at ASHRAE Winter Conference 2017

Simulation models enables us to expand the possibilities of investigation far beyond the limits of an experimental facility. For example, a simulation model gives the possibility of comparing the same system or construction under different climate conditions, which would be impossible with a stationary experimental facility. Similarly, a simulation model provides the possibility of running a parametric study in a very short period, and at the same ensuring that all the parameters remain constant. Keeping the rest of parameters constant is crucial, especially when the contingency of weather conditions is included, as it was shown in Chapter 4.1.2. Nevertheless, to ensure the credibility of a model, it is important to validate it against comparable experimental results.

4.2.1 Model description

A TRNSYS model was created to simulate the experimental setup that was described in Chapter 4.1.1. The model was representing a two-persons office. The office was

assumed to be in an intermediate floor of an office building and the external wall of the office was facing south. Therefore, the three internal walls, the roof and the floor were assumed to be adjacent to office rooms with identical thermal conditions, so no heat exchange occurred from these surfaces. The U-value of the external wall was 0.3 W/m²K while the internal surfaces had a U-value of 4.9 W/m²K. On the external wall there was a 3 m² window with a U-value of 1.4 W/m²K and a Solar Heat Gains Coefficient (SHGC) of 0.59. The heat gains of the office consisted of two occupants at sedentary activity level (1.2 Met), while the corresponding office equipment and artificial lighting was in total 540 W (23.8 W/m²). The heat gains were activated from 9:00 to 17:00.

The simulation period was from the 1st of May until the 30th of September, using the Copenhagen (CPH), Milano (MIL) and Athens (ATH) weather files. Apart from the geographic analysis, a parametric analysis also was conducted in which the performance of several parameters of the hydraulic system was evaluated. Table 4-2 shows the values that were examined for each parameter.

Table 4-2: Setpoint values for examined parameters

AWHP starting time, hh:mm	CWT temperature to activate the AWHP, K	Pump 3 starting time, hh:mm	CWT temperature to activate Pump 3, K	Panels- Tanks ΔT, K
03:00	15	03:00	15	1
04:00	16	04:00	16	2
05:00	17	05:00	17	3
06:00	18	06:00	18	4
07:00	19	07:00	19	5
	20		20	
	21		21	

Figure 4-7 shows an overview of the TRNSYS model. In the TRNSYS model, the main chiller of the experimental facilities was replaced with an air-to-water heat pump (AWHP). The AWHP was used as a supporting system for providing cold water when the production from nocturnal radiative cooling was not sufficient. The AWHP had a seasonal Coefficient Of Performance (COP) of 5.4 (18.4 Energy Efficiency Ratio (EER)), based on a datasheet of a market available product.
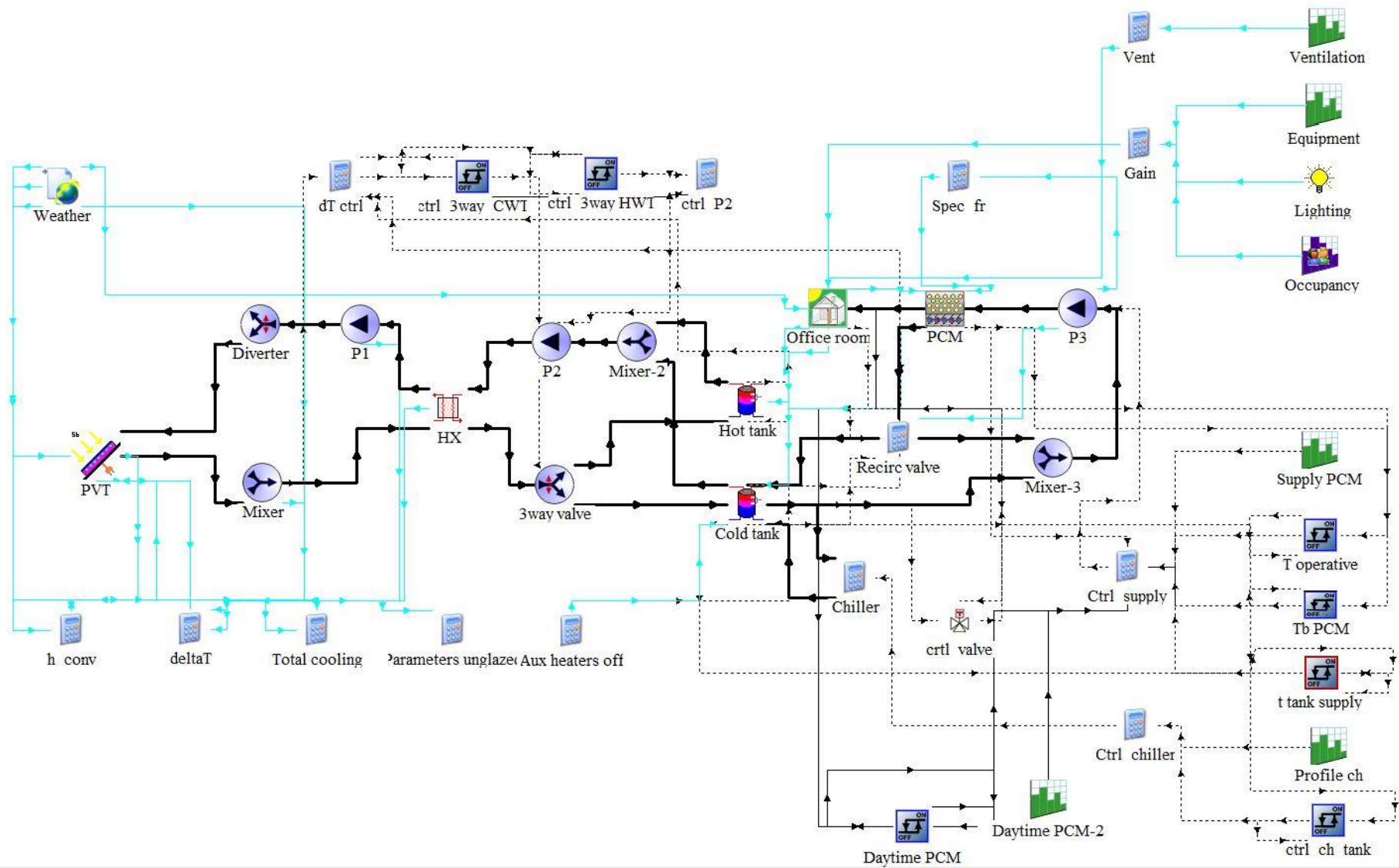
Figure 4-7: Overview of the TRNSYS validation model

4.2.2 Model validation

To validate the TRNSYS model the weather file was replaced with data extracted from a weather station installed next to the PVT panels on the roof of the building. Furthermore, there were no direct solar heat gains, as in reality the climate chamber used for the experiment was inside a bigger building. For the same reason, the air temperature outside the climate chamber was used as outdoor temperature for the simulation model and was applied as ambient condition to all four walls and the roof of the model. Figure 4-8 shows the air and operative temperatures for the simulation and the corresponding experimental case. Figure 4-9 shows the bottom surface temperature of PCM panels for the simulation and the corresponding experimental case. The simulation model predicted satisfactorily well the thermal performance in the room and the PCM panels.
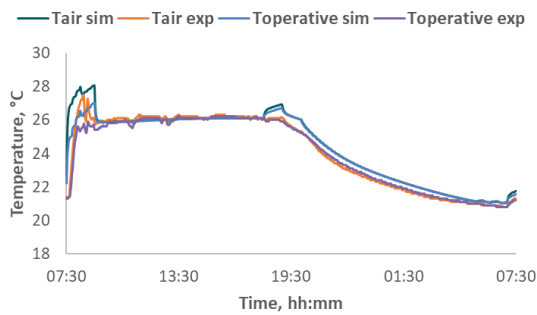
Figure 4-8: Air and operative temperature of simulation and experiment
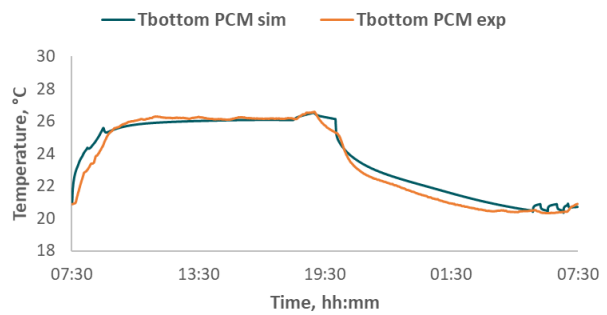
Figure 4-9: PCM bottom surface temperature of simulation and experiment

Figure 4-10 shows the specific cooling power of each night for the experiment and the corresponding simulations, while Figure 4-11 shows the corresponding energy that was released towards the atmosphere through the process of nocturnal radiative cooling. The simulation model underestimated the performance of the PVT in terms utilising nocturnal radiative cooling compared to the corresponding results extracted from the experiment. This inaccuracy was caused by the effective sky temperature values implemented in the TRNSYS model. Since this parameter was not possible to be measured by the weather station, a theoretical calculation was used as it is described by Péan et al. (2016).
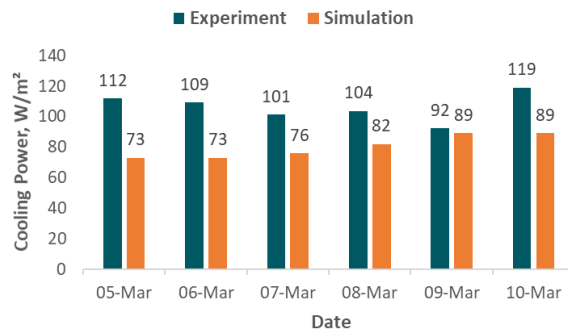
Figure 4-10: Average specific cooling power
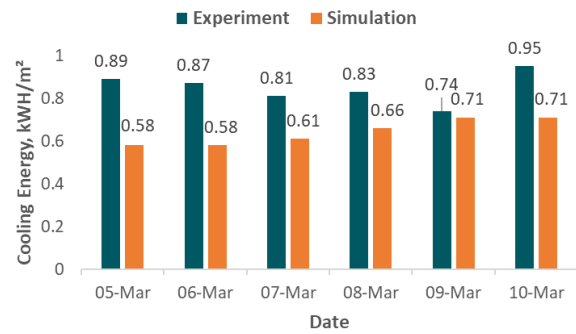
Figure 4-11: Energy released towards the atmosphere

4.2.3 Results

Table 4-3 shows the thermal performance of the office room in terms of operative temperature in the three simulated locations, as percentage in which the operative temperature was within the range of the corresponding category. It can be observed that Athens had the best thermal performance out of the three examined locations, but it was still not good enough for satisfying the requirements for category III of standard DS 15251. This means that the combination of PCM quantity used and the fixed ventilation flow rate was not adequate to maintain the desired thermal environment. Copenhagen had the worse thermal environment due to the position of the sun; in higher latitudes the sun was in a more horizontal position, resulting in higher solar heat gains compared to locations closer to the equator.

Table 4-3: Percentages of Occupancy Period in Categories of Standard EN 15251

	Category I (23.5 – 25.5°C)	Category II (23 – 26°C)	Category III (22 – 27°C)
CPH	27%	40%	63%
MIL	30%	44%	81%
ATH	26%	53%	82%

Figure 4-12 shows the percentage of cooling energy provided by nocturnal radiative cooling and the AWHP. The heat exchange of the solar collectors is a combination of radiation towards the sky and convection between the air and the surface of the collectors. Radiation towards the sky resulted in heat losses in all three cities. The air temperature was lower than the collectors' surface temperature only in Copenhagen resulting in heat loss in Copenhagen and heat gain in Milan and Athens. That resulted

in the limited performance of the nocturnal radiative cooling in Milan and almost negligible performance in Athens.
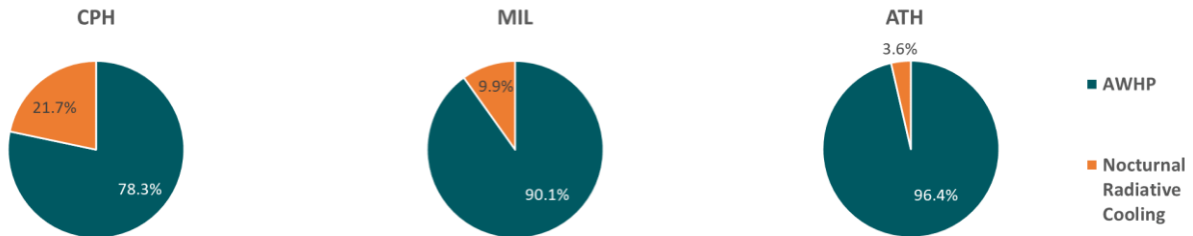
Figure 4-12: Percentage of cooling energy provided by nocturnal radiative cooling and the air-to-water heat pump (AWHP) in Copenhagen, Denmark (CPH), Milano, Italy (MIL) and Athens, Greece (ATH)

Table 4-4 shows the results from the simulation in which the starting time of the operation of Pump 3 (circulating water to the PCM ceiling panels) was examined. The earlier Pump 3 was starting to operate, the higher the percentage of time for all three categories, as it was expected. The later the operation started, the lower the energy use of the pumps was. The impact of the starting time of Pump 3 is significantly higher for the energy use of pumps and AWHP compared to the starting time setpoint of the AWHP itself. The reason why this is happening is that if Pump 3 is activated earlier than the AWHP, the temperature in the middle of the CWT will increase and then the AWHP will be required to operate for more time once it gets activated. On the other hand, if the AWHP is activated prior to Pump 3, the temperature in the middle of the CWT will not increase until Pump 3 is activated, and the AWHP will only need to operate if nocturnal radiative cooling is not enough for cooling down the water in the CWT.

Table 4-4: Results from the simulations examining the starting time of pump circulating water to the PCM ceiling panels

Pump starting time, hh:mm	Percentage of occupancy time in Category I, %	Percentage of occupancy time in Category II, %	Percentage of occupancy time in Category III, %	Pumps energy use, kWh	AWHP energy use, kWh
03:00	33.9	50.4	70.4	51.7	98.7
04:00	32.4	47.7	68.5	49.7	88.1
05:00	30.4	44.9	65.9	47.5	72.3
06:00	28.2	41.9	62.3	44.9	52.0
07:00	26.7	39.6	59.9	42.7	32.1

Figure 4-13 shows the correlation between the percentage of time outside Category III of EN 15251 and the energy use of the AWHP and Pump 3. There is a clear trend for all the examined setpoint values; the lower the percentage of occupancy period outside the range of Category III the higher the energy use.
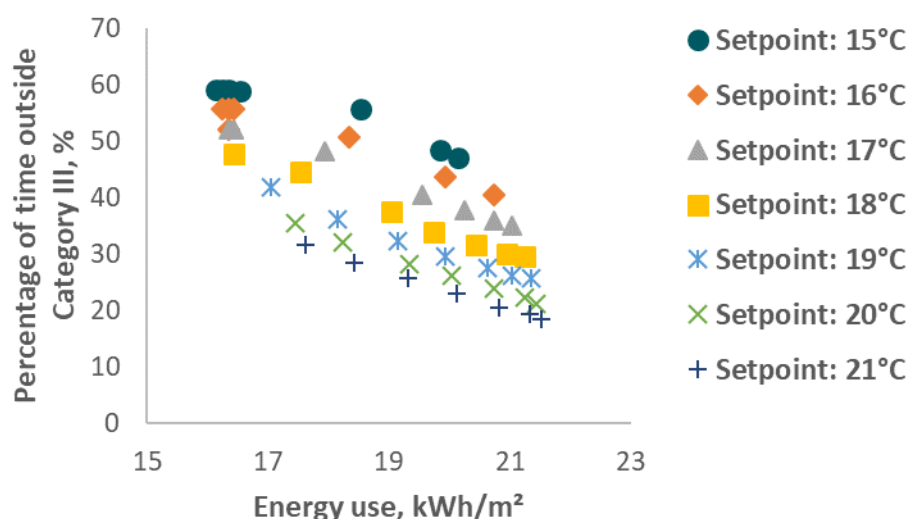
Figure 4-13: Percentage of time outside Category III of Standard EN 15251 (23-26°C) vs energy use for air-to-water heat pump (AWHP) and the pump circulating water in the PCM ceiling panels

The operation of the pump circulating water to the two tanks was examined in terms of activation sensitivity, namely how many times it was activated/deactivated on average during a day, depending on the ΔT between the PVT panels and the tanks. Table 4-5 shows the average number of times Pump 2 was activated and deactivated per day. The higher the ΔT between the water temperature exiting the solar panels and the middle of the storage tanks, the lower the number the pumps is activated or deactivated during a day. Therefore, the higher the ΔT the smoother the operation of the pump was.

Table 4-5: Activation sensitivity of the pump circulating water to the two tanks. The higher the ΔT, the lower the frequency of activation/deactivation of the pump

Panels – Tanks ΔT, K	1	2	3	4	5
Activation/deactivation times per day	16	12	8	6	4

4.2.4 Main findings and conclusions

1. The developed model simulating the chamber with the PCM ceiling panels proved to be satisfactorily accurate, while the solar loop containing the PVT panels needs to be further investigated and improved. The model should be compared with an experiment conducted during summer time for a more complete and accurate validation.

2. Nighttime ventilation can be exploited for discharging the PCM passively in areas with Nordic climate but is insufficient for Mediterranean climate conditions.

3. The PCM ceiling panels provided better thermal conditions in Athens and Milan than Copenhagen due to the position of the sun during daytime.

4. Nocturnal radiative cooling covered a higher percentage of the cooling demand at higher latitudes (e.g. Copenhagen or Oslo) despite the lower percentage of clear sky. because of the convective cooling due to lower outside night-temperatures

5. The performance of the installations could be improved by implementing a solar shading system on the window and an improved control strategy, with different values for the setpoint and the time for activating the pumps.

6. All the examined parameters had inverse results in terms of energy use and indoor thermal environment, namely the better the indoor thermal environment provided, the higher the energy use of circulation pumps and the heat pump. The only exception was the ΔT between the water temperature exiting the solar panels and the temperature in the middle of the storage tanks. For this ΔT, the highest examined value 5K performed the best by having the most stable operation.

7. When an output of a condition is based on a temperature difference, the set-point value should be carefully decided to avoid continuous activation/deactivation of the circulation pump or the heat pump, that could possibly damage it.

5   Parametric and statistical analysis of office ceiling panels containing PCM

This chapter summarises the findings from a simulation study conducted to develop a simplified method for estimating the performance of ceiling panels containing PCM for office buildings. These findings address the fourth objective of the PhD dissertation and has been based on Paper 4. Details can be found in this publication.

5.1   Development of a simplified method for designing office buildings with a PCM-enhanced suspended ceiling

Findings of this study have been submitted for publication in the Science and Technology for the Built Environment:

Eilersen E.C.R., Krintel C.H., Bourdakis E., Kazanci O.B., Olesen B.W. (2018). Development of a simplified method for designing office buildings with a PCM-enhanced suspended ceiling. Submitted at Science and Technology for the Built Environment

The biggest obstacles for the wide use of PCM in buildings are the many design parameters that must be considered and the lack of simplified and broadly accessible tools that can reliably predict the performance of a building with embedded PCM. Among the parameters that affect the performance of PCMs are the latent enthalpy, the melting point temperature, the phase change temperature range, the effective heat capacity curves, the thermal conductivity, the amount of PCM contained in the building structure, the thickness of the PCM layer, the climatic conditions, the level of internal heat gains and the heat transfer coefficient on the PCM panel surface. It is important to develop simplified design methods that incorporate the most critical parameters that affect the performance of PCM panels. Such a method would provide building designers with a fast but reliable tool to estimate whether the incorporation of PCM in their project would be beneficial.

5.1.1   Model description

In this parametric study, an office building section with a South-North orientation was simulated. The floor area of each office was 21 m² and the suspended ceiling height was 2.8 m. Above each office there was a plenum with a height of 0.5 m from which

air was supplied to the room. The PCM was in the ceiling panels separating the office from the plenum.

Two PCM quantities were simulated, one in which the whole ceiling area contained PCM and one where only half of the ceiling contained PCM. The two offices were separated by a 1.5 m wide corridor. Each office had a window, for which two window sizes were simulated, 5.25 m² and 7.88 m², corresponding to Equivalent Glazing Area (EGA) of 0.059 and 0.092, respectively. The windows were triple-glazed with a U-value of 0.5 W/m²K and a SHGC of 0.33. The exterior wall was a light-weight construction so that the PCM provided the main thermal mass of the construction, with a U-value of 0.11 W/m²K. The internal walls were considered as partition walls, having a low thermal capacity and a U-value of 0.57 W/m²K. The floor slabs consisted of concrete with a thickness of 240 mm. The floor construction was kept simple because it was considered that it would not affect the performance of the PCM ceiling panels. Each office had two occupants at sedentary activity level (1.2 Met). Two different heat gains from office equipment were simulated, 150 W (7.1 W/m²) and 300 W (14.2 W/m²) per office. All internal heat sources were activated during the occupancy period (08:00 to 16:00). Five locations whose climatic conditions differ substantially were simulated:

- Buenos Aires in Argentina (AR), with a humid subtropical climate
- Dori in Burkina Faso (BF), with a warm dessert climate
- Copenhagen in Denmark (DK), with an oceanic climate
- Madrid in Spain (ES), with an inland Mediterranean climate
- Santa Maria in California, USA (US), with a cool Mediterranean climate.

The thermal comfort range was calculated based on the adaptive method described in Standard EN 15251 [7]. The adaptive method is normally used in buildings in which passive means are adequate for maintaining the room temperature below the upper limit. Here it was used throughout, due to the significantly different weather files used in the present study. During the cooling season, the PCM should be discharged during the night to have its full latent capacity available to absorb heat the next day. On the other hand, during the heating season, the stored heat should be kept inside the building, to minimise energy use for heating. For discharging the PCM during the cooling period, nighttime ventilation was used. The ventilation was a constant air volume system (CAV) and three different airflow rates were examined, 14.7 L/s, 28.7

L/s and 60 L/s. The discharging period was outside the occupancy period, namely from 16:00 to 08:00.

5.1.2 Validation of PCM TRNSYS component

To increase the validity of the simulation model, it was compared with the benchmarking method known as Microbat, and developed by Kuznik and Virgone (2009). The Microbat test compared the thermal performance of two cubic cells; one with PCM and one without (NoPCM). Kuznik and Virgone placed the two cells in a climate chamber where they could adjust the room air temperature, and compared the cells under three scenarios: a step temperature increase from 15°C to 30°C, a step temperature decrease from 30°C to 15°C and a sinusoidal variation between 15°C and 30°C with a period of 24 hours. The NoPCM cell had a front wall of 2 mm aluminium, while the other walls were of 2 mm of aluminium, 60 mm of polyurethane insulation and 5 mm of cardboard, from outside to inside. In the PCM cell, the cardboard was replaced with a 5 mm PCM-wallboard which contained micro-encapsulated paraffin (60% by weight). For the present study, a similar TRNSYS model was created to simulate the same conditions. Figure 2 shows the air temperature inside the cells during the simulations in comparison with the corresponding cases from the Microbat experiment for the heating case, while the other cases can be found in Annex D. There was only a small discrepancy in the heating simulations for the PCM model: the root mean square errors (RMSE) were in the range 0.28 – 0.29. it was considered that the inaccuracies were caused because the software cannot simulate how the PCM behaves inside the micro-encapsulation. Nevertheless, the PCM component was considered accurate enough to be further investigated.
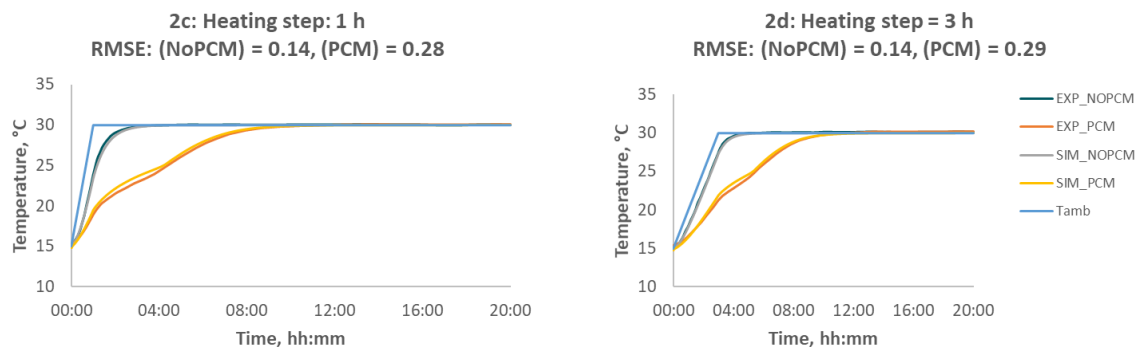
Figure 5-1: Comparison of the experimental and simulation results of the heating case of the Microbat test

5.1.3 Results

In this study, 2240 simulations with PCM and 20 reference cases without PCM were conducted using TRNSYS, in which 14 different types of PCM were simulated. PCMs differentiated in terms of phase change temperature range, melting point, solidifying point, hysteresis and latent heat.

Table 5-1 shows the total electrical energy in kWh/m² and for each office separately the energy use in kWh/m², the percentage of energy savings (ENS) and the utilisation ratio (UR) for the cases with the highest energy saving for each location (LOC), EGA and heat gains (HG) level simulated. The energy savings were calculated as the relative difference in energy use between the PCM simulation and the corresponding reference case.

Table 5-1: Cases where the highest energy savings were observed for each location, heat gains and window to floor ratio level simulated

Load case			PCM properties		Full PCM ceiling				Half PCM ceiling				Reference
HG level	EGA	LOC	PCM type	λ	Etot	ENS	UR S	UR N	Etot	ENS	UR S	UR N	Etot
-	%	-	-	W/mK	kWh/m²	%	%	%	kWh/m²	%	%	%	kWh/m²
L	0.059	AR	PCM_013	0.2	28.7	17.3	4.8	9.2	30.5	12.1	5.6	10.9	34.7
H			PCM_012	0.4	33.9	20.0	12.3	15.7	36.4	14.2	14.2	18.5	42.4
L	0.092		PCM_012	0.4	34.6	18.0	10.3	16.5	37.7	10.7	12.7	20.4	42.2
H			PCM_012	0.2	40.6	20.2	13.3	19.7	44.0	13.6	15.5	23.0	50.9
L	0.059	BF	PCM_008	0.4	68.2	25.6	11.1	8.9	76.9	16.1	12.3	9.9	91.7
H			PCM_013	0.4	86.8	24.0	21.3	12.1	97.3	14.8	24.1	14.9	114.2
L	0.092		PCM_013	0.4	89.9	25.0	22.7	11.3	101.5	15.3	25.5	13.9	119.9
H			PCM_013	0.4	110.7	23.3	23.9	12.7	124.0	14.1	26.4	15.5	144.4
L	0.059	DK	PCM_012	0.4	35.9	16.5	10.0	5.3	37.9	11.9	12.0	6.1	43.0
H			PCM_012	0.4	28.3	22.9	12.7	7.3	32.3	12.0	15.2	9.1	36.7
L	0.092		PCM_012	0.4	41.4	18.2	13.5	5.9	46.4	8.3	16.4	7.5	50.6
H			PCM_012	0.4	36.5	18.3	16.4	8.6	41.7	6.7	19.0	10.5	44.7
L	0.059	ES	PCM_012	0.2	27.4	16.7	16.5	8.3	29.2	11.2	19.7	9.8	32.9
H			PCM_012	0.4	29.6	22.7	19.6	10.7	32.6	14.9	23.6	12.8	38.3
L	0.092		PCM_012	0.2	32.5	23.2	20.9	9.0	36.1	14.7	24.8	11.5	42.3
H			PCM_012	0.4	36.5	25.5	24.2	11.8	42.2	13.9	28.4	14.5	49.0
L	0.059	US	PCM_012	0.2	22.6	15.0	17.2	8.3	24.4	8.3	20.7	10.1	26.6
H			PCM_012	0.2	24.4	14.7	19.5	11.1	26.0	9.1	23.4	13.8	28.6
L	0.092		PCM_012	0.4	26.3	22.6	23.5	10.0	29.3	13.8	28.0	12.2	34.0
H			PCM_012	0.2	28.1	24.7	25.0	12.9	31.2	16.4	29.5	15.7	37.3

As expected, the highest energy savings were observed when the PCM covered the whole ceiling. The energy saving for a full PCM ceiling ranged from 14.5% in Santa Maria to 25.7% in Madrid, while it ranged from 6.8% in Copenhagen to 16.5% in Santa Maria when half the ceiling contained PCM. For all cases, the optimal panel thickness was 20 mm. The PCM that provided the highest energy saving in Copenhagen, Madrid, Santa Maria and in most cases in Buenos Aires was PCM_012, while the most beneficial for Dori was PCM_013. Both PCM types have a high latent heat of fusion (80 kJ/kg). For Buenos Aires and Dori, the PCM with the highest melting temperature was the ideal option, because of the high mean outdoor temperature in these locations.

A linear model was formulated to calculate the energy saving for each location. Due to the differences in the distribution, for some locations it was necessary to transform the dependent variable (ENS) to bring the distribution closer to normal and improve homoscedasticity and the linear relationship assumed in the linear models. DK, ES and US are described by Equation (5-1), while AR and BF are described by Equations (5-2) and (5-3), respectively. The thermal conductivity was not included in these equations because its effect was found to be insignificant for the simulated panel thicknesses.

$$ENS \sim HG + EGA + PCM\ area + d + PCM \qquad \text{(5-1)}$$

$$log_{10}(ENS) \sim HG + EGA + PCM\ area + d + PCM \qquad \text{(5-2)}$$

$$1/ENS^{0.5} \sim HG + EGA + PCM\ area + d + PCM \qquad \text{(5-3)}$$

Table 5-2 shows the regression coefficients for the linear models and the corresponding significance level for each parameter and location examined. As an example, for DK, using a HG level of 16.8 W/m², an EGA of 0.059, a full PCM ceiling, a thickness of 20 mm and PCM of the 002 type, the statistical model calculated a potential energy saving of 9%. Simulations with the same parameters gave an energy saving of 7.6-8.1% depending on the thermal conductivity value used. For the ceiling coverage the values 0.5 and 1 should be used, corresponding to half and full ceiling

coverage with PCM, respectively. Regarding the panel thickness, the values should be written in meters, and in the previous example the panel thickness should be written as 0.020 m.

Table 5-2: Regression coefficient for the linear model

	AR		BF		DK		ES		US	
HG, m²/W	1.22E-02	***	2.77E-03	***	-5.34E-02		1.15E-01	***	-4.73E-01	***
EGA	-3.17E+00	***	1.25E+00	***	-7.94E+01	·	-3.97E-01	***	6.92E+01	***
PCM area	3.22E-01	***	-1.41E-01	***	3.47E+00	***	6.67E+00	***	7.13E+00	***
PCM d, 1/m	9.98E+00	***	-5.36E+00	***	1.11E+02	***	2.44E+02	***	2.04E+02	***
PCM_001	2.73E-01	***	5.87E-01	***	-5.51E+00	***	-8.22E+00	***	-6.78E+00	***
PCM_002	4.61E-01	***	5.57E-01	***	8.79E+00	***	6.70E-01	***	7.92E+00	***
PCM_003	5.77E-01	***	3.46E-01	***	4.42E+00	***	-6.91E+00	*	1.20E-01	***
PCM_004	3.28E-01	***	5.86E-01		-1.91E+00	***	-5.79E+00	***	-3.16E+00	***
PCM_005	3.37E-01	***	5.85E-01		3.31E+00	***	-5.81E+00	***	-5.08E+00	·
PCM_006	6.03E-01	***	4.85E-01	***	6.79E+00	***	2.38E+00	***	-4.80E-01	***
PCM_007	5.45E-01	***	4.93E-01	***	2.25E+00	***	-2.28E+00	***	-5.02E+00	·
PCM_008	3.94E-01	***	2.98E-01	***	1.39E+00	***	-9.81E+00	***	-1.19E+01	***
PCM_009	4.11E-01	***	5.69E-01	***	7.49E+00	***	-1.88E+00	***	6.92E+00	***
PCM_010	5.50E-01	***	3.90E-01	***	4.99E+00	***	-4.92E+00	***	2.19E+00	***
PCM_011	2.83E-01		5.95E-01	·	-8.51E+00	***	-6.78E+00	***	-4.48E+00	*
PCM_012	6.91E-01	***	5.27E-01	***	1.43E+01	***	6.38E+00	***	7.92E+00	***
PCM_013	6.69E-01	***	2.89E-01	***	7.37E+01	***	-7.73E+00		-1.25E+01	***
PCM_014	3.06E-01	*	5.93E-01		-2.69E+00	***	-4.29E+00	***	1.30E-01	***

Significance legend: '***' 0.001 '**' 0.01 '*' 0.05 '·' 0.1 ' ' 1

5.1.4 Main findings and conclusions

1. Implementing PCM in an office building can potentially reduce energy use by 14.5 – 25.6%, depending on the climatic conditions and the load. On the other hand, an incorrect choice of PCM could result in an increased energy use of up to 6%.

2. The utilisation ratio of the PCMs was strongly dependent on the season, with a utilisation ratio of 60-80% in winter and 20-50% in summer.

3. The best performance in terms of energy saving and the PCM utilisation ratio were both observed in the cities with the largest diurnal temperature range (Dori and Santa Maria.

4. From the statistical analysis, an equation was derived to predict the energy saving that would be achieved for each PCM type and location and this provided satisfactorily accurate results. It could therefore be used for estimating potential energy saving for the simulated locations and PCM types.

6 Investigation of the design of a new radiant ceiling panel containing PCM

This chapter summarises the findings from the studies carried to investigate the performance of a new radiant ceiling panel containing PCM numerically and comparing the performance of radiant ceiling panels with PCM tiles experimentally. These findings address the fifth objective of the PhD dissertation. The experiment reported in Chapter 6.1 is ongoing and has not been included in a publication yet. Chapter 6.2 is based on Paper 3. Detailed information in the numerical model and further results can be found in this publication.

6.1 Experimental comparison of conventional radiant ceiling panels with active ceiling panels containing phase change material

Both radiant and PCM ceiling panels are well documented in the literature. Nevertheless, no study was found that made a direct comparison between the two technologies.

6.1.1 Method

The same climate chamber described in Chapter 4.1.1 was used for that experiment as well. As mentioned in Chapter 4.1.1, since the chamber was not exposed to direct sunlight, an electrical heating wall panel was used to simulate the solar load of a window located in the south wall of an office located in Copenhagen. The control system responsible for the output of the heating panel could only be set in multiples of 25 W, therefore the schedule was adjusted as shown in Figure 6-1. A second solar heat gains schedule was used for each type of panel examined, which was 25 W lower in each step compared to the first schedule.
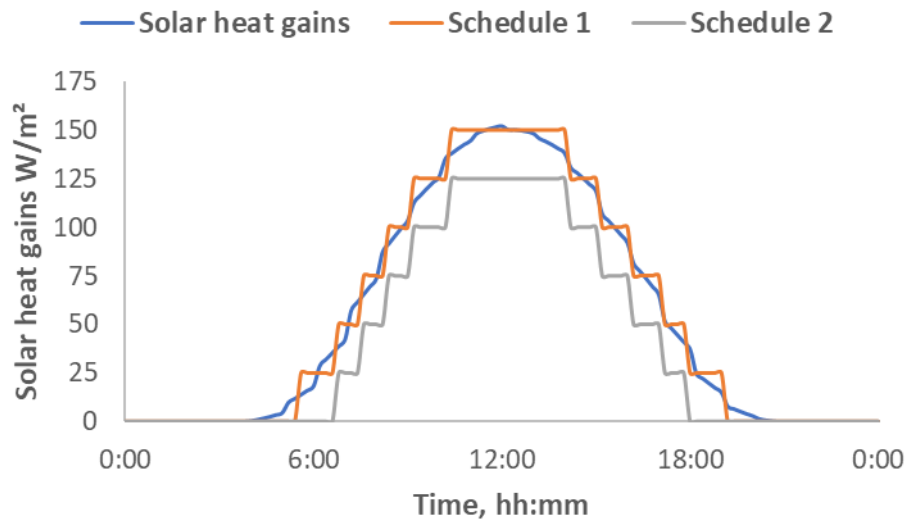
Figure 6-1: Solar heat gains schedule

The internal heat gains from the two occupants, the corresponding office equipment, the ceiling lights and a data logger required for the experiment were 386 W (17 W/m²). A temperature stand tree was located behind each "occupant," with an operative temperature sensor installed at 0.6 m above the floor, and four air temperature sensors installed at 0.1, 0.6, 1.1, and 1.7 m above the floor. Those heights correspond to the ankle, abdomen, and neck of a seated person and the neck of a standing person, respectively, as recommended by Standard ISO 7726 (ISO 2001). The accuracy of these sensors was ±0.2°C. At 2.5 m above the floor, the radiant panels were installed as a suspended ceiling. Both types of radiant panels examined had the same dimensions, namely 0.595 m x 0.595 m which are the most common dimensions for ceiling panels in Europe. Forty-eight panels were installed in each case, covering 75% of the total suspended ceiling area. To evaluate the performance of the two ceiling panels, 12 heat flux sensors and 16 surface temperature sensors were installed in different panels, as shown in Figure 6-2. The accuracy of the heat flux sensors was ±2.5% while the surface temperature sensors had an accuracy of ±0.2°C. All sensors were calibrated prior to the experiment start.
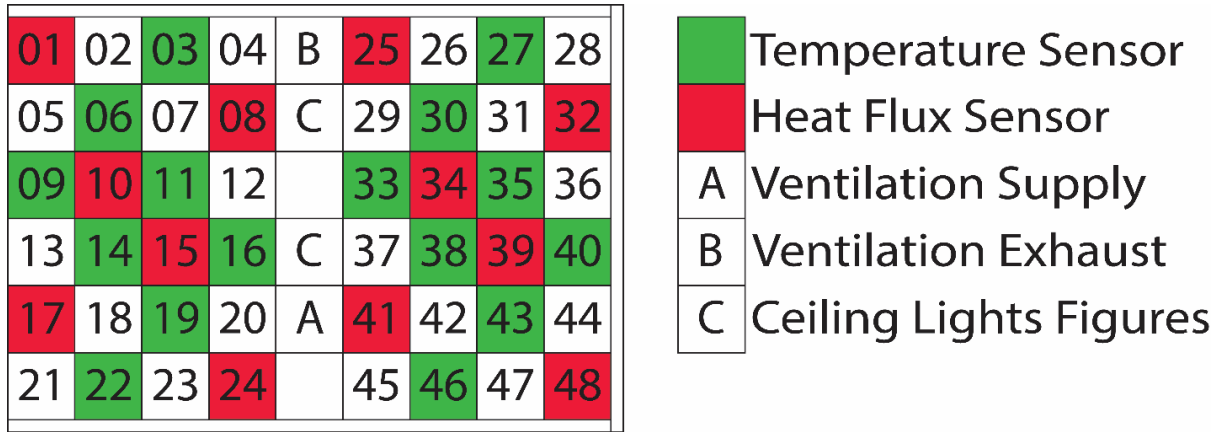
Figure 6-2: Ceiling map with temperature and heat flux sensors locations

The radiant ceiling panels (RCPs) had a lower surface made of 2 mm thick steel. Copper pipes were attached on the back side of the steel surface. For more uniform temperature distribution on the panel surface, an aluminum heat-conducting profile was embracing the pipes. The pipe distance was 150 mm, the outer diameter of the pipe was 10 mm and the pipe thickness 1 mm.

Each PCM tile contained 550 g (12.5% w/w) of organic microencapsulated PCM with an enthalpy of 96kJ/kg. The phase temperature range of the PCM was 19 – 23°C and the total heat capacity 123 Wh/m² at peak melting temperature of 23°C. For discharging the PCM tiles actively, the coper pipes of the RCPs were used, but the steel sheets were removed, and the aluminum heat-conducting profile was attached to the PCM tiles upper surface using thermal paste. Figure 6-3 shows the construction of the tested panels with their dimensions.
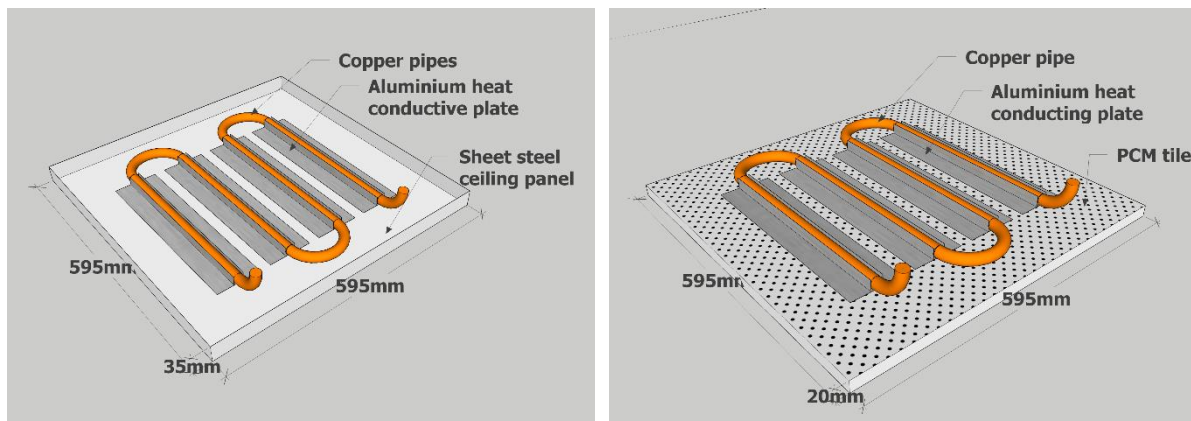
Figure 6-3: Construction of the tested panels with dimensions, RCP in the left and PCM tiles in the right

The water circulation was activated during the occupancy period (08:00 – 18:00) for the RCPs while for the cases with the PCM tiles they were activated when the office was not occupied (18:00 – 08:00). In all cases the water supply temperature was 19°C. Since no latent heat sources were used in the experiment, and to have less contingencies, it was decided to deactivate the ventilation system during the whole experiment. Table 6-1 shows the changes between the three experimental cases examined.

Table 6-1: Experimental cases examined for each panel type

	Water flow rate, kg/h	Solar heat gains profile
Case 1	140	Schedule 1
Case 2	220	Schedule 1
Case 3	140	Schedule 2

6.1.2 Results

Figure 6-4 shows the operative temperature and the water flow rate for the two cases testing the radiant ceiling panels. The shaded boxes show the occupancy period. The temperature difference between the two cases during the occupancy period varied between 0.6°C and 1.7°C. The lowest temperature different was observed at the beginning of the occupancy period while the highest one around 09:30 when the water circulation was activated. In the case with the low solar heat gains the water circulation was activated approximately 1.5 hour later. The highest operative temperature for the high SHG case was 24.1°C while for the low SHG case was 22.8°C.
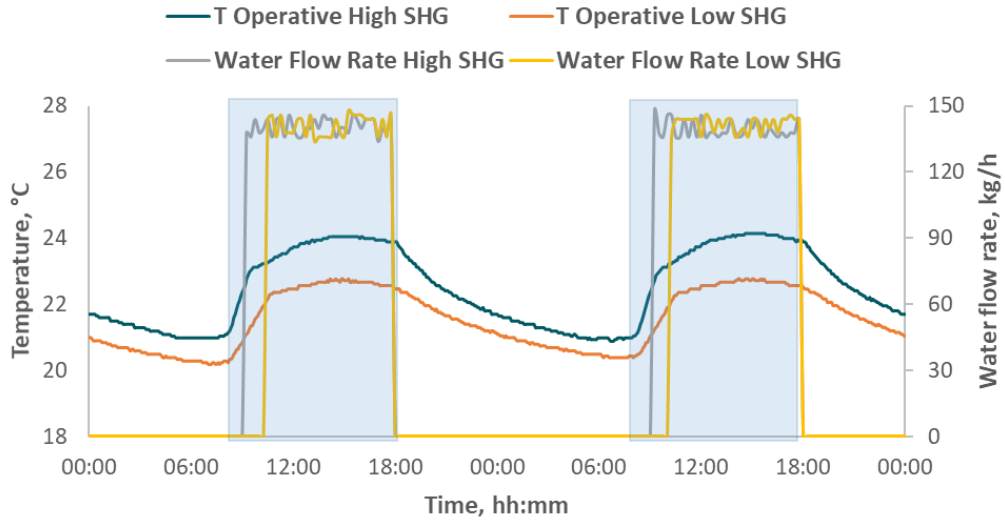
Figure 6-4: Operative temperature for the cases with high and low Solar Heat Gains (SHG) for the radiant ceiling panels. The shaded areas show the occupancy period

Figure 6-5 shows the operative and air temperature measured at different heights inside the chamber. A clear stratification can be observed during the occupancy period, which can be explained by the absence of an operating ventilation system. The higher the sensor was placed, the higher the temperature was measured. On the other hand, outside the occupancy period, the temperature measured by all sensors coincided. Similar stratification was observed in all experimental cases, both with the RCPs and the PCM Tiles. Due to the absence of air motion (no ventilation system was operating), the operative temperature was identical with the air temperature measured at the same height.
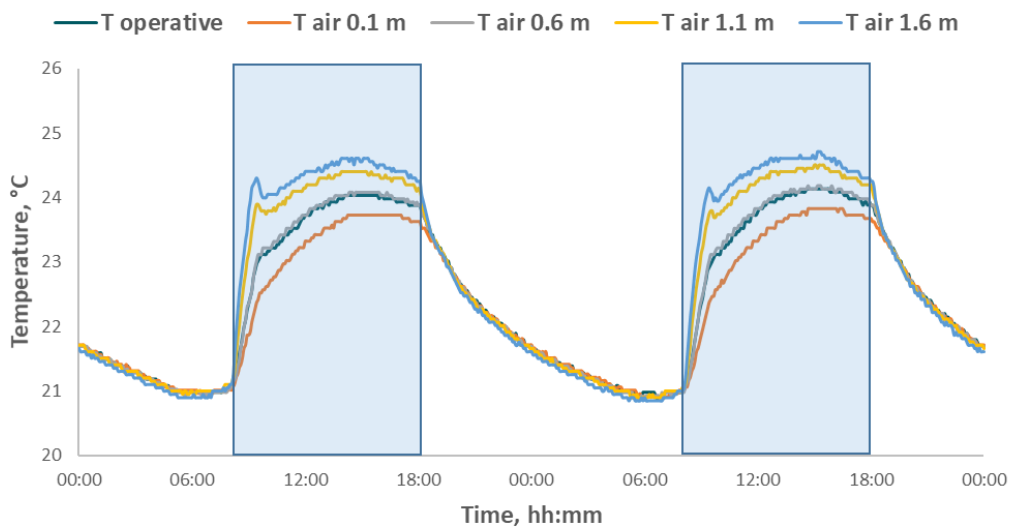
Figure 6-5: Temperature stratification for Case 1 with RCPs. The shaded areas show the occupancy period

Figure 6-6 and Figure 6-7 show the average temperature on the radiant ceiling panels surface during the occupancy period per surface temperature sensor for Case 1 (high solar heat gains) and Case 2 (low solar heat gains), respectively. Both figures also show the first (inlet) and last (outlet) panels for each water circulation loop. In both cases the highest average surface temperature was observed in the panels above the internal heat gains, in the middle of the room. Panel surface temperature is also affected by the position of the panel in relation to the water circulation loop. For example, in the bottom of Figure 6-6, although the two panels have a similar distance from both the solar and the internal heat gain sources, the surface temperature of the inlet panel is 1.1°C lower than the outlet panel. In Figure 6-7, the average surface temperature of each panel was lower by 0.1°C to 0.7°C compared to the average surface temperature of the corresponding panels shown in Figure 6-6, due to the lower solar heat gains.

Inlet		Outlet 22.2°C			Outlet		Inlet 20.9°C	
	21.2°C					21.7°C		
21.1°C		22.3°C			22.7°C		21.4°C	
	21.2°C		22.6°C			22.6°C		21.3°C
	21.9°C						21.5°C	
	Inlet 21.1°C		Outlet			Outlet 22.2°C		Inlet

Figure 6-6: Plan view of the ceiling panels showing the average surface temperature for Case 1, for each panel with a surface temperature sensor attached

Inlet		Outlet 21.5°C			Outlet		Inlet 20.7°C		
	21.0°C					21.4°C			
20.9°C		21.8°C			22.4°C		21.2°C		
	20.9°C		22.0°C			22.2°C		21.1°C	
	21.4°C						21.2°C		
	Inlet 20.9°C		Outlet			Outlet 21.7°C		Inlet	

Figure 6-7: Plan view of the ceiling panels showing the average surface temperature for Case 2, for each panel with a surface temperature sensor attached

Figure 6-8 shows an overview of the average heat flux during the occupancy period on the ceiling panels. The underlined values are those measured with a heat flux sensor while the rest were calculated using Equation (6-1) taken from ISO Standard 11855-2 (ISO 2012).

$$Q_{surface} = 8.92 \cdot (T_{operative} - T_{surface})^{1.1} \qquad \text{(6-1)}$$

The highest heat flux was measured on the outer panels, namely those being away from the heat gain sources, and especially those that were the first panel in the circulation loops, and therefore the circulated water had a lower temperature. On the other hand, the lower heat flux values were measured above and close to the heat gain sources. Both observation can be explained by Equation (6-1). The panels above and close to the internal heat gain sources had a higher surface temperature compared to the panels close to the chamber walls, thus the temperature difference

57

$T_{operative} - T_{surface}$ in those panels was lower. For the same reason, the heat flux values measured with the low solar heat gains were insignificant.

Inlet 17.5 W/m²		Outlet 12.9 W/m²			**Outlet 18.5 W/m²**	Inlet 27.0 W/m²	
	22.5 W/m²		**10.8 W/m²**		17.7 W/m²		**20.4 W/m²**
24.3 W/m²	**17.1 W/m²**	12.3 W/m²			8.4 W/m²	**18.0 W/m²**	21.5 W/m²
	23.8 W/m²	**21.3 W/m²**	9.7 W/m²		8.8 W/m²	**16.0 W/m²**	22.1 W/m²
19.5 W/m²		16.1 W/m²			**19.3 W/m²**	20.4 W/m²	
	Inlet 24.3 W/m²		**Outlet 17.2 W/m²**			Outlet 12.1 W/m²	**Inlet 25.3 W/m²**

Figure 6-8: Average heat flux in each panel for the case with the high solar heat gains

Figure 6-9 show the operative temperature and water flow rate for the three cases tested with the PCM tiles. Due to the switch to daylight saving time in the controller of the water pump, the water operation was shifted one hour later, namely from 19:00 to 09:00. That is why the activation of the water circulation was delayed and it would continue to operate even after the beginning of the occupancy period (Figure 6-9). The additional thermal mass provided by the PCM tiles was insufficient to maintain an acceptable thermal comfort, as the operative temperature reached 29.4°C with the high water flow rate (Case 2) and even higher values in the other two cases. The operative temperature differed only slightly between Case 1 and Case 3 (low solar heat gains profile). Increasing the water flow rate from 140 kg/h to 220 kg/h had a higher impact on the operative temperature but still proved inadequate to provide an acceptable thermal environment.
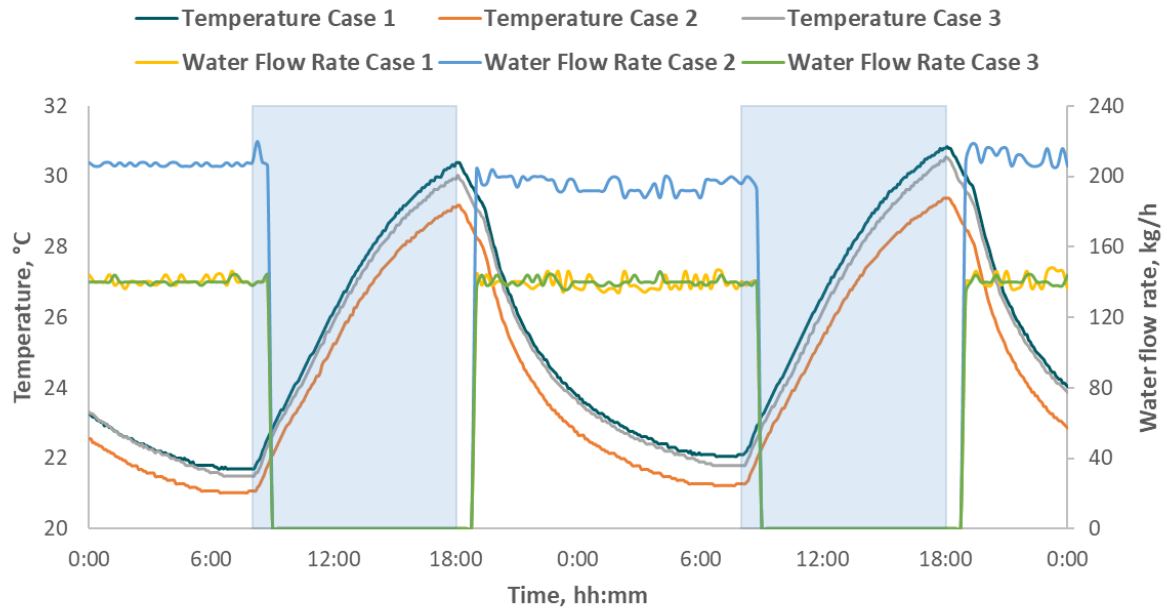
Figure 6-9: Operative temperature and water flow rate for the PCM tiles cases

Figure 6-10 shows the heat flux measured on the surface of the PCM tiles with the heat flux sensors for Case 1. The highest values were measured between 10:00 and 12:00, when the PCM temperature was between 22°C and 24°C, namely when the phase change was taking place. At 19:00, when the water circulation was activated, the heat flux measured was negative, indicating a reverse direction of heat flux. Similar pattern was observed in the other two cases examined, while the range of values was comparable to the one shown in Figure 6-10.
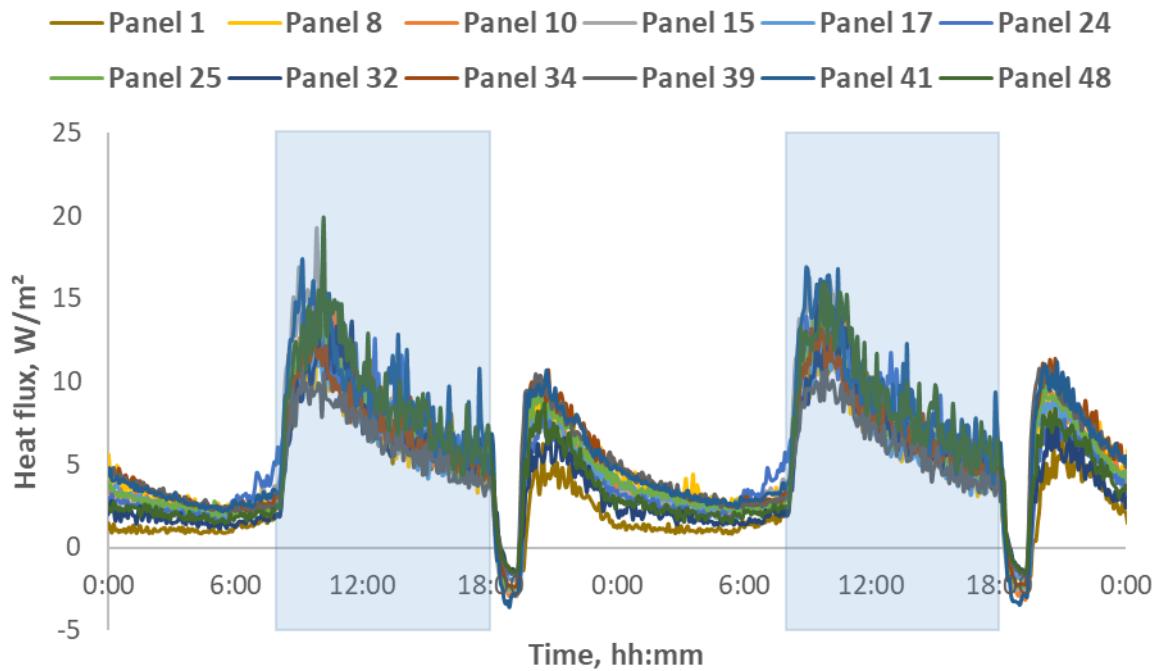
Figure 6-10: Heat flux over time for Case 1 of the PCM tiles

Figure 6-11 shows the average heat flux in each panel during occupancy period for Case 1 of the PCM tiles. As before, The underlined values are those measured with a heat flux sensor while the rest were calculated using Equation (6-1). Similarly to the case with the RCP panels, the lower heat flux values were measured above or close to the heat sources, while the highest values were measured on the outer panels closer to the chamber walls. By comparing Figure 6-8 with Figure 6-11 it can be observed that the heat flux in the case of the RCP panels were significantly higher. That was caused by the low thermal conductivity of the PCM tiles compared to the RCP panels and the high temperature on the panels surface, which was close to the room operative temperature. The low thermal conductivity of the PCM-plaster mixture was the reason why the PCM was not fully discharged at the end of the water circulation, the next morning. That issue might would be solved either by reducing the water supply temperature or increasing the water flow rate.

Inlet 7.63 W/m²		Outlet 6.54 W/m²			**Outlet 7.94 W/m²**		Inlet 4.93 W/m²	
	3.83 W/m²		**7.15 W/m²**			2.96 W/m²		**7.72 W/m²**
5.83 W/m²	**8.63 W/m²**	3.03 W/m²			1.90 W/m²	**7.50 W/m²**	5.10 W/m²	
	5.40 W/m²	**8.57 W/m²**	3.61 W/m²			1.08 W/m²	**6.52 W/m²**	4.11 W/m²
7.33 W/m²		5.14 W/m²			**9.31 W/m²**		5.41 W/m²	
	Inlet 4.22 W/m²		**Outlet 8.62 W/m²**			Outlet 5.13 W/m²		**Inlet 8.83 W/m²**

Figure 6-11: Average heat flux in each panel for the Case 1 with the PCM tiles

6.1.3 Main findings and conclusions

1. When using the Radiant Ceiling Panels (RCPs), the examined water flow rate was adequate to provide an acceptable thermal environment with the high solar heat gains. However, in the case of the low solar heat gains it resulted in overcooling.

2. The absence of a ventilation system resulted in temperature stratification and unevenly distribution of the heat on the panels surfaces, in both the RCP and PCM cases.

3. The additional thermal mass provided by the PCM proved inadequate to provide an acceptable thermal environment without a supplementary active system operating during the occupancy period (ventilation or activation of the water circulation).

4. The thermal conductivity of the PCM panels was too low to ensure complete discharging of the PCM during the nighttime.

6.2 Simulation study for the design of radiant ceiling panels containing Phase Change Material (PCM)

Findings of this study have been submitted for publication in the Applied Thermal Engineering journal:

Bourdakis E., Gkoufas N.A., & Olesen B.W. (2018). Simulation study for the design of radiant ceiling panels containing phase change material. Submitted at Applied Thermal Engineering

One of the drawbacks identified in the literature in Chapter 2, was the low thermal conductivity of the construction of radiant ceiling panels containing PCM and of the material itself. Due to the chemical complexity of PCMs, prior to developing and testing a new PCM panel, it is important to simulate its thermal and heat transfer performance to identify possible limitations of the design and suggest possible improvements. In that way, numerous cases can be examined and compared at a minimal time.

6.2.1 Model description

The geometry selected for the study was of a typical European square ceiling panel with side dimensions of 595 mm, having a total ceiling exposed surface area of 0.35 m². The thickness of the panel was one of the variables in the study and was 25-40 mm. The outer casing was of aluminium sheet, to ensure effective and homogeneous heat transfer to the enclosed PCM, with a thickness of 1 mm. For discharging the PCM, copper pipes were embedded, with an external diameter of 10 mm and pipe thickness of 1 mm. The distance between the pipes was chosen as 150 mm, so that there was uniform distribution throughout the panel. The properties of a commercially available PCM were used in the current study. Table 6-2 shows the thermophysical properties of the materials of the panel, which were implemented in the simulation model. The melting point temperature of the PCM was 24°C with a ΔT of 3 K and the latent heat capacity was 201 kJ/kg.

Table 6-2: Thermophysical properties of the simulated panel materials

	Cp, J/kg·K	K, W/m·K	ρ, kg/m^3
Solid PCM	1840	0.25	910
Liquid PCM	1990	0.25	810
Aluminium	900	238	2700
Copper	384	401	8960

Three different parameters were examined, to investigate the optimal discharge practice of the PCM:

- the panel height,

- the water supply temperature in the pipes,

- the water flow rate in the pipes.

For each parameter, four realistic values were chosen, and all the possible combinations were simulated, yielding a total of 64 different cases. Table 6-3 shows the set-point values for each examined parameter. The water flow rate values were selected to ensure turbulent flow in the pipes. The duration of the simulation was 12 hours, corresponding to the available time from the end of the occupancy period until the beginning of the occupancy period the next day. The time step was 6 minutes. A detailed description of the COMSOL numerical model can be found in Paper 3 in Annex C.

Table 6-3: Setpoint values for the examined parameters

Panel height, mm	Water flow, kg/h	Water supply temperature, °C
25	240	7
30	280	12
35	320	15
40	360	18

6.2.2 Results

Figure 6-12 shows the state of the PCM as a fraction of melted PCM. PCM phase equal to 1 means that the PCM is fully melted while PCM phase equal to 0 corresponds to fully solidified PCM. Colour variations represent different water supply

temperatures, while the marker variations represent different water flow rates in the embedded pipes. For example, the yellow line with a star marker corresponds to water supply temperature of 15°C and 280 kg/h of water flow rate in the embedded pipes.

In all four cases, the lower the water supply temperature the faster the PCM was discharged. On the other hand, disregarding the panel thickness, the impact of the water flow rate was insignificant, since in all cases the lines of the same colour coincided. When the thickness of the panel was 25 mm the PCM was completely solidified before the end of the discharging period in all cases. With a panel of 30 mm, when the water supply temperature was 18°C it failed to discharge the PCM completely. When the panel thickness was 35 mm only the water supply temperatures of 7°C and 12°C were sufficient to discharge the PCM completely, while with a panel thickness of 40 mm the PCM was completely discharged only when the water supply temperature was 7°C. When the panel thickness was 40 mm and the water supply temperature 18°C, only approximately 50% of the PCM became solidified. Since the impact of the water flow rate is insignificant, the lowest water flow rate from the simulated values would be sufficient for discharging the PCM. Lower water flow rate allows water pumps and chillers to be down-sized, providing lower first cost and running cost. The water flow rate must be high enough to ensure turbulent flow but the velocity must be lower than 1.2 m/s to minimise noise generated by the flow (ISO 2012).
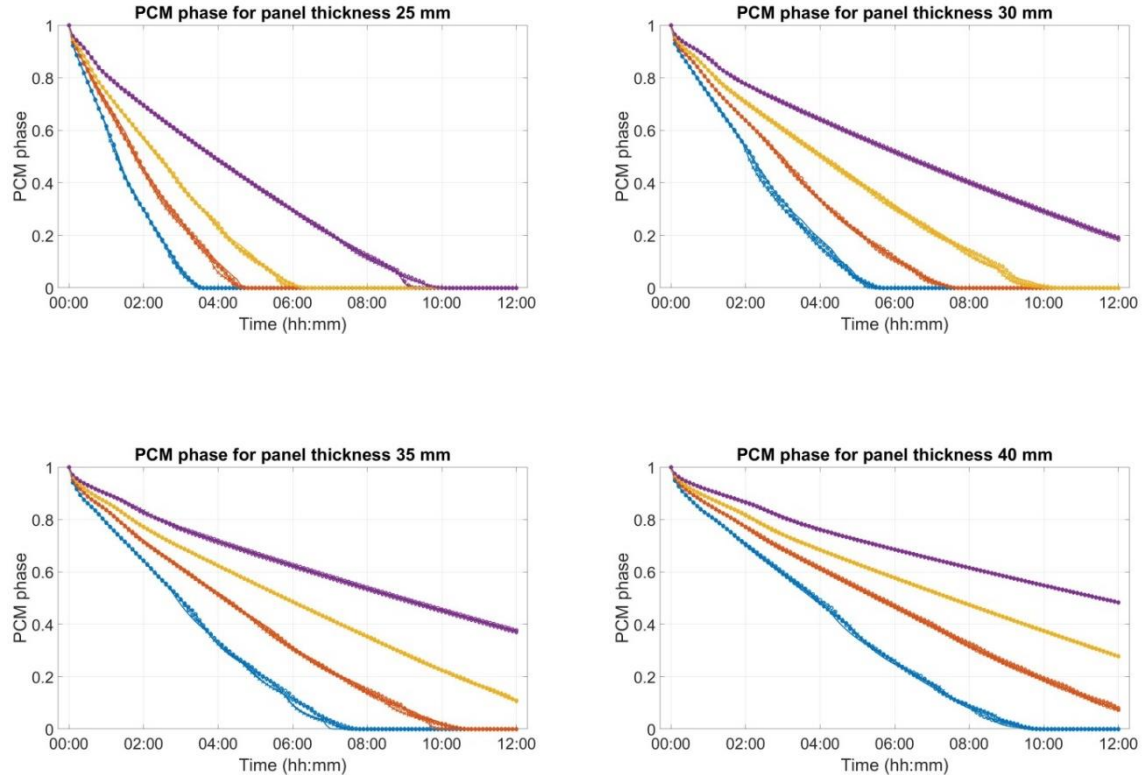
Figure 6-12: PCM phase as a function of the panel thickness

Table 6-4 shows the duration of the discharging process for each combination of water supply temperature and panel thickness. The values are the average of the four simulations with different water flow rate, since the impact of the water flow rate was insignificant. Cells with "–" are the cases where the PCM did not solidify completely. When the water supply temperature was 7°C, for every additional 5 mm of panel thickness the discharging period was increased by approximately two hours. Similarly, the discharging period was longer by approximately three and four hours when the water supply temperature was 12°C and 15°C, respectively. For every combination of water supply temperature and panel thickness, the increase in the discharging duration caused by increasing the water supply temperature was lower than by increasing the panel thickness. This was due to the low thermal conductivity of the PCM, which had a greater impact when increasing the panel thickness, namely the

mass of the PCM. This table can operate as a comparison for future studies examining radiant ceiling panels with PCM with similar properties.

Table 6-4: Discharging duration for each water supply temperature – panel thickness combination

	H=25 mm	H=30 mm	H=35 mm	H=40 mm
T=7°C	3:37	5:39	7:54	10:52
T=12°C	4:49	7:34	10:36	–
T=15°C	6:19	10:19	–	–
T=18°C	9:48	–	–	–

To examine the possibility of condensation on the bottom surface of the panels, Table 6-5 shows the temperature of the lower surface at the point when the PCM had become fully solidified. The underlined cells are the cases where the PCM was not fully discharged before the end of the discharging period. Keeping the panel thickness constant and increasing the water supply temperature, the temperature of the lower surface increased. On the other hand, keeping the water supply temperature constant and increasing the panel thickness, the temperature of the lower surface also decreased, though only slightly. For example, when the water supply temperature was 12°C and the panel thickness was increased from 25 mm to 30 mm, the temperature of the lower surface decreased by 0.2°C. In some cases that drop was insignificant, for example when the water supply temperature was 7°C and the panel thickness increased from 30 mm to 35 mm, the temperature drop was less than 0.1°C. This was not the case when the increase of the panel thickness would result in incomplete solidification of the PCM layer; for example, when the water supply temperature was 12°C and the panel thickness increased from 35 mm to 40 mm, the temperature of the lower surface increased by 0.9°C. This was because the PCM did not solidify homogenously. The temperature was therefore higher during the process, but as soon as the PCM had completely solidified a further decrease in the temperature of the lower panel surface was observed.

Even with the combination of the lowest water supply temperature and the thinnest panel, the surface temperature was high enough to ensure that there would be no risk of condensation. Although there is no risk for condensation on the panel surface, a water supply temperature as low as 7°C or 12°C should be avoided in residential or commercial buildings because there is still a high risk of condensation earlier in the

hydronic loop, e.g. on the manifold. Such low water supply temperatures should be used only in specific industrial applications.

Table 6-5: Panel lower surface temperature when the PCM had been fully discharged

	H=25 mm	H=30 mm	H=35 mm	H=40 mm
T=7°C	19.2	18.8	18.7	18.6
T=12°C	20.8	20.6	20.5	**21.3**
T=15°C	21.6	21.4	**22.0**	**22.7**
T=18°C	22.3	**22.7**	**23.1**	**23.4**

6.2.3 Main findings and conclusions

1. It was found that in the range examined, the water flow rate had no impact on the discharging process of the PCM.

2. The thickness of a panel of this type should not be above 30 mm, as the PCM was not fully discharged on time in thicker panels.

3. Thicker panels would be feasible only if the PCM was combined with graphite foam or other methods of enhancing its thermal conductivity.

4. Water supply temperatures as low as 7°C or 12°C should be avoided in residential and commercial buildings due to the risk of condensation.

5. In the range examined, the ideal combination for a PCM ceiling panel of this type was a panel thickness of 25 mm and a water supply temperature of 15°C.

7 Overall findings and conclusions

7.1 Discussion

To achieve the objectives stemming from the EU targets for 2030 and the Paris agreement we need to vastly reduce the energy use of the construction sector. To do so, all passive means should be utilised efficiently, one of which is nighttime cooling wherever this is possible. That would be possible if lower temperature were acceptable in office buildings at the beginning of the occupancy period, especially in buildings having a radiant cooling system, because in those building the room temperature drifts, rather than remaining constant around a setpoint temperature. In that way, a longer temperature drift would be possible, before the room temperature would exceed the upper limit of the comfort range resulting in overheating. It was shown that people who had elevated metabolic rate than sedentary activity due to walking to work, were accessible to lower temperature than what suggested by the European Standard EN 15251 at the beginning of the occupancy period. That would enable higher utilisation of nighttime cooling by having a lower temperature at the beginning of the occupancy period. Then the operative temperature would increase passively to reach the comfort range due to the presence of solar and internal heat gains, before an active system is activated to maintain the operative temperature within the comfort range. In that way, the active cooling system will be activated for shorter period than the whole occupancy period, resulting in energy savings. However, in most office buildings not all occupants arrive simultaneously, and they do not commute the same way (private car, public transportation, by bicycle or on foot). That means that any suggested starting temperature might not be considered as comfortable by all occupants. In the same study, it was shown that although developed using data from experiments conducted under steady-state, Fanger's thermal comfort model is applicable also in cases with non-steady conditions.

Although the benefits of incorporating PCM in constructions elements are well documented in the literature, the percentage of real life project incorporating PCM is insignificant. Even in those few projects that PCM was installed, the option of passive system was selected, either by impregnation, e.g. concrete-PCM mixture or by installing PCM-plaster panels as a layer inside the walls or the ceiling. For that reason, active PCM panels were tested, combined with PVT panels installed on the roof of the experimental building, to provide the cold water required to discharge the PCM by

exploiting the principle of nocturnal radiative cooling. It was shown that active ceiling panels containing PCM are an efficient method for providing an acceptable thermal environment. PCM panels provided a better thermal environment when a better air mixing was provided in the chamber. Furthermore, it was shown that the nocturnal radiative cooling process can reduce the energy use of the refrigerant equipment substantially and combined with the electricity produced by the PVT during daytime, it can result in a surplus of electricity, if the weather conditions are in favour. The effectiveness of nocturnal radiative cooling in producing cold water depends on several climate parameters (fraction of sky covered by opaque clouds, cloud emittance, dew point temperature, etc.). Therefore, a detailed weather prediction in situ is required to estimate the performance of the PVT panels in advance. If water was circulated in the PCM panels only during nighttime, the cold water tank could be removed, and the cold water from the PVT panels would be circulated directly in the PCM panels. In the tested conditions it was required to circulate water also during daytime, therefore the use of a storage tank was necessary.

Nevertheless, the contingency of the outdoor conditions did not allow the comparison between different setting in the solar loop. For that reason, a simulation model was developed that was validated against experimental data. That model enabled possibility of simulating different locations, setpoints values and discharging techniques. It was found that nocturnal radiative cooling can be beneficial in all locations simulated, although the performance varied significantly among the different locations, covering 4% to 22% of the cooling demand depending on the location. The higher the latitude, the higher the effectiveness of the nocturnal radiative cooling, due to the lower negative impact from convection. On the other hand, the lower the latitude, the better the thermal environment provided by the active ceiling PCM panels. That was due to the position of the sun; in higher latitudes the sun was in a more horizontal position, resulting in higher solar heat gains compared to locations closer to the equator. It should be taken into consideration though, that nocturnal radiative cooling is only a supplementary reason for investing in PVT panels, while the main reason should be of course the production of electricity and hot water. Nocturnal radiative cooling will increase the utilisation factor by enabling the exploitation of the panels also during nighttime and therefore decrease the payback period of the investment. Furthermore, an auxiliary cooling system should be installed as well, to ensure the

production of cold water, when the outdoor conditions are not in favour of exploiting nocturnal radiative cooling.

The literature has shown the complexity of the PCM and the many parameters that needs to be taken into consideration when selecting the appropriate PCM for a specific application. The complexity of the PCM can also explain why they have not penetrated the construction sector at a higher degree. To contribute in solving that issue, a simplification method was developed that can estimate the potential savings by incorporating passive PCM ceiling panels in an office building. It was found that although a correct choice of PCM can result in substantial energy savings, a wrong choice can result in increasing the energy use of the building to maintain the desired thermal environment. Furthermore, a panel thickness of 20 mm resulted in the highest energy savings. Thinner panels did not have adequate thermal mass to maintain the desired temperature resulting in the auxiliary cooling system to operate for longer period. In panels that were thicker than 20 mm, the heat did not penetrate the panel deep enough to take advantage of the additional thermal mass due to the low thermal conductivity of the PCM. Thus, thicker panels did not provide any additional advantage. The limitation of the developed method is that it provides an equation for each location and PCM types simulated. Therefore, it provides an indication of performance of the PCM only in already simulated locations and cannot be safely generalised to include also other locations without before simulating them.

No direct comparison between radiant ceiling panels (RCPs) and ceiling tiles containing PCM was identified during the literature review. For that reason, an experiment was conducted, where the performance of RCPs and PCM tiles was compared in terms of thermal comfort provided and heat flux on the surface of the panels. It was found that the quantity of the PCM was insufficient for ensuring an acceptable thermal environment. On the other hand, the radiant ceiling panels provided an acceptable thermal environment with the high solar heat gains, while the same water flow rate in the case with the low solar heat gains resulted in overcooling. Due to the absence of an operating ventilation system during the occupancy period, a substantial temperature difference was observed between the panels above and close to the internal heat gain sources compared to the panels installed at a greater distance from the heat sources. That resulted in lower heat flux at the panels close to the heat internal heat sources, due to the smaller temperature difference between the operative

temperature and the panel surface. When using the PCM tiles, the water circulation should be activated also during occupancy period, to ensure the operative temperature remains within the comfort range. In that case, the operation of the water circulation should be compared with the corresponding operation of the RCP panels in terms of hours being activated and energy use. Furthermore, the long duration of discharging the PCM tiles showed that the pipes should be inside the PCM layer, due to the low conductivity of the PCM material.

Prior to design a new active ceiling panel containing PCM, an extensive simulation study is required to identify possible limitations of the design and improve them prior to producing it. The parametric simulation study conducted in COMSOL to test the discharging performance of a new active PCM panel showed that the impact of the simulated range of water flow rate values was insignificant, and therefore the lowest water flow rate should be selected to enable the use of smaller cooling equipment and water pumps. That would result in lower investment and operation cost. Furthermore, it was shown that the maximum panels thickness should be 30 mm to ensure full discharging the PCM, and thicker panels would be possible only by enhancing the thermal conductivity of the construction, for example by incorporating in the panel a graphite foam. Nevertheless, this is still thicker than in the case of passive PCM panels, for which the ideal thickness was 20 mm, as mentioned earlier. That was due to the more direct contact with the cooling medium (water circulating in embedded pipes) in the case of the active PCM panels. Therefore, the added thermal mass would be significantly higher in the case of active PCM panels. Active PCM panels require temperature sensors monitoring the panel surface temperature and the temperature of the material, to ensure that the water circulation is stopped once the material is fully discharged. Continuing cooling the PCM would result in excess energy use, without providing any additional benefit. Monitoring the panel surface temperature would ensure that no condensation is occurring due to low panel surface temperature.

To summarise, active ceiling panels containing PCM and PVT panels are two technologies that can greatly contribute in achieving the targets for reduction of the energy use in the construction sector and realise a decarbonised building stock, and at the same provide the desired thermal environment. PCM tiles require further investigation before they can be considered a potential option for providing an acceptable thermal environment.

7.2 Conclusions

- People who had elevated metabolic rate than sedentary activity due to walking to work, were accessible to lower temperature than what suggested by the European Standard EN 15251 at the beginning of the occupancy period.

- Coupling PVT panels for the production of electricity, domestic hot water and cold water for space cooling with active PCM ceiling panels for space conditioning can significantly reduce the energy use of heating and cooling equipment and at the same time provide the desired thermal environment.

- Although nocturnal radiative cooling can provide the required energy for space cooling, its performance varies depending on the outdoor conditions. A secondary system is required to provide the required energy when nocturnal radiative cooling is insufficient, while a detailed weather prediction is necessary to predict the performance of nocturnal radiative cooling in advance.

- The performance of passive PCM panels varies significantly depending on the outdoor conditions. Furthermore, a correct design of the PCM board (PCM quantity, PCM surface area, panel thickness, etc.) results in energy savings while an incorrect design could result in increased energy use.

- Although PCM tiles add additional thermal and contribute in reducing the energy use of the HVAC equipment, they cannot stand alone as a cooling system and should only be considered as a secondary system supplementing the main system, either all-air or radiant system.

- In case of active PCM panels, to ensure the full discharge of the PCM, the pipes should be embedded in the PCM layer to take advantage of the better contact between PCM and the cooling medium.

- For passive PCM panels the ideal thickness was 20 mm, while for active PCM panels 30 mm. That would result in significantly higher thermal mass in the case of incorporating active PCM panels compared to passive panels.

8 Future investigations and recommendations

Based on the findings of this study the following proposals are recommended as future investigation

- Different temperature ramps should be tested to identify the one that provides the best thermal environment both at the beginning of the occupancy period but also afterwards. A smaller ramp, e.g. 0.5 K/h would take more time to reach the comfort range (23-26°C) and thus might result in discomfort. The tested ramps should comply with the limitations of Table 5.3.5.3 of Standard ASHRAE 55 [8].

- Different age groups should also be exposed to similar experiments, since the study was intended for office buildings and a significant fraction of the occupants of an office building are older than the group 20-30 years old.

- The experiment should also last longer, e.g. 8-10 hours, to simulate a complete working day.

- Since the PCM-PVT validation experiment was conducted during March, this discharging method should also be examined during summer time or ideally during a whole year to have a more comprehensive view of the performance of the PVT panels. To have the complete performance of the PVT panels, also the production of hot water and electricity should be taken into consideration.

- More locations should be simulated using the validated PCM-PVT TRNSYS model, to create a map of locations with high, medium and low benefit from incorporating such a system.

- Similarly, different parameters should be tested for the PVT panels, e.g. place the panels vertical or horizontal, representing PVT panels integrated on a building, either on the wall or the roof, respectively.

- The TRNSYS model created to develop a simplified method for estimating the potential of incorporating PCM in an office building, should be validated against a real building to ensure the reliability of the model.

- Properties of PCM available on the market should be used as inputs in the model and more locations should be simulated to provide the corresponding equation for additional cities.

- The active panels with the embedded PCM developed in COMSOL, should be produced and tested using similar conditions as in the simulation study to validate the model.

- To have a reference case for all tested panels, the heat gains should be activated without any active system or PCM panel installed. In that way, we could compare what is the impact of the added thermal mass of the PCM tiles.

- A ventilation system sized accordingly to remove latent heat gains and pollutants should be operating during the occupancy period of the experiment.

- RCP panels should be tested with a higher level of heat gain sources to identify the highest level of heat the panels can remove before the operative temperature exceeds the upper limit of the comfort range.

- Since in an office building usually only approximately half of the ceiling is covered with RCPs, the same conditions should be tested with only two panel loops open for water circulation.

- Since the active panels with embedded PCM are a custom-made product, their performance in terms of fire safety should be assessed.

- A feasibility analysis should be conducted to calculate the payback period for an investment such as RCP, PCM tiles or PCM radiant panels. The concluded prices should be in €/m² to provide an indication also for larger scale projects.

- Once a control method that maintains the operative temperature within the comfort range is identified, PCM tiles and PCM radiant panels should be assessed in a field study, both in terms of energy use and thermal environment provided through questionnaires distributed to the occupants of the building.

References

[1]   Heat Roadmap Europe (HRE), "EU Profile of heating and cooling demand in 2015," 2017.

[2]   United Nations (UN), "Adoption of the Paris agreement," 2015.

[3]   European Commission (EC), "Public consultation on the Energy Performance of Buildings Directive," 2016.

[4]   European Commission (EC), "Commission launches plans to curb energy use in heating and cooling," 2016. [Online]. Available: https://ec.europa.eu/energy/en/news/commission-launches-plans-curb-energy-use-heating-and-cooling. [Accessed: 16-Jun-2018].

[5]   European Commission (EC), "Launch of the EU Energy Poverty Observatory (EPOV)," 2018. [Online]. Available: https://ec.europa.eu/energy/en/events/launch-eu-energy-poverty-observatory-epov. [Accessed: 16-Jun-2018].

[6]   ISO, *ISO 7730:2005 Ergonomics of the thermal environment – Analytical determination and interpretation of thermal comfort using calculation of the PMV and PPD indices and local thermal comfort criteria*. 2005.

[7]   EN, *EN 15251:2007 Indoor environment input parameters for design and assessment of energy performance of buildings adressing indoor air quality, thermal environment, lighting and acoustics*. 2007.

[8]   ASHRAE, *ASHRAE Standard 55: Thermal Environmental Conditions for Human Occupancy*. 2013.

[9]   L. Lan, P. Wargocki, and Z. Lian, "Quantitative measurement of productivity loss due to thermal discomfort," *Energy Build.*, vol. 43, no. 5, pp. 1057–1062, 2011.

[10]   P. Wargocki and D. P. Wyon, "Ten questions concerning thermal and indoor air quality effects on the performance of office work and schoolwork," *Build. Environ.*, vol. 112, pp. 359–366, 2017.

[11]   D. P. Wyon and P. Wargocki, "Room temperature effects on office work," in *Creating the Productive Workplace*, 2006, pp. 181–192.

[12]   J. Kolarik, J. Toftum, B. W. Olesen, and A. Shitzer, "Occupant Responses and Office Work Performance in Environments with Moderately Drifting Operative Temperatures (RP-1269)," *HVAC&R Res.*, vol. 15, no. 5, pp. 931–960, 2009.

[13]   United Nations Environment Programme, "Buildings and Climate Change - Summary for Decision-Makers," 2009.

[14]   B. Lehmann, V. Dorer, and M. Koschenz, "Application range of thermally activated building systems tabs," *Energy Build.*, vol. 39, no. 5, pp. 593–598, 2007.

[15]   J. Babiak, B. W. Olesen, and Dušan Petráš, *Low Temperature Heating and High Temperature Cooling*, no. 7. Finland, Forssa Print: REHVA, 2013.

[16]   S. H. Park, W. J. Chung, M. S. Yeo, and K. W. Kim, "Evaluation of the thermal performance of a Thermally Activated Building System (TABS) according to the thermal load in a residential building," *Energy Build.*, vol. 73, pp. 69–82, 2014.

[17]   K. N. Rhee, B. W. Olesen, and K. W. Kim, "Ten questions about radiant heating and cooling systems," *Build. Environ.*, vol. 112, pp. 367–381, 2017.

[18]   K. Zhao, X.-H. Liu, and Y. Jiang, "Application of radiant floor cooling in a large open space

building with high-intensity solar radiation," *Energy Build.*, vol. 66, no. 11, pp. 246–257, 2013.

[19]   B. W. Olesen and L. Mattarolo, "Thermal comfort and energy performance of hydronic radiant cooling systems compared to convective systems," in *Healthy Buildings 2009 Proceedings*, 2009.

[20]   B. W. Olesen, "Possibilities and limitations of radiant floor cooling," *ASHRAE Trans.*, vol. 50, no. 9, pp. 42–48, 1997.

[21]   B. W. Olesen, "Radiant floor cooling systems," *ASHRAE J.*, vol. 50, no. 9, pp. 16–20, 2008.

[22]   J. Pereira da Cunha and P. Eames, "Thermal energy storage for low and medium temperature applications using phase change materials - A review," *Appl. Energy*, vol. 177, pp. 227–238, 2016.

[23]   A. M. Khudhair and M. M. Farid, "A review on energy conservation in building applications with thermal storage by latent heat using phase change materials," *Energy Convers. Manag.*, vol. 45, no. 2, pp. 263–275, 2004.

[24]   M. Xiao, B. Feng, and K. Gong, "Preparation and performance of shape stabilized phase change thermal storage materials with high thermal conductivity," *Energy Convers. Manag.*, vol. 43, no. 1, pp. 103–108, 2002.

[25]   Z. Dong, H. Cui, W. Tang, D. Chen, and H. Wen, "Development of hollow steel ball macro-encapsulated PCM for thermal energy storage concrete," *Materials (Basel).*, vol. 9, no. 1, 2016.

[26]   P. Schossig, H. M. Henning, S. Gschwander, and T. Haussmann, "Micro-encapsulated phase-change materials integrated into construction materials," *Sol. Energy Mater. Sol. Cells*, vol. 89, no. 2–3, pp. 297–306, 2005.

[27]   A. Jamekhorshid, S. M. Sadrameli, and M. Farid, "A review of microencapsulation methods of phase change materials (PCMs) as a thermal energy storage (TES) medium," *Renew. Sustain. Energy Rev.*, vol. 31, pp. 531–542, 2014.

[28]   V. V. Tyagi, S. C. Kaushik, S. K. Tyagi, and T. Akiyama, "Development of phase change materials based microencapsulated technology for buildings: A review," *Renew. Sustain. Energy Rev.*, vol. 15, no. 2, pp. 1373–1391, 2011.

[29]   N. Soares, J. J. Costa, A. R. Gaspar, and P. Santos, "Review of passive PCM latent heat thermal energy storage systems towards buildings' energy efficiency," *Energy Build.*, vol. 59, pp. 82–103, 2013.

[30]   Z. Khan, Z. Khan, and A. Ghafoor, "A review of performance enhancement of PCM based latent heat storage system within the context of materials, thermal stability and compatibility," *Energy Convers. Manag.*, vol. 115, pp. 132–158, 2016.

[31]   S. S. Chandel and T. Agarwal, "Review of current state of research on energy storage, toxicity, health hazards and commercialization of phase changing materials," *Renew. Sustain. Energy Rev.*, vol. 67, pp. 581–596, 2017.

[32]   Y. Cui, J. Xie, J. Liu, and S. Pan, "Review of Phase Change Materials Integrated in Building Walls for Energy Saving," *Procedia Eng.*, vol. 121, pp. 763–770, 2015.

[33]   H. Akeiber *et al.*, "A review on phase change material (PCM) for sustainable passive cooling in building envelopes," *Renew. Sustain. Energy Rev.*, vol. 60, pp. 1470–1497, 2016.

[34]   X. Py, R. Olives, and S. Mauran, "Paraffin/porous-graphite-matrix composite as a high and

constant power thermal storage material," *Int. J. Heat Mass Transf.*, vol. 44, no. 14, pp. 2727–2737, 2001.

[35]   B. Xu and Z. Li, "Paraffin/diatomite composite phase change material incorporated cement-based composite for thermal energy storage," *Appl. Energy*, vol. 105, pp. 229–237, 2013.

[36]   X. Xiao, P. Zhang, and M. Li, "Preparation and thermal characterization of paraffin/metal foam composite phase change material," *Appl. Energy*, vol. 112, pp. 1357–1366, 2013.

[37]   K. Pielichowska and K. Pielichowski, "Phase change materials for thermal energy storage," *Prog. Mater. Sci.*, vol. 65, pp. 67–123, 2014.

[38]   J. Kośny, *PCM-Enhanced Building Components - An Application of Phase Change Materials in Building Envelopes and Internal Structures*. 2015.

[39]   H. Johra and P. Heiselberg, "Influence of internal thermal mass on the indoor thermal dynamics and integration of phase change materials in furniture for building energy storage: A review," *Renew. Sustain. Energy Rev.*, vol. 69, no. September 2015, pp. 19–32, 2017.

[40]   Hasnain S.M., "Review on sustainable thermal energy storage technologies, Part I: heat storage materials and techniques," *Energy Convers. Manag.*, vol. 39, no. 11, pp. 1127–1138, 1998.

[41]   W. Su, J. Darkwa, and G. Kokogiannakis, "Review of solid-liquid phase change materials and their encapsulation technologies," *Renew. Sustain. Energy Rev.*, vol. 48, pp. 373–391, 2015.

[42]   D. Feldman, M. M. Shapiro, D. Banu, and C. J. Fuks, "Fatty acids and their mixtures as phase-change materials for thermal energy storage," *Sol. Energy Mater.*, vol. 18, no. 3, pp. 201–216, 1989.

[43]   D. Feldman, D. Banu, and D. W. Hawes, "Development and application of organic phase change mixtures in thermal storage gypsum wallboard," *Sol. Energy Mater. Sol. Cells*, vol. 36, no. 2, pp. 147–157, 1995.

[44]   D. Rozanna, T. G. Chuah, A. Salmiah, T. S. Y. Choong, and M. Sa'ari, "Fatty Acids as Phase Change Materials (PCMs) for Thermal Energy Storage: A Review," *Int. J. Green Energy*, vol. 1, no. 4, pp. 495–513, 2005.

[45]   Y. Yuan, N. Zhang, W. Tao, X. Cao, and Y. He, "Fatty acids as phase change materials: A review," *Renew. Sustain. Energy Rev.*, vol. 29, pp. 482–498, 2014.

[46]   S. Karaman, A. Karaipekli, A. Sar, and A. Biçer, "Polyethylene glycol (PEG)/diatomite composite as a novel form-stable phase change material for thermal energy storage," *Sol. Energy Mater. Sol. Cells*, vol. 95, no. 7, pp. 1647–1653, 2011.

[47]   Y. Deng and L. Yang, "Preparation and characterization of polyethylene glycol (PEG) hydrogel as shape-stabilized phase change material," *Appl. Therm. Eng.*, vol. 114, pp. 1014–1017, 2017.

[48]   A. Sarı, A. Bicer, F. A. Al-Sulaiman, A. Karaipekli, and V. V. Tyagi, "Diatomite/CNTs/PEG composite PCMs with shape-stabilized and improved thermal conductivity: Preparation and thermal energy storage properties," *Energy Build.*, vol. 164, pp. 166–175, 2018.

[49]   M. Iten and S. Liu, "A work procedure of utilising PCMs as thermal storage systems based on air-TES systems," *Energy Convers. Manag.*, vol. 77, pp. 608–627, 2014.

[50]   M. Kenisarin and K. Mahkamov, "Salt hydrates as latent heat storage materials:Thermophysical properties and costs," *Sol. Energy Mater. Sol. Cells*, vol. 145, pp.

255–286, 2016.

[51]   Y. E. Milián, A. Gutiérrez, M. Grágeda, and S. Ushak, "A review on encapsulation techniques for inorganic phase change materials and the influence on their thermophysical properties," *Renew. Sustain. Energy Rev.*, vol. 73, no. February, pp. 983–999, 2017.

[52]   F. C. Porisini, "Salt hydrates used for latent heat storage: Corrosion of metals and reliability of thermal performance," *Sol. Energy*, vol. 41, no. 2, pp. 193–197, 1988.

[53]   A. J. Farrell, B. Norton, and D. M. Kennedy, "Corrosive effects of salt hydrate phase change materials used with aluminium and copper," *J. Mater. Process. Technol.*, vol. 175, no. 1–3, pp. 198–205, 2006.

[54]   A. Sharma, V. V. Tyagi, C. R. Chen, and D. Buddhi, "Review on thermal energy storage with phase change materials and applications," *Renew. Sustain. Energy Rev.*, vol. 13, no. 2, pp. 318–345, 2009.

[55]   S. N. Gunasekara, V. Martin, and J. N. Chiu, "Phase equilibrium in the design of phase change materials for thermal energy storage: State-of-the-art," *Renew. Sustain. Energy Rev.*, vol. 73, no. February 2016, pp. 558–581, 2017.

[56]   R. Baetens, B. P. Jelle, and A. Gustavsen, "Phase change materials for building applications: A state-of-the-art review," *Energy Build.*, vol. 42, no. 9, pp. 1361–1368, 2010.

[57]   H. Fauzi, H. S. C. Metselaar, T. M. I. Mahlia, and M. Silakhori, "Sodium laurate enhancements the thermal properties and thermal conductivity of eutectic fatty acid as phase change material (PCM)," *Sol. Energy*, vol. 102, pp. 333–337, 2014.

[58]   S. Kahwaji, M. B. Johnson, A. C. Kheirabadi, D. Groulx, and M. A. White, "Stable, low-cost phase change material for building applications: The eutectic mixture of decanoic acid and tetradecanoic acid," *Appl. Energy*, vol. 168, pp. 457–464, 2016.

[59]   A. Sharma, A. Shukla, C. R. Chen, and S. Dwivedi, "Development of phase change materials for building applications," *Energy Build.*, vol. 64, pp. 403–407, 2013.

[60]   T. K. Stovall and J. J. Tomlinson, "What are the potential benefits of including latent storage in common wallboard?," *J. Sol. Energy Eng. - Trans. ASME*, vol. 11, no. 4, pp. 318–325, 1995.

[61]   A. K. Athienitis, C. Liu, D. Hawes, D. Banu, and D. Feldman, "Investigation of the thermal performance of a passive solar test-room with wall latent heat storage," *Build. Environ.*, vol. 32, no. 5, pp. 405–410, 1997.

[62]   D. Banu, D. Feldman, and D. Hawes, "Evaluation of thermal storage as latent heat in phase change material wallboard by differential scanning calorimetry and large scale thermal testing," *Thermochim. Acta*, vol. 317, pp. 39–45, 1998.

[63]   S. M. Vakilaltojjar and W. Saman, "Analysis and modelling of a phase change storage system for air conditioning applications," *Appl. Therm. Eng.*, vol. 21, no. 3, pp. 249–263, 2001.

[64]   M. Koschenz and B. Lehmann, "Development of a thermally activated ceiling panel with PCM for application in lightweight and retrofitted buildings," *Energy Build.*, vol. 36, pp. 567–578, 2004.

[65]   S. Takeda, K. Nagano, T. Mochida, and K. Shimakura, "Development of a ventilation system utilizing thermal energy storage for granules containing phase change material," *Sol. Energy*, vol. 77, no. 3, pp. 329–338, 2004.

[66]   W. Saman, F. Bruno, and E. Halawa, "Thermal performance of PCM thermal storage unit for a

roof integrated solar heating system," *Sol. Energy*, vol. 78, no. 2, pp. 341–349, 2005.

[67]   L. F. Cabeza, C. Castellón, M. Nogués, M. Medrano, R. Leppers, and O. Zubillaga, "Use of microencapsulated PCM in concrete walls for energy savings," *Energy Build.*, vol. 39, no. 2, pp. 113–119, 2007.

[68]   N. Artmann, *Cooling of the building structure by night-time ventilation*. 2009.

[69]   M. Alam, H. Jamil, J. Sanjayan, and J. Wilson, "Energy saving potential of phase change materials in major Australian cities," *Energy Build.*, vol. 78, pp. 192–201, 2014.

[70]   J. P. Arzamendia Lopez, F. Kuznik, D. Baillis, and J. Virgone, "Numerical modeling and experimental validation of a PCM to air heat exchanger," *Energy Build.*, vol. 64, pp. 415–422, 2013.

[71]   I. Mandilaras, M. Stamatiadou, D. Katsourinis, G. Zannis, and M. Founti, "Experimental thermal characterization of a Mediterranean residential building with PCM gypsum board walls," *Build. Environ.*, vol. 61, pp. 93–103, 2013.

[72]   S. Álvarez, L. F. Cabeza, A. Ruiz-Pardo, A. Castell, and J. A. Tenorio, "Building integration of PCM for natural cooling of buildings," *Appl. Energy*, vol. 109, pp. 514–522, 2013.

[73]   F. Ascione, N. Bianco, R. F. De Masi, F. de' Rossi, and G. P. Vanoli, "Energy refurbishment of existing buildings through the use of phase change materials: Energy savings and indoor comfort in the cooling season," *Appl. Energy*, vol. 113, pp. 990–1007, 2014.

[74]   A. Bastani, F. Haghighat, and J. Kozinski, "Designing building envelope with PCM wallboards: Design tool development," *Renew. Sustain. Energy Rev.*, vol. 31, no. 2014, pp. 554–562, 2014.

[75]   F. Bruno, N. H. S. Tay, and M. Belusko, "Minimising energy usage for domestic cooling with off-peak PCM storage," *Energy Build.*, vol. 76, pp. 347–353, 2014.

[76]   K. Biswas and R. Abhari, "Low-cost phase change material as an energy storage medium in building envelopes: Experimental and numerical analyses," *Energy Convers. Manag.*, vol. 88, pp. 1020–1031, 2014.

[77]   P. Atkin and M. M. Farid, "Improving the efficiency of photovoltaic cells using PCM infused graphite and aluminium fins," *Sol. Energy*, vol. 114, pp. 217–228, 2015.

[78]   J. Borderon, J. Virgone, and R. Cantin, "Modeling and simulation of a phase change material system for improving summer comfort in domestic residence," *Appl. Energy*, vol. 140, pp. 288–296, 2015.

[79]   R. Barzin, J. J. J. Chen, B. R. Young, and M. M. Farid, "Application of PCM energy storage in combination with night ventilation for space cooling," *Appl. Energy*, vol. 158, pp. 412–421, 2015.

[80]   M. Alam, J. Sanjayan, P. X. W. Zou, S. Ramakrishnan, and J. Wilson, "Evaluating the passive and free cooling application methods of phase change materials in residential buildings: A comparative study," *Energy Build.*, vol. 148, pp. 238–256, 2017.

[81]   A. Bastani, F. Haghighat, and C. J. Manzano, "Investigating the effect of control strategy on the shift of energy consumption in a building integrated with PCM wallboard," *Energy Procedia*, vol. 78, pp. 2280–2285, 2015.

[82]   Dansk Standard (DS), *DS/EN 13501-1: Fire classification of construction products and building elements – Part 1: Classification using data from reaction to fire tests*. 2009.

[83]   Dansk Standard (DS), *DS/EN 13501-2: Fire classification of construction products and building elements – Part 2: Classification using data from fire resistance tests, excluding ventilation services*. Charlottenlund, 2009.

[84]   Dansk Standard (DS), *DS/EN ISO 1182: Reaction to fire tests for products – Non-combustibility test*. Charlottenlund, 2010.

[85]   M. G. Meir, J. B. Rekstad, and O. M. Løvvik, "A study of a polymer-based radiative cooling system," *Sol. Energy*, vol. 73, no. 6, pp. 403–417, 2002.

[86]   G. Clark and P. Berdahl, "Radiative cooling: resources and applications," in *5th National Passive Solar Conference*, 1980, pp. 167–201.

[87]   J. A. Duffie and W. A. Beckmann, *Solar Engineering of Thermal Processes*, 2nd ed. New York: Wiley Interscience, 1991.

[88]   T. Q. Péan, L. Gennari, O. B. Kazanci, E. Bourdakis, and B. W. Olesen, "Influence of the environmental parameters on nocturnal radiative cooling capacity of solar collectors," in *Klima*, 2016.

[89]   E. Erell and Y. Etzion, "Radiative cooling of buildings with flat-plate solar collectors," *Build. Environ.*, vol. 35, no. 4, pp. 297–305, 2000.

[90]   U. Eicker and A. Dalibard, "Photovoltaic-thermal collectors for night radiative cooling of buildings," *Sol. Energy*, vol. 85, no. 7, pp. 1322–1335, 2011.

[91]   E. Hosseinzadeh and H. Taherian, "An experimental and analytical study of a radiative cooling system with unglazed flat plate collectors," *Int. J. Green Energy*, vol. 9, no. 8, pp. 766–779, 2012.

[92]   T. Anderson, M. Duke, and J. Carson, "Performance of an unglazed solar collector for radiant cooling," *Aust. Sol. Cool.*, 2013.

[93]   T. Péan, L. Gennari, B. W. Olesen, and O. B. Kazanci, "Nighttime radiative cooling potential of unglazed and PV / T solar collectors : parametric and experimental analyses," in *Proceedings of the 8th Mediterranean Congress of Heating, Ventilation and Air-conditioning (climamed 2015)*, 2015.

[94]   M. Fiorentini, P. Cooper, and Z. Ma, "Development and optimization of an innovative HVAC system with integrated PVT and PCM thermal storage for a net-zero energy retrofitted house," *Energy Build.*, vol. 94, pp. 21–32, 2015.

[95]   W. Lin, Z. Ma, M. I. Sohel, and P. Cooper, "Development and evaluation of a ceiling ventilation system enhanced by solar photovoltaic thermal collectors and phase change materials," *Energy Convers. Manag.*, vol. 88, pp. 218–230, 2014.

[96]   European Union (EU), *DIRECTIVE 2010/31/EU OF THE EUROPEAN PARLIAMENT AND OF THE COUNCIL of 19 May 2010 on the energy performance of buildings*. 2010.

[97]   J. Kolarik, J. Toftum, B. W. Olesen, and K. L. Jensen, "Simulation of energy use, human thermal comfort and office work performance in buildings with moderately drifting operative temperatures," *Energy Build.*, vol. 43, no. 11, pp. 2988–2997, 2011.

[98]   E. Arens, H. Zhang, and C. Huizenga, "Partial- and whole-body thermal sensation and comfort - Part I: Uniform environmental conditions," *J. Therm. Biol.*, vol. 31, no. 1–2 SPEC. ISS., pp. 53–59, 2006.

[99]   A. Melikov, B. Yordanova, L. Bozhkov, V. Zboril, and R. Kosonen, "Human response to thermal

environment in rooms with chilled beams," in *Proceedings of Clima 2007 WellBeing Indoors*, 2007.

[100] M. Dalewski, A. K. Melikov, and M. Vesely, "Performance of ductless personalized ventilation in conjunction with displacement ventilation: Physical environment and human response," *Build. Environ.*, vol. 81, pp. 354–364, 2014.

[101] A. Lipczynska, J. Kaczmarczyk, B. Marcol, W. Kierat, and A. K. Melikov, "Human Response to Personalized Ventilation Combined with Chilled Ceiling," *Proc. 13th Int. Conf. Air Distrib. Rooms*, pp. 1–7, 2014.

[102] T. Arghand *et al.*, "Individually controlled localized chilled beam in conjunction with chilled ceiling: Part 2 – Human response," *Proc. Indoor Air 2016 Publ.*, 2016.

[103] Q. Jin, A. Simone, B. W. Olesen, S. K. M. Holmberg, and E. Bourdakis, "Laboratory study of subjective perceptions to low temperature heating systems with exhaust ventilation in Nordic countries," *Sci. Technol. Built Environ.*, vol. 23, no. 3, 2017.

[104] Z. D. Bolashikov, P. Mustakallio, S. Kolencikova, K. Kostov, A. K. Melikov, and R. Kosonen, "Thermal comfort in simulated office environment with four convective and radiant cooling systems," *Proc. 11th REHVA World Congr. 8th Int. Conf. Indoor Air Qual. Vent. Energy Conserv. Build.*, p. Paper ID: 375, 2013.

[105] H. Zhang, C. Huizenga, E. Arens, and D. Wang, "Thermal sensation and comfort in transient non-uniform thermal environments," *Eur. J. Appl. Physiol.*, vol. 92, no. 6, pp. 728–733, 2004.

[106] C. Huizenga, H. Zhang, E. Arens, and D. Wang, "Skin and core temperature response to partial- and whole-body heating and cooling," *J. Therm. Biol.*, vol. 29, no. 7–8 SPEC. ISS., pp. 549–558, 2004.

[107] H. Zhang, E. Arens, C. Huizenga, and T. Han, "Thermal sensation and comfort models for non-uniform and transient environments, Part I: Local sensation of individual body parts," *Build. Environ.*, vol. 45, no. 2, pp. 380–388, 2010.

[108] H. Zhang, E. Arens, C. Huizenga, and T. Han, "Thermal sensation and comfort models for non-uniform and transient environments, part II: Local comfort of individual body parts," *Build. Environ.*, vol. 45, no. 2, pp. 389–398, 2010.

[109] H. Zhang, E. Arens, C. Huizenga, and T. Han, "Thermal sensation and comfort models for non-uniform and transient environments, part III: Whole-body sensation and comfort," *Build. Environ.*, vol. 45, no. 2, pp. 399–410, 2010.

[110] E. Arens, H. Zhang, and C. Huizenga, "Partial- and whole-body thermal sensation and comfort—Part II: Non-uniform environmental conditions," *J. Therm. Biol.*, vol. 31, no. 1–2, pp. 60–66, 2006.

[111] A. P. Gagge, J. A. J. Stolwijk, and J. D. Hardy, "Comfort and thermal sensations and associated physiological responses at various ambient temperatures," *Environ. Res.*, vol. 1, no. 1, pp. 1–20, 1967.

[112] I. D. Griffiths and D. A. McIntyre, "Sensitivity to Temporal Variations in Thermal Conditions," *Ergonomics*, vol. 17, no. 4, pp. 499–507, 1974.

[113] D. A. McIntyre and R. R. Gonzalez, "Man's Thermal Sensitivity During Temperature Changes at Two Levels of Clothing Insulation and Activity," *ASHRAE Trans.*, vol. 82, no. 2, pp. 219–233, 1976.

[114] J. L. M. Hensen, "Literature Review on Thermal Comfort in Transient Conditions," vol. 25, no.

4, pp. 309–316, 1990.

[115] T. Goto, J. Toftum, R. de Dear, and P. O. Fanger, "Thermal sensation and thermophysiological responses to metabolic step-changes," *Int. J. Biometeorol.*, vol. 50, no. 5, pp. 323–332, 2006.

[116] P. O. Fanger, *Thermal comfort*. Copenhagen, Denmark: Danish Technical Press, 1970.

[117] G. K. Pavlov, *Building Thermal Energy Storage*. Copenhagen, Denmark: DTU-Tryk, 2014.

[118] F. Kuznik and J. Virgone, "Experimental investigation of wallboard containing phase change material: Data for validation of numerical modeling," *Energy Build.*, vol. 41, no. 5, pp. 561–570, 2009.

[119] DS/EN ISO, "ISO 7726: Ergonomics of the thermal environment - Instruments for measuring physical quantities," 2001.

[120] (ISO) International Organization for Standardization, *ISO 11855-2: Building Environment Design — Design, Dimensioning, Installation and Control of the Embedded Radiant Heating and Cooling Systems —Part 2: Determination of the design heating and cooling capacity*. 2012.

[121] International Organization for Standardization, *ISO 11855-1: Building Environment Design — Design, Dimensioning, Installation and Control of the Embedded Radiant Heating and Cooling Systems —Part 1: Definition, symbols, and comfort criteria*. 2012.

Paper 1: Bourdakis E., Péan T. Q., Gennari L., & Olesen B. W. (2016). Daytime space cooling with phase change material ceiling panels discharged using rooftop photovoltaic/thermal panels and nighttime ventilation. Science and Technology for the Built Environment, 4731(June), 1–9. https://doi.org/10.1080/23744731.2016.1181511

Daytime space cooling with phase change material ceiling panels discharged using rooftop photovoltaic/thermal panels and night-time ventilation

Eleftherios Bourdakis, Thibault Q. Péan, Luca Gennari & Bjarne W. Olesen

Taylor & Francis
Taylor & Francis Group

Daytime space cooling with phase change material ceiling panels discharged using rooftop photovoltaic/thermal panels and night-time ventilation

ELEFTHERIOS BOURDAKIS*, THIBAULT Q. PÉAN, LUCA GENNARI, and BJARNE W. OLESEN

International Centre of Indoor Environment and Energy, Technical University of Denmark, Nils Koppels Allé, Building 402, office 227, Kgs, Lyngby 2800, Denmark

The possibility of using photovoltaic/thermal panels for producing cold water through the process of night-time radiative cooling was experimentally examined. The cold water was used to discharge phase change material in ceiling panels in a climatic chamber. Both night-time radiative cooling and night-time ventilation were used as the discharging method in five experiments, simulating summer conditions. The operative temperature remained within the range of Category III of standard DS/EN 15251 for 50% to 99% of the occupancy period. The percentage of electrical energy usage covered from the photovoltaic/thermal varied from 56% to 122%. The phase change material ceiling panels were thus, capable of providing an acceptable thermal environment and the photovoltaic/thermal panels were able to provide most of the required electricity and cold water needed for cooling.

Introduction

The European Parliament (EP) has used ambitious and demanding legislation to stop the continuous increase in energy demand and reduce CO_2 emission by EU Member States (EP 2009; EP 2010). In the EU Directive for the Energy Performance of Building (EPBD) it is stipulated that by the January 1, 2019, all new public buildings must be "nearly zero energy buildings" (nZEBs), and that by January 1, 2020, all new buildings should be nZEB (EP 2010). These directives must be followed by all Member States. Two preconditions have to be met in order for the spread of nZEB to be realized. First, the energy usage of buildings has to be reduced drastically, and second, buildings have to be equipped with some means of producing their own energy, such as photovoltaic panels, to cover their electrical energy demand, either on an individual building or district scale.

Thermally active building systems (TABS) could contribute to the reduction of the energy required for heating, cooling, and ventilation systems. Their high thermal mass results in the distribution of cooling over a longer period of time which leads to lower peaks of cooling/heating demand (Babiak, Olesen, and Petráš 2013). By reducing the size of the

suspended ceiling required for ventilation, since a lower air volume is required, the height of the building can be reduced which results in reduction of building's materials (Babiak et al. 2013). In addition, when using high temperature cooling and low temperature heating systems where the medium temperature needed for cooling/heating is closer to the room temperature, it increases the energy efficiency of heat pumps and ground source heat exchangers (Babiak et al. 2013; Zhao, Liu, and Jiang 2013). The ventilation noise level and the risk of draught are reduced and they provide a more uniform thermal environment compared to mixing ventilation systems (Olesen 1997; Olesen 2008).

Although TABS seem to be a promising solution for new construction, they are not always applicable to renovation, since it is technically difficult to include a new 150 mm concrete ceiling in an existing building. This drawback could be solved by installing radiant systems which include phase change material (PCM), since they have the thickness of a lightweight construction but their effective thermal mass is comparable to that of a heavyweight construction (Koschenz and Lehmann 2004). PCMs can be either organic or inorganic substances that absorb latent heat when they melt and release it when they solidify. The biggest benefits of implementing PCM in the structure or ceiling panels are the reduction of peak cooling demand, the shift of part of the cooling demand to night-time (when lower electricity tariffs occur in several countries), the reduced fluctuation of the room temperature, the reduction in the size of the HVAC system that is required and the more rapid charge and discharge rates that can be achieved compared to conventional concrete (BASF 2010; Cabeza et al. 2007; Krasimirov Pavlov 2014).

Eleftherios Bourdakis, Student Member ASHRAE, is a PhD Candidate. **Thibault Q. Péan,** Student Member ASHRAE, is a Research Assistant. **Luca Gennari** is a Research Assistant. **Bjarne W. Olesen, PhD,** Fellow ASHRAE, is a Professor.
*Corresponding author e-mail: elefbur@byg.dtu.dk
Color versions of one or more of the figures in the article can be found online at www.tandfonline.com/uhvc.
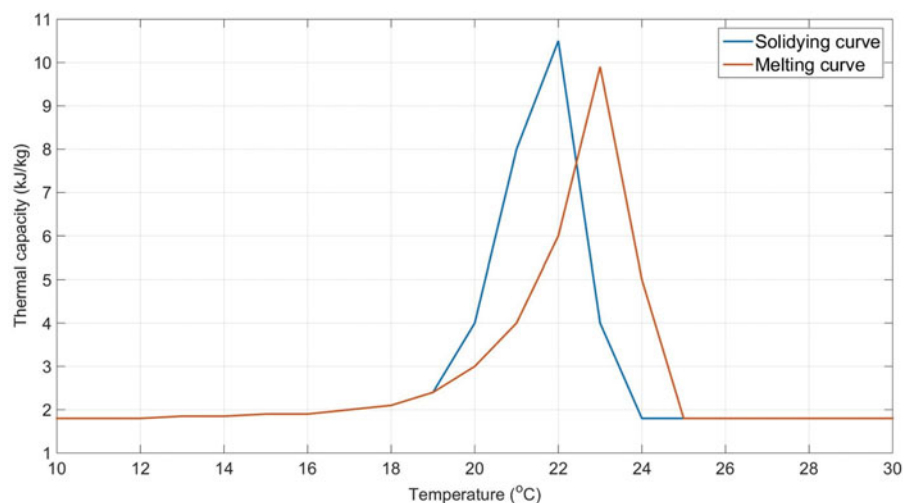
Fig. 1. Thermal capacity versus temperature.

Radiative heat transfer to the night sky is a method which could be used as the cooling source for discharging PCMs inside the building. Solar panels release heat in the form of longwave radiation toward the night sky (–40°C/–40°F). The benefits of night-time radiative cooling are the low energy usage (since only a water circulation pump is required); the higher utilization factor of the solar panels (since they are exploited also during night-time); that cold water production and cooling demand are in phase, since clear skies occur more often during the summer period, and that they can be coupled with thermal storage systems such as TABS and PCM (Eicker and Dalibard 2011; Hosseinzadeh and Taherian 2012; Meir, Rekstad, and Løvvik 2002).

The use of photovoltaic/thermal (PV/T) panels for night-time radiative cooling together with PCM for space cooling has been reported by (Eicker and Dalibard 2011; Fiorentini, Cooper, and Ma 2015; Lin et al. 2014) and in the first of these the PCM was part of the radiant cooling system. The purpose of the present experiment was to demonstrate that the coupling of PV/T panels with a radiant ceiling cooling system containing PCM can contribute to the realization of nZEB. The system was evaluated in terms of the resulting indoor thermal conditions, the cooling output and electricity production of the PV/T panels, and the heat stored in the PCM panels.

Method

A climate chamber at the International Centre for Indoor Environment and Energy (ICIEE) at the Technical University of Denmark (DTU) was used. The chamber was located inside a larger building, so it was not exposed to the ambient weather conditions. The floor area was 22.7 m^2 (5.4 m × 4.2 m) while the height was 3 m. The walls and the roof of the chamber consisted of two steel sheets separated by 100 mm of mineral wool.

At 2.5 m above the floor, the PCM panels were installed as a suspended ceiling. The plenum that was formed between the suspended ceiling and the chamber's roof was used to supply fresh air inside the room through the gaps between the PCM panels. Twenty-four PCM panels were installed, and the dimensions of each panel were 1.25 m × 0.625 m × 0.025 m, containing 6 kg of PCM each. The PCM that was used is microencapsulated paraffin with a melting point of 23°C. The curves of the thermal capacity versus the temperature for the melting and solidifying processes are shown in Figure 1. For discharging the PCM, Alu-PEX pipes were embedded inside the panels to circulate cold water. The external diameter of the pipes was 8 mm, the thickness 1 mm and the pipe spacing 100 mm. As it can be seen in Figure 2, eight panels had surface temperature sensors attached both on the upper and the lower surface, while in three panels a heat flux sensor was attached.

The chamber interior was arranged to simulate a two-person office, as shown in Figure 3. Heated manikins were used to simulate two occupants and office equipment was simulated using heated dummies. They were activated only during typical office hours, namely from 9:00 to 17:00 and only on weekdays. The total power from the two occupants, the office equipment and the four ceiling lamps was 540 W (23.8 W/m^2). The office
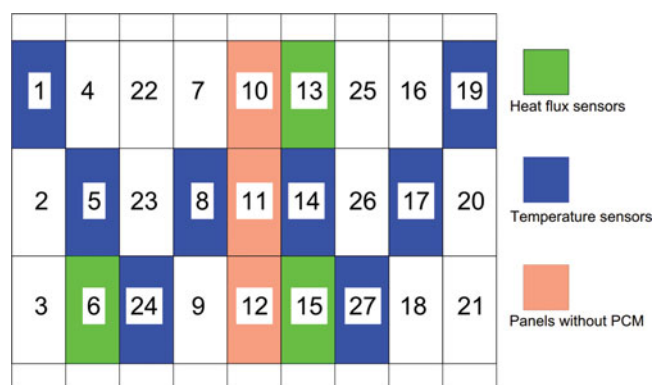
Fig. 2. Sensors' location on PCM panels.

Fig. 3. Chamber's interior.

equipment consisted of two laptops with an additional screen each and two desktop lamps. Behind each "occupant," there was a stand with an operative temperature sensor 0.6 m above the floor, and four air temperature sensors at heights of 0.1, 0.6, 1.1, and 1.7 m. Those heights correspond to the ankle, abdomen, and neck of a seated person and the neck of a standing person, respectively, as recommended by Standard ISO 7726 (2001).

The chamber was not directly exposed to sunlight, but an electrical heating wall panel was used to simulate the solar load of a window located on the south wall of the office, as may be seen in the background of Figure 3. For defining the daily solar heat gains profile, a simulation in TRNSYS was run using the International Weather for Energy Calculations (IWEC) file for Copenhagen. From this simulation, the average value of longwave radiation passing a window located on the south wall per minute was defined for the cooling period (namely from May 1st until October 30th). Since the control system

for the electrical heating panel could only be set in multiples of 25 W, the daily schedule was adjusted as shown in Figure 4.

The air supply temperature was varying from 18°C to 20°C, while the ventilation flow rate was set to 30 l/s. This airflow rate judged adequate for providing fresh air and removing latent heat gains and pollutants to an office the size of the climate chamber, based on Annex B.1.2 of the standard DS/EN 15251 (DS/EN 2007b). The ventilation was operated from 9:00 to 17:00. As stated above, the air was supplied from a plenum above the PCM panels, while the exhaust diffuser was located behind one of the "occupants," as may be seen in Figure 2. The ventilation was also operated to discharge the PCM at night in three experimental cases, as set out in Table 1.

On the roof of the building where the chamber was located, three polycrystalline PV/T panels were installed. The surface of each panel was 1.3 m² and they were facing south with a tilt angle of 45°. The water flow rate in the solar loop was 94 L/h. As shown in Figure 5, the PV/T panels were connected
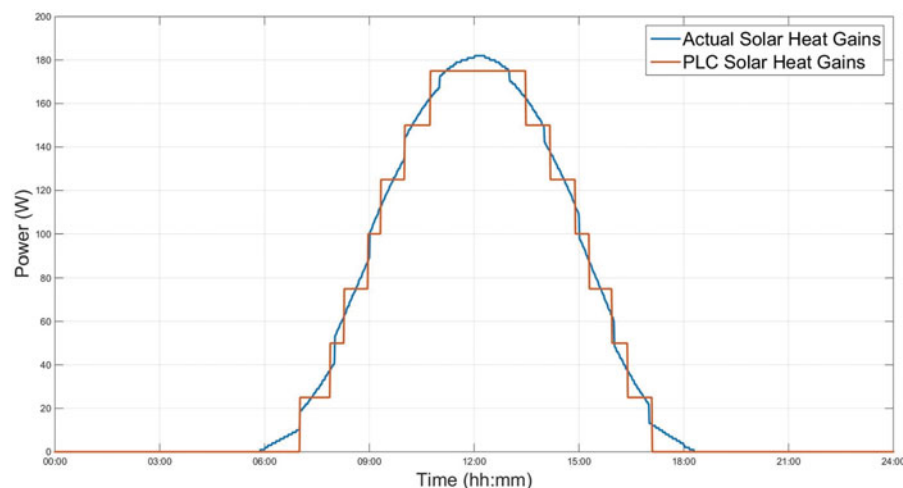
Fig. 4. Daily solar heat gains profile.

Table 1. Cases examined.

Case number	Nighttime ventilation	Improved air mixing	Activation of embedded water system
1	No	No	Yes
2	No	Yes	Yes
3	30 l/s at 18°C–20ºC	Yes	Yes
4	30 l/s at 18°C–20ºC	No	Yes
5	30 l/s at 18°C–20ºC	No	No

through a heat exchanger with two storage tanks. The volume of each tank was 255 L. One tank was used to store hot water (hot water tank; HWT) while in the second one, cold water (cold water tank; CWT) was stored. A plate heat exchanger was installed between the panels and the tanks due to different water pressure in the solar loop and the tanks. This restricted the quantity of glycol as much as possible, which was required as antifreeze in the solar loop. The direction of the water after the heat exchanger toward the HWTs or CWTs was determined automatically based on the two following conditions:

If $T_{PV/T} - T_{HWT} > 1K$ then water directed toward HWT

$$(1)$$

If $T_{CWT} - T_{PV/T} > 1K$ then water directed toward CWT

$$(2)$$

Where

$T_{PV/T}$ is the water temperature exiting the PV/T panels
T_{HWT} is the temperature in the middle of the HWT
T_{CWT} is the temperature in the middle of the CWT

The location of the three sensors measuring $T_{PV/T}$, the T_{HWT}, and the T_{CWT} are shown in Figure 5. If neither of the two conditions was met, then the pump between the heat exchanger and the tanks was switched off. The CWT had two internal spiral heat exchangers. As it is shown in Figure 5, the upper one was connected to the plate heat exchanger, while the lower one was connected to the main chiller of the laboratory facilities. The main chiller was used as an auxiliary system for providing cold water whenever the production from nighttime radiative cooling was not sufficient. The water supply temperature of the main chiller was 7°C. The water from the bottom of the CWT was circulated to the PCM panels and from there it was returned to the top of the CWT. The water flow rate was 210 kg/h and the circulation of the water was started at 5:00 and continued until 9:00, provided that the following conditions were met:

- The average lower surface temperature of the PCM panels was above 21°C
- The operative temperature of the room was above 21°C
- The temperature of the water in the middle of the CWT was below 20°C

During the occupant period, the water circulation to the PCM panels was activated automatically if the temperature at the middle of the CWT was below 20°C and the operative temperature of the room was above 25.5°C.

In Table 1 the configurations that were examined are tabulated. The duration for each of them was five weekdays and the experiment was performed from July 2015 to September 2015. In addition to night-time radiative cooling, night-time ventilation, and the combination of the two were examined as methods for discharging the PCM. In the second and the third configuration the air mixing was improved by turning on two floor fans. In the last configuration, the embedded water cooling system was deactivated and only night-time ventilation was used for discharging the PCM panels.

In Figure 6 the operative temperature for all six configurations is presented. The grey shaded areas are the occupancy
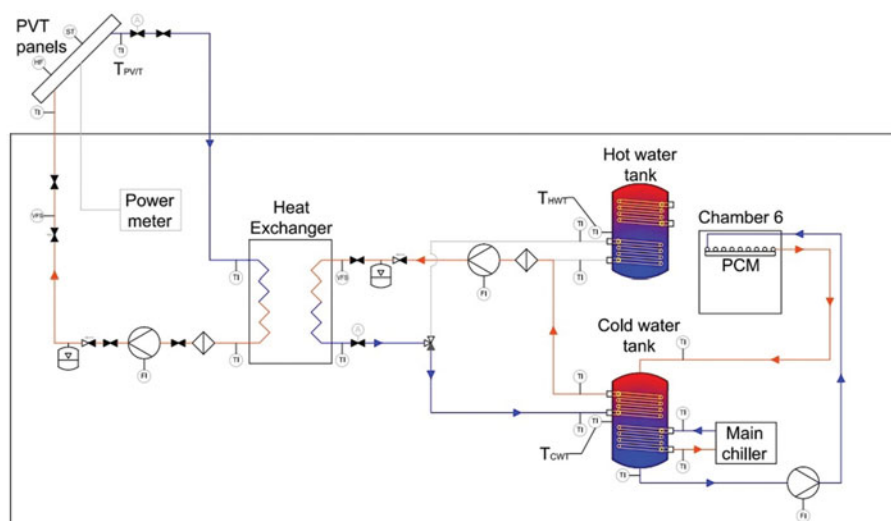
Fig. 5. Schematic drawing of the hydraulic system.
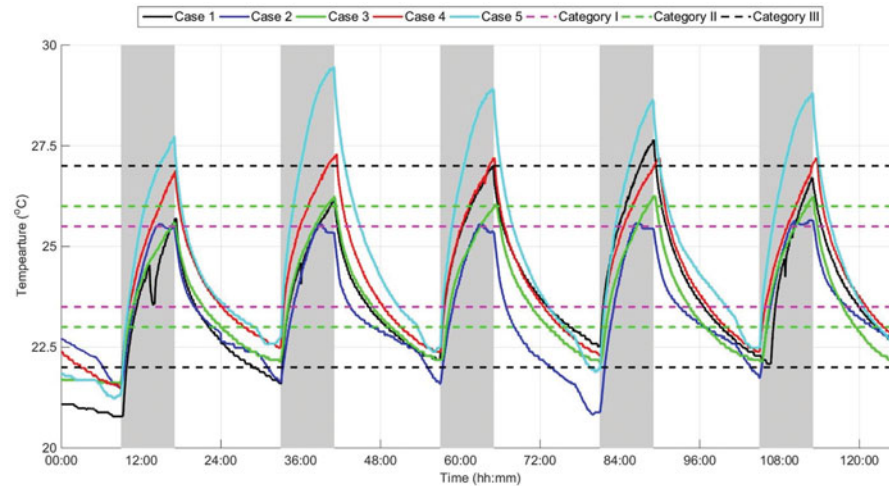
Fig. 6. Operative temperature.

periods, while the three pairs of horizontal dashed lines show the lower and upper limits of the Categories I, II, and III of Standard DS/EN 15251 (DS/EN 2007b).

The percentages of the occupancy period where the operative temperature was within the limits of each category of standard DS/EN 15251 (DS/EN 2007b) are presented in Table 2. The temperature should be within the ranges 23.5–25.5°C, 23–26°C, and 22–27°C for Category I, II, and III, respectively. Table 3.

It can be observed that the configuration which achieved the highest percentage of time within the range of Category III was the third configuration, in which the operative temperature was within the limits for 99% of the occupancy period. The configuration in which the worst thermal conditions were provided was the fifth case, in which the embedded water cool-

Table 2. Percentages of occupancy period in categories of standard EN 15251.

Case number	Category I,%	Category II,%	Category III,%
1	45	63	92
2	59	84	95
3	57	81	99
4	37	58	95
5	19	29	50

Table 3. Average power of the PV/T panels.

Case number	Average electrical power, W/m²	Average hot water production power, W/m²	Average cold water production power, W/m²
1	51	35	70.8
2	51.9	27	56.3
3	63.2	72.1	76.5
4	31.9	39.7	67.1
5	28	72.2	82.1

ing system was deactivated and the PCM was discharged only by night-time ventilation.

In Figure 7 the total energy output of the PV/Ts and the PCM for each configuration is shown (in each case, the energy accumulated over 5 days). It may be seen that the amount of energy stored in the CWT is significantly higher than the energy stored in the HWT. For the energy stored in the CWT, only the operation of the PV/Ts was taken into consideration, while the impact of the main chiller was not included in the calculations. It can be seen that in Configurations 1–4 the energy removed by the PCM was 38 to 59% lower than the energy stored in the CWT. The last configuration was not taken into consideration since the water stored in the CWT tank was not utilized for discharging the PCM.

The average power per m² of the PV/T panels in terms of producing electricity, hot water, and cold water is presented in Table 3

In Figure 8, a comparison between the electrical energy production and electrical energy usage is presented. The latter is tabulated separately for the office equipment, the pumps, the ventilation, and the main chiller. The energy usage of the office equipment was always 9.1 kWh. The pumps bar shows the energy usage of all three pumps shown in Figure 5. The solar loop pump was operated continuously, while the operation of the other two pumps differed between configurations. The total energy usage of the three pumps varied from 1.3 kWh (Configuration 5) to 1.6 kWh (Configurations 1 and 4). The lower energy usage in the fifth case was expected since the PCM pump was deactivated. The ventilation bar includes the energy usage of the fan and the cooling coil. The energy usage of the ventilation system varied from 1.2 kWh in Configurations 1 and 2, to 3.6 kWh in the others. The higher energy usage in the last three cases was because the ventilation was also operated during the night. Since the specific fan power (SFP) was not known, an SFP of 1000 W/(m³/s) was assumed, which corresponds to Category SFP 3 of the standard DS/EN 13779 (DS/EN 2007a). In order to calculate the energy usage of the cooling coil and the chiller it was assumed that an air-to-water heat pump was used. The specifications of a heat pump
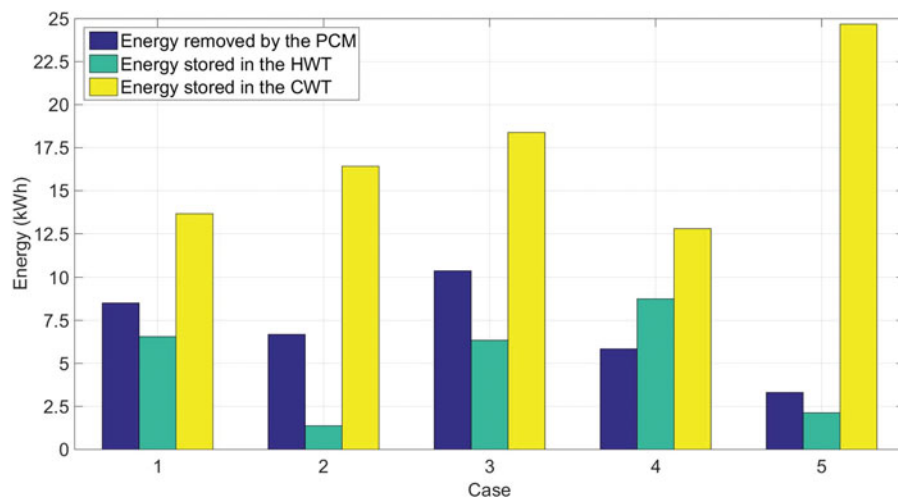
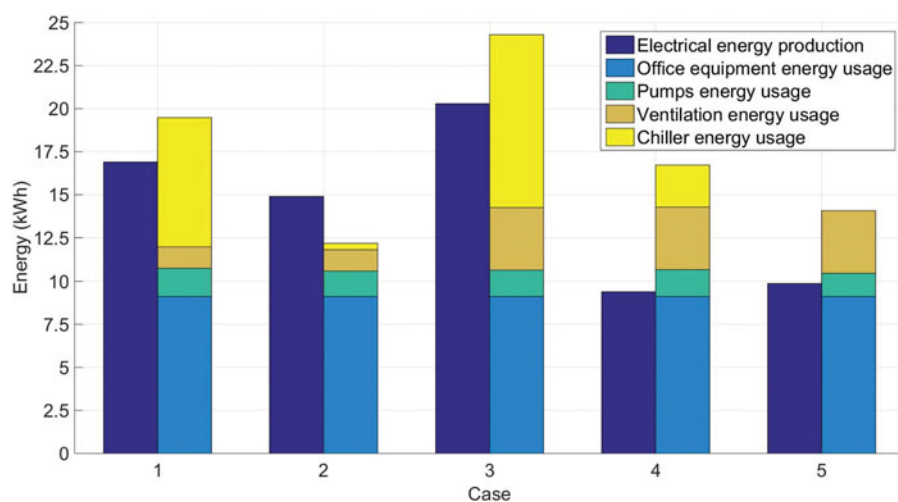**Fig. 7.** Energy output of the PV/Ts and the PCM.

Fig. 8. Energy production and usage comparison.

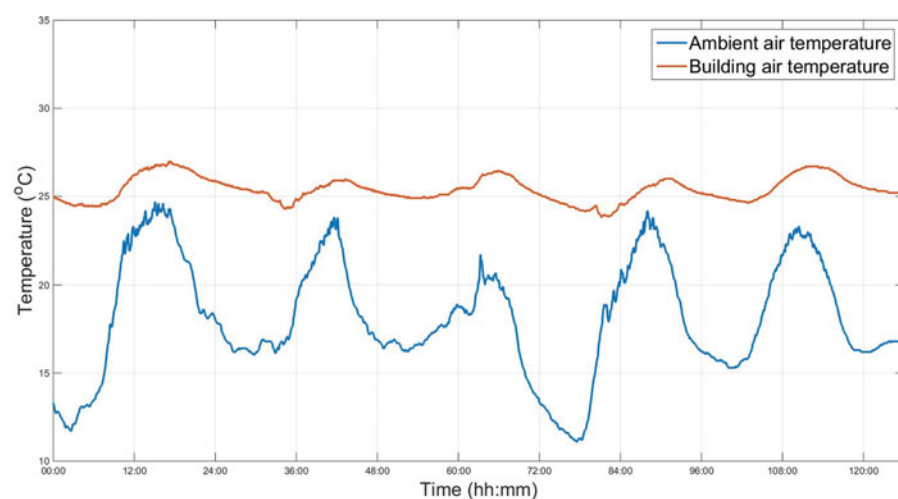**Fig. 9.** Ambient and building air temperature (August 10–14, 2015).

Table 4. Ambient weather conditions during the experiments.

Case number	Min. outside air temperature, °C	Max. outside air temperature, °C	Avg. outside air temperature, °C	Solar radiation on the panels, kWh/m^2	Total rain precipitation, mm	Max. wind speed, m/s	Aver. wind speed, m/s
1	11.1	24.7	18.2	1656	4.8	5.4	1.1
2	7.2	19.2	13.5	1276	0.4	4.9	1.1
3	13.5	25.6	19.0	1908	0.0	4.9	1.7
4	10.1	21.8	15.6	898	14.8	6.7	1.5
5	9.1	20.4	14.8	1130	24.8	7.2	1.8

available on the market were used, based on which a seasonal coefficient of performance (COP) of 4.5 was calculated. With this COP, the electricity usage of the chiller in Configurations 1–4 varied from 0.4 kWh in Configurations 2, to 10 kWh in Configurations 3, while in the fifth configuration it was deactivated. The electrical energy production from the PV/Ts varied from 9.4 kWh (Configuration 4) to 20.3 kWh (Configuration 3). This considerable difference between the different configurations can be explained by the different weather conditions to which the panels were exposed at during the experiment. The percentage of electricity usage covered from PV/Ts varied from 56% in case 4, to 122% in case 2 which was the only case in which the electrical energy production from the PV/Ts covered the electrical energy demand of the chamber.

Discussion

Analyzing the performance of each configuration in terms of Category III, it may be seen that improving the air mixing in the second configuration resulted in a slight improvement in the percentage of time within the Category III range by 3%, while adding night-time ventilation resulted in a further improvement of 4% in the third configuration. When air mixing was no longer increased artificially, the percentage dropped back to 95%. By comparing the second and the fourth

configuration, it may be seen that although they were within the Category III range for the same percentage of time, in Configuration 2 the percentage of time within the Category I and II ranges was significantly higher than in Configuration 4, in which these percentages were less than that of the first configuration. Thus, improving the air mixing had a bigger impact in improving thermal conditions than implementing night-time ventilation. In Configuration 5, the airflow rate or air temperature proved insufficient for discharging the PCM which resulted in overheating during the occupied period.

Since the chamber was not exposed to the weather conditions, the ambient conditions for the chamber and the PV/Ts were not always the same. The ambient air temperature and the air temperature inside the building housing the chamber during Configuration 1 are shown in Figure 9. The ambient air temperature was measured at a weather station installed next to the PV/T panels, while the building air temperature was measured just outside the chamber. The small fluctuation in the building's air temperature ensured that the performance of the PCM was affected only by the configuration employed and not by external factors such as the ambient weather conditions.

All the parameters that were related to the PV/T panels, e.g., water flow rate, tilt angle, and orientation, were kept constant through all five different configurations. Therefore, the fluctuations observed in the results presented in Figure 7 and Table 3 were caused by changes in the ambient weather
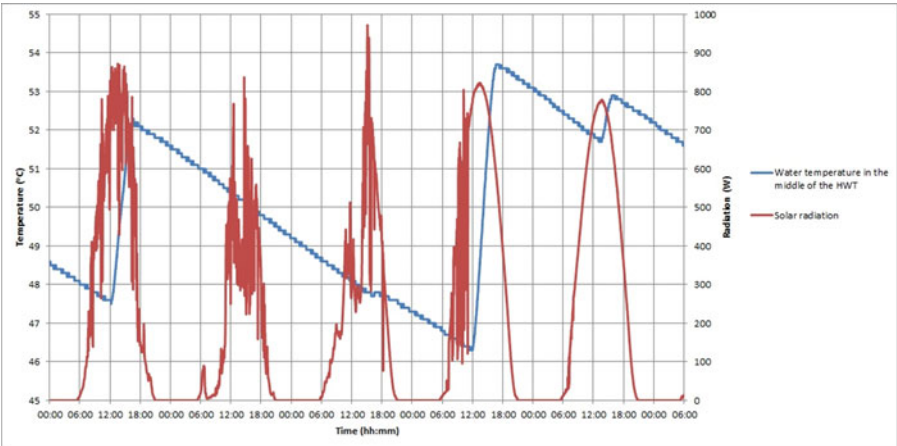
Fig. 10. Correlation between solar radiation and HWT temperature (August 10–14, 2015).

conditions which are shown in Table 4. An accurate performance of the panels thus cannot be estimated without a detailed weather prediction.

The experiment was mainly focused on examining the performance of the night-time radiative cooling principle, so the hot water stored in the HWT was not utilized. During a sunny day the temperature in the HWT increased considerably. Since the hot water was not used, the only temperature drop in the HWT was caused by heat losses. Therefore, the following day the pump placed after the heat exchanger would hardly be activated since Condition (1; as stated in the Method paragraph) would not be fulfilled, even if the weather conditions were capable of producing hot water. This can be seen in Figure 10, which shows the temperature in the middle of the HWT and the solar radiation measured during the first experiment. This resulted in an underestimation of the performance of the PV/Ts in terms of domestic hot water production.

As it is shown in Figure 7, in order to discharge the PCM panels completely, more energy was required than the actual energy that is stored in the panels. This is due to the low thermal conductivity of the PCM used in the specific panels. Connecting directly the PV/Ts with the PCM panels would reduce the heat losses, but since cold water was also circulated during daytime, the storage tank could not be avoided.

Péan et al. (2015) measured the cooling power of PV/T panels for 2 weeks and an average value of 89.6 W/m² was measured. Only the result of the fifth configuration was comparable to the results obtained by Péan et al., while it was significantly lower in all of the other configurations. For the two experiments the same panels were used. The fluctuation observed in the values of the two experiments were attributed to the different values of the water flow rate (94 L/h in the present experiment while 120 L/h in Pèan's et al. [2015] experiment) and the variation of the weather conditions during the two experiments.

Although in most of the configurations the PV/Ts did not provide all of the electrical energy required, the production of hot and cold water from the PV/Ts would reduce the operating time of chillers or heaters. If a water-to-water heat pump or a ground source heat exchanger was used instead of an air-to-water heat pump a higher COP would be achieved and the energy usage of the chiller would be reduced.

Conclusions

1. The PCM ceiling panels were capable of providing an acceptable thermal environment in the office room when the embedded cooling pipes were in use.
2. The airflow rate proved insufficient when only night-time ventilation was used as discharging method.
3. PV/T panels can be an efficient solution for producing electrical energy, domestic hot water and cold water for space cooling, contributing to the spread of nZEBs.

4. Although the PV/T panels performed satisfactorily, their performance cannot be accurately predicted due to variation in the weather conditions to which they were exposed.

References

Babiak, J., B.W. Olesen, and Dušan Petráš, 2013. *Low Temperature Heating and High Temperature Cooling*. Finland: REHVA.

BASF. 2010. Micronal PCM–intelligent temperature management for buildings. http://www.micronal.de/portal/load/fid774774/ Catalogue Micronal PCM.pdf.

Cabeza, L.F., C. Castellón, M. Nogus, M. Medrano, R. Leppers, and O. Zubillaga. 2007. Use of microencapsulated PCM in concrete walls for energy savings. *Energy and Buildings* 39(2):113–9.

DS/EN. 2007a. 13779: Ventilation for non-residential buildings. Performance requirements for ventilation and room-conditioning systems. (2).

DS/EN. 2007b. DS/EN 15251: 2007 Indoor environment input parameters for design and assessment of energy performance of buildings adressing indoor air quality, thermal environment, lighting, and acoustics.

DS/EN ISO. 2001. ISO 7726: Ergonomics of the thermal environment—instruments for measuring physical quantities.

Eicker, U., and A. Dalibard, 2011. Photovoltaic-thermal collectors for night radiative cooling of buildings. *Solar Energy* 85(7):1322–35. http://dx.doi.org/10.1016/j.solener.2011.03.015.

EP. 2009. Directive 2009/28/EC of the European Parliament and of the Council of April 23, 2009 on the promotion of the use of energy from renewable sources and amending and subsequently repealing Directives 2001/77/EC and 2003/30/EC. *Official Journal of the European Union* 140(16):16–62.

EP. 2010. Directive 2010/31/EU of the European Parliament and of the Council of May 19, 2010 on the energy performance of buildings (recast). *Official Journal of the European Union* 152(13):13–35.

Fiorentini, M., P. Cooper, and Z. Ma, 2015. Development and optimization of an innovative HVAC system with integrated PVT and PCM thermal storage for a net-zero energy retrofitted house. *Energy and Buildings* 94:21–32. http://www.sciencedirect.com/science/article/pii/S0378778815001139.

Hosseinzadeh, E. and H. Taherian. 2012. An experimental and analytical study of a radiative cooling system with unglazed flat plate collectors. *International Journal of Green Energy* 9(October):766–79. http://www.scopus.com/inward/record.url?eid = 2-s2.0-84870328 243&partnerID = tZOtx3y1

Koschenz, M., and B. Lehmann, 2004. Development of a thermally activated ceiling panel with PCM for application in lightweight

and retrofitted buildings. *Energy and Buildings* 36(6):567–78. http://www.sciencedirect.com/science/article/pii/S037877880400-0702

Krasimirov Pavlov, G. 2014. Building thermal energy storage (April):313.

Lin, W., Z. Ma, M. I. Sohel, and P. Cooper. 2014. Development and evaluation of a ceiling ventilation system enhanced by solar photovoltaic thermal collectors and phase change materials. *Energy Conversion and Management*, 88:218–30. http://www.sciencedirect.com/science/article/pii/S0196890414-007432

Meir, M.G., J.B. Rekstad, and O.M. Løvvik. 2002. A study of a polymer-based radiative cooling system. *Solar Energy* 73(6):403–17.

Olesen, B. 1997. Possibilities and limitations of radiant floor cooling. *ASHRAE Transactions-American* 50(9):42–8.

Olesen, B. 2008. Radiant floor cooling systems. *Ashrae Journal* 50(9):16–20.

Zhao, K., X.-H. Liu, and Y. Jiang. 2013. Application of radiant floor cooling in a large open space building with high-intensity solar radiation. *Energy and Buildings* 66(11):246–57.

Paper 2: Bourdakis E., Simone A., & Olesen B.W. (2018). An experimental study of the effect of different starting room temperatures on occupant comfort in Danish summer weather. Building and Environment. https://doi.org/10.1016/j.buildenv.2018.03.046

Contents lists available at ScienceDirect

Building and Environment

An experimental study of the effect of different starting room temperatures on occupant comfort in Danish summer weather

Eleftherios Bourdakis[*], Angela Simone, Bjarne W. Olesen

International Centre for Indoor Environment and Energy (ICIEE), Department of Civil Engineering, Technical University of Denmark (DTU), Building 402, Kongens Lyngby, 2800, Denmark

ABSTRACT

As office workers will usually have a slightly elevated metabolic rate when arriving at work, they may prefer a room temperature below the comfort range for sedentary activity in the morning. This possibility was studied in an experiment with 25 young people, male and female, exposed to four different conditions. Each condition consisted of two sessions, the simulated commute (activity equivalent to walking to work) and the office session. Each office session had a different starting room temperature, namely 18.5 °C, 20 °C, 21.5 °C or 23 °C, followed by an increasing temperature "ramp" of 1.5 K every 30 min. During the last 30 min the temperature remained constant. Physical measurements were continuously recorded and subjective evaluation questionnaires were completed every 30 min. It was observed that, upon arrival at the office-lab, a room temperature of 20 °C provided a thermal environment with neutral thermal sensation (0.23), low thermal dissatisfaction (8.6%) and a high level of thermal comfort for the whole body (3.3). It was concluded that, in the cooling season, to improve the thermal sensation of occupants, a lower temperature than is suggested by the existing standards should be maintained in the early office hours, and that this will lead to a lower maximum room temperature during the day, which would result in less demand for cooling during the summer period.

1. Introduction

According to ISO Standard 7730 [1], thermal comfort is "the condition of mind that expresses satisfaction with the thermal environment". Warm or cold discomfort of the whole body, or unwanted heating or cooling of a human body part, can cause dissatisfaction and lead to thermal conditions being judged unacceptable. Several studies have correlated thermal discomfort with low productivity in school and office working environments [2–4]. In addition, according to Wyon and Wargocki [5], thermal discomfort also causes distraction, generates complaints and increases the intensity of Sick Building Syndrome (SBS) symptoms. SBS symptoms include headache, nose irritation (stuffy, running), irritated throat, fatigue, dry eyes, difficulty in concentrating, a lack of alertness etc. The literature shows that increased room air temperature resulted in increasing the intensity of symptoms of fatigue, headache and difficulty in concentrating [6], [7]. A field study conducted in an office building, showed that lower temperature, even within the comfort range, reduced the intensity of SBS symptoms [8].

Due to fluctuations in solar heat gains, occupancy level and equipment, steady-state conditions are rarely observed in practice. Nevertheless, the majority of human subject experiments examining

thermal comfort have been conducted under steady-state conditions and in a thermally uniform environment [7] [9–16] or in a non-uniform but constant thermal environment [8] [17–22]. Only a few studies have been conducted under transient uniform conditions. Kolarik et al. examined different temperature ramps and observed a linear relationship between mean thermal sensation and operative temperature [7]. In another study examining thermal sensation under transient conditions for sedentary unclothed men, it was found that when the temperature was increasing, the rate of rise of skin temperature caused a sensation that reduced the discomfort caused by the lower skin temperature [15]. Griffiths and McIntyre examined steady state and 3 levels of temperature ramps, both increasing and decreasing, and developed a method for estimating the degree of dissatisfaction produced by temperature changes [23]. Goto et al. investigated the impact of different activity intensity and duration on thermal sensation and concluded that participants' thermal sensation was more sensitive to changes in core temperature caused by a reduction in activity than by increased activity [24]. McIntyre and Gonzalez examined the impact of clothing insulation and activity level on men's thermal sensitivity during rapid temperature drops and found that for resting subjects, thermal sensitivity was not affected by clothing insulation or season [25]. A literature

---

review study of thermal comfort in transient conditions showed that ramps between 0.5 K/h and 1.5 K/h have no impact on the range of the comfort zone [26]. In all of these studies, either the participants had been acclimatized for a period of time in an environment similar to that of the experiment, to negate any effect of previous activities, or no information was provided about their previous metabolic rate. No study was found that correlated thermal sensation in an office environment with previous activity, e.g. commuting on foot or bicycling.

Adaptive thermal comfort has attracted the attention of the thermal comfort community and has been implemented in ASHRAE and CEN standards [27], [28]. The principle of the adaptive approach is that occupants have the possibility to adjust their clothing level, open or close the windows, draw the curtains to reduce solar heat gains, etc. Moujalled et al. conducted a field study in four office buildings in southeast France during Summer-Autumn and found that the subjects' vote was in close agreement with the adaptive control for naturally ventilated buildings [29]. In another study, a survey was conducted in nine schools in Australia during summer and it was found that the more thermally sensitive group of students originated from naturally ventilated schools than air-conditioned schools [30]. Damiati et al. conducted a field study in 13 office buildings in Malaysia, Indonesia, Singapore and Japan running in three different modes (heating, cooling and free-running mode) and found that the results for the free-running mode very mostly within the comfort range of EN 15251 [27]. They also observed that the most frequent personal adaptive behaviour varied among the four countries, namely, turning on the air-condition in Malaysia, or drinking cold beverages in Indonesia and Japan [31]. Liu et el. introduced a method to quantify the physiological, behavioural and psychological portions of the adaptation process and concluded that the physiological adaptation was the dominant factor in the creation of an acceptable thermal environment [32]. It should be stated though, that the adaptive approach incorporated in standards is used for the evaluation of buildings where no mechanical system is in use for the condition of the indoor temperature, and the occupants have the freedom to open or close the windows and adjust their clothing level.

Most offices need cooling even in temperate climates like Denmark due to more airtight building envelopes. Several papers and studies show the benefits of using night cooling combined with the active use of thermal mass in the building [33–37]. These benefits are mainly due to transferring some of the cooling from day-time to night-time and reduction of the peak load. During night-time the potential for using free cooling (evaporative cooling, increased ventilation with cooler outside temperatures) and the use of lower electricity rates, will result in significant energy benefits. During the day the temperature drifts upwards due to solar heat gains and the internal loads from occupants and equipment. It is however important that the temperature drift within the comfort zone [27], [28]. The study by Kolarik et al. showed that a drift even up to 4.8 K/h was acceptable as long as the room temperature stayed in the comfort range [7].

In the existing standards [27] [28], there is a seasonal effect on both the adaptive model and the PMV-PPD approach mainly due to change in clothing level from winter to summer. The effect of a change in metabolic rate (activity level) during the day on the acceptable room temperature has not been studied in detail. Most people will have an increased activity (higher than sedentary) coming to work. This may result in a feeling of warmth arriving in an office controlled for sedentary comfort. A little lower temperature than the comfort range may improve the comfort when arriving in the office and at the same time increase the potential use of night-cooling. The present study investigated that issue, focusing on the conditions in office buildings that can exploit the possibility of night-cooling.

The aim of this study was to examine the impact of increased metabolic rate on thermal sensation when entering an office room that has a lower temperature than is recommended by European Standard 15251 [27]. The authors conducted a human subject experiment in which the effect of commuting to work on foot (estimated and planned to be 2 met on average) was taken into consideration when the participants were asked to evaluate thermal sensation, acceptability and comfort when entering a climate chamber simulating an office space.

2. Experimental methods

The experiment was carried out in the climatic chambers of the International Centre for Indoor Environment and Energy (ICIEE) at the Technical University of Denmark (DTU) in the period mid of April to beginning of May. Based on the Köppen-Geiger climate classification, Copenhagen is classified as category Cfb, namely, temperate oceanic climate, fully humid with a warm summer. Chamber 3 was constructed to accurately control the thermal environment [38]. Its dimensions are 5 m × 6 m x 2.5 m and the walls are made of two layers of porous vinyl sheets. Air was supplied to the chamber through the floor (equally distributed), and by penetrating the vinyl wall-sheets. This construction ensured identical room air and mean radiant temperature, and consequently an operative temperature equal to air temperature. Prior to the experiment, the authors took air speed measurements in several locations inside the room, using heat dummies in the positions to be occupied by the subjects, to simulate the conditions and the heat gains of the actual experiment. This pre-test study of the distributed physical room conditions was conducted to ensure that the office-lab had the standardized acceptable room conditions without causing any draft, thermal discomfort or air movement discomfort. The anemometers were installed on a vertical stand at 0.1 m, 0.3 m, 0.6 m, 0.9 m, 1.1m, 1.4 m, 1.7 m, and 2 m above the floor to examine the vertical stratification. The highest air speed measured was 0.09 m/s, which was considered unlikely to affect the thermal comfort of the participants. Fig. 1 shows the results of the air speed measurements, while the location of the points of measurement are shown in Fig. 2.

Initially, 30 DTU students were recruited and allocated randomly to groups of five. Their age varied from 22 to 27 years old, they were healthy and physically fit and they all had a normal Body Mass Index (BMI), namely between 18.5 and 25 kg/m^2. BMI is obtained by dividing a person's weight (in kg) by the square of his/her height (in metres). The participants were requested to wear light summer clothing and this resulted in an effective clo-value of 0.5 when the insulation of an office chair was included (ASHRAE Standard 55 Table 5.2.2.2C [28]). Each subject participated in four different sessions, experiencing each session only once. Two sessions were executed per day, one starting at 8:30 and one starting 13:00. To minimize possible bias caused by the order of exposure, the four sessions were spread randomly during the three weeks of the experiment, and it was ensured that no participant would come twice on the same day or on consecutive days. By the end of the experiment, only 25 subjects had participated in all four sessions, so only their responses were processed. Due to absence, the number of participants in each session varied from three to five, as is common in an open-office work situation. Table 1 shows the anthropometric information for the 25 remaining participants.

Each session consisted of two phases: the commute phase, which simulated commuting to work on foot, and the office phase. This climatic chamber was furnished to represent a five-person landscape office: each participant was provided with a desk, a chair, and a laptop connected to the internet. Upon arrival, all participants were fitted with a heart rate sensor. In addition, four iButton skin temperature sensors (accuracy ± 0.5 °C) were placed on each participant, on the forehead, the right palm, the right scapula and the right shin, so that local skin temperature and an estimate of the area-weighted mean skin temperature could be recorded. The level of skin temperature can cause both local and whole body thermal discomfort. Therefore, the authors recorded the participants' skin temperature to examine whether any extremely low or high skin temperature values were recorded. Heart rate and skin temperature were measured throughout each session.

The first part of the experiment was conducted in a HVAC controlled office room with a view of the garden outside. In this room the average
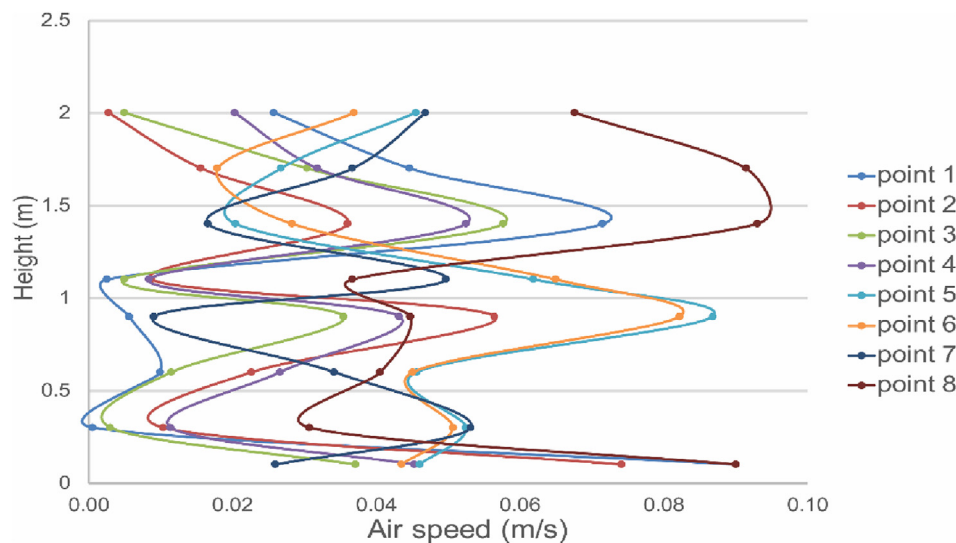
Fig. 1. Air speed measurements at different heights and locations in Chamber 3.
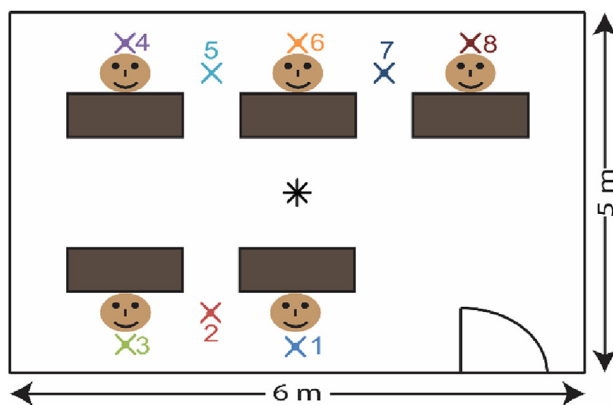

Fig. 2. Graphical representation of the conditioned office room, the location of the five desks, the air speed measurements and the stand with the control air and operative temperature sensors.

Table 1
Anthropometric data of the experiment participants.

Genre	Age	Height, cm	Weight, kg	BMI, kg/m²
Female	25 ± 1.4	1.67 ± 0.07	61.2 ± 6.7	21.9 ± 2.4
Male	25 ± 1.6	1.81 ± 0.07	75.9 ± 5.8	23.2 ± 0.8
Both	25 ± 1.5	1.74 ± 0.1	68.5 ± 9.7	22.5 ± 1.8

outdoor air temperature for Northern European summer weather conditions at the typical working day commuting time, from 07:00 to 09:00, was maintained (18 °C). For this commute session, three treadmills and two steps were installed on which the subjects exercised for 15 min at an average activity level of 1.5 met. In order for all participants to have equivalent activity levels, the subjects switched positions so that they exercised for a total of 9 min on the treadmill and 6 min on the steps.

After the commuting session, the participants walked directly into the conditioned office room and sat down at their assigned desk (second experimental session). Fig. 2 shows a graphical representation of the conditioned office room, the location of the five desks and the locations where the air speed measurements shown in Fig. 1 were taken. The star in the centre of figure shows the location of the stand with the air and operative sensors controlling the conditions in the chamber. The distance between the subjects was 1 m, to ensure that any effect of

convective or radiative heat exchange with adjacent subjects was negligible.

At the beginning and end of each session and at 30-min intervals throughout the session, the participants were requested to complete an online questionnaire. In the meantime, participants played various simple games on the computer (e.g. Sudoku) to replicate a normal office activity level. In the questionnaires, the participants reported thermal sensation, thermal comfort, the acceptability of the thermal conditions at that specific moment and the intensity of any SBS symptoms. The SBS symptoms included in the questionnaires were headache, nose irritation (stuffy, running), irritated throat, fatigue, dry eyes, difficulty in concentrating and sleepiness. When conducting a human subject experiment, the questionnaire should include more questions than those necessary for the particular study, to have a complete knowledge of the indoor environment quality (IEQ) parameters of the built offices' environment and to ensure that the participants will work blind of the aim the investigation to avoid bias. In the present case, the authors had included questions about air quality, noise level, lighting intensity etc. Fig. 3 shows some of the questions included in the questionnaires.

During this phase of the experiment, the air temperature was increased by 1.5 °C every 30 min, and then kept constant during the last 30 min. According to ASHRAE Standard 55 [28], the room temperature increase within 30 min should be no more than 1.7 K, so the temperature ramp complied with the suggested limits. The relative humidity was kept constant around 50%. Table 2 shows the temperature schedule for the four different sessions examined, whose duration varied.

3. Results

3.1. Gender comparison

Random- and mixed-effects models were used to examine the significance of differences between temperatures for all three thermal comfort questions (sensation, acceptability and comfort). Quantile-quantile plots (QQ-plots) were used to test whether the residuals were normally distributed. The P-level for significance was set to 0.05 as in a similar study [7]. Table 3 shows the p-values for the responses of thermal sensation, thermal acceptability and thermal comfort between the male and female participants. No significant gender difference was found, so in the rest of the thermal comfort analysis their responses were pooled. When combining the two gender results (as no significant difference was observed), the results were very close to being normally distributed. Therefore, it was decided to use mean values and standard deviation to describe them.
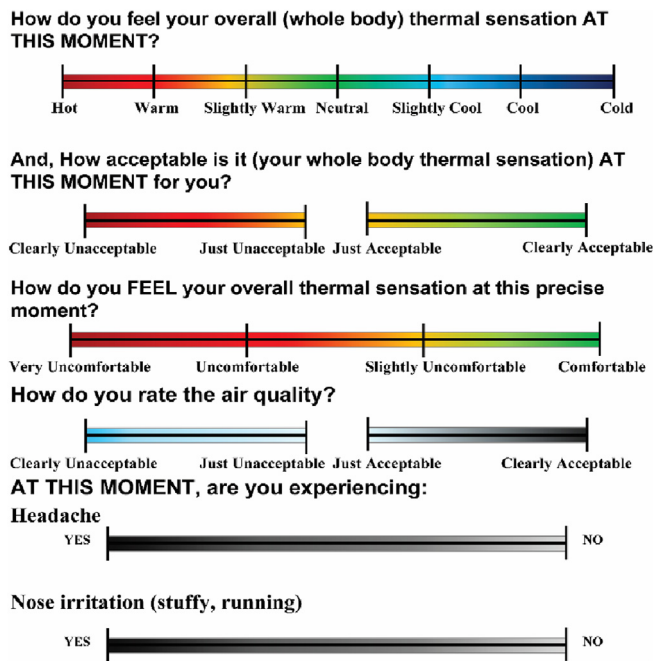
Fig. 3. Some of the questions included in the questionnaires.

Table 2
Temperature schedule for the 4 sessions.

Time of change	00:00	00:30	01:00	01:30	02:00	02:30	03:00
Case 1	18.5 °C	20 °C	21.5 °C	23 °C	24.5 °C	24.5 °C	
Case 2	20 °C	21.5 °C	23 °C	24.5 °C	26 °C	27.5 °C	27.5 °C
Case 3	21.5 °C	23 °C	24.5 °C	26 °C	26 °C		
Case 4	23 °C	24.5 °C	26 °C	27.5 °C	27.5 °C		

Table 3
p-values for a gender difference in responses to the thermal comfort questions.

	Whole body thermal sensation	Thermal sensation acceptability	Thermal sensation comfort
Case 1	0.78	0.74	0.87
Case 2	0.70	0.57	0.91
Case 3	0.66	0.71	0.70
Case 4	0.58	0.33	0.28

3.2. Skin temperature

As for the responses to the thermal comfort questions, it was first determined whether there was a significant difference between the responses of male and female participants. Table 4 shows the p-values for the skin temperature measurements. No significant differences were observed for the sensors placed on the right hand and the forehead of the participants, namely the two sensors that were exposed directly to room air. On the other hand, for the two sensors that were covered by the participants' clothing, significant differences were observed between the responses of the two genders. The cells highlighted in bold

Table 4
p values for a gender difference in skin temperatures.

	Right hand	Forehead	Right scapula	Right shin
Case 1	0.51	0.53	**0.01**	0.41
Case 2	0.52	0.47	**0.02**	0.15
Case 3	0.38	0.36	0.14	**0.03**
Case 4	0.48	0.83	0.98	**0.01**

were the cases in which a significant difference was found. Female participants had higher skin temperature on the right scapula during the whole session, while male participants had higher skin temperature on their right shin throughout the whole session.

Fig. 4 shows the average skin temperature of all participants on the forehead, the right palm, the right scapula and the right shin, for each case separately. The vertical black dashed line separates the figures into the exercise phase on the left side of the line and the office phase on the right side of the line. At the end of the exercise period, all four cases had almost the same skin temperature in all four locations measured, since the PV Lab maintained a constant temperature throughout the experiment. The temperature differences measured in the four cases on the scapula and the shin were not significant, since these two sensors were covered by the participants' clothing. A similar trend was also observed on the forehead, although this sensor was exposed and in direct contact with room air. On the other hand, the temperature differences measured on the palm sensor differed markedly between cases. At thermal neutrality, skin temperature is around 33 °C and the flow of energy to and from the skin determines a person's sense of hot and cold. No extreme values were recorded, that could have caused local or whole-body thermal discomfort.

3.3. Whole body thermal sensation

Fig. 5 shows the whole body thermal sensation and its standard deviation as a function of the room temperature. At the starting temperature of 18.5 °C, the subjects felt closest to neutral when they entered the chamber, compared to the other three cases. The effect of exercising quickly decreased, and subjects reported feeling slightly cool in the second questionnaire of Case 1. This indicates that after half an hour, the results are largely dependent on the room temperature, and unaffected by any preceding activity. The responses were close to neutral again only when the room temperature was at least 23 °C. This corresponds to what was proposed by European Standard 15251 [27]. A temperature range of 23–24.5 °C was proposed as the most neutral. When the participants entered the chamber at the room temperatures of 21.5 °C and 23 °C (Cases 3 and 4 respectively), they reported slightly warm thermal sensations. Fig. 5 confirms that 24.5 °C was the most neutral temperature. When the temperature remained constant at 27.5 °C (the last 30 min of Cases 2 and 4), the subjects adapted to it even though it is above the upper limit of Category III of the Standard 15251, namely 27 °C [27]. Furthermore, although the starting temperature of Cases 2 and 4 differed by 3 K, after 26 °C the participants' responses were almost identical. The starting point of each session thus had no influence at the end of each session. By calculating the area under each curve, it was found that the case that deviated the least from the neutral point was Case 3. This was due to the fact that after the initial 30 min, the room temperature was 23 K and therefore remained for most of the time period within the neutral range of Category II of Standard 15251, namely 23 °C–26 °C [27].

Kolarik et al. [7] reported whole body thermal sensation of approximately -0.5 when the starting room air temperature was 22 °C, the clo-value 0.5 and the metabolic rate 1.2 met. In the present study, the closest starting room air temperature was 21.5 °C (Case 3) for which the mean whole-body thermal sensation was 1.06. Although in the present study the room air temperature was 0.5 K lower, whole-body thermal sensation was significantly higher when entering the chamber. This difference is attributed to the different metabolic rate values in the two experiments.

Fig. 6 shows the whole-body thermal sensation in boxplots, separately for male and female participants, for the first questionnaire. In all four cases, the responses from each gender were quite similar. In Cases 1 and 2 the median and the ± 25% of the responses were around neutral, while in Cases 3 and 4 they reached a slightly warm value. In Cases 3 and 4 the box indicating the central 50% of responses is smaller, which indicates less variation between the responses of different
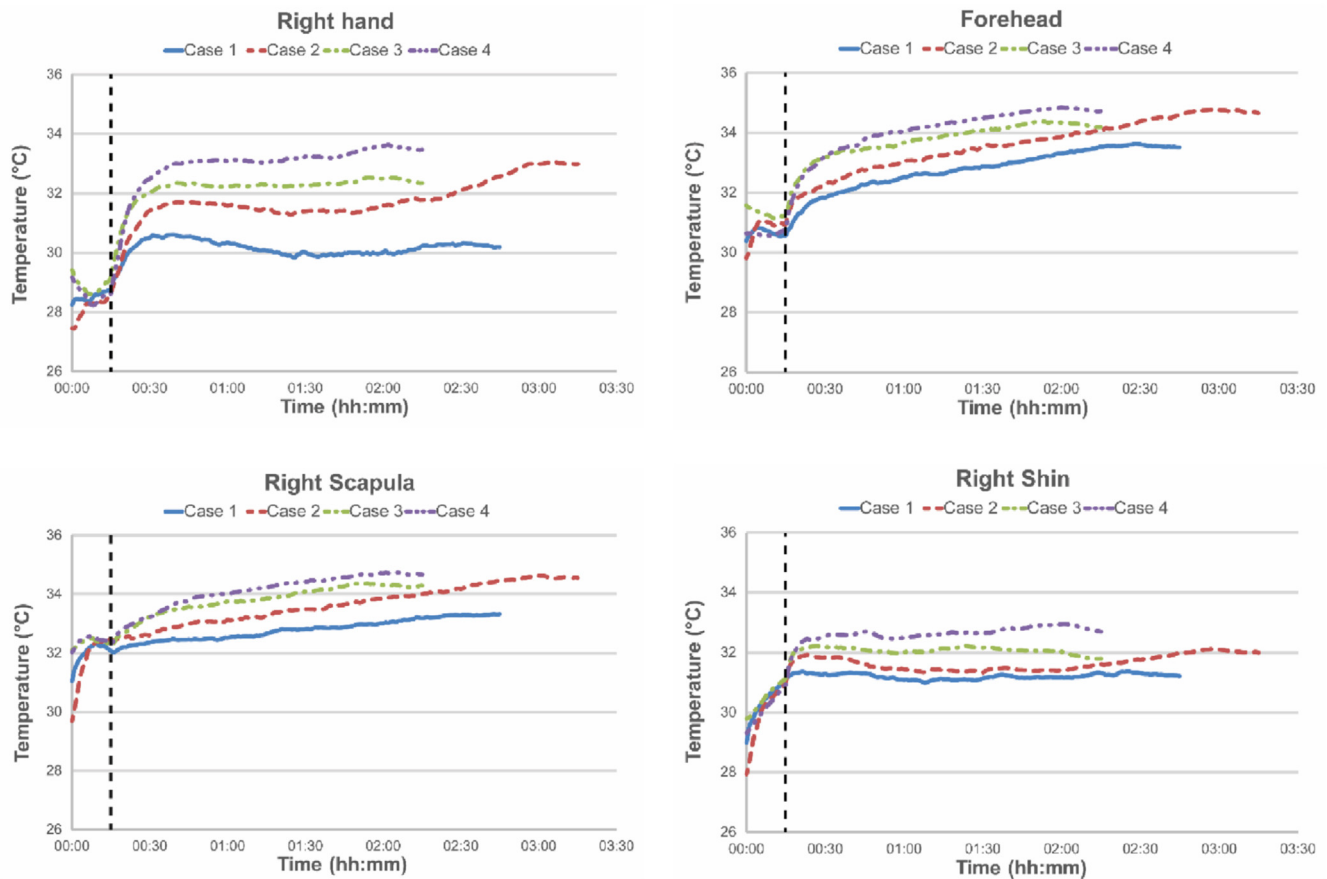
Fig. 4. Average skin temperature for each case.

subjects. This figure also supports the previous conclusion that the differences between male and female subjects were small.

3.4. Whole-body thermal acceptability

Fig. 7 shows the mean values of the whole-body thermal acceptability as a function of the room temperature. As before, the lower the room temperature at the beginning of the session, the higher the acceptability. Case 1 was the only case that returned a lower acceptability value at the second questionnaire compared to the first one, meaning that once the participants' metabolic rate dropped to a value typical of office work, a room air temperature of 20 °C proved to be too low. On the other hand, Case 2, with a starting temperature of 20 °C followed by the 1.5K/0.5 h ramp, had the highest acceptability value before it exceeded 26 °C, which is the upper limit of Category II of Standard 15251 [27]. Case 2 yielded the highest acceptability: from 21 °C to 26 °C the thermal acceptability remained almost unchanged. The lowest acceptability was recorded in the initial questionnaire of Case 4, when the
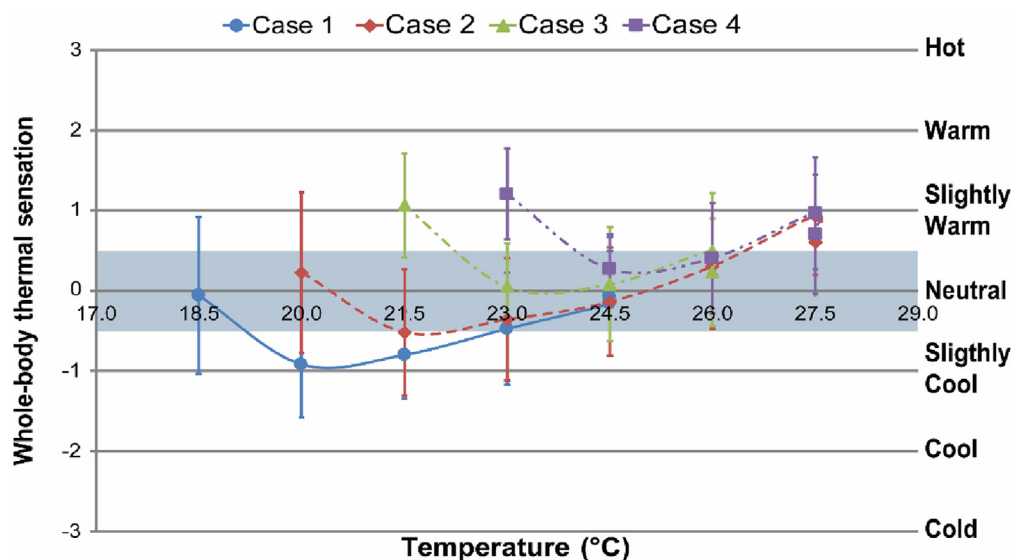
Fig. 5. Whole-body thermal sensation as a function of the room air temperature. Whiskers show the standard deviation for each questionnaire.
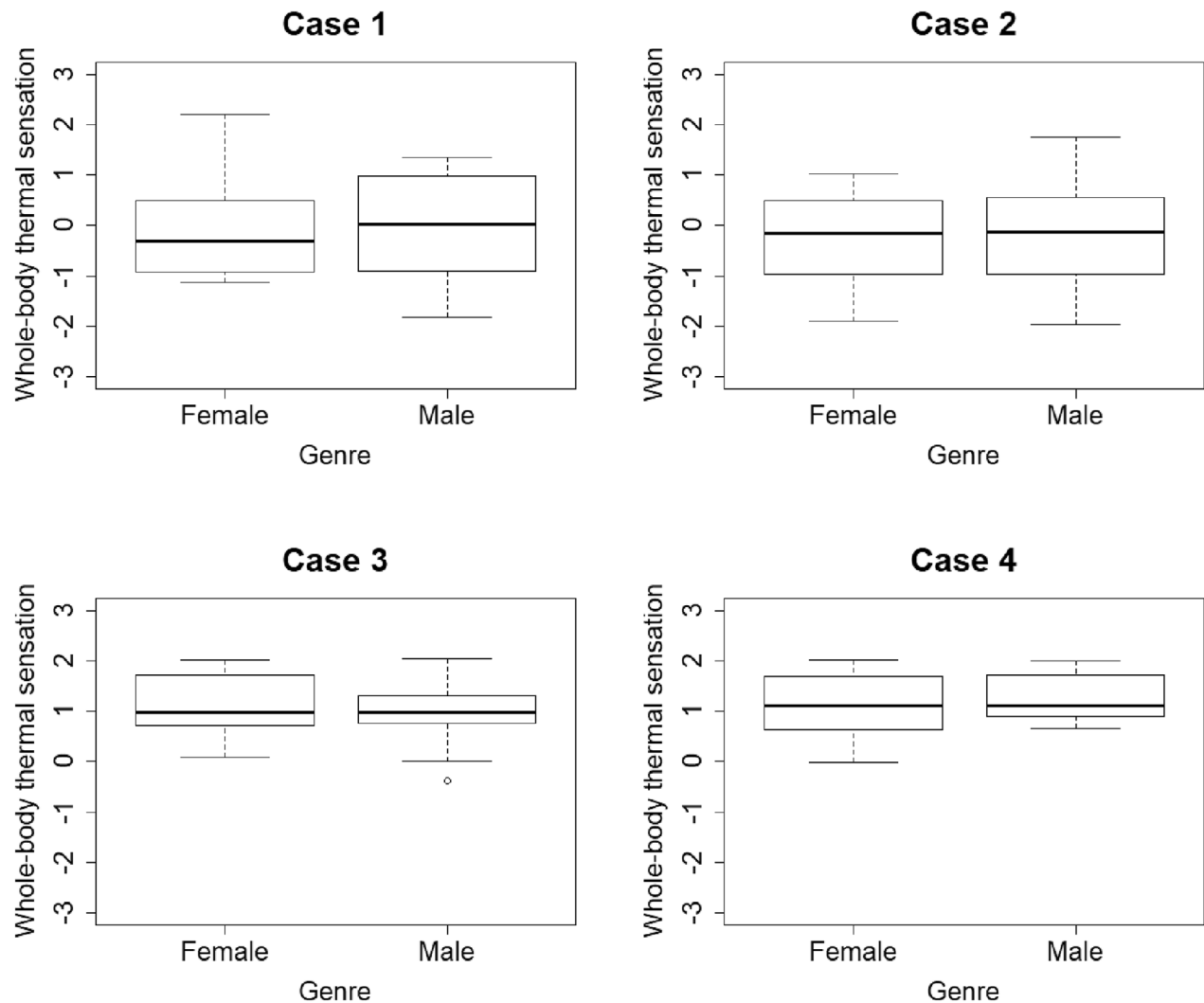
Fig. 6. Whole-body thermal sensation for the first questionnaire of each case separately.

room temperature was 23 °C. Although this is the lower limit of Category II of Standard 15251, it was considered as just acceptable. Due to the decrease in the subjects' metabolic rate, the increased room temperature at the second questionnaire was reported as more acceptable. A similar trend was also observed in Case 3, but with slightly higher

values of thermal acceptability.

3.5. Whole body thermal comfort

Fig. 8 shows whole-body thermal comfort as a function of room

Fig. 7. Whole-body thermal acceptability as a function of the room temperature. Whiskers show the standard deviation for each questionnaire.

Fig. 8. Whole-body thermal comfort as a function of the room temperature. Whiskers show the standard deviation for each questionnaire.

temperature. As before, the lower starting room temperature of the first two experimental cases yielded the highest values of thermal comfort at the beginning of each session, 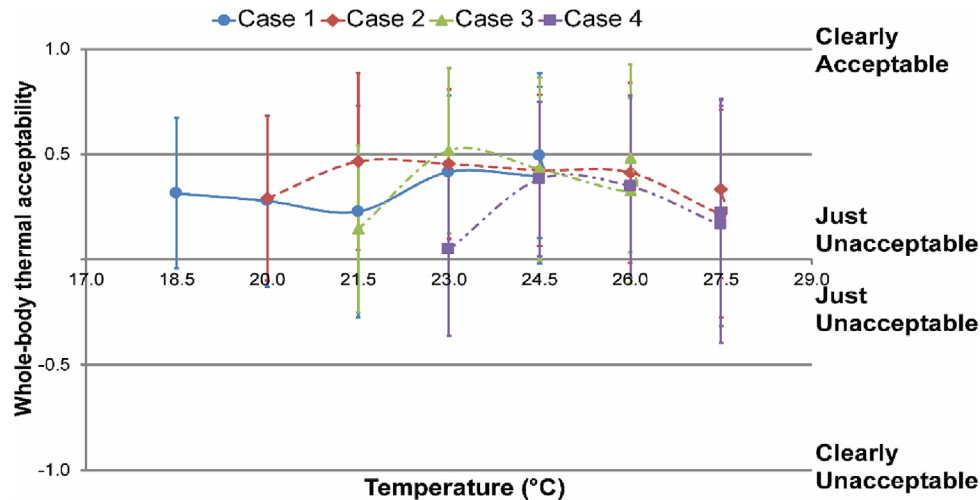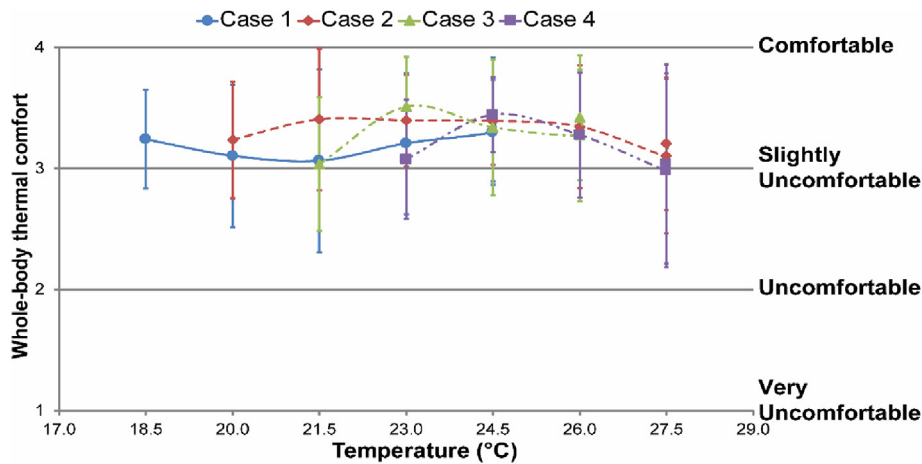although this time the differences were smaller. For all the experimental cases, whole-body thermal comfort was always above the "slightly uncomfortable" level. When the room temperature exceeded 26 °C (Cases 2 and 4), the room temperature was evaluated as less comfortable. In all four cases, when the room temperature remained constant at the end of the sessions, participants felt slightly more comfortable after being exposed to the same temperature for 30 min. The most comfortable temperature range was 23 °C–26 °C. Case 1 was the only case in which the participants felt less comfortable at the second questionnaire than at the first questionnaire. Overall, Case 2 was considered the most comfortable.

3.6. Percentage dissatisfied

Fig. 9 shows the percentage of the subjects dissatisfied with the thermal environment as a function of the mean thermal sensation, for each case separately. The predicted percentage dissatisfied (PPD) curve derived from Fanger's model is also included in these figures for comparison [39]. For every questionnaire, the thermal sensation was the average value of the thermal sensation responses of all the participants. Cases 1, 2 and 4 follow Fanger's curve quite closely, while Case 3 does not. Fig. 10 shows all the results combined in order to plot the trendline more accurately. Although the conditions in this experiment were transient (temperature ramp of 1.5K/0.5 h), the results in the neutral zone follow Fanger's model quite closely, although it was developed from data obtained in steady-state studies. Kolarik et al. [7] made a similar observation in their study. These are strong indications that
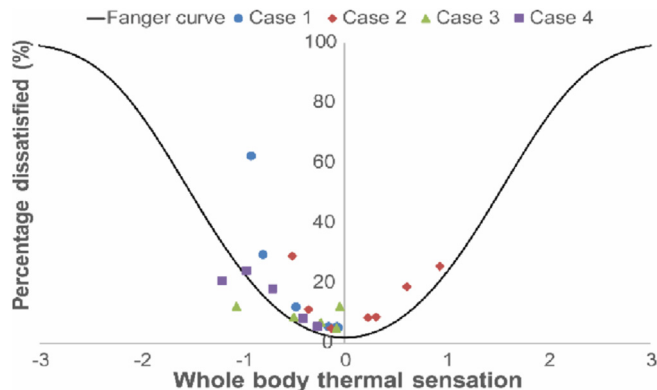
Fig. 9. Percentage of subjects dissatisfied with the thermal environment, for each case separately.
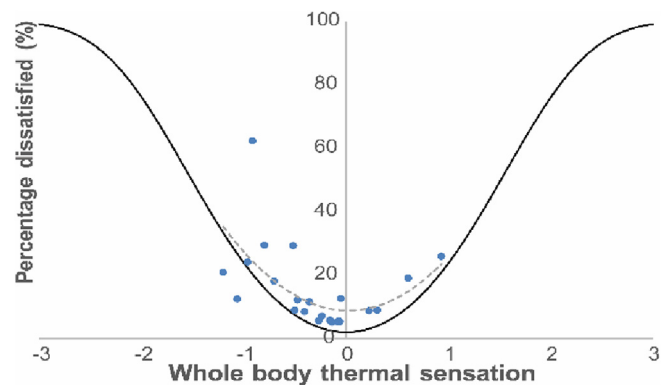
Fig. 10. Combined results of percentage of subjects dissatisfied with the thermal environment.

Fanger's model has a broader range of application and this should be further investigated to well outside the limits of a steady-state condition.

3.7. Sick building syndrome (SBS) symptoms

Table 5 summarizes the results of the subjects' responses to questions about their sick building syndrome symptoms. An arrow pointing downwards means that there was a significant deterioration in that symptom as room air temperature increased, while NS means that there was no significant change, either positive or negative. In most cases a deterioration was observed in the general symptoms (fatigue, lack of concentration, sleepiness) and less often in the specific symptoms (headache, nose irritation, etc.). The cause of the deterioration of the general symptoms could be the quality of the artificial light in the climatic chamber or the fact that this chamber has no windows.

Fig. 11 shows examples of the evolution of the intensity of a specific symptom (throat irritation) and a general symptom (difficulty in concentrating). A symptom intensity of 100 means that the subject felt no irritation, while 0 mean severe irritation. For throat irritation, a deterioration was observed in all cases, but the effect was small. For example, in Case 1, the maximum value was 97 (recorded at the first questionnaire), while the lowest was 90 (recorded at the last questionnaire). On the other hand, in every case the ability to concentrate showed the most significant deterioration. For example, in Case 1, the maximum value was 92 (first questionnaire), while the lowest value recorded was 74 (penultimate questionnaire). Regardless of the symptom, in most cases an improvement was observed when the temperature was kept constant during the last 30 min. A deterioration of

Table 5
Intensity of SBS symptoms.

	Headache	Nose Irritation	Throat Irritation	Eyes Irritation	Fatigue	Concentration	Sleepiness
Case 1	NS	NS	NS	NS	↓	↓	NS
Case 2	NS	NS	NS	↓	NS	↓	NS
Case 3	↓	NS	NS	NS	↓	↓	NS
Case 4	↓	NS	NS	NS	↓	↓	↓

the SBS symptoms observed with an increase in room air temperature is consistent with other findings in the literature [6]– [8].

4. Discussion

The significant differences observed between the four experimental cases in Fig. 5 were not reflected in similar differences in Fig. 7 or Fig. 8. Whole-body thermal sensation varied from slightly cool to slightly warm, thermal acceptability was always better than "just acceptable" while whole-body thermal comfort was always better than "slightly uncomfortable". The course of the curves of thermal acceptability and thermal comfort shown in Figs. 7 and 8 are almost identical, although the question that was used to report thermal comfort was a continuous scale while for thermal acceptability it was not, as shown in Fig. 3.

There are certain limitations in the present study that should be taken into consideration. These limitations are related to the experimental factors that were restricted to a specific value or range of values, to avoid possible bias. These factors include the clo-value of the participants and the anthropometric parameters of the subjects. The clo-value was limited to 0.5, the subjects' age was in a narrow range (22-27 years old) and only subjects with normal body mass index were accepted. In other words, underweight, overweight or obese people were

excluded from this study. The interior of the climate chamber used for the experiment was designed to simulate a landscape office. The dimensions of the climate chamber could not be changed however, so not more than 5 participants at the same time could be present. Nevertheless, the findings of the study would not be affected whether the authors had simulated a landscape or a cellular office room. When selecting the temperature rate of change, the limitation of 1.7 K/0.5 h had to be taken into consideration, based on ASHRAE Standard 55 [28]. Apart from that restriction, the choice was arbitrary. The ramp of 1.5K/0.5 h used in this study is close to the maximum allowed. Increasing the ramp to 1.7K/0.5 h most probably would not cause significant differences since 0.2 K is a very small temperature difference and unlikely to be perceived. Reducing the slope of the ramp to e.g. 1K/0.5 h would result in increased thermal discomfort after the first 30 min, as Figs. 5, Figs. 7 and 8 show, because it will take more time to reach the comfort range of 23–26 °C for sedentary activity. The authors therefore believe that no useful findings would be obtained by examining different ramps in relation to the purpose of the present study. No extensive study of typical office temperatures in Denmark in summer was found and using one-building cases would be too risky due to the high degree of variability (building orientation, construction properties, occupancy level, etc.). Nevertheless, the Danish building code, which is based on ISO 7730 [1], recommends that office buildings should operate in the
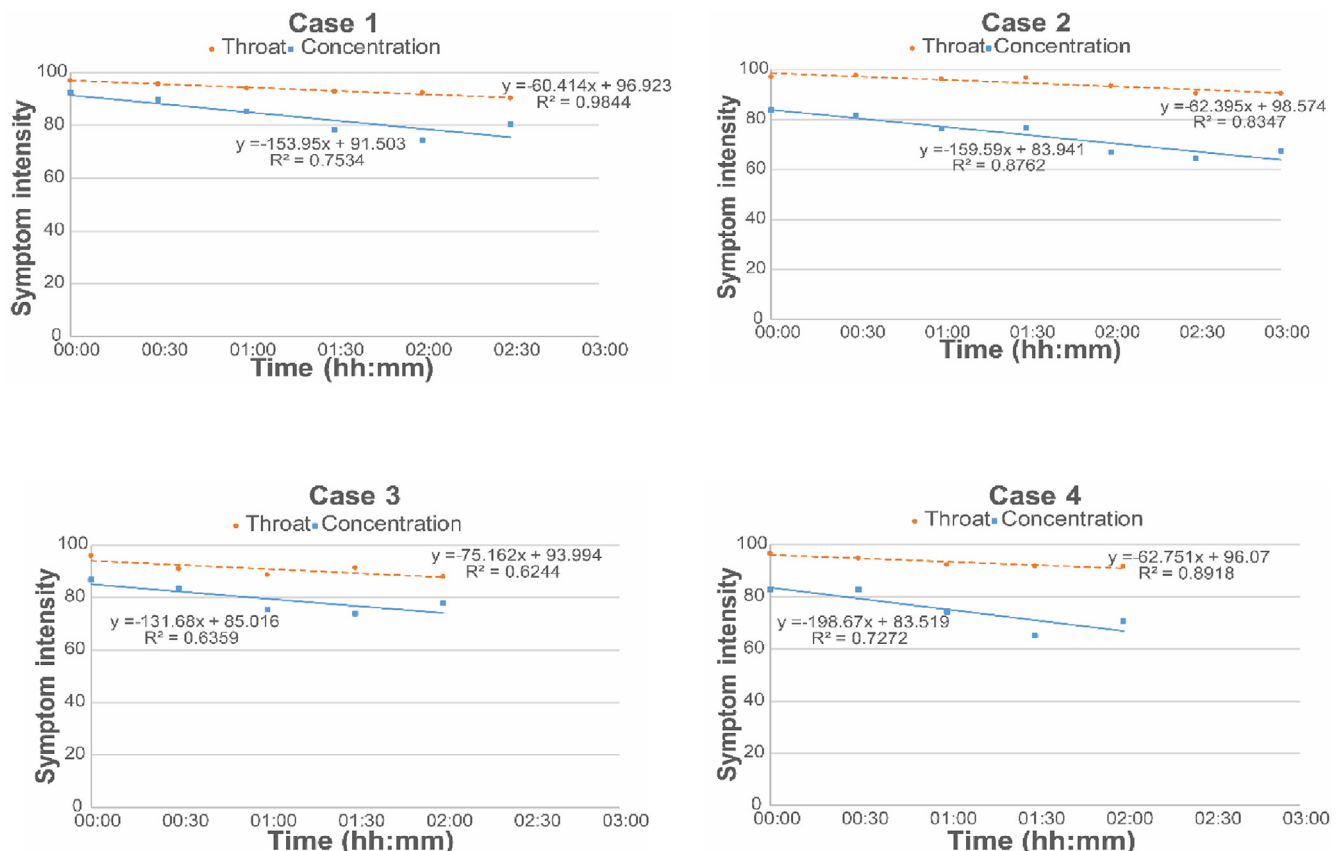
Fig. 11. Examples of development of sick building syndrome symptoms for each case examined.

range of 20–24 °C during winter and 23-26 °C during summer. Therefore, most buildings may be assumed to operate in this interval.

After having exercised for 15 min the participants preferred a lower room air temperature than is suggested by the standards, so in countries where most people commute on foot or on a bicycle, at the beginning of the occupancy period the office room temperature should be lower than 23 °C. Although 18.5 °C as a starting temperature had the highest thermal acceptability and comfort value, it must be considered as too low, as it took longer to reach the range of 23 °C–26 °C, because the maximum allowed room temperature increase in 30 min is 1.7 K [28]. We therefore suggest that the starting room temperature should be 20 °C–21.5 °C and that room temperature should then increase at the rate of 1.5K/0.5 h to reach the comfort range of 23 °C–26 °C. It should be taken into consideration though, that in landscape offices not all occupants commute the same way (private car, public transportation, bicycle or on foot) and they do not all arrive at the office at the same time. This means that any given room temperature control might not be ideal for all occupants. However, it would be more appropriate in educational and public service buildings, where the arrival times of all building occupants are identical.

Rijal et al. investigated 11 office buildings in Japan for more than a year and developed an equation for buildings in heating, cooling and free-run mode [40]. Fig. 12 shows the comparison between the results from their equation for the cooling mode with the current experimental data. The responses for the first questionnaire are presented separately because the participants had higher metabolic rate at that time. It can be seen that the experimental responses of the second questionnaire and onwards are very close to the results extracted from equation developed by Rijal et al. while the responses of the first questionnaire differ substantially. Therefore, when the metabolic rate of the responses from the current experiment was similar to that of the field study, the two sets of subjects' responses almost coincide, in spite the difference of the season (summer during the field study compare to spring during the current experiment). This shows that the dominant factor that affected the subject's thermal perception was not the season or the outdoor conditions during the experiment execution, but the high metabolic rate that the subjects had while filling the first questionnaire.

While there is a seasonal effect on the preferred room temperature level, the relative effect of an increased activity in the morning on the decrease preferred room temperature in the morning is minor. There is some effect as the acceptable change in room temperature for an increased activity level will depend on the clothing level. At a lower clothing insulation, the acceptable decrease in room temperature for an increased activity level will be less than for a heavier clothing. In the present study the authors focused on one level of clothing (0.5 clo) considered typical for summer clothing in a temperate climate.
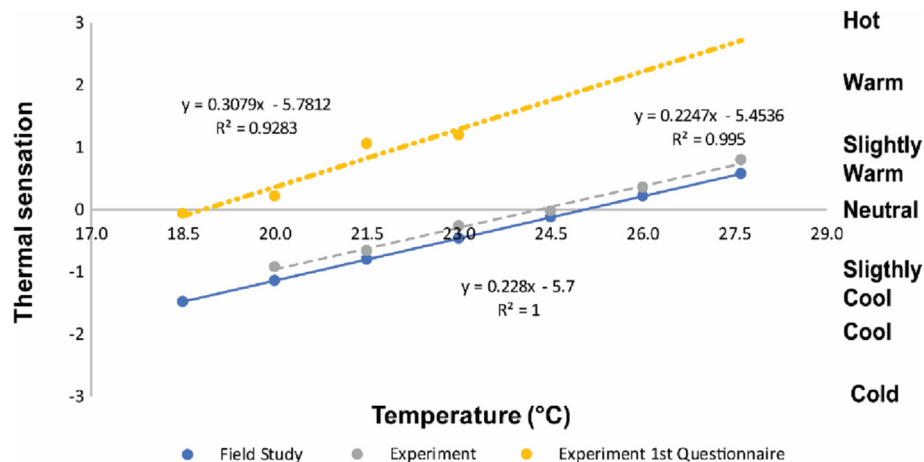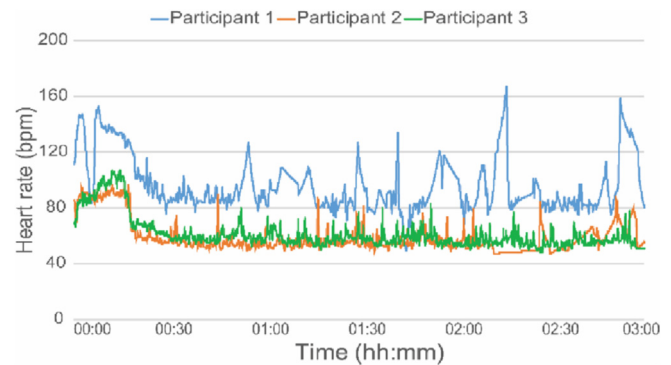
Fig. 13. Example of heart rate measured during an experimental session.

The temperature ranges suggested by the European standard EN 15251 [27] for office buildings assume a metabolic rate of 1.2 met, which is typical for sedentary activity. The authors believe that similar findings would be observed for a person with elevated metabolic rate entering an office building, independent of the season, the geographical location or climate conditions, due to the difference in the metabolic rate. This naturally requires further investigation.

For Figs. 9 and 10, the PMV – PPD values were calculated based on the program designated by Appendix B of ASHRAE Standard 55 [28]. For the metabolic rate, the ISO Standard 8996 (ISO 2004) was applied, using the heart rate measured during the experiment. In some cases, the wireless connection between the sensor and the receiver failed, resulting in unrealistic values of heart rate. Fig. 13 shows an example of such a session, where the heart rate of Participant 1 exceeded 160 heart beats at a time when the subject was sitting at a desk performing office work. This resulted in a metabolic rate of five or six met during the walking phase and up to three met during their stay in the office-chamber. In those cases, the metabolic rate was set by the authors to 2 met during the walking phase and when responding to the first questionnaire, and to 1 met during the rest of their stay in the chamber. These values of metabolic rate were taken from Table A.2 of the ISO Standard 8996 [41].

5. Conclusions

The present study examined whether building occupants with slightly elevated metabolic rate due to commuting on foot may accept a room temperature below the comfort range for sedentary activity in the morning. This was studied in an experiment with 25 young people, male and female, exposed to four different conditions. It was concluded that.

Fig. 12. Thermal sensation comparison between current study results with field study results.

- No significant differences were observed between the subjective responses of male and female participants
- Due to the increased metabolic rate from walking, lower room temperature than are suggested by EN Standard 15251 were reported as acceptable at the beginning of the occupancy period.
- The impact of the physical exercise had disappeared after approximately 30 min
- Although the conditions in this experiment were transient (an increasing temperature ramp of 1.5K/0.5 h), the results in the neutral zone followed Fanger's model quite closely, although his model was developed from data obtained in steady-state exposures
- In countries where most people commute on foot or by bike, the room air temperature at the beginning of the occupancy period could be 20 °C–21.5 °C, namely lower than EN Standard 15251 suggests. It should then increase steadily at a rate of 1.5K/0.5 h to reach the comfort range of 23 °C–26 °C.

These results could be used by researchers examining thermal comfort or energy use in office buildings and could be taken into consideration in international standards for the indoor environment or the operation of HVAC equipment.

Acknowledgements

References

[1] ISO, ISO 7730:2005 Ergonomics of the thermal environment, Analytical Determination and Interpretation of Thermal Comfort Using Calculation of the PMV and PPD Indices and Local Thermal Comfort Criteria, (2005).

[2] L. Lan, P. Wargocki, Z. Lian, Quantitative measurement of productivity loss due to thermal discomfort, Energy Build. 43 (5) (2011) 1057–1062.

[3] L. Lan, P. Wargocki, Z. Lian, Thermal effects on human performance in office environment measured by integrating task speed and accuracy, Appl. Ergon. 45 (3) (2014) 490–495.

[4] P. Wargocki, D.P. Wyon, Ten questions concerning thermal and indoor air quality effects on the performance of of fi ce work and schoolwork, Build. Environ. 112 (2017) 359–366.

[5] D.P. Wyon, P. Wargocki, Room temperature effects on office work, Creating the Productive Workplace, 2006, pp. 181–192.

[6] L. Fang, D.P. Wyon, G. Clausen, P.O. Fanger, Impact of indoor air temperature and humidity in an office on perceived air quality, SBS symptoms and performance, Indoor Air J 14 (7) (2004) 74–81.

[7] J. Kolarik, J. Toftum, B.W. Olesen, A. Shitzer, Occupant responses and office work performance in environments with moderately drifting operative temperatures (RP-1269), HVAC R Res. 15 (5) (2009) 931–960.

[8] M.J. Mendell, et al., Enhanced particle filtration in a non-problem office environment: preliminary results from a double-blind crossover intervention study, Am. J. Ind. Med. 36 (1) (1999) 55–57.

[9] A. Melikov, B. Yordanova, L. Bozkhov, V. Zboril, R. Kosonen, Human response to thermal environment in rooms with chilled beams, Proc. Clima 2007 WellBeing Indoors, 2007.

[10] M. Dalewski, A.K. Melikov, M. Vesely, Performance of ductless personalized ventilation in conjunction with displacement ventilation: physical environment and human response, Build. Environ. 81 (2014) 354–364.

[11] Z. Dimitrov, A. Krikor, Thermal conditions in a simulated office environment with convective and radiant cooling systems ventilation and energy conservation in buildings publication date, World Congress and the 8th International Conference on Indoor Air Quality, Ventilation an, 2013.

[12] A. Lipczynska, J. Kaczmarczyk, B. Marcol, W. Kierat, A.K. Melikov, Human response to personalized ventilation combined with chilled ceiling, Proc. 13th Int. Conf. Air Distrib. Rooms, 2014, pp. 1–7.

[13] T. Arghand, et al., Individually controlled localized chilled beam in conjunction with chilled ceiling: Part 2 – human response, Proc. Indoor Air 2016 Publ. (2016) 482.

[14] Q. Jin, A. Simone, B.W. Olesen, S.K.M. Holmberg, E. Bourdakis, Laboratory study of subjective perceptions to low temperature heating systems with exhaust ventilation in Nordic countries, Sci. Technol. Built Environ 0 (0) (2017) 1–12.

[15] A.P. Gagge, J.A.J. Stolwijk, J.D. Hardy, Comfort and thermal sensations and associated physiological responses at various ambient temperatures, Environ. Res. 1 (1) (1967) 1–20.

[16] E. Arens, H. Zhang, C. Huizenga, Partial- and whole-body thermal sensation and comfort - Part I: uniform environmental conditions, J. Therm. Biol. 31 (no. 1–2 SPEC. ISS) (2006) 53–59.

[17] H. Zhang, C. Huizenga, E. Arens, D. Wang, "Thermal sensation and comfort in transient non-uniform thermal environments, Eur. J. Appl. Physiol. 92 (6) (2004) 728–733.

[18] H. Zhang, E. Arens, C. Huizenga, T. Han, Thermal sensation and comfort models for non-uniform and transient environments, Part I: local sensation of individual body parts, Build. Environ. 45 (2) (2010) 380–388.

[19] H. Zhang, E. Arens, C. Huizenga, T. Han, Thermal sensation and comfort models for non-uniform and transient environments, part II: local comfort of individual body parts, Build. Environ. 45 (2) (2010) 389–398.

[20] H. Zhang, E. Arens, C. Huizenga, T. Han, Thermal sensation and comfort models for non-uniform and transient environments, part III: whole-body sensation and comfort, Build. Environ. 45 (2) (2010) 399–410.

[21] C. Huizenga, H. Zhang, E. Arens, D. Wang, Skin and core temperature response to partial- and whole-body heating and cooling, J. Therm. Biol. 29 (no. 7–8 SPEC. ISS) (2004) 549–558.

[22] E. Arens, H. Zhang, C. Huizenga, Partial- and whole-body thermal sensation and comfort—Part II: non-uniform environmental conditions, J. Therm. Biol. 31 (no. 1–2) (2006) 60–66.

[23] I.D. Griffiths, D.A. McIntyre, Sensitivity to temporal variations in thermal conditions, Ergonomics 17 (4) (1974) 499–507.

[24] T. Goto, J. Toftum, R. de Dear, P.O. Fanger, Thermal sensation and thermophysiological responses to metabolic step-changes, Int. J. Biometeorol. 50 (5) (2006) 323–332.

[25] D.A. McIntyre, R.R. Gonzalez, Man's thermal sensitivity during temperature changes at two levels of clothing insulation and activity, ASHRAE Trans 82 (2) (1976) 219–233.

[26] J.L.M. Hensen, Literature review on thermal comfort in transient conditions, 25 (4) (1990) 309–316.

[27] EN, EN 15251, 2007 Indoor Environment Input Parameters for Design and Assessment of Energy Performance of Buildings Adressing Indoor Air Quality, Thermal Environment, Lighting and Acoustics, (2007).

[28] ASHRAE, ASHRAE Standard 55: Thermal Environmental Conditions for Human Occupancy, (2013).

[29] B. Moujalled, R. Cantin, G. Guarracino, Adaptive thermal comfort evaluation in a field study, Int. Conf. "Passive Low Energy Cool. Built Environ (2005) 225–230 May.

[30] R. De Dear, J. Kim, C. Candido, M. Deuble, Adaptive thermal comfort in australian school classrooms, Build. Res. Inf. 43 (3) (2015) 383–398.

[31] S.A. Damiati, S.A. Zaki, H.B. Rijal, S. Wonorahardjo, Field study on adaptive thermal comfort in office buildings in Malaysia, Indonesia, Singapore, and Japan during hot and humid season, Build. Environ. 109 (2016) 208–223.

[32] J. Liu, R. Yao, R. McCloy, A method to weight three categories of adaptive thermal comfort, Energy Build. 47 (2012) 312–320.

[33] N. Artmann, H. Manz, P.K. Heiselberg, Potential for passive cooling of buildings by night-time ventilation in present and future climates in Europe, 23rd Int. Conf. Passiv. Low Energy Archit, 2006, p. 6.

[34] S.P. Corgnati, A. Kindinis, Thermal mass activation by hollow core slab coupled with night ventilation to reduce summer cooling loads, Build. Environ. 42 (9) (2007) 3285–3297.

[35] J. Kolarik, B.W. Olesen, Energy use and thermal comfort in a building with thermo active building system (TABS), Indoor Climate of Buildings 2007 (2007).

[36] J. Kolarik, J. Toftum, B.W. Olesen, K.L. Jensen, Simulation of energy use, human thermal comfort and office work performance in buildings with moderately drifting operative temperatures, Energy Build. 43 (11) (2011) 2988–2997.

[37] E. Bourdakis, T.Q. Péan, L. Gennari, B.W. Olesen, Daytime space cooling with phase change material ceiling panels discharged using rooftop photovoltaic/thermal panels and night-time ventilation, Sci. Technol. Built Environ. 4731 (June, 2016) no.

[38] P. Kjerulf-Jensen, Y. Nishi, H. Graichen, R. Rascati, A test chamber design for investigating man's thermal comfort and physiological response, ASHRAE Trans 82 (1) (1975) 73–82.

[39] P.O. Fanger, Thermal comfort, Danish Technical Press, Copenhagen, Denmark, 1970.

[40] H.B. Rijal, M.A. Humphreys, J.F. Nicol, Towards an adaptive model for thermal comfort in Japanese offices, Build. Res. Inf. 45 (7) (2017) 717–729.

[41] ISO, ISO 8996: Ergonomics of the thermal environment, Determination of the Metabolic Rate, (2004).

Paper 3: Bourdakis E., Gkoufas N.A., & Olesen B.W. (2018). Simulation study for the design of radiant ceiling panels containing phase change material. Submitted at Applied Thermal Engineering

Simulation study for the design of radiant ceiling panels containing phase change material

Eleftherios Bourdakis[1], Nikolaos A. Gkoufas[1], Bjarne W. Olesen[1]
[1]International Centre for Indoor Environment and Energy
Technical University of Denmark

Abstract

The authors conducted a simulation parametric study to identify the effect of different parameters on the discharging process of the PCM contained in radiant ceiling panels designed for commercial buildings. The examined parameters were the panel thickness, the water flow rate and the water supply temperature. Four realistic values were selected for each parameter and all the possible combinations were examined. It was found that the examined range of water flow rate had insignificant impact on the discharging process of the PCM and therefore the lowest water flow rate that ensures turbulent flow rate should be used. It was concluded that among the examined combinations the ideal combination for a PCM ceiling panel was a panel thickness of 25 mm and a water supply temperature of 15°C.

Keywords

Radiant ceiling panel, phase change material, cooling systems, energy efficiency.

Nomenclature

Symbol	Unit	Quantity
C_p	J/kg·K	Specific heat capacity
$C_{p,phase1}$	J/kg·K	Specific heat capacity of PCM when solid
$C_{p,phase2}$	J/kg·K	Specific heat capacity of PCM when liquid
h	mm	Panel height
H	J/kg	Specific enthalpy
H_{phase1}	J/kg	Specific enthalpy of PCM when solid
H_{phase2}	J/kg	Specific enthalpy of PCM when liquid
l	mm	Panel length
L	J/kg	Latent heat of fusion
T_{PC}	°C	Phase change temperature

Q	W/m²	Additional heat source
q	W/m²	Heat flux
T	K	PCM Temperature
u_{trans}	m/s	Velocity vector of translational motion
w	mm	Panel width
α_m	-	Mass fraction
θ	-	Fraction of phase before transition
λ	W/m·K	Thermal conductivity
λ_{phase1}	W/m·K	Thermal conductivity of PCM when solid
λ_{phase2}	W/m·K	Thermal conductivity of PCM when liquid
ρ	kg/m³	Density
ρ_{phase1}	kg/m³	Density of PCM when solid
ρ_{phase2}	kg/m³	Density of PCM when liquid

Introduction

The past few decades, an increase in the energy demand for space cooling has been observed even in northern European countries, especially in buildings with airtight envelopes and large glazing façades [1]. The past few years several studies have been conducted to address that issue and reduce the energy use of the buildings sector. Literature shows that utilizing the thermal mass in well-insulated buildings can result in up to 30% of reduction in energy use for space heating and cooling [2]–[4]. Although sensible heat storage is the most widespread method of heat storage, latent heat storage has attracted attention through the utilization of phase change materials (PCM), due to their high energy storage density with a small variation in their temperature [5]–[7].

PCMs are chemical substances that absorb and release "latent" heat almost at a constant temperature, during which their physical state changes, e.g. from solid to liquid and allows them to store large amounts of thermal energy. In fact, PCMs have 5-14 times higher heat capacity per unit volume compared to conventional storage materials such as masonry and rock [6].

Figure 1 shows the difference in stored energy between a sensible and latent thermal storage system. The continuous line is the latent heat storage system. When the PCM is solid, it behaves as a sensible storage system. Once its temperature reaches the phase change temperature (PCT) the PCM starts to melt. At that point, the temperature of the

PCM remains constant but it continues to store energy. When it is fully melted it behaves again as sensible storage system and the temperature increases as it stores energy. On the other hand, in a sensible storage system (dashed line) the temperature increases continuously as the material stores more energy. Therefore, for a specific temperature it has stored less energy than a fully melted PCM at the same temperature as shown by the grey dashed lines in Figure 1. It should be stated that usually the phase change process does not take place only on a specific temperature but within a certain temperature range around the phase change temperature of the PCM.
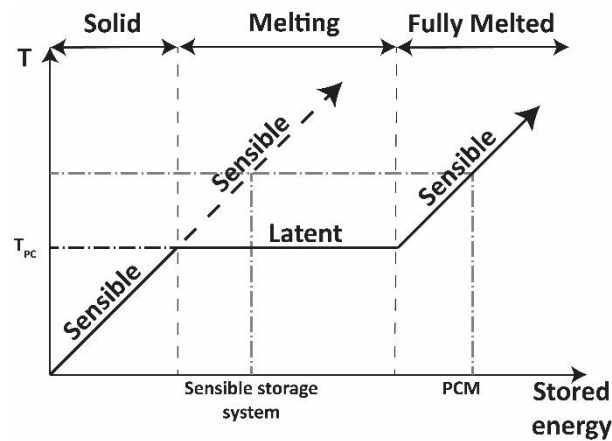
Figure 1: Sensible and latent heat storage

PCMs are classified based on the phase change process in the following categories

- Solid – solid
- Solid – liquid
- Solid – gas
- Liquid – gas

Detailed lists with numerous PCMs of different phase change temperatures and chemical properties can be found in the literature [8]–[10]. Among the four phase change processes the most popular is the solid – liquid since it has a higher latent heat capacity than the solid – solid process and a lower volumetric change compared to the solid – gas and the liquid – gas processes [6], [11], [12].

According to the literature, the following properties should be taken into consideration in order to select the appropriate PCM [7], [13]–[16]:

- Appropriate phase change temperature based on the application
- High latent heat of fusion per unit of mass
- High thermal conductivity

- Reproducible phase change to repeatedly store heat as many times as required

- Limited or no super-cooling (super-cooling occurs when the solidification process starts only after the PCM has reached a lower temperature than the phase change temperature

- Small volumetric change during the phase change process

- Chemical stability

- Compatibility with other materials, e.g. no occurrence of corrosion

- Not flammable

- Not toxic

- High availability

Since it is almost impossible to find materials that fulfill all the aforementioned conditions, Zhou et al. (2012) identified the phase change temperature, the latent heat of fusion and the thermal conductivity as the most critical parameters in a PCM selection process.

A major drawback of PCMs is their low thermal conductivity [17]. The use of metal foams, aluminum powder, carbon fibers and expanded graphite structure has been examined as a heat transfer enhancement technique [18]–[20]. Other techniques examined are finned tubes [21]–[23], thin aluminum plates filled with PCM [24] and metal or graphite matrix structure with embedded PCM [25], [26].

Various PCM applications in the building sector have been tested academically, but lately, the industrial interest is fast increasing as well [7]. Dinçer & Rosen (2010) listed several PCM-enhanced building applications. PCM has been implemented in wallboards [28], in concrete [29], ceiling and floor [17], [30]–[33], insulation [29], shutters or window blinds [7], cooled ceilings [34], [35] and air-conditioning systems [36].

Although PCMs in general have impressive thermal performance, their implementation in buildings is minimal, due to modeling and simulating limitations, the lack of real examples, [37], high cost of implementation [16], [38] and technical limitations [7], [17], [29].

PCMs have been incorporated in both passive and active ceiling systems. The findings showed that a solar heating system with PCM had 17-36% heat recovery compared to a system without PCM [39]. Furthermore, in a room with PCM ceiling tiles, the temperature rise only 2°C instead of 6°C if PCM was not used [40]. In another study, 5 cm of gypsum panel containing 25% by weight PCM, was able to maintain the room air temperature within the comfort range [41].

For achieving higher efficiency and complying with the international fire-safety standards [42]–[45], a PCM container should meet the following requirements:

- Strength, flexibility, corrosion resistance and thermal stability

- Sufficient surface area for heat transfer

- Structural stability and easy handling

The most common techniques for containing PCM are impregnation in building materials like plaster, concrete or gypsum [14], [30], [46]–[53], microencapsulation [54], [55] and shape-stabilized PCM [54], [56], [57]. Impregnation has the disadvantage of leakage occurrence, which could be solved with the microencapsulation [54]. Microencapsulation is the method in which PCM is enclosed in capsules with diameter ~ 20 μm. Shape-stabilized PCMs are prepared by a liquid mixture of the PCM and a supporting material. The disadvantage of shape-stabilized PCMs is their low thermal conductivity.

The scope of this study was to design a new ceiling panel containing PCM. The PCM was enclosed in an aluminum frame, for higher thermal conductivity, with embedded pipes for discharging the PCM actively. The examined parameters were the panel thickness, the water flow rate in the embedded pipes and the water supply temperature. The performance of the panel was evaluated in terms of duration of discharging phase, energy released, temperature of the PCM layer and the lower surface of the panel and utilization ratio of the PCM.

Model description

System, Geometry and materials

The geometry selected, was of a typical European square ceiling panel with side dimensions of length $l = 595$ mm and width $w = 595$ mm, having a total ceiling exposed surface area of 0.35 m^2 (Figure 2 top). The height of the panel was one of the upon research parameters, as it is directly connected with the thermal mass capacity of the enclosed phase change material. Therefore, the height varied depending on the simulated case.
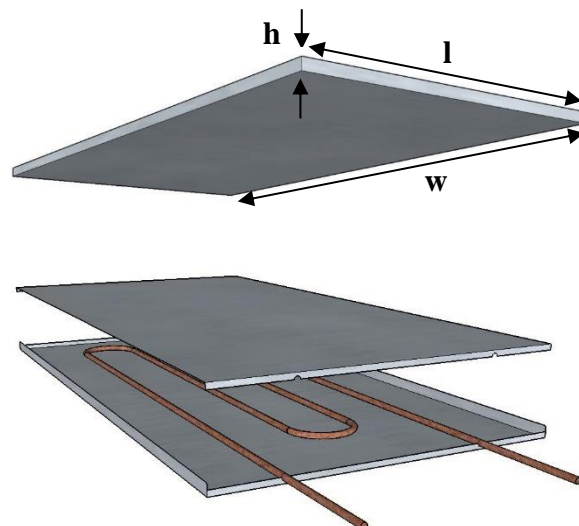
The outer construction was made of aluminum sheets, to ensure effective and homogeneous heat transfer to the enclosed PCM, with thickness of l = 1 mm. For discharging the PCM, copper pipes were embedded as shown in Figure 2 bottom, with external diameter 20 mm and pipe thickness of 0.5 mm. The distance between the pipes was set to 150 mm, so that there is uniform distribution within the panel. The properties of a commercially available PCM were used in the current study. Table 1 shows the thermophysical properties of the materials of the panel, which were manually implemented in the simulation model. The transition temperature of the PCM was 24°C with a ΔT of 3 K and the latent heat capacity was 201 kJ/kg.

Table 1. Thermophysical properties of the simulated panel materials

	Cp [J/kg·K]	K [W/m·K]	ρ [kg/m^3]
Solid PCM	1840	0.25	910
Liquid PCM	1990	0.25	810
Aluminum	900	238	2700
Copper	384	401	8960

Numerical Model in COMSOL

A two-dimensional cross-section (Figure 3) numerical model was created in COMSOL, in order to simulate the discharge performance of the previously presented PCM ceiling panel under different conditions.

Figure 3: 2D cross-section of the ceiling panel simulated in Comsol

Regarding initial conditions; the entire PCM was considered in liquid state at a temperature of $T_0 = 27$°C. Since discharging of PCM through the water pipes was the main concern of the study, all boundary surfaces were considered adiabatic, but heat transfer within the aluminum though, was still taking place since it was defined in the model as thin layer. For the discharge through the water pipes, an internal forced convective heat flux was defined from an isothermal tube containing water as fluid. The velocity and the temperature of the water were among the investigated parameters.

The heat transfer in fluids physics interface was employed for the simulations, while solid components were simply simulated as thin layers. The study was time dependent, driven by the following main heat transfer equation:

$$\rho C_p \left(\frac{\partial T}{\partial t} + u_{trans} \cdot \nabla T \right) + \nabla q = Q \qquad \text{Eq. 1}$$

While the heat flux was calculated as follows:

$$q = -\lambda \cdot \nabla T \qquad \text{Eq. 2}$$

However, since phase change is taking place in the process, latent heat, was added in the energy balance equation, within a temperature range of $T_{pc} \pm \Delta T/2$. The density ρ, the effective thermal conductivity λ, the specific enthalpy H and the specific heat capacity C_p are expressed as:

$$\rho = \theta \rho_{phase1} + (1 - \theta)\rho_{phase2} \qquad \text{Eq. 3}$$

$$\lambda = \theta \lambda_{phase1} + (1 - \theta)\lambda_{phase2} \qquad \text{Eq. 4}$$

$$H = \frac{1}{\rho}\left(\theta \rho_{phase1} H_{phase1} \right) + \frac{1}{\rho}\left((1 - \theta)\, \rho_{phase2} H_{phase2} \right) \qquad \text{Eq. 5}$$

$$C_p = \frac{1}{\rho}\left(\theta \rho_{phase1} C_{p,phase1} \right) + \frac{1}{\rho}\left((1 - \theta)\rho_{phase2}\, C_{p,phase2} \right) + \left(H_{phase2} - H_{phase1} \right)\frac{da_m}{dt} \qquad \text{Eq. 1}$$

θ was a smoothed function representing the fraction of phase before transition while a_m was the mass fraction defined according to the following equation.

$$\alpha_m = \frac{1}{2}\frac{\left((1 - \theta)\rho_{phase2} - \theta \rho_{phase1} \right)}{\rho} \qquad \text{Eq. 2}$$

Cases examined

Three different parameters were examined, in order to investigate the optimal discharge practice of the PCM, the panel height, the water supply temperature in the pipes and the water speed in the pipes. For each parameter, four realistic values were selected and all the possible combinations were simulated, giving in total 64 different cases. Table 2 shows the setpoint values for each examined parameter. The water flow rate values were selected to ensure turbulent flow on the pipes. The duration of the simulation was 12 hours, corresponding to the available time from the end of the occupancy period until the beginning of the occupancy period the next day. The timestep was 6 minutes.

Table 2: Setpoint values for the examined parameters

Panel height, mm	Water flow, kg/h	Water supply temperature, °C
25	240	7
30	280	12
35	320	15
40	360	18

Results

PCM phase

Figure 4 shows the state of the PCM as a fraction of melted PCM. PCM phase equal to 1 means that the PCM is fully melted while PCM phase equal to 0 corresponds to fully solidified PCM. Color variations represent different water supply temperature, while the marker variations represent different water flow rate in the embedded pipes. For example, the yellow line with star marker corresponds to T_s of 15°C and 280 kg/h of water flow rate in the embedded pipes.

In all four cases, the lower the water supply temperature the faster the PCM got discharged. On the other hand, disregarding of the panel thickness, the impact of the water flow rate was insignificant, since in all cases the lines of the same color coincided. When the thickness of the panel was 25 mm the PCM was completely solidified before the end of the discharging period in all cases simulated. In the cases of panel of 30 mm when the water supply temperature was 18°C failed to discharge the PCM completely. When the panel thickness was increased to 35 mm only the water supply temperature of 7°C and 12°C were sufficient to discharge the PCM completely, while in the cases of panel thickness of 40 mm the PCM got completely discharged only when the water supply temperature was 7°C. When the panel thickness was 40 mm and the water supply temperature 18°C, only approximately 50% of the PCM was solidified.

Since the impact of the water flow rate is insignificant, the lowest water flow rate from the simulated values would be sufficient for discharging the PCM. Lower water flow rate results in smaller size of water pumps and chillers, thus lower acquisition cost and energy use for their operation. The water flow rate though, should be high enough to ensure turbulent flow but with water speed lower than 1.2 m/s to minimize noise generated by the flow [58].

$$—T_{supply} = 7°C \quad —T_{supply} = 12°C \quad —T_{supply} = 15°C \quad —T_{supply} = 18°C$$

$$—W_{flow} = 240\ kg/h \quad —■—W_{flow} = 280\ kg/h \quad —○—W_{flow} = 320\ kg/h \quad —✱—W_{flow} = 360\ kg/h$$
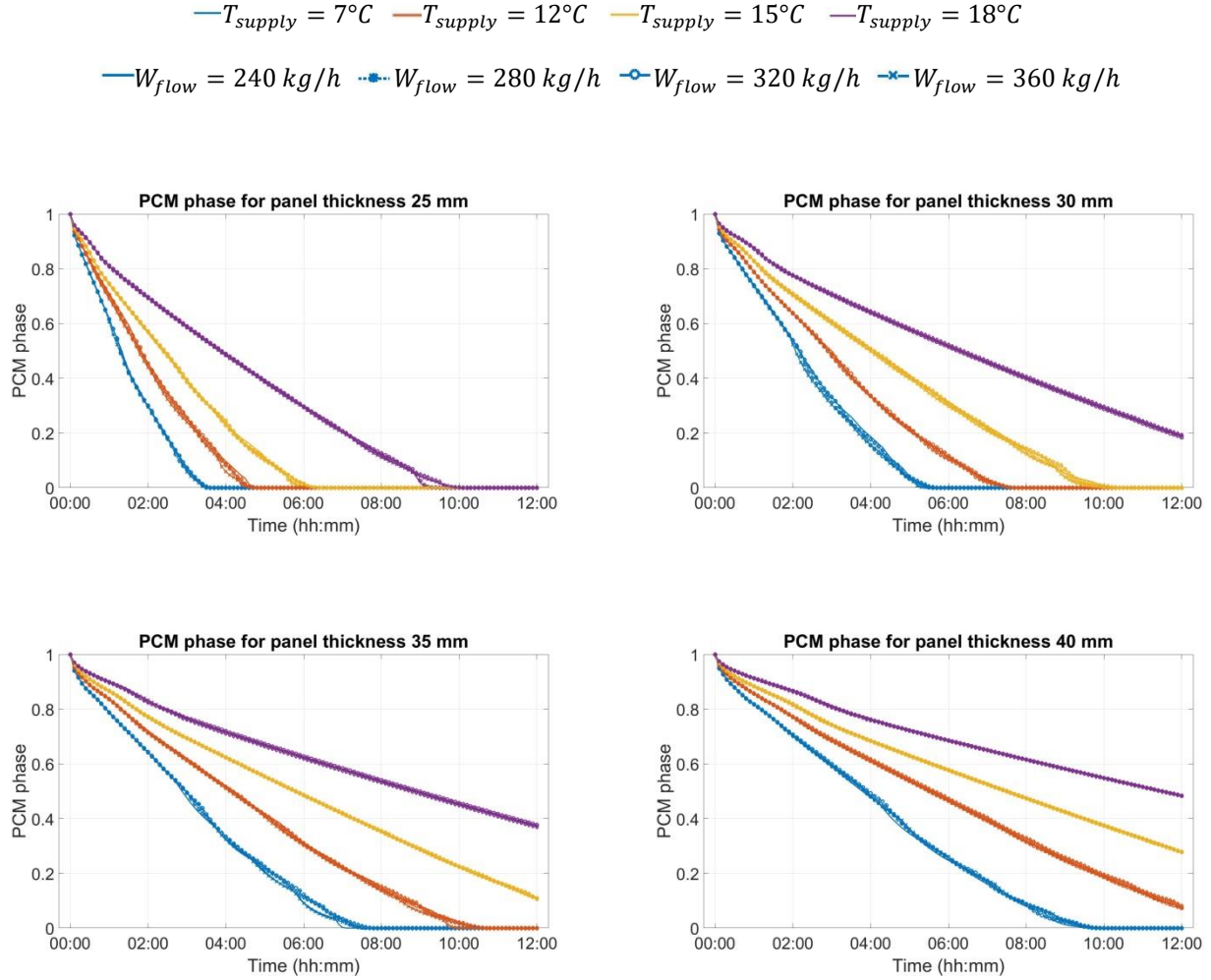
Figure 4: PCM phase as a function of the panel thickness

Table 3 shows the duration of the discharging process for each combination of water supply temperature and panel thickness. The shown values are the average of the four simulations with different water flow rate, since the impact of the water flow rate was insignificant. Cells with "–" are the cases where the PCM did not solidify completely. When the water supply temperature was 7°C, for every additional 5 mm of panel thickness the discharging period was increased by approximately two hours. Similarly, the discharging period was increasing by approximately three and four hours when the water supply temperature was 12°C and 15°C, respectively. For every combination of water supply

temperature and panel thickness, the increase on the discharging duration from increasing the water supply temperature was lower than by increasing the panel thickness. That was due to the low thermal conductivity of the PCM, which had a higher impact when increasing the panel thickness, namely the mass of the PCM. This table can operate as a comparison for future studies examining radiant ceiling panels with PCM with similar properties.

Table 3: Discharging duration for each water supply temperature – panel thickness combination

	H=25 mm	H=30 mm	H=35 mm	H=40 mm
T=7°C	3:37	5:39	7:54	10:52
T=12°C	4:49	7:34	10:36	–
T=15°C	6:19	10:19	–	–
T=18°C	9:48	–	–	–

PCM average temperature

Figure 5 shows the average temperature of the PCM layer as a function of the water supply temperature. Color variations represent different panel thickness, while the different marker represents different water flow rate in the embedded pipes. For example, the red line with "x" marker corresponds to panel thickness of 30 mm and 360 kg/h of water flow rate in the embedded pipes.

In all cases, initially, due to the high temperature difference between the water circulated in the pipes and the PCM layer, the temperature drop of the PCM was steeper, until it reached 24°C which is the melting temperature point of the used PCM and the inclination of the temperature curve was more horizontal. Once the bigger portion of the PCM was solidified the temperature curve was becoming steep again until it was reaching steady state, namely the value of the water supply temperature. The higher the water supply temperature, the less steep the temperature curve was after the PCM temperature was below the melting point temperature.

$—Height = 25\ mm$ $—Height = 30\ mm$ $—Height = 35\ mm$ $—Height = 40\ mm$
$—W_{flow} = 240\ kg/h$ $\text{-■-}W_{flow} = 280\ kg/h$ $\text{-○-}W_{flow} = 320\ kg/h$ $\text{-✕-}W_{flow} = 360\ kg/h$
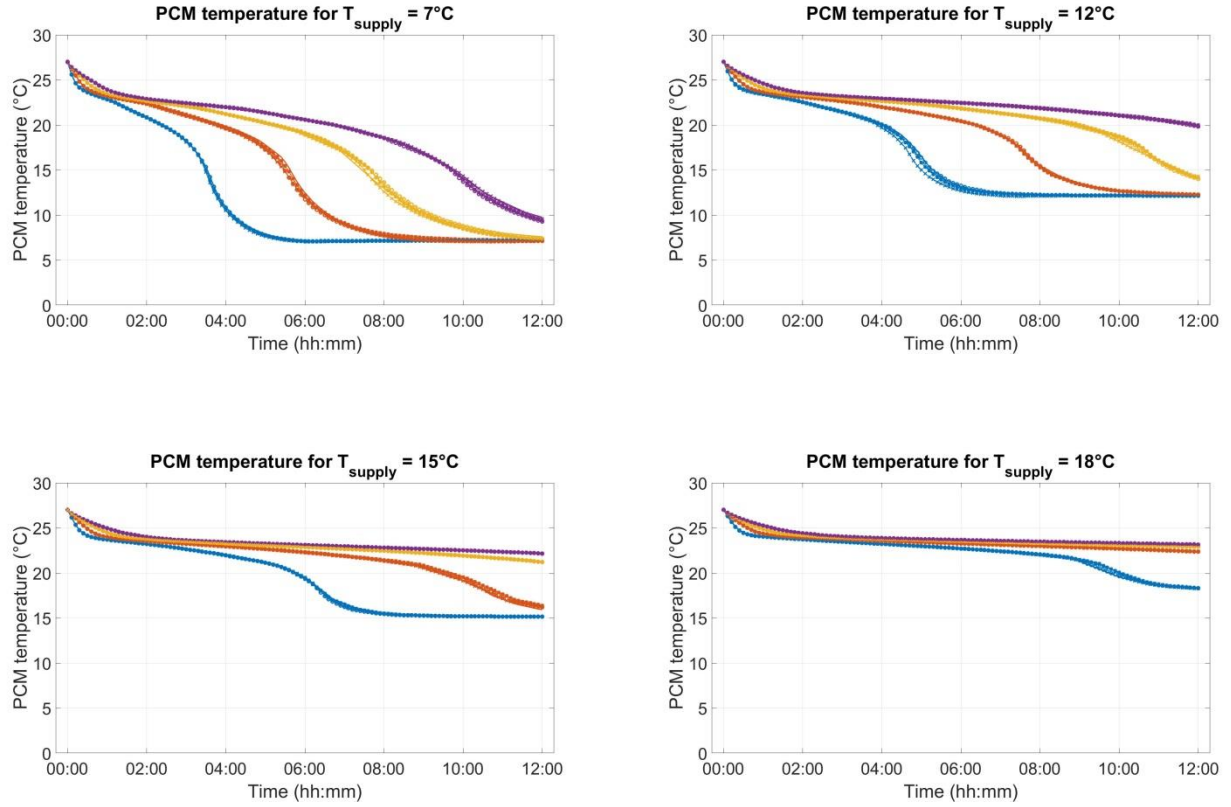
Figure 5: PCM average temperature as a function of the water supply temperature

Since the water flow was continuing disregarding of the phase of the PCM, the temperature continued to drop even after the PCM was completely solidified until the average PCM temperature was reaching the value of the water supply temperature. In reality, the water flow should have stopped once the PCM was fully solidified to avoid overcooling, wasting energy and increasing the operation cost for no actual benefit. For that reason, Table 4 shows the average temperature of the PCM layer when the PCM was fully discharged, for each combination of water supply temperature and panel thickness. The underlined values represent the cases where the PCM was not fully discharged. The average temperature of the PCM was increasing less when increasing the panel thickness than when increasing the water supply temperature. For example, in the case of panel thickness of 30 mm and water supply temperature of 12°C, when the panel thickness was increased to 35 mm the temperature increased by only 0.3°C while by keeping the thickness constant and increasing the water supply temperature to 15°C the average temperature of the PCM increased by 1.9°C. The only exception was when the water supply temperature was 12°C and the panel thickness was increased from 25 mm to 30 mm. In that case, the average PCM temperature was slightly decreased although the panel thickness was increased to 30 mm.

Table 4: PCM average temperature for each water supply temperature – panel thickness combination

	H=25 mm	H=30 mm	H=35 mm	H=40 mm
T=7°C	13.7	14.2	14.9	15.5
T=12°C	16.9	16.8	17.1	**_19.9_**
T=15°C	18.3	18.7	**_21.2_**	**_22.2_**
T=18°C	20.1	**_22.4_**	**_22.9_**	**_23.2_**

Panel bottom surface temperature

Figure 6 shows the temperature at the bottom surface of the panel, as a function of the water supply temperature. Color variation represents different panel thickness, while the marker variation represents different water flow rate in the embedded pipes. For example, the blue line without marker corresponds to panel thickness of 25 mm and 240 kg/h of water flow rate in the embedded pipes.

By comparing Figure 6 with Figure 5, it can be seen that there is a significant time hysteresis of several hours before the bottom surface of the panel reaches the average temperature of the PCM layer, due to the low thermal conductivity of the PCM layer. As it was expected, the thinner the panel, the faster the surface temperature would drop. When the water supply temperature was 18°C, the differences among all cases examined were insignificant, despite of the panel thickness.
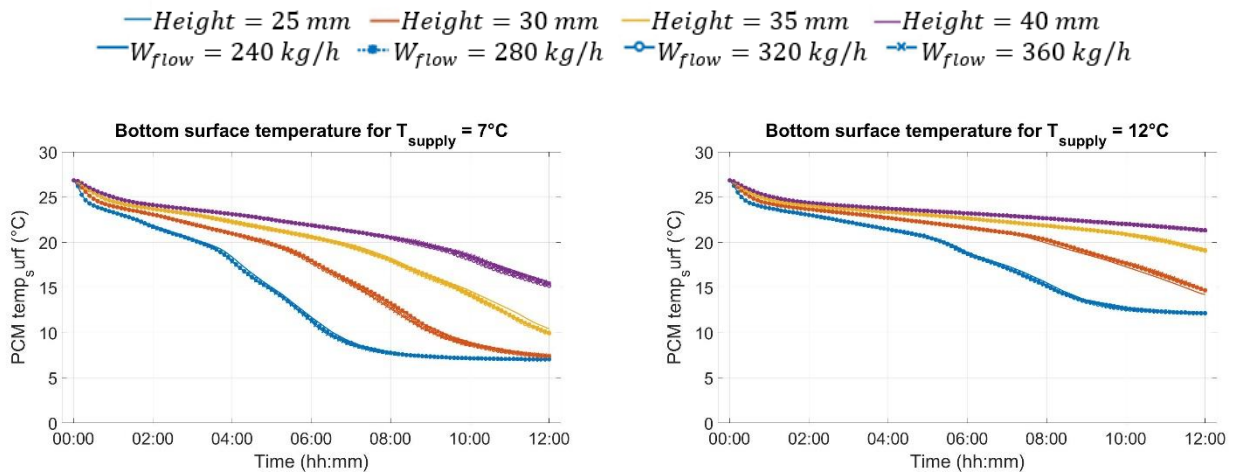
Figure 6: Panel bottom surface temperature as a function of the water supply temperature

To examine the possibility of condensation occurrence on the bottom surface of the panels, Table 5 shows the bottom surface temperature when the PCM was fully solidified. The underlined cells are the cases where the PCM did not get fully discharged until the end of the discharging period. When keeping the panel thickness constant and increasing the water supply temperature, the bottom surface temperature w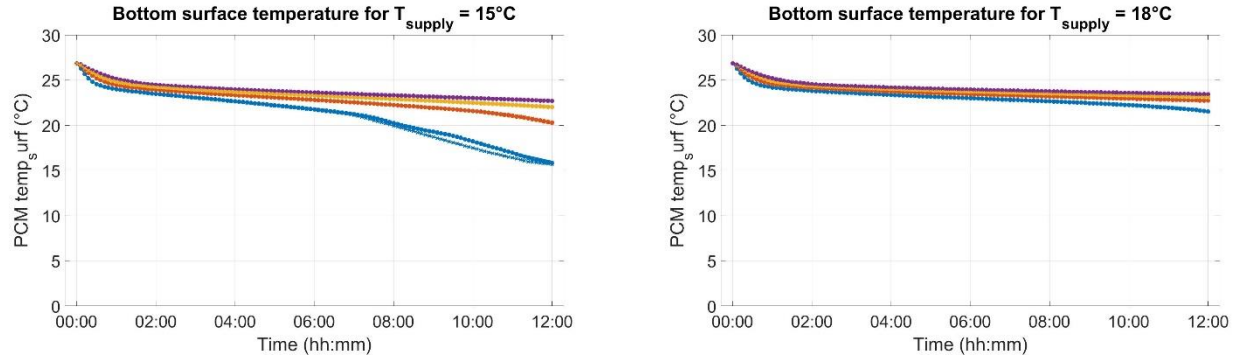as increasing. On the other hand, when keeping the water supply temperature constant and increasing the panel thickness, the bottom surface temperature was decreasing slightly. For example, when the water supply temperature was 12°C and increasing the panel from 25 mm to 30 mm, the temperature dropped 0.2°C. In some cases that drop was insignificant, for example when the water supply temperature was 7°C and the panel thickness increased from 30 mm to 35 mm, the temperature drop was less than 0.1°C. That was not the case when the increase of the panel thickness would result in incomplete solidification of the PCM layer; for example, when the water supply temperature was 12°C and the panel thickness increased from 35 mm to 40 mm, the bottom surface temperature increased by 0.87°C. That was because PCM was not solidifying homogenously. Therefore, the temperature was higher during the process, but when the PCM was completely solidified a further decrease in the temperature of the lower panel surface occurred.

Even with the combination of lowest water supply temperature and thinnest panel the surface temperature is high enough to ensure that there is no risk for condensation occurrence. Although there is no risk for condensation occurrence on the panel surface, water supply temperature low as 7°C or 12°C should be avoided in residential or commercial buildings because there is still high risk of condensation earlier in the hydronic loop, e.g. on the manifold. Such low water supply temperatures should be used only in specific industrial applications.

Table 5: Panel bottom surface temperature when PCM was fully discharged

	H=25 mm	H=30 mm	H=35 mm	H=40 mm

T=7°C	19.2	18.7	18.8	18.6
T=12°C	20.8	20.6	20.5	**21.3**
T=15°C	21.6	21.4	**22.0**	**22.7**
T=18°C	22.3	**22.7**	**23.1**	**23.4**

Heat flux

Figure 7 shows the heat flux on the lower surface of the PCM panel as a function of the water supply temperature. Color variation represents different panel thickness, while marker variation represents different water flow rate in the embedded pipes. For example, the purple line with circular marker corresponds to panel thickness of 40 mm and 320 kg/h of water flow rate in the embedded pipes.

The highest heat flux was observed when the panel thickness and water supply temperature had the lowest examined value, namely 25 mm and 7°C respectively. The peak heat flux was reducing when either the water supply temperature or the panel thickness was increasing, but increasing the water supply temperature caused a more significant decrease on the peak heat flux. The heat flux would become zero once the temperature of the PCM had reached the value of the water supply temperature, therefore reaching steady state.
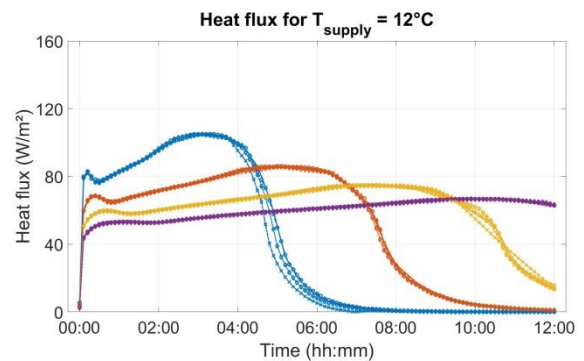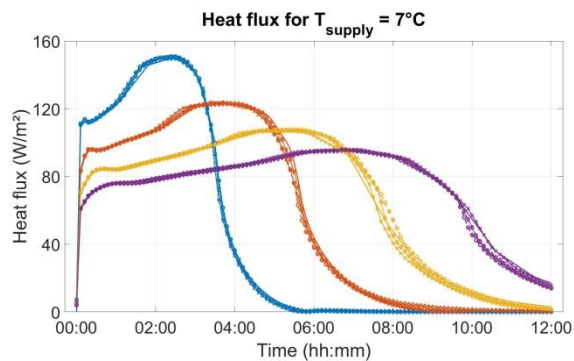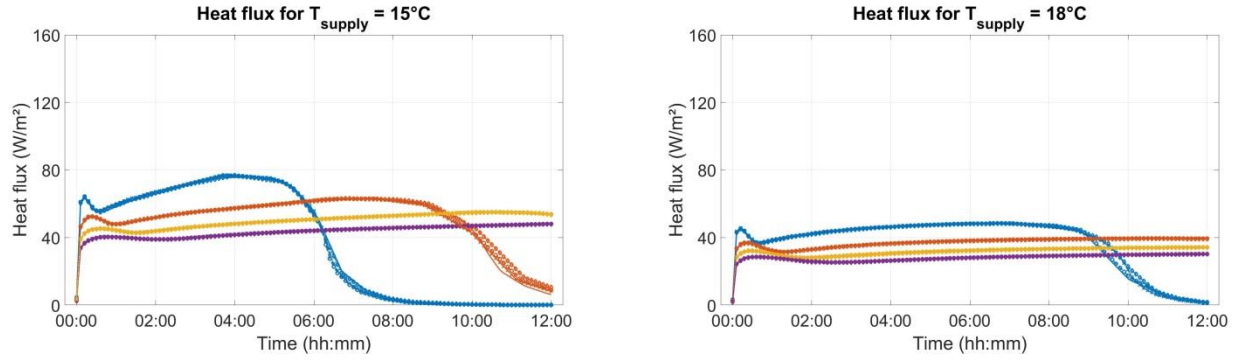
Figure 7: Heat flux on the lower surface of the PCM panels based on the panel thickness

Energy released

Figure 8 shows the accumulated energy per m² of panel area released by the PCM to change state from liquid to solid, as a function of the panel thickness. The accumulated energy was calculated as a fraction of the panel area to be indicative for applications with different floor area. Colour variation represents different water supply temperature, while the different marker represents different water flow rate in the embedded pipes. For example, the yellow line with star marker corresponds to T_s of 15°C and 280 kg/h of water flow rate in the embedded pipes.

The presented values refer to thermal energy and should not be misinterpreted with electrical energy use. Among cases with the same panel thickness, the accumulated energy released by the PCM increased as the water supply temperature was increasing. Similarly, among cases with the same water supply temperature, the accumulated energy released by the PCM increased, as the panel thickness was increasing. In the cases where the PCM got fully discharged, there was no energy released after the PCM was fully solidified although the temperature of the PCM was continuing to decrease as shown in Figure 5. When the panel thickness was 25 mm, before the PCM was fully discharged the difference among the cases with different supply water temperature was insignificant; see Figure 8a between 00:00 and 04:00. The difference among the cases with different water supply temperature was becoming more profound as the panel thickness was increasing, for example in Figure 8d.

$$\text{---}T_{supply} = 7°C \quad \text{---}T_{supply} = 12°C \quad \text{---}T_{supply} = 15°C \quad \text{---}T_{supply} = 18°C$$
$$\text{---}W_{flow} = 240\ kg/h \quad \text{--•--}W_{flow} = 280\ kg/h \quad \text{--o--}W_{flow} = 320\ kg/h \quad \text{--×--}W_{flow} = 360\ kg/h$$
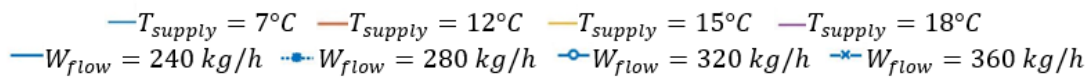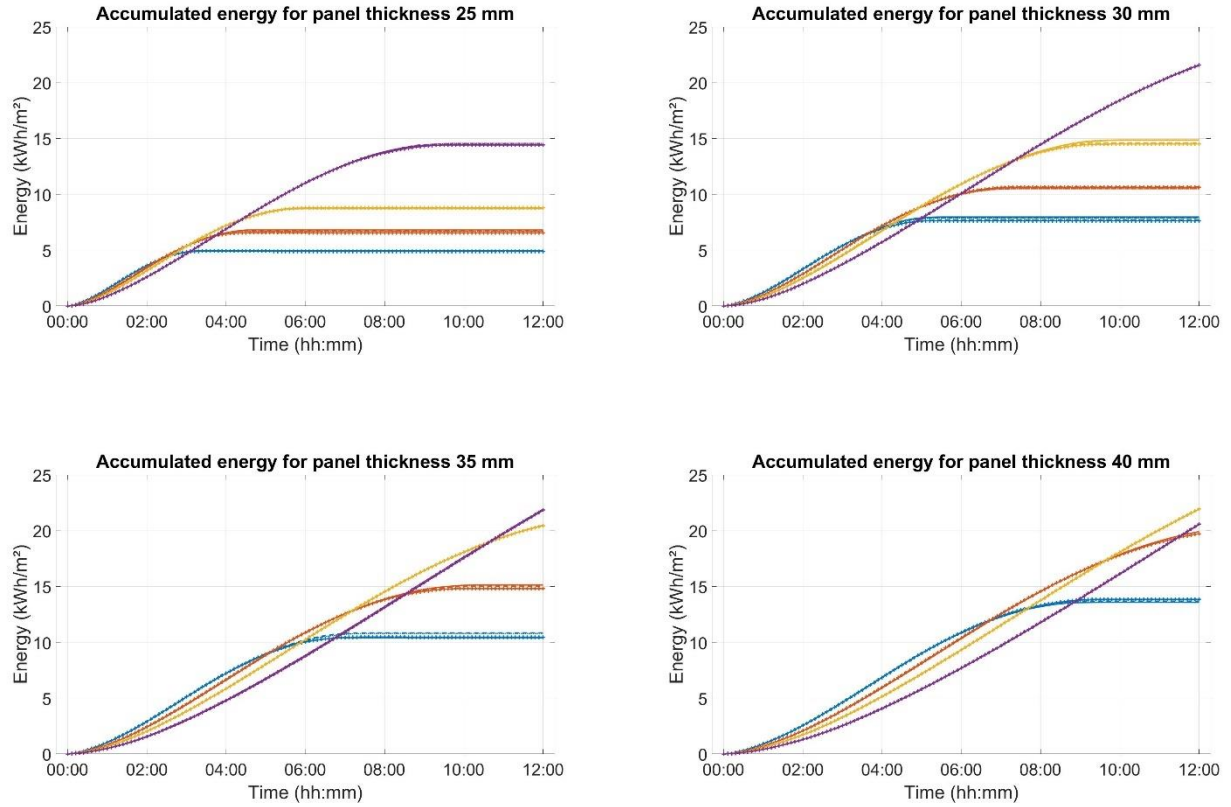
Figure 8: Accumulated energy released from the PCM layer

As it was discussed earlier, water supply temperature of 7°C and 12°C should be avoided. Therefore, the only cases where the PCM got fully discharged were when the panel thickness was 25 mm and the water supply temperature either 15°C or 18°C and when the panel thickness was 30 mm and the water supply temperature was 18°C. Out of these cases, the combination of water supply temperature of 15°C and panel thickness of 25 mm was considered as ideal, since the discharging period lasted significantly less compared to the other two cases, as shown in Table 3. That means less hours of operation for the cooling equipment (chiller, heat pump, etc.) and pumps and therefore reduced energy use.

The panel thickness could be higher only if the PCM thermal conductivity was enhanced either by adding an additive to the PCM layer, e.g. metal filings, adding a structural form with a high thermal conductivity, e.g. graphite foam or by adding copper vertical or horizontal fins as shown in Figure 9. It should be taken into consideration though that some of these solutions would increase the cost of the panels substantially. Therefore, a feasibility analysis would be required to examine whether the increase of the cost due to the additional PCM quantity and the thermal conductivity enhancement is a viable investment.
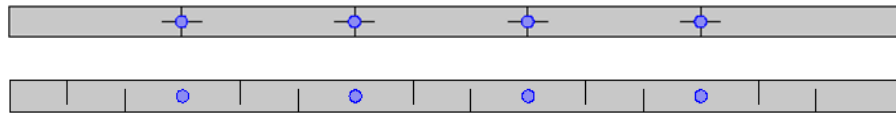
Figure 9: Proposals for enhancing the thermal conductivity of the PCM layer by installing metal fins

Conclusions

The subject of this study was to examine the discharging performance of a PCM ceiling panel. The parameters that were examined were the panel thickness, the water supply temperature and the water flow rate.

It was found that the examined range of water flow rate had no impact on the discharging process of the PCM. Furthermore, the thickness of the panel should not be above 30 mm since the PCM did not get fully discharged on time in cases of thicker panels. Higher thickness values would be feasible only if PCM is combined with graphite foam or other methods for enhancing the thermal conductivity of the PCM. Water supply temperature low as 7°C or 12°C should be avoided in residential and commercial buildings due to the risk of condensation. Finally, based on the present study the ideal combination for a PCM ceiling panel among the examined cases was a panel thickness of 25 mm and a water supply temperature of 15°C.

Reference

[1]   J. Adnot, P. Riviere, D. Marchio, M. Holmstrom, J. Naeslund, J. Saba, and I. Blanco, "Energy Efficiency and Certification of Central Air Conditioners (EECCAC) Volume 2," 2003.

[2]   T. K. Stovall and J. J. Tomlinson, "What are the potential benefits of including latent storage in common wallboard?," *J. Sol. Energy Eng. - Trans. ASME*, vol. 11, no. 4, pp. 318–325, 1995.

[3]   P. Schossig, H. M. Henning, S. Gschwander, and T. Haussmann, "Micro-encapsulated phase-change materials integrated into construction materials," *Sol. Energy Mater. Sol. Cells*, vol. 89, no. 2–3, pp. 297–306, 2005.

[4]   C. Castellón, M. Medrano, J. Roca, G. Fontanals, and L. F. Cabeza, "Improve thermal comfort in concrete buildings by using phase change material," in *Proceedings of the Energy Sustainability Conference 2007*, 2007, pp. 457–463.

[5]   A. Pasupathy, R. Velraj, and R. V. Seeniraj, "Phase change material-based building architecture for thermal management in residential and commercial establishments," *Renew. Sustain. Energy Rev.*, vol. 12, no. 1, pp. 39–64, 2008.

[6]   A. Sharma, V. V. Tyagi, C. R. Chen, and D. Buddhi, "Review on thermal energy storage with phase change materials and applications," *Renew. Sustain. Energy Rev.*, vol. 13, no. 2, pp. 318–345, 2009.

[7]   T. R. Whiffen and S. B. Riffat, "A review of PCM technology for thermal energy storage in the built environment: Part I," *Int. J. Low-Carbon Technol.*, vol. 8, no. 3, pp. 147–158, 2013.

[8]   H. G. Lorsch, K. W. Kauffman, and J. C. Denton, "Thermal energy storage for heating and air conditioning," *Futur. energy Prod. Syst. Heat mass Transf. Process.*, vol. 1, pp. 69–81, 1976.

[9]   W. R. Humphries and E. I. Griggs, *A design handbook for phase change thermal control and energy storage devices*. 1977.

[10]   G. A. Lane, "Solar Heat Storage : Latent Heat Materials - Vol . I : Background and Scientific Principles," *Sol. Energy Mater.*, vol. 33, no. 5, p. 476, 1984.

[11]   Hasnain S.M., "Review on sustainable thermal energy storage technologies, Part I: heat storage materials and techniques," *Energy Convers. Manag.*, vol. 39, no. 11, pp. 1127–1138, 1998.

[12]   J. Kośny, *PCM-Enhanced Building Components - An Application of Phase Change Materials in Building Envelopes and Internal Structures*. 2015.

[13]   B. Zalba, J. M. Marín, L. F. Cabeza, and H. Mehling, *Review on thermal energy storage with phase change: Materials, heat transfer analysis and applications*, vol. 23, no. 3. 2003.

[14]   M. M. Farid, A. M. Khudhair, S. A. K. Razack, and S. Al-Hallaj, "A review on phase change energy storage: Materials and applications," *Energy Convers. Manag.*, vol. 45, no. 9–10, pp. 1597–1615, 2004.

[15]   Y. Zhang, G. Zhou, K. Lin, Q. Zhang, and H. Di, "Application of latent heat thermal energy storage in buildings: State-of-the-art and outlook," *Build. Environ.*, vol. 42, no. 6, pp. 2197–2209, Jun. 2007.

[16]   H. Mehling and L. F. Cabeza, *Heat and cold storage with PCM*. 2008.

[17]   D. Zhou, C. Y. Zhao, and Y. Tian, "Review on thermal energy storage with phase change materials (PCMs) in building applications," *Appl. Energy*, vol. 92, pp. 593–605, 2012.

[18]   F. Agyenim, N. Hewitt, P. Eames, and M. Smyth, "A review of materials, heat transfer and phase change problem formulation for latent heat thermal energy storage systems (LHTESS)," *Renew. Sustain. Energy Rev.*, vol. 14, no. 2, pp. 615–628, 2010.

[19]   W. Lu and S. A. Tassou, "Experimental study of the thermal characteristics of phase change slurries for active cooling," *Appl. Energy*, vol. 91, no. 1, pp. 366–374, 2012.

[20]   L. Zhong, X. Zhang, Y. Luan, G. Wang, Y. Feng, and D. Feng, "Preparation and thermal properties of porous heterogeneous composite phase change materials based on molten salts/expanded graphite," *Sol. Energy*, vol.

107, pp. 63–73, 2014.

[21]   P. V. Padmanabhan and M. V. Krishna Murthy, "Outward phase change in a cylindrical annulus with axial fins on the inner tube," *Int. J. Heat Mass Transf.*, vol. 29, no. 12, pp. 1855–1868, 1986.

[22]   V. Morcos, "Investigation of a latent heat thermal energy storage system," *Sol. Wind Technol.*, vol. 7, no. 2–3, pp. 197–202, 1990.

[23]   M. Costa, D. Buddhi, and A. Oliva, "Numerical simulation of a latent heat thermal energy storage system with enhanced heat conduction," *Energy Convers. Manag.*, vol. 39, no. 3–4, pp. 319–330, 1998.

[24]   C. A. Bauer and R. A. Wirtz, "Thermal characteristics of a compact, passive thermal energy storage device," *Am. Soc. Mech. Eng. Heat Transf. Div.*, vol. 366, pp. 283–289, 2000.

[25]   M. Kamimoto, Y. Abe, S. Sawata, T. Tani, and T. Ozawa, "Latent thermal storage unit using form-stable high density polyethylene. I. Performance of the storage unit," *Trans. ASME. J. Sol. Energy Eng.*, vol. 108, no. 4, pp. 282–289, 1986.

[26]   X. Py, R. Olives, and S. Mauran, "Paraffin/porous-graphite-matrix composite as a high and constant power thermal storage material," *Int. J. Heat Mass Transf.*, vol. 44, no. 14, pp. 2727–2737, 2001.

[27]   I. Dinçer and M. A. Rosen, *Thermal Energy Storage: Systems and Applications*. 2010.

[28]   K. Peippo, P. Kauranen, and P. D. Lund, "A multicomponent PCM wall optimized for passive solar heating," *Energy Build.*, vol. 17, no. 4, pp. 259–270, 1991.

[29]   R. Baetens, B. P. Jelle, and A. Gustavsen, "Phase change materials for building applications: A state-of-the-art review," *Energy Build.*, vol. 42, no. 9, pp. 1361–1368, 2010.

[30]   M. Koschenz and B. Lehmann, "Development of a thermally activated ceiling panel with PCM for application in lightweight and retrofitted buildings," *Energy Build.*, vol. 36, pp. 567–578, 2004.

[31]   W. Saman, F. Bruno, and E. Halawa, "Thermal performance of PCM thermal storage unit for a roof integrated solar heating system," *Sol. Energy*, vol. 78, no. 2, pp. 341–349, 2005.

[32]   E. Bourdakis, T. Q. Péan, L. Gennari, and B. W. Olesen, "Daytime space cooling with phase change material ceiling panels discharged using rooftop photovoltaic/thermal panels and night-time ventilation," *Sci. Technol. Built Environ.*, vol. 4731, no. June, 2016.

[33]   E. Bourdakis, T. Q. Péan, L. Gennari, and B. W. Olesen, "Experimental study of discharging PCM ceiling panels through nocturnal radiative cooling," in *9th International Conference on Indoor Air Quality, Ventilation and Energy Conservation in Buildings (IAQVEC) 2016*, 2016.

[34]   D. Feldman, M. M. Shapiro, D. Banu, and C. J. Fuks, "Fatty acids and their mixtures as phase-change materials

for thermal energy storage," *Sol. Energy Mater.*, vol. 18, no. 3, pp. 201–216, 1989.

[35]   X. Wang and J. Niu, "Performance of cooled-ceiling operating with MPCM slurry," *Energy Convers. Manag.*, vol. 50, no. 3, pp. 583–591, 2009.

[36]   S. Álvarez, L. F. Cabeza, A. Ruiz-Pardo, A. Castell, and J. A. Tenorio, "Building integration of PCM for natural cooling of buildings," *Appl. Energy*, vol. 109, pp. 514–522, 2013.

[37]   Y. Dutil, D. Rousse, S. Lassue, L. Zalewski, A. Joulin, J. Virgone, F. Kuznik, K. Johannes, J. P. Dumas, J. P. Bédécarrats, A. Castell, and L. F. Cabeza, "Modeling phase change materials behavior in building applications: Comments on material characterization and model validation," *Renew. Energy*, vol. 61, pp. 132–135, 2014.

[38]   C. C. Menassa, "Evaluating sustainable retrofits in existing buildings under uncertainty," *Energy Build.*, vol. 43, no. 12, pp. 3576–3583, 2011.

[39]   J. M. Gutherz and M. E. Schiler, "A PASSIVE SOLAR HEATING-SYSTEM FOR THE PERIMETER ZONE OF OFFICE BUILDINGS," *Energy Sources*, vol. 13, no. 1, pp. 39–54, 1991.

[40]   T. Kondo and S. Iwamoto, "Research on Thermal Storage using Rock Wool PCM Ceiling Board PCM ceiling board Rock Wool ceiling board," *ASHRAE Trans.*, vol. 112, pp. 526–531, 2006.

[41]   J. Li, P. Xue, H. He, W. Ding, and J. Han, "Preparation and application effects of a novel form-stable phase change material as the thermal storage layer of an electric floor heating system," *Energy Build.*, vol. 41, no. 8, pp. 871–880, 2009.

[42]   Dansk Standard (DS), *DS/EN 13501-1: Fire classification of construction products and building elements – Part 1: Classification using data from reaction to fire tests*. 2009.

[43]   Dansk Standard (DS), *DS/EN 13501-2: Fire classification of construction products and building elements – Part 2: Classification using data from fire resistance tests, excluding ventilation services*. Charlottenlund, 2009.

[44]   Dansk Standard (DS), *DS/EN 1991-1-2: Eurocode 1: Actions on structures – Part 1-2: General actions – Actions on structures exposed to fire*. Charlottenlund, 2007.

[45]   Dansk Standard (DS), *DS/EN ISO 1182: Reaction to fire tests for products – Non-combustibility test*. Charlottenlund, 2010.

[46]   J. R. Turnpenny, D. W. Etheridge, and D. A. Reay, "Novel ventilation cooling system for reducing air conditioning in buildings. Part I: Testing and theoretical modelling," *Appl. Therm. Eng.*, vol. 20, no. 11, pp. 1019–1037, 2000.

[47]   S. Scalat, D. Banu, D. Hawes, J. Paris, F. Haghighata, and D. Feldman, "Full scale thermal testing of latent heat storage in wallboard," *Sol. Energy Mater. Sol. Cells*, vol. 44, no. 1, pp. 49–61, 1996.

[48]   D. Banu, D. Feldman, and D. Hawes, "Evaluation of thermal storage as latent heat in phase change material wallboard by differential scanning calorimetry and large scale thermal testing," *Thermochim. Acta*, vol. 317, pp. 39–45, 1998.

[49]   D. Feldman, D. Banu, and D. W. Hawes, "Development and application of organic phase change mixtures in thermal storage gypsum wallboard," *Sol. Energy Mater. Sol. Cells*, vol. 36, no. 2, pp. 147–157, 1995.

[50]   D. W. Hawes, D. Feldman, and D. Banu, "Latent heat storage in building materials," *Energy Build.*, vol. 20, no. 1, pp. 77–86, 1993.

[51]   D. Feldman, D. Banu, D. Hawes, and E. Ghanbari, "Obtaining an energy storing building material by direct incorporation of an organic phase change material in gypsum wallboard," *Sol. Energy Mater.*, vol. 22, no. 2–3, pp. 231–242, 1991.

[52]   D. Feldman and D. Banu, "DSC analysis for the evaluation of an energy storing wallboard," *Thermochim. Acta*, vol. 272, no. 1–2, pp. 243–251, 1996.

[53]   T. Lee, D. W. Hawes, D. Banu, and D. Feldman, "Control aspects of latent heat storage and recovery in concrete," *Sol. Energy Mater. Sol. Cells*, vol. 62, no. 3, pp. 217–237, 2000.

[54]   F. Kuznik, D. David, K. Johannes, and J. J. Roux, "A review on phase change materials integrated in building walls," *Renew. Sustain. Energy Rev.*, vol. 15, no. 1, pp. 379–391, 2011.

[55]   G. K. Pavlov, *Building Thermal Energy Storage*. Copenhagen, Denmark: DTU-Tryk, 2014.

[56]   A. Sari, "Form-stable paraffin/high density polyethylene composites as solid-liquid phase change material for thermal energy storage: Preparation and thermal properties," *Energy Convers. Manag.*, vol. 45, no. 13–14, pp. 2033–2042, 2004.

[57]   M. Xiao, B. Feng, and K. Gong, "Preparation and performance of shape stabilized phase change thermal storage materials with high thermal conductivity," *Energy Convers. Manag.*, vol. 43, no. 1, pp. 103–108, 2002.

[58]   International Organization for Standardization, *ISO 11855-1: Building Environment Design — Design, Dimensioning, Installation and Control of the Embedded Radiant Heating and Cooling Systems —Part 1: Definition, symbols, and comfort criteria*. 2012.

Paper 4: Eilersen E.C.R., Krintel C.H., **Bourdakis E.**, Kazanci O.B., Olesen B.W. (2018). Development of a simplified method for designing office buildings with a PCM-enhanced suspended ceiling. Submitted at Science and Technology for the Built Environment

Development of a simplified method for designing office buildings with a suspended ceiling containing Phase Change Material (PCM)

Esben C.R. Eilersen, Christian H. Krintel, Eleftherios Bourdakis, Ongun B. Kazanci, Bjarne W. Olesen

International Centre for Indoor Environment and Energy – ICIEE, Department of Civil Engineering, Technical University of Denmark, Nils Koppels Allé, Building 402, 2800 Kgs. Lyngby, Denmark

Abstract

The authors conducted a parametric simulation study to identify the effect of different phase change material (PCM) types and heat loading on the energy used by the heating and cooling system of two office rooms. The intention was to create a simplified method for calculating the potential energy savings from implementing ceiling panels containing PCM in office buildings. The parametric analysis showed that choosing the correct PCM can result in energy savings of up to 26%, while a poor decision can result in an increase in the energy use of up to 6%. From the statistical analysis, the authors developed an equation calculating the energy savings for each simulated location and PCM type examined.

Nomenclature

Symbol	Unit	Quantity
A_g	m^2	Glazing area
A_f	m^2	Floor area
$c_{p,eff}$	kJ/kgK	Effective heat capacity
$c_{p,eff,peak}$	kJ/kgK	Peak effective heat capacity
$c_{p,sens}$	kJ/kgK	Specific sensible heat capacity
d	m	PCM panel thickness
DTR	^oC	Diurnal temperature range
DTR_{avg}	^oC	Average diurnal temperature range
E_{tot}	kWh/m^2	Total energy use
ENS	%	Percentage of energy savings
EGA	-	Equivalent glazing area

H	^oC	Hysteresis
HG		Heat gain
LH	kJ/kg	Latent heat
LOC	-	Location
$PCTR$	^oC	Phase change temperature range
RMSE	-	Root-mean-square error
T_{avg}	^oC	Annual average outdoor temperature
$T_{m,s}$	^oC	Start melting temperature
$T_{m,end}$	^oC	Temperature at the end of the melting phase
T_p	^oC	Temperature corresponding to the peak c_p-value $c_{p,eff,peak}$
T_{PCM}	^oC	PCM temperature
$T_{s,s}$	^oC	Initial solidifying temperature
T_{tcr}	^oC	Thermal comfort range
UR N	%	Utilization ratio for north oriented office room
UR S	%	Utilization ratio for south oriented office room
WFAR	%	Window to floor area ratio
a	-	Coefficients for drawing the effective heat capacity curve
β	-	
γ	-	
λ	W/mK	Thermal conductivity

Introduction

Background theory on phase change materials

Reducing the energy used in the building sector is currently a priority, to reach to the global goal for reducing greenhouse gas emissions that was agreed at the recent Paris agreement [1]. The building sector is responsible for 41% of all energy use in the European Union and the US and 50% of that is used to operate heating, ventilation and air-conditioning (HVAC) equipment (DoE 2012; European Commission 2016). Several studies shows optimal use of the thermal mass of buildings can reduce this energy use substantially [4]–[7].

Heat could be stored in the structure of a building either in the form of sensible or latent heat. Sensible heat storage is when the accumulated energy in the building elements results in an increase in their temperature. Latent heat storage is when a material is heated to a its melting point temperature, after which the material undergoes a phase transition from a stable state to a more dispersed state, e.g. ice melting. This endothermic process absorbs energy to break the molecular bonds and the energy is stored as latent energy in the material. When the temperature of the material is reduced to the temperature at which it solidifies, it releases its stored energy and starts to solidify.

A solution that could increase the thermal mass of buildings, especially lightweight constructions, is the implementation of Phase Change Material (PCM) in the structural elements. During daytime, room air is heated up by solar radiation and internal heat gains. PCM implemented in the structure absorbs that heat and its temperature increases, as in the case of a conventional building material, until it reaches the PCM's phase change temperature range (PCTR). At that point, the PCM continues to absorb heat but instead of heating up, its thermal capacity increases significantly, and it starts to melt. When all the PCM has melted, its temperature starts to increase again and the PCM behaves like a conventional building material (Figure 1).
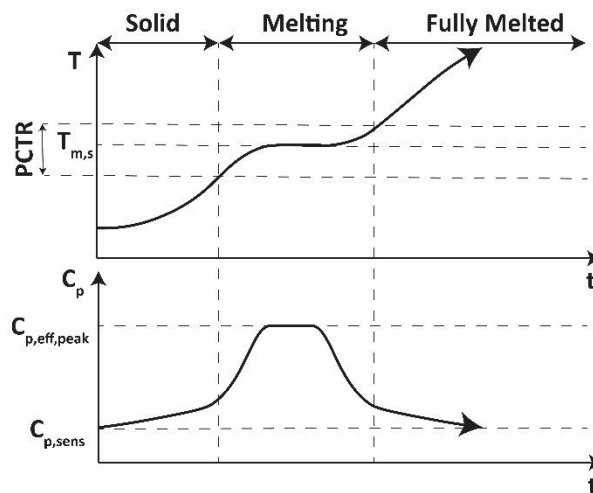

Figure 1: Correlation of temperature and thermal capacity during the melting process

During the night, the PCM releases the stored heat back to the room and it solidifies again. The ideal daily performance for the PCM would be achieved if it was completely solid at the beginning of the occupancy period, and completely melted at the end of it. The PCM can be discharged (i.e. solidified) either passively, e.g. by natural ventilation, or actively, e.g. by mechanical ventilation or by circulating water in pipes embedded in the PCM.

Several types of PCM are utilized in different industrial sectors and they are divided in three main categories: organic, inorganic and eutectic PCMs. Organic PCMs include paraffins, fatty acids, polyethylene glycols (PEG) and sugar alcohols, while inorganic PCMs are mainly salt hydrates [8]. Eutectic PCMs are chemical mixtures of multiple PCMs, which results in a melting point lower than that of each component separately [9]. Paraffins have a high heat of fusion, narrow enthalpy curves, good melting congruency and no super-cooling occurs [10]. Their biggest drawbacks are that they cost more than salt hydrates and are flammable [10]. Fatty acids have good melting congruency, are chemically stable, non-toxic and they can be produced sustainably from plant and animal waste. On the other hand, they have a lower heat of fusion than paraffins and they are slightly corrosive [10], [11]. PEGs have a heat of fusion that is comparable to that of fatty acids, they are non-toxic and chemically stable, they display congruent melting and no super-cooling occurs [12]. Sugar alcohols have the highest heat of fusion among the organic PCMs but their melting temperature of $90 - 200^{\circ}C$ makes them inappropriate for building envelope applications [10]. Salt hydrates are non-toxic, non-flammable and have a higher heat of fusion than organic PCMs. On the other hand, corrosion occurs when they are combined with metals, they are subject to volumetric change and super-cooling and they have incongruent melting [10], [13]. Table 1 summarizes the different PCM categories with their advantages and disadvantages.

Table 1: PCM types and characteristics

PCM category	PCM subcategory	Advantages	Disadvantages
Organic	Paraffins	+ high heat of fusion + narrow enthalpy curves + good melting congruency + no super-cooling	− high cost − flammability
	Fatty acids	+ good melting congruency + chemically stable + not toxic + can be produced sustainably by utilizing plant and animal waste	− lower heat of fusion than paraffins − slightly corrosive

	polyethylene glycols (PEG)	+	comparable heat of fusion to fatty acids	− high cost
		+	non-toxic	− low heat storage capacity per unit volume
		+	chemically stable	
		+	congruent melting	
		+	no super-cooling occurs	
	sugar alcohols	+	highest heat of fusion among the organic PCMs	− Inappropriate for building applications due to high melting temperature (90ºC – 200ºC)
Inorganic	salt hydrates	+	non-toxic	− corrosion when combined with metals
		+	non-flammable	− subject to volumetric change
		+	higher heat of fusion than organic PCMs	− subject to super-cooling
				− incongruent melting
	metals	+	high heat of fusion per unit volume	− very high melting point for building applications
		+	high thermal conductivity	− high weight
Eutectic	chemical mixtures of multiple PCMs	+	higher phase change enthalpy compared to paraffin and salt hydrate PCMs	− low information on thermophysical properties
		+	long-term durability	− some have a strong odour which makes them unapplicable for building applications
		+	easy impregnation in porous materials	

PCMs can be implemented in the building structure or in building components using three different methods, impregnation, macro-encapsulation and microencapsulation. [10], [14]–[16]. Impregnation is when liquid PCM is implemented directly in porous materials. This is the cheapest among the containment methods, but leakage problems often occur. Macro-encapsulation is implementation of PCM in capsules of a radius of 1-10 cm. This method prevents leakage, but the capsules are very fragile. Micro-encapsulation is the implementation of PCM in capsules with a radius of 1-100 μm. These capsules are very durable; however, they increase the cost of the PCM installation significantly.

The use of PCMs in buildings has not attained high market penetration, despite their well-documented benefits [10], [13], [15], [17], [18].

Parametric literature review

The biggest obstacles for the wide use of PCM in buildings are the many design parameters that have to be considered and the lack of simplified and accessible tools that can reliably predict the performance of a building with embedded PCM (Soares et al. 2013; IEA 2013). The most important parameters that affect the performance of PCMs are the latent

enthalpy, the melting temperature, the phase change temperature range, the effective heat capacity curves, the thermal conductivity, the amount of PCM contained in the building structure, the thickness of the PCM layer, the climatic conditions, the level of internal heat gains and the heat transfer coefficient on the PCM surface.

The latent enthalpy is the amount of energy stored and released when the phase change occurs. A higher latent enthalpy means that the PCM is capable of storing a larger amount of energy [20]. The melting temperature is the temperature at which the phase changes from solid to liquid and should be within the thermal comfort range [21], [22]. PCTR is the range around the melting temperature where the latent enthalpy is higher. Contradictory results are to be found in the literature, with cases where a low or a wider PCTR proved to be better [21], [23]. The effective heat capacity curve describes the thermal characteristic of the PCM-enhanced product and is shown in Equation 1 [21]

$$
c_{p,eff}(T_{PCM}) = \begin{cases} c_{p,sens} + a(T_p - T_{PCM})^\beta \cdot e^\gamma (T_p - T_{PCM}) & if\ T_{PCM} \leq T_p \\ \dfrac{c_{p,sens} - c_{p,eff,peak}}{T_{m,end} - T_p} \cdot (T_{PCM} - T_p) + c_{p,eff,peak} & if\ T_p < T_{PCM} \leq T_{m,end} \\ c_{p,sens} & otherwise \end{cases} \qquad 1
$$

where $\alpha, \beta\ and\ \gamma$ are coefficients that affect the shape of the curve. The thermal conductivity of the PCM affects how fast the PCM can absorb and release energy. The thermal conductivity of PCMs can be enhanced with high conductivity additives such as aluminium powder, metal oxide and graphite foam [10]. The thickness of the PCM layer is crucial due to the low thermal conductivity of the PCMs. Beyond a critical value, the additional thickness has no impact, as the heat does not penetrate the PCM panel [23], [24]. The PCM amount determines the total amount of energy the building element can store. If the quantity is lower than is required, excess heat remains in the room and overheating occurs, while if the PCM quantity is too high, the discharging period will take longer than intended [10], [18], [24]. In addition to that, if the quantity of the PCM is higher than is required, the installation and operation costs will be significantly increased with no additional benefits.

Several studies have been conducted on the correlation of the diurnal temperature range (DTR) with thermal mass utilization but they obtained contradictory results, depending on the climate conditions they examined. Shaviv et al. found a linear correlation between the reduction of the maximum indoor temperature and the DTR for the hot-humid Israeli climate [25]. In other studies, it was found that the free cooling potential was positively correlated with a higher DTR and that the average outdoor temperature had only a minor effect on the cooling potential of the PCM [21], [26]. In contrast, Alam et al., who simulated a one-room house in six climate zones of Australia found that in cold, mild and hot temperate climates, PCMs had a better potential for energy savings than in hot humid climates [22]. Other studies showed that a DTR higher than 12-15°C was ideal for free cooling systems [17], [27].

Internal heat gains affect the performance of PCMs because a high heat gain will heat up the room quickly and, depending on the PCM conductivity, it might not be able to absorb it. Furthermore, the distribution of the heat sources also affects the performance of the PCM [16], and if possible, they should be distributed evenly across the room. The heat transfer coefficient on the surface should be as high as possible to achieve a higher energy transfer to the PCM. It is worth noting that a higher convective heat transfer coefficient is achieved by high air velocities, although they might increase the risk of draught.

The literature review shows that a simplified design method is required, one that incorporates the most critical parameters that affect the performance of PCM panels. The intention of the present study was to facilitate the use of PCM panels in buildings, as this could lead to significant energy savings, by introducing a simplified method for estimating whether and how PCMs would be beneficial for a building.

A parametric study using dynamic building simulations was conducted, to identify the effect of different PCM types and cooling loads on the energy use of HVAC systems. The PCM-related parameters that were included were the phase change temperature range, different melting and solidifying temperature points, the hysteresis and the latent heat of fusion. The following parameters were also simulated for each PCM, resulting in a total of 2240 simulations:

- five locations with different climates

- two levels of glazing area

- two levels of ceiling coverage with PCM

- two levels of panel thickness

- two levels of internal heat gains

Method

Validation of PCM component

In order to increase the validity of a simulation model, the International Energy Agency (2013) suggested comparing it with a standardized benchmark method. Kuznik & Virgone (2009) described a benchmarking method known as Microbat and this was used in the present study. The Microbat test compared the thermal performance of two cubic cells; one with PCM and one without (NoPCM). Kuznik and Virgone placed the two cells in a climate chamber where they could adjust the room air temperature. They compared the cells under three scenarios: a step temperature increase from 15ºC to 30ºC, a step decrease from 30ºC to 15ºC and a sinusoidal variation between 15ºC and 30ºC with a period of 24 hours. The first two scenarios were tested with one-hour and three-hour time steps. The NoPCM cell had a front wall of 2 mm aluminium, while the other walls were of 2 mm of aluminium, 60 mm of polyurethane insulation and 5 mm of

cardboard, from outside to inside. In the PCM cell, the cardboard was replaced with a 5 mm PCM-wallboard which contained micro-encapsulated paraffin (60% by weight).

For the present study, a similar TRNSYS model was created to simulate the same conditions. Figure 2 shows the air temperature inside the cells during the simulations in comparison with the corresponding cases from the Microbat experiment. There was only a small discrepancy in the heating simulations for the PCM model: the root mean square errors (RMSE) were in the range 0.28 – 0.29. On the other hand, a significant discrepancy was observed in the case of cooling: the RMSE was in the range 0.71 – 0.81. For the NoPCM, the simulations predicted the air temperature very well; the RMSE was in the range 0.14 – 0.34. The authors consider that the inaccuracies were caused because the software cannot simulate how the PCM behaves inside the micro-encapsulation. Nevertheless, the PCM component was considered accurate enough to be further investigated.

2a: Cooling step = 1 h
RMSE: (NoPCM) = 0.17, (PCM) = 0.81

2b: Cooling step = 3 h
RMSE: (NoPCM) = 0.30, (PCM) = 0.72

2c: Heating step: 1 h
RMSE: (NoPCM) = 0.14, (PCM) = 0.28

2d: Heating step = 3 h
RMSE: (NoPCM) = 0.14, (PCM) = 0.29

2e: Sinusoidal variation RMSE: (NoPCM) = 0.34, (PCM) = 0.62

EXP_NOPCM — EXP_PCM — SIM_NOPCM — SIM_PCM — Tamb
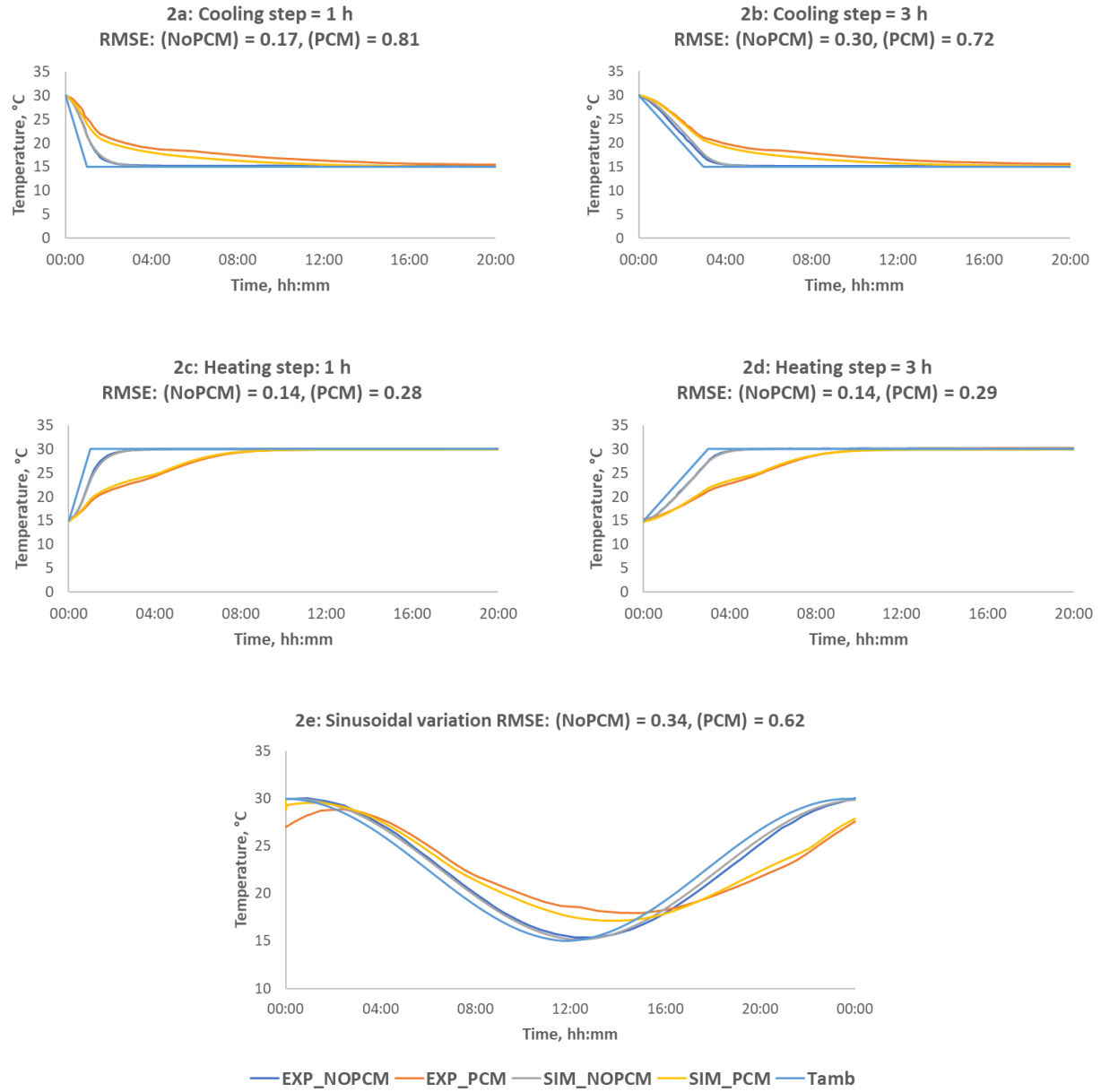
Figure 2: Results of the validation simulations

Model description

In this parametric study, an office building section with a South-North orientation was simulated. The floor area of each office was 21 m² and the suspended ceiling height was 2.8 m. Above each office there was a plenum with a height of 0.5 m from which air was supplied to the room. The PCM was in the ceiling panels separating the office from the plenum.

Two PCM quantities were simulated, one in which the whole ceiling area contained PCM and one where only half of the ceiling contained PCM. The two offices were separated by a 1.5 m wide corridor. Each office had a window, for which

two window sizes were simulated, 5.25 m² and 7.88 m², corresponding to a window-to-floor-area ratio of 21% and 33%, respectively. The windows were triple-glazed with a U-value of 0.5 W/m²K and a g-value of 0.33. The windows were described by the equivalent glazing area (EGA) which was calculated using Equation 2 and resulted in 0.059 and 0.092 respectively for the two window-to-floor ratios (WFAR). Figure 3 shows a drawing of the office section with the wall dimensions.

$$EGA = \frac{A_g}{A_f} g_{value} \qquad\qquad 2$$
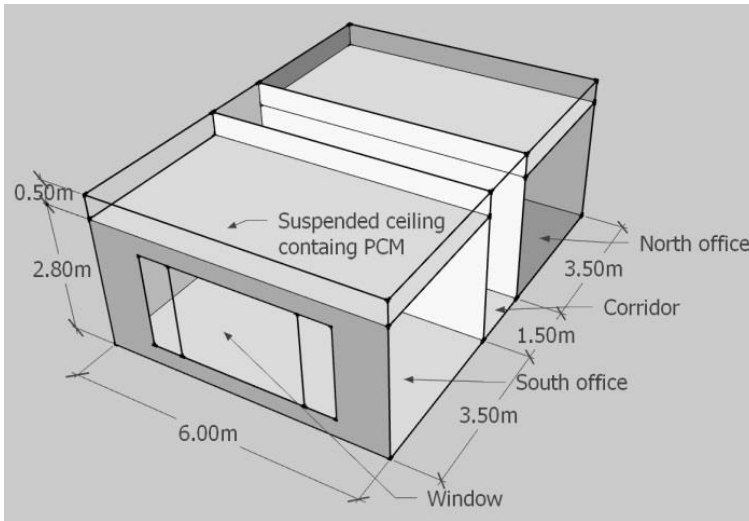
Figure 3: Office section drawing

The exterior wall was a light-weight construction so that the PCM provided the main thermal mass of the construction, with a U-value of 0.11 W/m²K. The internal walls were considered as partition walls, having a low thermal capacity and a U-value of 0.57 W/m²K. The floor and ceiling slabs consisted of concrete with a thickness of 240 mm. Table 2 shows the properties for all materials used for each wall type.

		Thickness, mm	λ, W/mK	ρ, kg/m3
Internal wall	Gypsum board (outer side)	26	0.23	800
	Insulation	50	0.04	50
	Gypsum board (inner side)	26	0.23	800
External wall	Fibrocement (outer side)	8	1.25	1536
	Insulation	315	0.04	50
	Gypsum board (inner side)	26	0.23	800
Floor	Concrete	240	2.03	2400

Each office had two occupants engaged in sedentary office activity (1.2 met), as this is assumed by the ISO Standard 7730 (EN ISO 2006). The artificial lighting had a power of 2.5 W/m² in the offices and 2 W/m² in the corridor. Two different heat gains from office equipment were simulated, 150 W (7.1 W/m²) and 300 W (14.2 W/m²) per office. All internal heat sources were activated during the occupancy period, i.e. 08:00 to 16:00.

To make this study more representative, the authors simulated five locations whose climatic conditions differ substantially. These locations were Buenos Aires in Argentina, Dori in Burkina Faso, Copenhagen in Denmark, Madrid in Spain and Santa Maria in California, USA. For the rest of this paper, the abbreviations AR, BF, DK, ES and US will be used for these five locations, respectively. The thermal comfort range was calculated based on the adaptive method described in EN Standard 15251 (EN 2007). The adaptive method is normally used in buildings in which passive means are adequate for maintaining the room temperature below the upper limit. Here it was used throughout, due to the significantly different weather files used in the present study.

The option of ideally specified heating and cooling systems was used, so the effect of the PCM was evaluated in terms of a reduction (or an increase) in the energy use from the heating and cooling equipment. During the cooling season, the PCM should be discharged during the night to have its full latent capacity available to absorb heat the next day. On the other hand, during the heating season, the stored heat should be kept inside the building, to minimize energy use for heating. For discharging the PCM during the cooling period, night-time ventilation was used. The ventilation was a

constant air volume system (CAV) and three different airflow rates were examined, 14.7 L/s, 28.7 L/s and 60 L/s. The

discharging period was outside the occupancy period, namely from 16:00 to 08:00. The ventilation system contained a

heat recovery heat exchanger. A controller regulated the return flow passing through the heat exchanger to condition the

supply temperature. The air supply temperature was the same for each of the two offices. The supply temperature varied

between the outdoor temperature, when the heat exchanger was bypassed, and the maximum heat recovery temperature.

The effectiveness of the heat exchanger was 90%. During the heating period, the air supply temperature setpoint was at

the upper limit of the comfort range, in order to utilize heat recovery as much as possible. During the cooling period,

during occupancy and after occupancy when the PCM was discharged, the supply air temperature setpoint was at the

lower limit of the thermal comfort range so as to use ambient air if it was cold outside, or to utilize the heat exchanger to

precool the supply air. When neither heating nor cooling was required, the air supply setpoint was in the middle of the

comfort range.

Table 3 shows the climatic and geographic details for the five simulated locations. The diurnal temperature range has

been correlated with a high free cooling potential [21], [25], [26].

Table 3: Climatic and geographic details of the simulated locations

Location	DTR>12°C, months	DTR_{avg}, ^oC	T_{avg}, ^oC	TCR, ^oC	Latitude, $^\circ$	Longitude, $^\circ$	Elevation, m
AR	0	8.8	16.9	20.4 – 28.4	-34.58	-58.48	24
BF	8	14.3	29.1	22.9 – 29.9	14.03	-0.05	276
DK	0	6.4	8.4	19.3 – 26.1	55.67	12.3	28
ES	5	11.7	14.1	20.1 – 27.4	40.45	-3.55	582
US	9	13.0	14.4	19.3 – 27.0	34.9	-12.45	72

By using Equation 1, 14 C_p-curves were created with latent heat levels of 40 kJ/kg and 80 kJ/kg, PCTRs of 6°C, 8°C and

10°C, three melting starting temperatures of 20°C, 24°C and 26°C and two solidifying start temperatures of 23°C and 27°C.

Figure 4 shows as an example the C_p-curve generated for $T_{m,s}$ equal to 16°C, $T_{s,s}$ equal to 19°C, PCTR of 8°C, hysteresis

of 5°C and LH of 80 kJ/kg. The melting start temperature is defined as the intersection between the tangent to the Cp

curve at $C_{p,eff} = 0.5(C_{p,eff,peak} - C_{p,sens)}$ and the baseline ($C_{p,sens}$) $\cdot$ $C_{p,sens}$ is fixed at 1.8 J/gK for all curves for both

solid and liquid phase, and the linear part of the curve spans 2 K. Hysteresis is the horizontal difference between the peaks

of the melting and solidifying curves. Table 4 shows the values for the 14 generated curves that were simulated for each
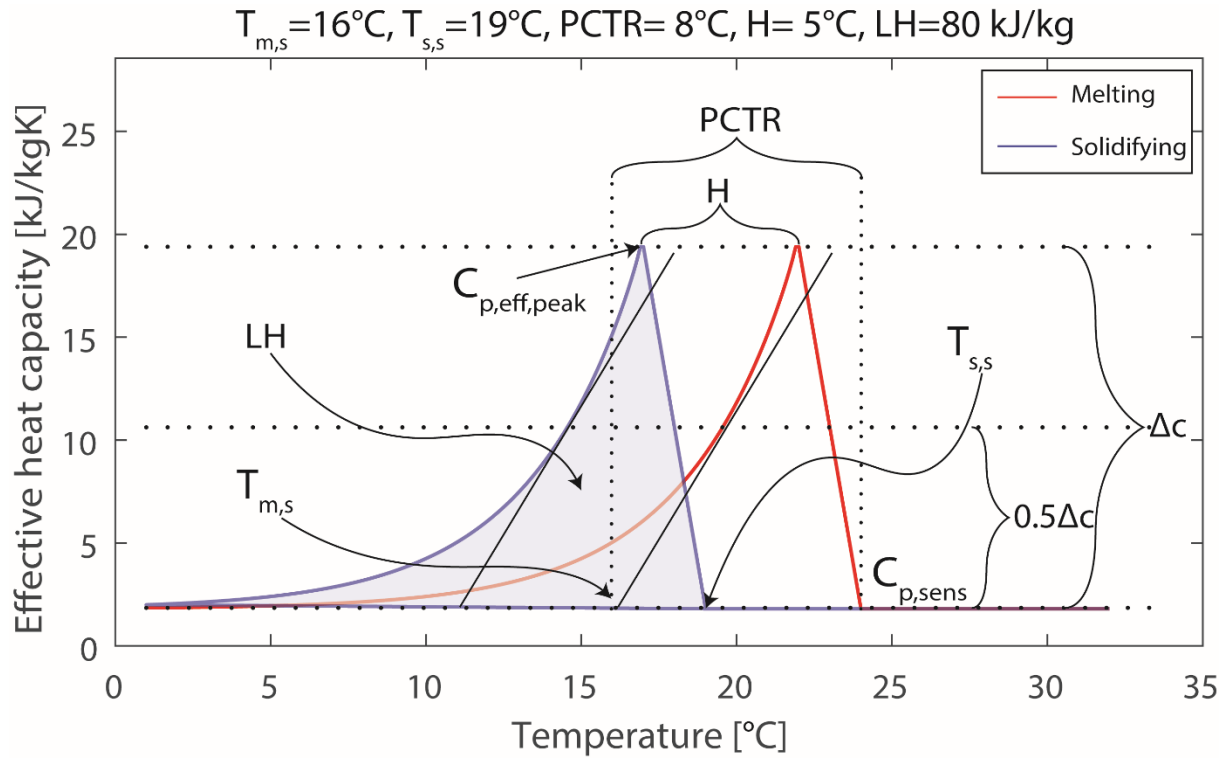
location.

Figure 4: C_p-curve generated using Equation 1

Table 4: PCMs generated using Equation 1

Name of C_p − curve	Temperature range, ^oC	$T_{m,s}$, ^oC	$T_{s,s}$, ^oC	PCTR, ^oC	H, ^oC	LH, kJ/kg
PCM_001	17 – 26	20	23	6	3	40
PCM_002	21 – 30	24	27	6	3	40
PCM_003	21 – 32	26	27	6	5	40
PCM_004	15 – 28	20	23	8	5	40
PCM_005	19 – 28	20	27	8	1	40
PCM_006	19 – 32	24	27	8	5	40
PCM_007	17 – 30	20	27	10	3	40
PCM_008	17 – 26	20	23	6	3	80
PCM_009	21 – 30	24	27	6	3	80
PCM_010	21 – 32	26	27	6	5	80
PCM_011	15 – 28	20	23	8	5	80
PCM_012	19 – 28	20	27	8	1	80

| PCM_013 | 19 - 32 | 24 | 27 | 8 | 5 | 80 |
| PCM_014 | 17 – 30 | 20 | 27 | 10 | 3 | 80 |

Results

Parametric analysis

There were 2240 simulations with PCM and 20 reference cases without PCM.

Table 5 shows the total energy use in kWh/m² and for each office separately the energy use in kWh/m², the percentage of energy savings and the utilization ratio for the cases with highest energy saving for each location, window to floor ratio and heat gain simulated. The energy savings were calculated as the relative difference in energy use between the PCM simulation and the corresponding reference case. As expected, the highest energy savings were observed when the PCM covered the whole ceiling. The energy saving for a full PCM ceiling ranged from 14.5% in US to 25.7% in ES, while it ranged from 6.8% in DK to 16.5% in US when half the ceiling contained PCM. For all cases, the optimal panel thickness was 20 mm. Table 6 shows the simulations with the highest PCM utilization ratio for each location, heat gain and window-to-floor ratio simulated. The utilization ratio was calculated as the ratio between the stored latent energy during a day and the maximum possible latent energy the PCM could store. All the simulations had a low latent heat level and a thickness of 10 mm. In some cases, the energy saving ratio was negative, meaning that the energy use increased compared to the corresponding reference case. The highest utilization ratios were observed in BF and US which had the largest diurnal temperature range among the simulated cities.

Table 5: Cases where the highest energy savings were observed for each location, heat gains and window to floor ratio level simulated

Load case			PCM properties		Full PCM ceiling				Half PCM ceiling				Reference
HG level	EGA	LOC	PCM type	λ	Etot	ENS	URS	URN	Etot	ENS	URS	URN	Etot
-	%	-	-	W/mK	kWh/m²	%	%	%	kWh/m²	%	%	%	kWh/m²
L	0.059	AR	PCM_013	0.2	28.7	17.3	4.8	9.2	30.5	12.1	5.6	10.9	34.7
H			PCM_012	0.4	33.9	20.0	12.3	15.7	36.4	14.2	14.2	18.5	42.4
L	0.092		PCM_012	0.4	34.6	18.0	10.3	16.5	37.7	10.7	12.7	20.4	42.2
H			PCM_012	0.2	40.6	20.2	13.3	19.7	44.0	13.6	15.5	23.0	50.9

			PCM type	λ									
L	0.059		PCM_008	0.4	68.2	25.6	11.1	8.9	76.9	16.1	12.3	9.9	91.7
H		BF	PCM_013	0.4	86.8	24.0	21.3	12.1	97.3	14.8	24.1	14.9	114.2
L	0.092		PCM_013	0.4	89.9	25.0	22.7	11.3	101.5	15.3	25.5	13.9	119.9
H			PCM_013	0.4	110.7	23.3	23.9	12.7	124.0	14.1	26.4	15.5	144.4
L	0.059		PCM_012	0.4	35.9	16.5	10.0	5.3	37.9	11.9	12.0	6.1	43.0
H		DK	PCM_012	0.4	28.3	22.9	12.7	7.3	32.3	12.0	15.2	9.1	36.7
L	0.092		PCM_012	0.4	41.4	18.2	13.5	5.9	46.4	8.3	16.4	7.5	50.6
H			PCM_012	0.4	36.5	18.3	16.4	8.6	41.7	6.7	19.0	10.5	44.7
L	0.059		PCM_012	0.2	27.4	16.7	16.5	8.3	29.2	11.2	19.7	9.8	32.9
H		ES	PCM_012	0.4	29.6	22.7	19.6	10.7	32.6	14.9	23.6	12.8	38.3
L	0.092		PCM_012	0.2	32.5	23.2	20.9	9.0	36.1	14.7	24.8	11.5	42.3
H			PCM_012	0.4	36.5	25.5	24.2	11.8	42.2	13.9	28.4	14.5	49.0
L	0.059		PCM_012	0.2	22.6	15.0	17.2	8.3	24.4	8.3	20.7	10.1	26.6
H		US	PCM_012	0.2	24.4	14.7	19.5	11.1	26.0	9.1	23.4	13.8	28.6
L	0.092		PCM_012	0.4	26.3	22.6	23.5	10.0	29.3	13.8	28.0	12.2	34.0
H			PCM_012	0.2	28.1	24.7	25.0	12.9	31.2	16.4	29.5	15.7	37.3

Table 6: Cases where the highest utilization ratio of the PCM were observed for each location, heat gains and window to floor ratio level simulated

Load case			Full PCM ceiling					Half PCM ceiling				
HG level	EGA	LOC	PCM type	λ	ENS	UR S	UR N	PCM type	λ	ENS	UR S	UR N
-	%		-	W/mK	%	%	%	-	W/mK	%	%	%
L	0.059		PCM_006	0.4	11.2	14.3	22.2	PCM_006	0.4	6.7	15.3	24.5
H		AR	PCM_006	0.2	11.9	18.9	26.9	PCM_006	0.4	9.2	20.3	28.9
L	0.092		PCM_006	0.4	8.0	16.6	29.1	PCM_006	0.4	5.8	18.4	32.0
H			PCM_006	0.4	11.0	21.5	33.7	PCM_006	0.4	7.7	23.2	36.5
L	0.059	BF	PCM_003	0.4	12.2	31.5	22.4	PCM_003	0.4	7.7	32.8	24.8
H			PCM_003	0.4	11.1	33.2	25.1	PCM_003	0.4	6.9	34.0	27.1

L	0.092		PCM_003	0.4	10.7	33.1	23.2	PCM_003	0.4	6.5	34.0	25.6
H			PCM_003	0.4	10.2	33.9	25.4	PCM_003	0.4	6.1	34.2	27.6
L	0.059		PCM_005	0.2	2.1	18.0	10.2	PCM_005	0.2	0.3	19.6	11.3
H		DK	PCM_004	0.4	-3.2	24.7	15.1	PCM_005	0.2	0.9	26.3	16.5
L	0.092		PCM_004	0.2	-6.1	25.6	12.4	PCM_004	0.4	-5.5	27.2	13.5
H			PCM_004	0.4	-4.7	31.3	17.8	PCM_005	0.2	-4.9	32.3	19.3
L	0.059		PCM_002	0.4	8.5	32.0	16.8	PCM_002	0.4	4.6	34.1	18.1
H		ES	PCM_002	0.4	10.7	35.9	20.6	PCM_002	0.4	6.1	38.6	22.5
L	0.092		PCM_002	0.4	6.6	38.1	18.1	PCM_002	0.2	0.7	40.0	19.3
H			PCM_002	0.4	10.0	41.1	22.1	PCM_002	0.2	4.7	43.8	24.1
L	0.059		PCM_002	0.4	6.9	31.1	13.8	PCM_002	0.4	3.9	32.7	14.2
H		US	PCM_002	0.4	9.6	36.0	19.8	PCM_002	0.4	5.9	37.8	20.2
L	0.092		PCM_002	0.4	15.5	40.7	15.9	PCM_002	0.4	11.5	42.9	16.7
H			PCM_002	0.4	18.4	44.7	21.4	PCM_002	0.4	13.3	46.9	22.7

Figure 5 shows the case with the highest utilization factor for the whole annual simulation. For all the simulations, the highest values were calculated during the winter period and the lowest during summer.
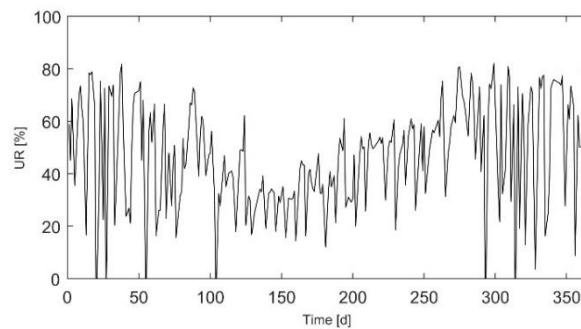

*Figure 5: Annual utilization ratio for Santa Maria, USA*

Figure 6 shows as an example, the accumulated energy for Santa Maria when the area of the ceiling containing PCM and the thickness of the PCM panels were altered. In Figure 6a, each time the PCM ceiling area was increased, it resulted in an energy use reduction by approximately 4.5 kWh/m² (a 12% reduction). In Figure 6b, when the panel changed from the reference case, it resulted in a reduction in energy use of 6.2 kWh/m² (a 16.7% reduction), while when the PCM panel

thickness was increased, the energy use was reduced by 9.3 kWh/m² (a 24.9% reduction). Similar trends were observed in the other simulated locations.
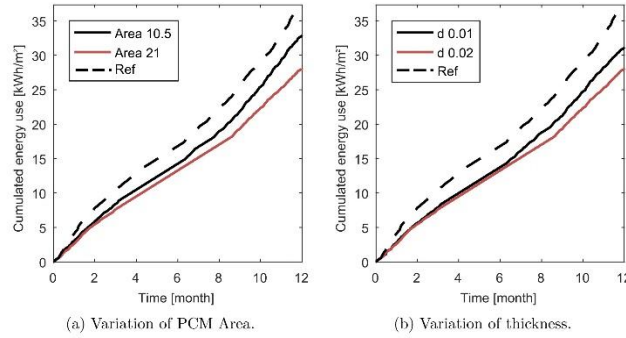
Figure 6: Example of cumulated energy use for Santa Maria, USA as a function of PCM ceiling area and PCM panel thickness

Figure 7 shows an example of the air temperature of the south office in Santa Maria, USA during the cooling period. The case with the PCM had a smaller diurnal temperature fluctuation. Similar trends were observed in the other simulated locations, which supports the findings in the literature [10], [13], [18].
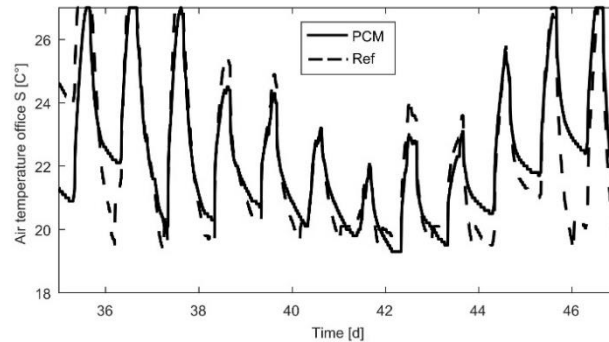
Figure 7: Air temperature during cooling period in Santa Maria, USA

Statistical analysis

The purpose of the statistical analysis was to identify the impact of the parameters on energy saving and propose a statistical model that could be used in building designs. Figure 8 shows the density histogram of the percentage energy savings. The data follow an approximately normal distribution with its mean equal to 4.11 and a standard deviation of 6.5. Figure 8 shows that a poor choice of PCM panel can result in an increase in energy use, while a correct design can result in significant energy savings.
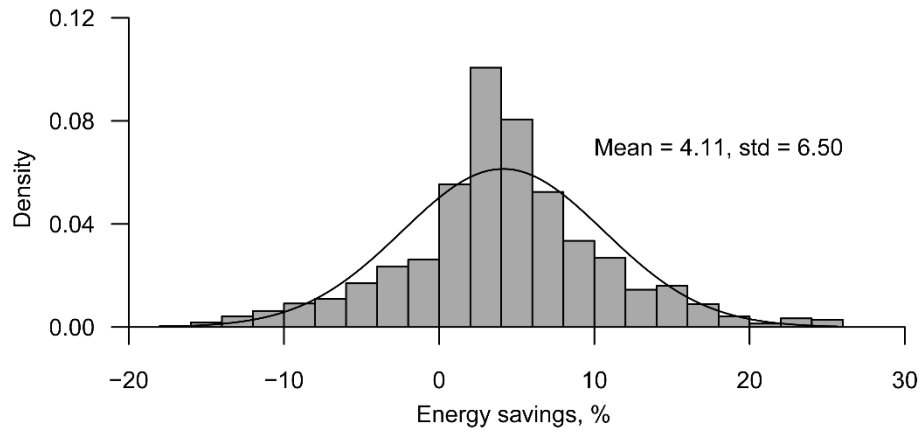
Figure 8: Histogram of the energy saving potential

Figure 9 illustrates the energy saving for each simulated location in the form of a boxplot. Even the worst performing PCM cases resulted in energy savings for AR and BF. On the other hand, several PCM cases resulted in an increase in the energy use in DK and US. This is caused because the phase change was shifted towards the lower end of the comfort range. The temperature reached a lower maximum during the day in the PCM case than in the reference case, so the temperature dropped faster to the lower comfort bound during the night and the heater was therefore activated for a longer period, than in the reference case. That was because the energy used to discharge the PCM was higher than the energy savings on the heating and cooling operation from the implementation of the PCM.
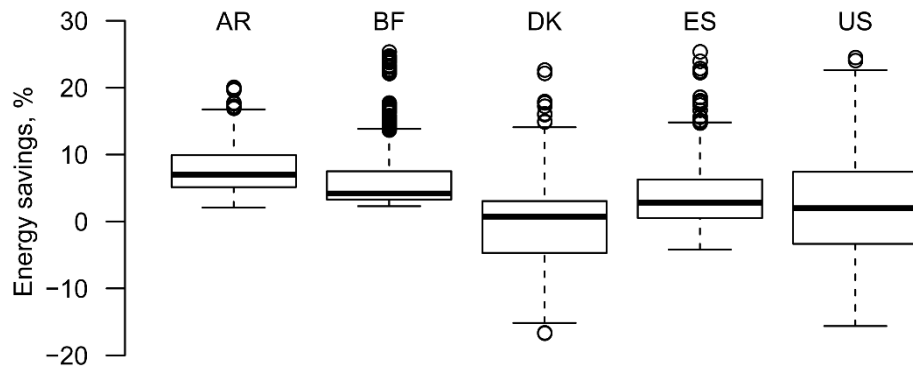

Figure 9: Boxplot of the energy savings for simulated locations

A linear model was formulated to calculate the energy saving for each location. Due to the differences in the distribution, for some locations it was necessary to transform the dependent variable (ENS) to bring the distribution closer to normal and improve homoscedasticity and the linear relationship assumed in the linear models. DK, ES and US are described by

Equation 3, while AR and BF are described by Equations 4 and 5, respectively. The thermal conductivity was not included in these equations because its effect was found to be insignificant for the simulated panel thicknesses.

$$ENS \sim HG + EGA + PCM\ area + d + PCM \tag{3}$$

$$log_{10}(ENS) \sim HG + EGA + PCM\ area + d + PCM \tag{4}$$

$$1/ENS^{0.5} \sim HG + EGA + PCM\ area + d + PCM \tag{5}$$

Table 7 shows the regression coefficients for the linear models and the corresponding significance level for each parameter and location examined. As an example, for DK, using a HG level of 16.8 W/m², an EGA of 0.059, a full PCM ceiling, a thickness of 20 mm and PCM of the 002 type, the statistical model calculated a potential energy saving of 8.9%. Simulations with the same parameters gave an energy saving of 7.6-8.1% depending on the thermal conductivity value used. For the ceiling coverage the values 0.5 and 1 should be used, corresponding to half and full ceiling coverage with PCM, respectively. Accordingly, the panel thickness should be written in meters, and in the previous example the panel thickness should be written as 0.020 m.

Table 7: Regression coefficient for the linear model

	AR		BF		DK		ES		US	
HG, m²/W	1.22E-02	***	2.77E-03	***	-5.34E-02		1.15E-01	***	-4.73E-01	***
EGA	-3.17E+00	***	1.25E+00	***	-7.94E+01	·	-3.97E-01	***	6.92E+01	***
PCM area	3.22E-01	***	-1.41E-01	***	3.47E+00	***	6.67E+00	***	7.13E+00	***
PCM d, 1/m	9.98E+00	***	-5.36E+00	***	1.11E+02	***	2.44E+02	***	2.04E+02	***
PCM_001	2.73E-01	***	5.87E-01	***	-5.51E+00	***	-8.22E+00	***	-6.78E+00	***
PCM_002	4.61E-01	***	5.57E-01	***	8.79E+00	***	6.70E-01	***	7.92E+00	***
PCM_003	5.77E-01	***	3.46E-01	***	4.42E+00	***	-6.91E+00	*	1.20E-01	***
PCM_004	3.28E-01	***	5.86E-01		-1.91E+00	***	-5.79E+00	***	-3.16E+00	***
PCM_005	3.37E-01	***	5.85E-01		3.31E+00	***	-5.81E+00	***	-5.08E+00	·
PCM_006	6.03E-01	***	4.85E-01	***	6.79E+00	***	2.38E+00	***	-4.80E-01	***

PCM_007	5.45E-01	***	4.93E-01	***	2.25E+00	***	-2.28E+00	***	-5.02E+00	·
PCM_008	3.94E-01	***	2.98E-01	***	1.39E+00	***	-9.81E+00	***	-1.19E+01	***
PCM_009	4.11E-01	***	5.69E-01	***	7.49E+00	***	-1.88E+00	***	6.92E+00	***
PCM_010	5.50E-01	***	3.90E-01	***	4.99E+00	***	-4.92E+00	***	2.19E+00	***
PCM_011	2.83E-01		5.95E-01	·	-8.51E+00	***	-6.78E+00	***	-4.48E+00	*
PCM_012	6.91E-01	***	5.27E-01	***	1.43E+01	***	6.38E+00	***	7.92E+00	***
PCM_013	6.69E-01	***	2.89E-01	***	7.37E+01	***	-7.73E+00		-1.25E+01	***
PCM_014	3.06E-01	*	5.93E-01		-2.69E+00	***	-4.29E+00	***	1.30E-01	***

<div align="center">Significance legend: '***' 0.001 '**' 0.01 '*' 0.05 '·' 0.1 ' ' 1</div>

Figure 10 shows the fitted ENS against the simulated ENS and the corresponding R^2 values for all simulated locations. The R^2 values were in the range 0.78 – 0.98, which was considered satisfactorily accurate. R^2 values can only be considered reliable if the corresponding residual plots are free from bias. Figure 11 shows the residuals against the fitted ENS, where ideally, the residuals should be scattered randomly. This is the case for AR, BF and US. On the other hand, DK and ES show some bias in the residuals plots and probably the results would have been improved by a data transformation as in the case of AR and BF. It is assumed that in linear regression the residuals are normally distributed. This assumption was tested with Quantile-Quantile plots (QQ-plots), as shown in Figure 12. The standardized residuals should follow the quantiles of the standard normal distribution if the residuals are normally distributed.
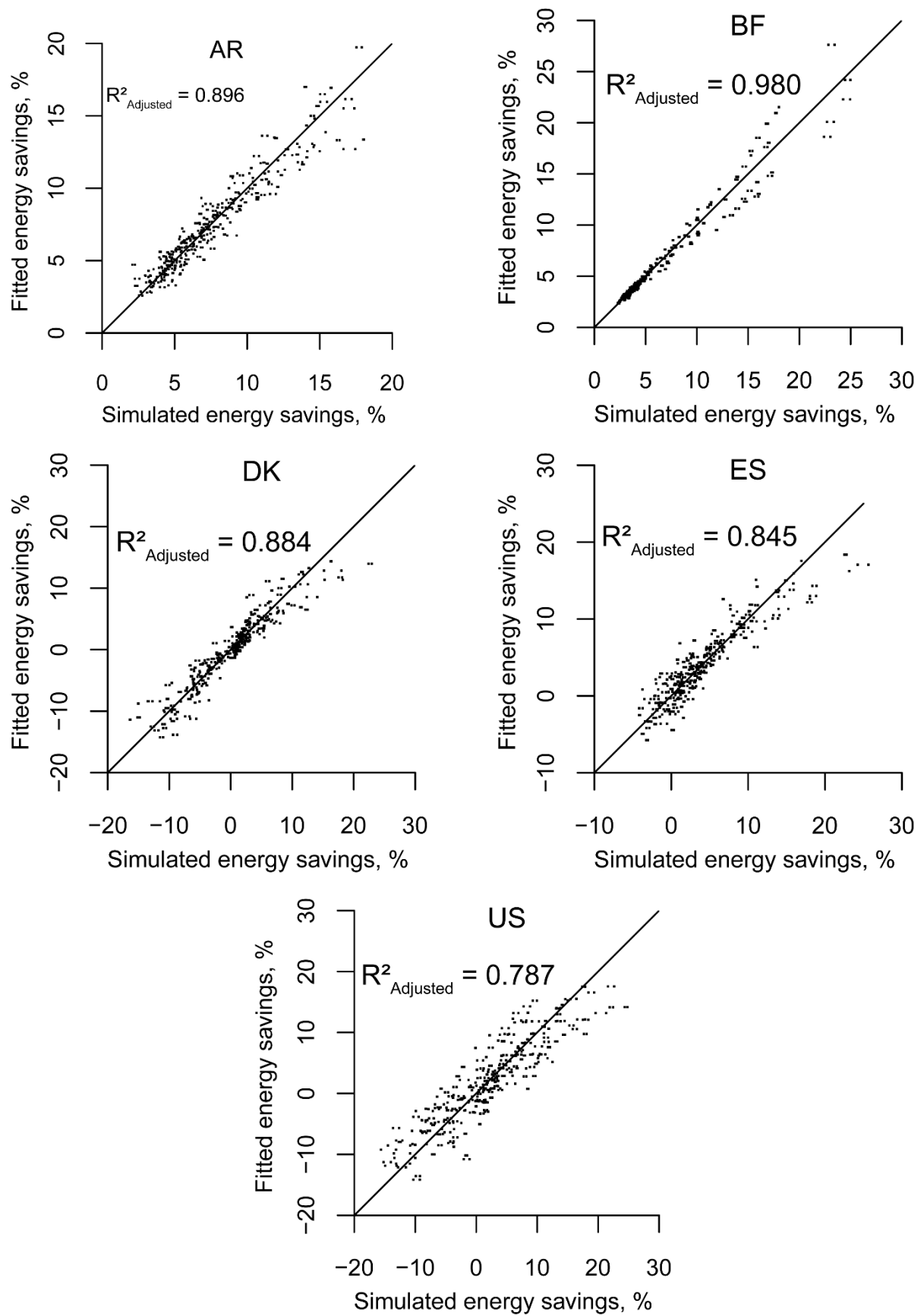
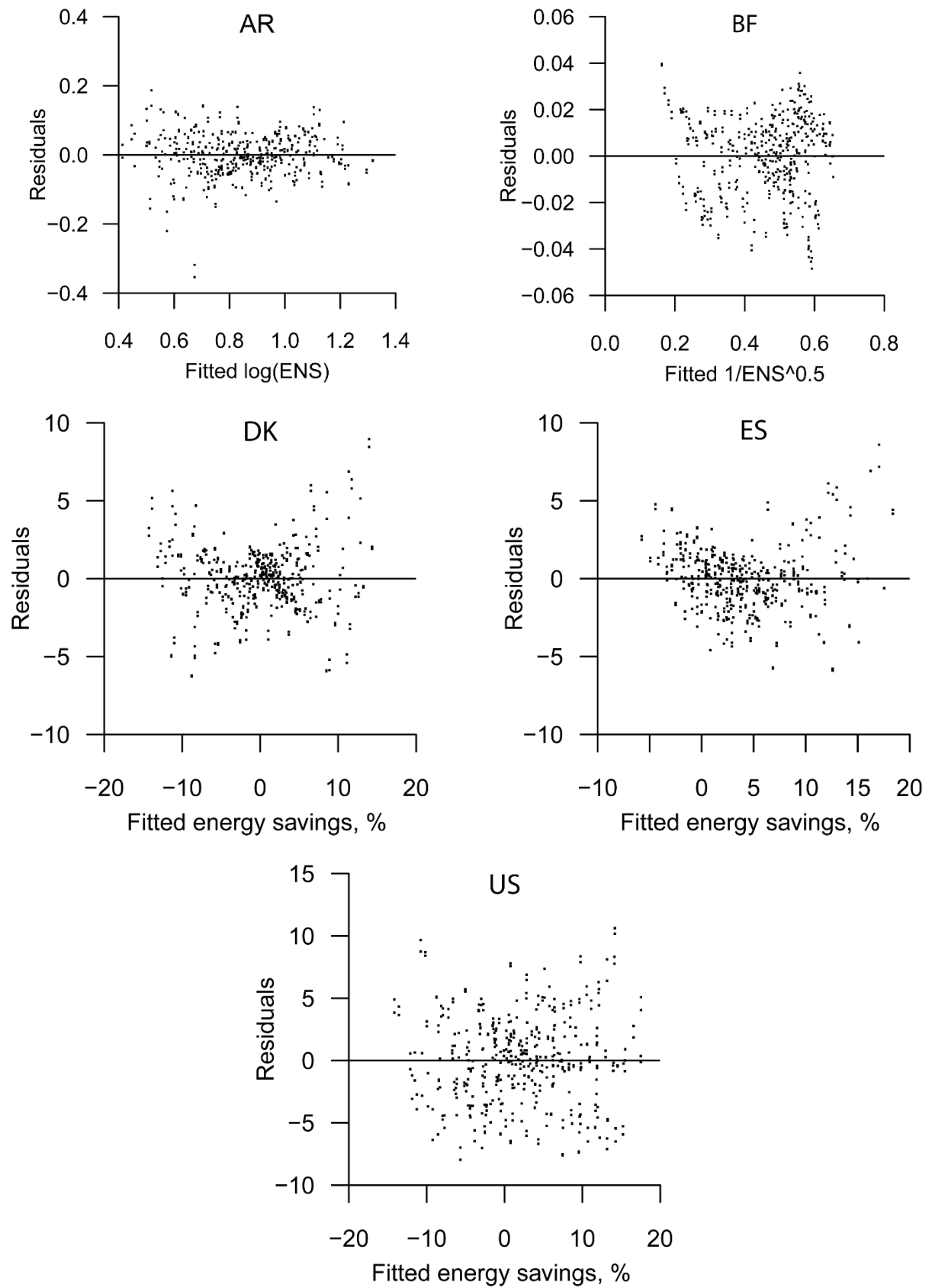*Figure 10: Goodness-of-fit plots with fitted values of ENS plotted against simulated values of ENS*

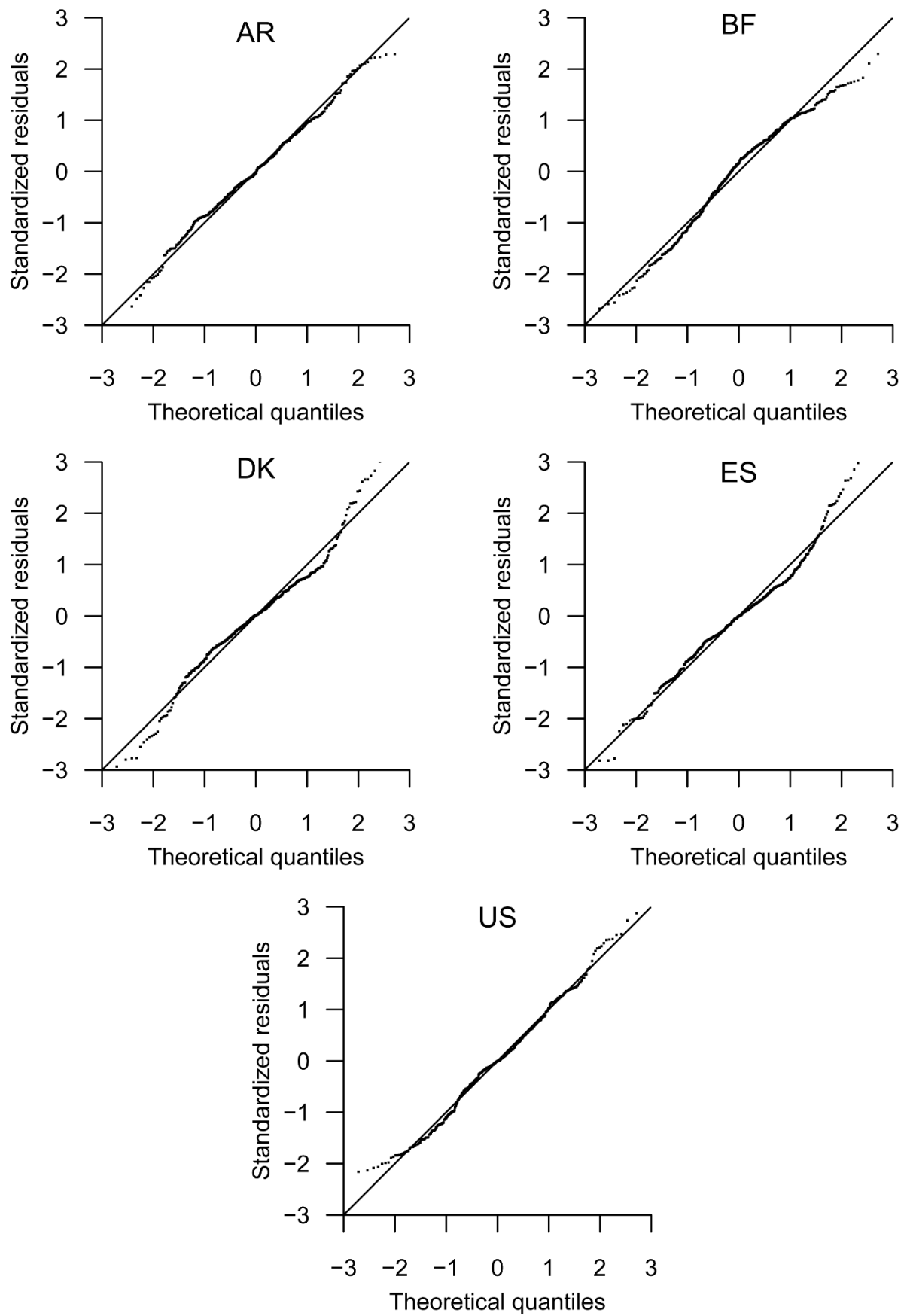*Figure 11: Residuals plotted against the fitted values of ENS*

Figure 12: QQ-plots of standardized residuals plotted against the quantiles of the standard normal distribution

Discussion

The PCM that provided the highest energy saving in DK, ES, US and in most cases in AR was PCM_012, while the most beneficial for BF was PCM_013. Both PCM types have a high latent heat of fusion (80 kJ/kg). For AR and BF, the PCM with the highest melting temperature was the ideal option, because of the high mean outdoor temperature in these locations.

In all load cases, a panel thickness of 20 mm resulted in the highest energy savings, due to the increased thermal capacity compared to the reduced thickness of 10 mm. For the 10 mm thickness, the authors calculated a low utilization ratio in all the examined cases, with the highest being 29%. To increase the utilization ratio, the authors investigated the impact of reducing the panel thickness. By reducing the panel thickness to 10 mm for DK with a high heat gain, an EGA of 0.059 and a full PCM ceiling, the ENS decreased by 4%, and the utilization ratio in the south office increased by only 5%. Thus decreasing the panel thickness, instead of utilizing more of the unused latent energy potential, resulted in a reduction in the energy saving potential. A similar trend was observed in the other simulated locations. A possible reason for the low utilization ratios was that the small fluctuation of the indoor temperature resulted in a failure to exploit the whole phase change temperature range.

Regarding the thermal conductivity of the PCM, the authors did not observe any clear pattern among the five simulated locations. This was in line with the statistical analysis, in which the impact of thermal conductivity for the simulated thicknesses was found to be insignificant.

A high latent heat capacity increased the effect of the PCM system for both positive and negative ENS values. Thus in a poorly designed PCM ceiling panel, a higher latent heat will result in an increase in the energy use.

The PCM types that provided the highest energy savings had the peak of their effective heat capacity curve shifted towards the upper comfort range limit. For climates with heating energy use, having the peak of the effective heat capacity curve shifted towards the lower comfort range limit increased energy use for heating, resulting in negative energy savings.

The PCM utilization ratio changed during the year. The highest utilization ratios were calculated to occur in winter, reaching 80% in some cases, while the lowest utilization ratios were calculated to occur in the summer period, dropping up to 20%. The utilization ratio was low during the summer period because the discharging was not sufficient during the night. This means that in locations with a long summer period it is not beneficial to increase the PCM quantity beyond a certain value, since only a small percentage of it will be utilized. During winter, with a low outdoor temperature during the night, the PCMs were cooled to lower temperature, making it possible to store more thermal energy during the next day. Discharging through embedded pipes might have been a more effective way of discharging the PCM and the system would be less dependent on the season and the climatic conditions. The cities that benefited the most from implementation

of PCM both in terms of energy saving and utilization ratio were the BF and the US, as they had the largest diurnal temperature range.

As mentioned earlier, there were several cases in which an increase in energy use was observed in DK and US. This was because the phase change was shifted towards the lower end of the comfort range in these locations. The temperature reached a lower maximum during the day in the PCM case than in the reference case, so the temperature dropped faster to the lower comfort bound during the night and the heater was therefore activated for a longer period than in the reference case.

The statistical analysis resulted in an equation for each simulated location that calculated the energy saving potential satisfactorily close to the energy saving calculated from the simulations. In order for this model to become broadly applicable, it should be expanded to simulate several different locations with different climatic conditions, to identify possible trends among locations with similar weather conditions and to confirm the observation that a large diurnal temperature range is beneficial for implementation of PCM materials.

Conclusions

The present parametric simulation study examined the potential energy saving that could be achieved by using 14 different PCM types under various conditions and five different climate conditions. It was concluded that:

- Implementing PCM in an office building can potentially reduce energy use by 14.5 – 25.6%, depending on the climatic conditions and the load. On the other hand, an incorrect choice of PCM could result in an increased energy use of up to 6%;

- The utilization ratio of the PCMs was strongly dependent on the season, with a utilization ratio of 60-80% in winter and 20-50% in summer;

- The best performance in terms of energy saving and the PCM utilization ratio were both observed in the cities with the largest diurnal temperature range;

- From the statistical analysis, an equation was derived to predict the energy saving that would be achieved for each PCM type and location and this provided satisfactorily accurate results. It could therefore be used for estimating potential energy saving for the simulated locations and PCM types.

Aknowledgements

Reference

[1]   United Nations (UN), "Adoption of the Paris Agreement," 2015.

[2]   U.S. Department of Energy (DoE), "Buildings energy data book 2011," 2012.

[3]   European Commission, "EU energy in figures - Statistical Pocketbook 2016," 2016.

[4]   A. K. Athienitis, "Investigation of thermal performance of a passive solar building with floor radiant heating," *Sol. Energy*, vol. 61, no. 5, pp. 337–345, 1997.

[5]   G. Reynders, T. Nuytten, and D. Saelens, "Potential of structural thermal mass for demand-side management in dwellings," *Build. Environ.*, vol. 64, pp. 187–199, 2013.

[6]   K.-N. Rhee and K. W. Kim, "A 50 year review of basic and applied research in radiant heating and cooling systems for the built environment," *Build. Environ.*, vol. 91, pp. 166–190, 2015.

[7]   K.-N. Rhee, B. W. Olesen, and K. W. Kim, "Ten questions about radiant heating and cooling systems," *Build. Environ.*, pp. 1–15, 2016.

[8]   H. Akeiber *et al.*, "A review on phase change material (PCM) for sustainable passive cooling in building envelopes," *Renew. Sustain. Energy Rev.*, vol. 60, pp. 1470–1497, 2016.

[9]   R. Baetens, B. P. Jelle, and A. Gustavsen, "Phase change materials for building applications: A state-of-the-art review," *Energy Build.*, vol. 42, no. 9, pp. 1361–1368, 2010.

[10]   J. Kośny, *PCM-Enhanced Building Components - An Application of Phase Change Materials in Building Envelopes and Internal Structures*. 2015.

[11]   D. Rozanna, T. G. Chuah, A. Salmiah, T. S. Y. Choong, and M. Sa'ari, "Fatty Acids as Phase Change Materials (PCMs) for Thermal Energy Storage: A Review," *Int. J. Green Energy*, vol. 1, no. 4, pp. 495–513, 2005.

[12]   S. Karaman, A. Karaipekli, A. Sar, and A. Biçer, "Polyethylene glycol (PEG)/diatomite composite as a novel form-stable phase change material for thermal energy storage," *Sol. Energy Mater. Sol. Cells*, vol. 95, no. 7, pp. 1647–1653, 2011.

[13]   A. Sharma, V. V. Tyagi, C. R. Chen, and D. Buddhi, "Review on thermal energy storage with phase change materials and applications," *Renew. Sustain. Energy Rev.*, vol. 13, no. 2, pp. 318–345, 2009.

[14]   X. Gu, P. Xi, B. Cheng, and S. Niu, "Synthesis and characterization of a novel solid-solid phase change

luminescence material," *Polym. Int.*, vol. 59, no. 6, pp. 772–777, 2010.

[15] C. Y. Zhao and G. H. Zhang, "Review on microencapsulated phase change materials (MEPCMs): Fabrication, characterization and applications," *Renew. Sustain. Energy Rev.*, vol. 15, no. 8, pp. 3813–3832, 2011.

[16] G. K. Pavlov, *Building Thermal Energy Storage*. Copenhagen, Denmark: DTU-Tryk, 2014.

[17] V. A. A. Raj and R. Velraj, "Review on free cooling of buildings using phase change materials," *Renew. Sustain. Energy Rev.*, vol. 14, no. 9, pp. 2819–2829, 2010.

[18] N. Soares, J. J. Costa, A. R. Gaspar, and P. Santos, "Review of passive PCM latent heat thermal energy storage systems towards buildings' energy efficiency," *Energy Build.*, vol. 59, pp. 82–103, 2013.

[19] International Energy Agency (IEA), "Annex 23: Energy storage in buildings of the future - Applying Energy Storage in Ultra-low Energy Buildings," 2013.

[20] S. N. Al-Saadi and Z. Zhai, "A new validated TRNSYS module for simulating latent heat storage walls," *Energy Build.*, vol. 109, pp. 274–290, 2015.

[21] S. Medved and C. Arkar, "Correlation between the local climate and the free-cooling potential of latent heat storage," *Energy Build.*, vol. 40, no. 4, pp. 429–437, 2008.

[22] M. Alam, H. Jamil, J. Sanjayan, and J. Wilson, "Energy saving potential of phase change materials in major Australian cities," *Energy Build.*, vol. 78, pp. 192–201, 2014.

[23] J. Koo, H. So, S. W. Hong, and H. Hong, "Effects of wallboard design parameters on the thermal storage in buildings," *Energy Build.*, vol. 43, no. 8, pp. 1947–1951, 2011.

[24] F. Kuznik, J. Virgone, and J. Noel, "Optimization of a phase change material wallboard for building use," *Appl. Therm. Eng.*, vol. 28, no. 11–12, pp. 1291–1298, 2008.

[25] E. Shaviv, A. Yezioro, and I. G. Capeluto, "Thermal mass and night ventilation as passive cooling design strategy," *Renew. Energy*, vol. 24, no. 3–4, pp. 445–452, 2001.

[26] S. Takeda, K. Nagano, T. Mochida, and K. Shimakura, "Development of a ventilation system utilizing thermal energy storage for granules containing phase change material," *Sol. Energy*, vol. 77, no. 3, pp. 329–338, 2004.

[27] A. Waqas and Z. Ud Din, "Phase change material (PCM) storage for free cooling of buildings - A review," *Renew. Sustain. Energy Rev.*, vol. 18, pp. 607–625, 2013.

[28] F. Kuznik and J. Virgone, "Experimental investigation of wallboard containing phase change material: Data for validation of numerical modeling," *Energy Build.*, vol. 41, no. 5, pp. 561–570, 2009.

[29] ISO, *ISO 7730:2005 Ergonomics of the thermal environment – Analytical determination and interpretation of thermal comfort using calculation of the PMV and PPD indices and local thermal comfort criteria*. 2005.

[30]   EN, *EN 15251:2007 Indoor environment input parameters for design and assessment of energy performance of buildings adressing indoor air quality, thermal environment, lighting and acoustics*. 2007.

Paper 5: Bourdakis E., Grossule F., & Olesen B. W. (2016). Night time cooling by ventilation or night sky radiation combined with in-room radiant cooling panels including Phase Change Materials. Presented at AIVC 2015

Night time cooling by ventilation or night sky radiation combined with in-room radiant cooling panels including Phase Change Materials

Eleftherios Bourdakis[1], Bjarne W. Olesen[*1], Fabio Grossule[1]

[1]Technical University of Denmark
International Centre for Indoor Environment and Energy
Nils Koppels Allé, Building 402
Kongens Lyngby, Denmark
* bwo@byg.dtu.dk

ABSTRACT

Night sky radiative cooling technology using PhotoVoltaic/Thermal panels (PVT) and night time ventilation have been studied both by means of simulations and experiments to evaluate their potential and to validate the created simulation model used to describe it. An experimental setup has been constructed at the Technical University of Denmark, where the outside PVT panels are connected through a storage tank to in-room radiant ceiling panels. The radiant ceiling panels include phase change material (PCM) and embedded pipes for circulating water. Due to the phase change material it is possible to store the heat generated during the day from internal sources. Then during the night the panels can be cooled down again and regenerated. The possibility of cooling down the panels during the night with outside air was also studied. The night cooling power of the PVT panels ranged from 92 to 119 W/m^2 depending on the sky clearness. This cooling power was enough to remove the stored heat and regenerate the ceiling panels. The validation simulation model results related to PCM were close to the corresponding results extracted from the experiment, while the results related to the production of cold water through the night sky radiative cooling differed significantly. The possibility of night time ventilation was studied through simulations for three different latitudes. It was concluded that for Danish climatic conditions night time ventilation would also be able to regenerate the panels while its contribution is not sufficient in warmer South-European climates.

KEYWORDS
Night Time Ventilation, Night Sky Radiative Cooling, Phase Change Materials, Thermal Comfort, Renovation

1   INTRODUCTION

World energy consumption has been increasing rapidly the last decades, mainly due to the population growth and the industrial and technological development. In order to address this issue, European Union (EU) has put into force the agreement "20-20-20" (European Commission, 2007), which sets several ambitious targets to be met from the member states by the year 2020.

According to the International Energy Agency (IEA) (2013), energy consumption in buildings accounts for more than 40% of the primary energy consumption in many IEA member states. Therefore, vast changes have to be made in the building sector and especially in the Heating, Ventilation and Air-Conditioning (HVAC) systems, in order to reach the aforementioned targets. Most of the buildings which will exist by the year 2020 have already been built, since a building has a life span of more than 50 years. Thus, much effort must be put into retrofitting existing buildings.

One solution that could contribute in reducing the energy consumption caused by HVAC systems is the Thermo Active Building Systems (TABS). Main advantages of TABS are the distribution of cooling over a longer period which results in reduced peak loads, reduction in the buildings materials due to the reduced suspended ceiling for ventilation

purposes since the required air flow rate is reduced. Moreover, the fact that the cooling temperature is close to room temperature increases the energy efficiency of heat pumps and ground heat exchangers (Babiak et al., 2007). Many modern office buildings in Europe are using TABS to store heat in the slabs during the day and remove the stored heat during the night (Kolarik et al., 2015).

Nevertheless, this system is in most cases not applicable for energy renovation of buildings. A solution that could be effective in cases of buildings renovation is a radiant cooling system with the implementation of Phase Change Material (PCM) since it has the benefits of a heavyweight construction with the thickness of a lightweight construction (Koschenz & Lehmann, 2004). PCMs are organic or inorganic substances that absorb heat while melting and release it while solidifying. The most important advantages of the implementation of PCMs in the structure, as they have been reported in the literature (Cabeza et al., 2007; BASF, 2010; Pavlov, 2014; Grossule, 2015), are the improved thermal inertia compared to conventional concrete, the reduction of peak cooling load, the shift of part of the cooling demand to night time where lower electricity prices occure, the attenuation of the interior air temperature fluctuations and the reduction of the size of the HVAC system.

One passive method that could be utilized for discharging the PCM is the night sky radiative cooling. During night time the effective sky temperature is lower than the one of the solar panels surface, therefore the panels release heat in the form of radiation towards the atmosphere (Meir et al., 2002). There are several ways with which night sky radiative cooling can be exploited (Grossule, 2015), but in this study only a closed water based system will be examined. The advantages of such a system are the reduction of energy consumption, since the only energy required is that for the water pumps, a higher utilization factor for solar thermal panels is achieved since they are exploited also during night time, cooling demand and cold water production through night sky radiative cooling are in phase since clear sky occurs more often during summer time and it can be coupled with thermal storage materials like PCM (Meir et al., 2002; Eicker & Dalibard, 2011; Hosseinzadeh & Taherian, 2012). Another passive method that could be exploited is the night time natural ventilation when the ambient air temperature is low enough.

The purpose of this study was to examine and evaluate different methods for discharging the PCM, and to couple the PCM with solar panels for discharging it passively through night sky radiative cooling. The results of the experiment were used to validate the corresponding simulation model, which was then used to simulate the possibility of discharging the PCM by exploiting night time ventilation under Copenhagen's, Milan's and Athens' weather conditions.

2 EXPERIMENT

2.1 Experimental setup

For the purpose of the experiments a climatic chamber at the facilities of the International Centre for Indoor Environment and Energy (ICIEE) was used. The floor surface was 22.7 m^2 and the height from the floor to the suspended ceiling 2.5 m. The walls and the roof are made of two steel sheets separated by 10 cm of mineral wool for insulation, while the whole chamber is not exposed directly to the ambient weather conditions since it is enclosed in a bigger building.

The suspended ceiling consisted from panels made from a mixture of clay with 26% of PCM by weight. The PCM used was the type DS 5040X produced from BASF with melting point of 23°C (BASF, 2010). As it is shown in Figure 1, above the PCM ceiling panels there was a 0.5 m height plenum, from where the ventilation air was supplied in the chamber through the gaps between the ceiling panels. For discharging the PCM, the ceiling panels had embedded pipes inside for circulating water during night time. The chamber was designed

accordingly to simulate a two-person office, with the use of heat dummies for the occupants and the equipment. Therefore, the heat dummies were activated during typical office hours, namely from 9:00 to 17:00. The total power of the heat gains was 540 W.
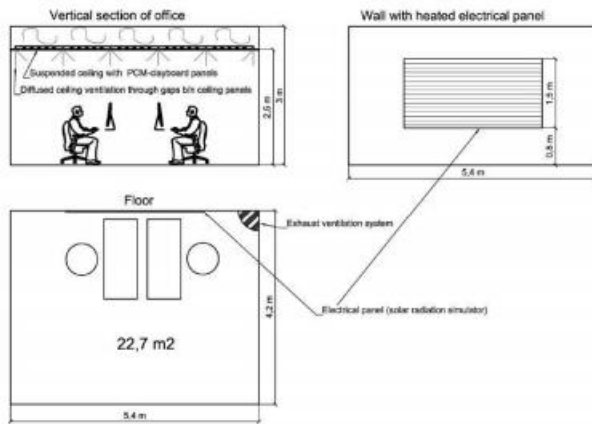

Figure 1: Chamber's layout (Pavlov, 2014)

Figure 2: Experimental Setup (Grossule, 2015)

The ventilation flow rate was set to 30 l/s, sized according to Annex B.1.2 of the standard DS 15251 (2007) for removing pollutants and providing fresh air, counting only on the performance of the PCM for removing the heat. The air supply temperature was set to 18.5°C. As in the case of the heat dummies, the ventilation was operating from 9:00 to 17:00. The exhaust of the ventilation can be seen in the far corner of the chamber in Figure 2. In the second experimental case the ventilation was also used from 22:00 to 06:00 as a method for discharging the PCM.

For the simulation of the solar heat gains, an electrical heating panel was used on the wall which was supposed to be facing south, as it can be seen in Figure 2. The schedule of the solar heat gains is illustrated in Figure 3.
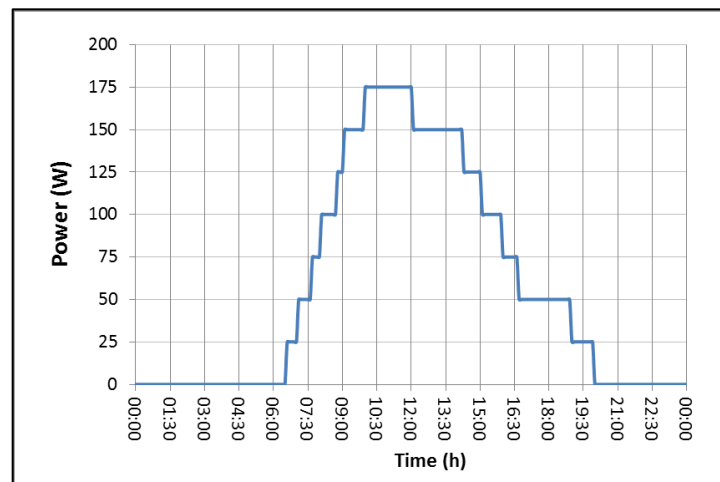
Figure 3: Daily solar heat gains profile

The second method used for discharging the PCM was by circulating water to the embedded pipes during night time. In experiment 1 the cold water was directly supplied from the main chiller of the laboratory's facilities. In experiment 2 the system was upgraded with

the implementation of 3 PhotoVoltaic/Thermal (PVT) panels for the production mainly of cold water, by circulating water in the PVT panels during night time. In this study the production of hot water and electricity was not taken into consideration. Each PVT panel had a surface area of 1.3 m^2, a tilt angle of 45° and they were facing south.

The PVT panels were connected with two storage tanks through a heat exchanger. Both tanks had a volume of 255 l and the one was used for storing cold water (CWT) while the other one for storing hot water (HWT). The reason why a heat exchanger was installed in between was due to different settings required in the PVT panels and the tanks regarding water pressure. Furthermore, in this way a smaller quantity of glycol was required which was used as antifreeze. The water from the heat exchanger was circulated to a heat exchanger enclosed in the upper part of the CWT, while a second enclosed heat exchanger was connected with the main chiller of the laboratory's facilities. The main chiller was used as an ancillary system for ensuring the production of cold water in case where the production from the night sky radiative cooling was not enough. The water from the bottom of the CWT was circulated to the PCM panels and from there it was returned to the top of the CWT. In Figure 4 the schematic drawing of the hydraulic system is presented.

In both cases (water provided either from the main chiller or the CWT) the circulation of the water would start at 20:00 and would continue until 7:30 if none of the two following conditions was met earlier:

- The average bottom surface temperature of the PCM panels dropped below 21°C
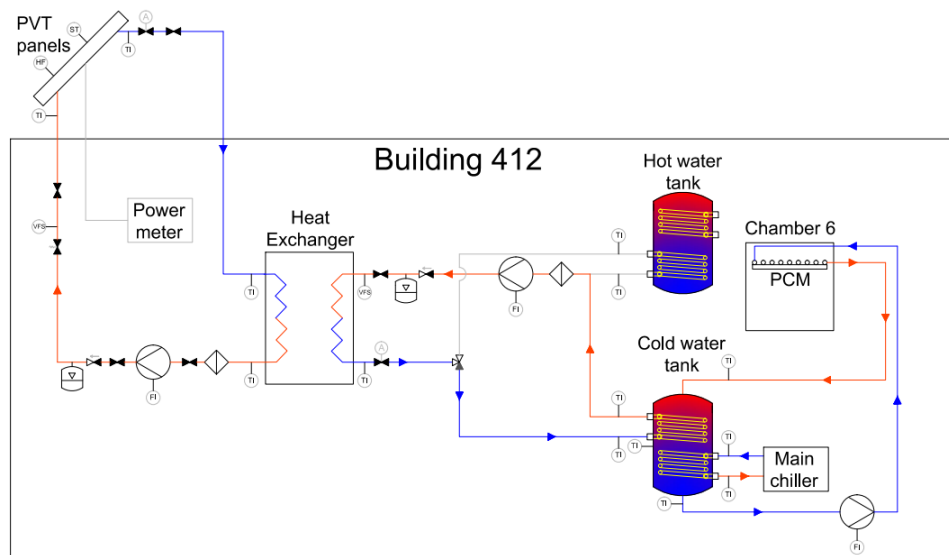- The operative temperature of the room dropped below 21°C

Figure 4: Schematic drawing of the hydraulic system

2.2 Experiment 1

As it was mentioned before, for experiment 1 the cold water for discharging the PCM was provided from the main chiller of the laboratory. Four cases were examined in the first experiment; the first two cases were identical to the cases A1 and B1 examined by Pavlov (2014), in order to ensure that the system works in the same way. In the third case the embedded pipes were used for discharging the PCM and two floor fans were installed in the corners to examine the impact of improved air mixing in the operative temperature and the PCM bottom surface temperature. Lastly, in the fourth case the two desks with the heat dummies where placed closer to the centre of the room and then split towards the walls, in order to distribute the heat sources more evenly in the room. The settings for the four cases are presented in Table 1. Each experimental case lasted four days.

Table 1: Examined cases of experiment 1

Case	Night ventilation (22:00 – 6:00)	Water air flow
1	Off	0.15 m³/h
2	62 l/s	Off
3	Off	0.15 m³/h
4	Off	0.15 m³/h

2.3 Experiment 2

For the second experiment two cases were examined. In the first one the air temperature inside the chamber was kept constantly at 26°C from 9:00 to 18:00, while in the second case it was kept constantly at 28°C for the same time period. During the rest of the day the ventilation was deactivated. In this experiment the heat dummies and the solar panel were deactivated and the room air temperature was controlled through the ventilation system. Each case lasted for three days.

2.4 Simulation study

The results extracted from experiment 2 were compared with a simulation model made in TRNSYS 17, in order to validate it. In order for the simulation model to be more accurate, the extracted data from a weather station installed next to the PVT panels were used as an input to the PVT component in the simulation model. All the rest of the settings of the simulation model were as close as possible to the conditions of experiment 2. Afterwards, the model was used for simulating the possibility of exploiting night time ventilation for discharging the PCM under the weather conditions of Copenhagen, Milan and Athens. The night time flow rate that was used was 62 l/s as it was set in the second case of experiment 1, while the air supply temperature was the ambient air temperature. The period simulated was the whole cooling period, namely from 1st of May until the 30th of September.

3 RESULTS

3.1 Experiment 1 results

In the Figure below the operative temperature in the interior of the chamber during the four examined cases of experiment 1 is presented. As it can be seen, both the improvement of the air mixing (case 3) and the separation of the internal heat sources (case 4) caused a reduction in the peak temperature during the occupancy period.
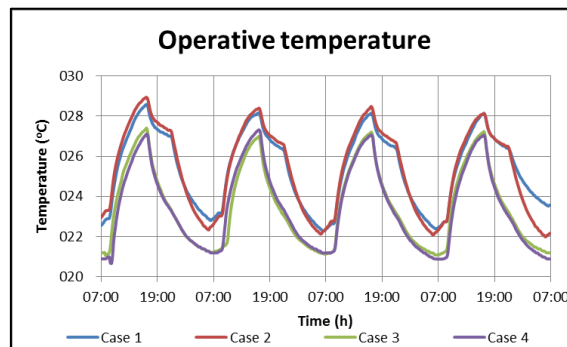

Figure 5: Operative temperature of experiment 1

In Figure 6 the temperature of the bottom surface of the PCM panels is presented. As before, a reduction in the peak temperature is observed in cases 3 and 4. Furthermore, the minimum surface temperature is lower in these two cases, which means that a higher

percentage of PCM was discharged during the night time. On the other hand, the examined combination of air supply volume and temperature during night time proved to be insufficient for discharging the PCM completely.
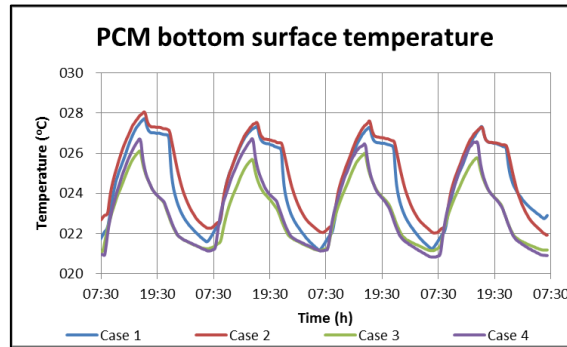

Figure 6: Bottom surface temperature of the PCM panels

One of the drawbacks of PCMs is their low thermal conductivity. In order to examine the impact of the changes examined during cases 3 and 4 to the energy absorbed by the PCM, the percentage of the utilised PCM was calculated. For this calculation the bottom and the top PCM surface temperatures were used, and the results can be seen in Table 2. As it can be seen the changes implemented in case 3 and 4 increased the percentage of the utilised PCM.

Table 2: Percentage of PCM utilization level

	Case 1	Case 2	Case 3	Case 4
Percentage of PCM utilized (%)	90.8	78.1	95.1	96.7

3.2 Experiment 2 and validation simulations results

The results from the second experiment will be presented in the following figures combined with the results from the validation simulations, in order to be compared directly. In Figure 7 the air temperature at height 0.6 m and the operative temperature from a representative experimental day of case 1 are presented. As it can be seen the results from the simulation match satisfactorily with the results extracted from the corresponding experiment case. In Figure 8 the average temperature of the bottom surface of the PCM panels is presented. As before, the two results are satisfactorily close. The three spikes that are observed in the simulation curve in the morning were caused by the fact that a deadband was not implemented.
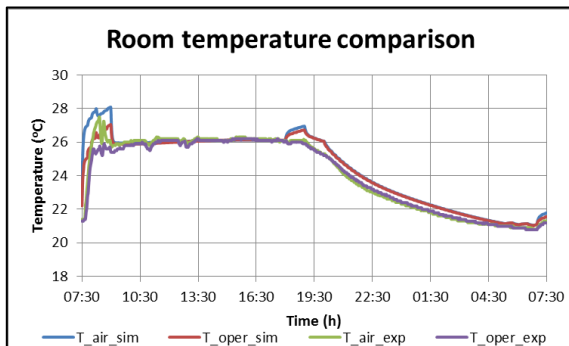

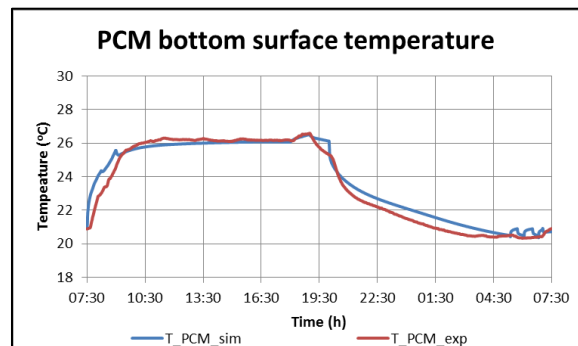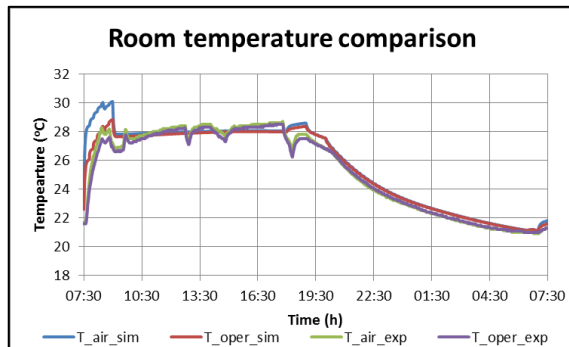Figure 7: Air and operative temperature of simulation and experiment for case 1

Figure 8: Bottom surface temperature of PCM panels of simulation and experiment for case 1

In Figure 9 the air temperature at height 0.6 m and the operative temperature from a representative experimental day of case 2 are shown. The downwards pikes that are observed in the experiment curves were caused by the opening of the door of the chamber. In Figure 10 the average temperature of the bottom surface of the PCM panels is presented. As in the previous case, the pike at the end of the curve is caused by the absence of a deadband. From both Figure 9 and Figure 10 it can be seen that the simulation results of case 2 matched to a large extent with the results from the corresponding experimental case.

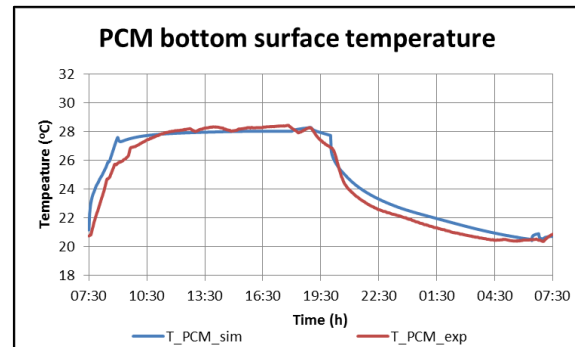Figure 9: Air and operative temperature of simulation and experiment for case 2

Figure 10: Bottom surface temperature of PCM panels of simulation and experiment for case 2

In the figures below the average specific cooling power of each night of the second experiment and the corresponding energy that was released towards the atmosphere are presented. As it can be seen, the results extracted from the simulations are underestimated compared to those extracted from the experiment.
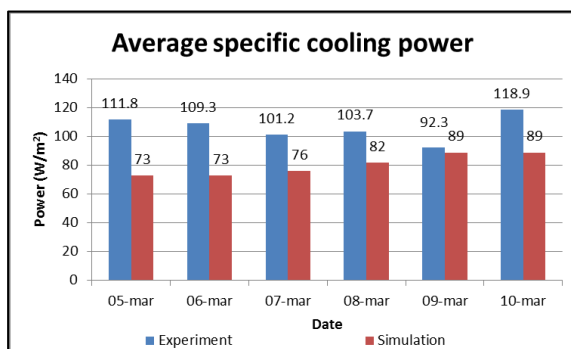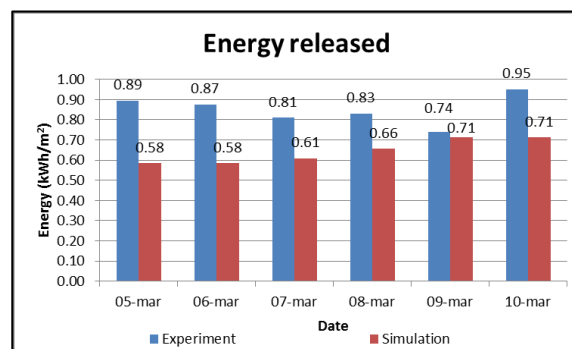

Figure 11: Average specific cooling power

Figure 12: Energy released towards the atmosphere

The reason why this inaccuracy was observed was caused by the effective sky temperature values implemented in the TRNSYS model. Since this parameter was not possible to be measured by the weather station, a theoretical calculation was used as it is described by Grossule (2015) in Appendix 12.1.3.

Moreover, the cooling output is affected by the difference between the water temperature entering and exiting the PVT panels. As it can be seen in **Error! Reference source not found.** the ΔT in the case of simulation is significantly lower compared to the case of the experimental results.
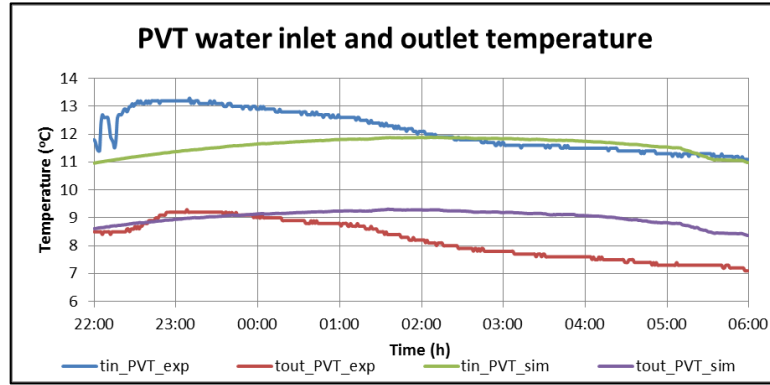
Figure 13: Water inlet and outlet temperature at the PVT panels

3.3 Simulation study results

In Table 3 the performance of the office room in terms of operative temperature in the three simulated location is presented. At this point, it should be reminded that standard DS 15251 requires the 95% of the occupancy period to be within the range $23.5 – 25.5^oC$, $23 – 26^oC$ or $22 – 27^oC$ in order for a building to be evaluated as category I, II or III respectively. The presented results are the percentages in which the operative temperature was within the suggested range. It can be observed that Athens had the best thermal performance out of the three examined locations, but it was still not good enough for satisfying the requirements for category III of standard DS 15251.

Table 3: Operative temperature performance based on standard DS 15251

	Category I (23.5 – 25.5^{o}C)	Category II (23 – 26°C)	Category III (22 – 27°C)
COP	25%	39%	43%
MIL	28%	42%	46%
ATH	29%	42%	72%

In Figure 14 the daily average performance of the PCM is illustrated. The percentage of charged PCM refers to the end of the occupancy period, namely shows the percentage of PCM that was utilized during that period. On the other hand, the percentage of the discharged PCM refers to the beginning of the occupancy period, thus it reflects the percentage that is still not discharged after the night time ventilation. It can be seen that while in Copenhagen and Milan PCM was almost fully discharged, in the case of Athens approximately the one third of it was not discharged.
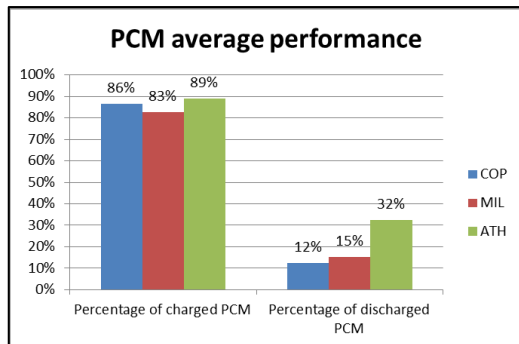

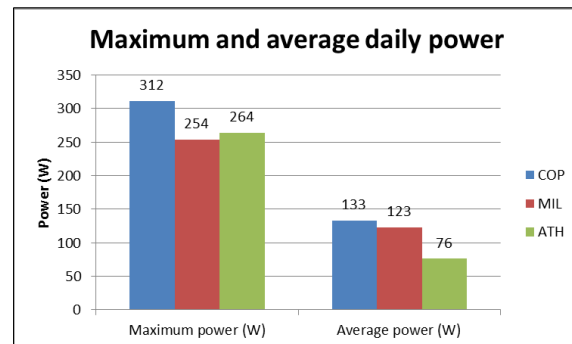Figure 14: Average daily percentage of charged and discharged PCM

Figure 15: Maximum and daily average power

In Figure 15 the maximum and the daily average cooling power are presented. As it can be seen, although the maximum cooling power in Athens is comparable with the one of Copenhagen, the daily average cooling power of Athens is approximately the half of the one of Copenhagen. The corresponding results of Milan are closer to the results of Copenhagen than those of Athens.

4   DISCUSSION

Regarding the experiment 1, the calculation regarding the percentage of utilization is just an indication, since the temperature distribution inside the panels is not known. This can be observed from the values for cases 1 and 2, which were expected to be closer, since the interior of the experiment was identical. Since the air flow rate that was examined as a discharging method proved to be insufficient for discharging the PCM panels, a higher air flow rate could be examined, or a lower air supply temperature. A lower supply temperature would be feasible in northern European climate areas, but not in Mediterranean climate areas.

The second experiment was conducted during March 2015, a period in which the ambient weather conditions were in favour for producing cold water through night sky radiative cooling. Thus, the experiment should be repeated during summer time, when it is expected that the cooling demand would be higher and the ambient air temperature as well.

The reason why Copenhagen performed worse than Milan and Athens in terms of thermal environment was the low position of the sun which increased significantly the solar heat gains in this location. The same simulations should be repeated with the implementation of a solar shading system.

5   CONLUSIONS

In this study two experiments were conducted to examine the performance of a radiant ceiling cooling system with PCM combined with PVT panels for discharging the PCM passively, while the results extracted from the second experiment were used to validate the corresponding TRNSYS simulation model. The validated model was used to simulate in three different locations the possibility of discharging the PCM by exploiting night time ventilation.

From the first experiment it can be concluded that the circulation of water in the embedded pipes is more effective in discharging the PCM compared to the tested night time ventilation flow rate. Furthermore, it can be concluded that the location of the PCM compared to the heat gain sources affects significantly the performance of the PCM. Therefore, special attention has to be given when designing a cooling system which includes PCM.

From the second experiment it can be concluded that the cold water produced through the night sky radiative cooling was sufficient for discharging the PCM for both examined cases. On the other hand, since – as it was mentioned before – the experiment was conducted during March, this discharging method should also be examined during summer time or ideally during a whole year in order to have a more comprehensive view of the performance of the PVT panels. In order to have the complete performance of the PVT panels, also the production of hot water and electricity needs to be taken into consideration.

Regarding the simulation model, the part simulating the chamber with the PCM ceiling panels proved to be satisfactorily accurate, while the solar loop containing the PVT panels needs to be further investigated and improved. The model should be compared with an experiment conducted during summer time for a more complete and accurate validation.

From the simulation study it can be concluded that the night time ventilation can be exploited for discharging the PCM passively in areas with Nordic climate but is insufficient for Mediterranean climate conditions.

6   REFERENCES

Babiak, J., Olesen, B. W., & Petráš, D. (2007). *Low temperature heating and high temperature cooling* (2nd ed., Vol. 7). Forssa, Finland: Forssan Kirjapaino Oy.

BASF. (2010). *Micronal ® PCM Intelligent temperature management for buildings.* Ludwigshafen, Germany: BASF.

Cabeza, L. F., Castellón, C., Nogués, M., Medrano, M., Leppers, R., & Zubillaga, O. (2007). Use of microencapsulated PCM in concrete walls for energy savings. *Energy and Buildings, 39*(2), 113 - 119.

Dansk standard. (2007). *DS 15251 Indoor environmental input parameters for design and assessment of energy performance of buildings addressing indoor air quality, thermal environment, lighting and acoustics.* Charlottenlund, Denmark: Dansk Standard.

Eicker, U., & Dalibard, A. (2011). Photovoltaic–thermal collectors for night radiative cooling of buildings. *Solar Energy, 85*(7), 1322 - 1335.

European Commission. (2007). *The EU climate and energy package.* Retrieved June 30, 2015, from http://ec.europa.eu/clima/policies/package/index_en.htm

Grossule, F. (2015). *The use of phase change materials for cooling of buildings combined with night sky radiant cooling.* Kongens Lyngby, Denmark: Technical University of Denmark.

Hosseinzadeh, E., & Taherian, H. (2012). An experimental and analytical study of a radiative cooling system with unglazed flat plate collectors. *International Journal of Green Energy, 9*, 766 - 779.

International Energy Agency. (2013). *Modernising Building Energy Codes to secure our Global Energy Future: Policy Pathway.* Retrieved 6 26, 2015, from http://www.iea.org/publications/freepublications/publication/policy-pathways-modernising-building-energy-codes.html

Kolarik, J., Toftum, J., & Olesen, B. W. (2015). Operative temperature drifts and occupant satisfaction with thermal environment in three office buildings using radiant heating/cooling system. *Healthy Buildings Europe 2015.*

Koschenz, M., & Lehmann, B. (2004). Development of a thermally activated ceiling panel with PCM for application in lightweight and retrofitted buildings. *Energy and Buildings, 36*(6), 567 - 578.

Meir, M. G., Rekstad, J. B., & Løvvik, O. M. (2002). A study of a polymer-based radiative cooling system. *Solar Energy, 73*(6), 403 - 417.

Pavlov, G. K. (2014). *Building thermal energy storage.* Kongens Lyngby: Technical University of Denmark.

Paper 6: Bourdakis E., Kazanci O. B., Grossule F., & Olesen B. W. (2016). Simulation Study of Discharging PCM Ceiling Panels through Night-time Radiative Cooling. Presented at ASHRAE Annual Conference 2016

Technical University of Denmark

DTU

Simulation Study of Discharging PCM Ceiling Panels through Night - time Radiative Cooling

Bourdakis, Eleftherios; Kazanci, Ongun Berk; Grossule, F.; Olesen, Bjarne W.

[Link to publication](#)

Simulation Study of Discharging PCM Ceiling Panels through Night-time Radiative Cooling

E. Bourdakis
Student Member ASHRAE

O.B. Kazanci
Student Member ASHRAE

F. Grossule

B.W. Olesen, PhD
Fellow ASHRAE

ABSTRACT

A simulation study was conducted to examine the possibility of using PhotoVoltaic/Thermal (PV/T) panels and unglazed solar collectors for producing cold water through night-time radiative cooling. The cold water was used as the medium for cooling an office in three different cities (Copenhagen, Denmark, Milan, Italy and Athens, Greece) during the cooling period (1st of May – 30th of September). For cooling the office, radiant ceiling panels including Phase Change Material (PCM) were used. In Athens and Milan the operative temperature was within the range of Category III of EN 15251 (23 – 26ºC, 73.4 – 78.8 ºF) for 81% and 82% of the occupancy period respectively, while in Copenhagen it was within the same range for 63%. Night-time radiative cooling provided for Copenhagen 22%, for Milan 10% and for Athens 4% of the cooling energy required for discharging the PCM. The total electricity produced in Copenhagen for the simulated period was 94.4 kWh/m² (29900 Btu/ft²), while for Milan and Athens it was 96.7 kWh/m² (30700 Btu/ft²) and 111.7 kWh/m² (35400 Btu/ft²)respectively. It was concluded that night-time radiative cooling can be a satisfying solution for providing space cooling to office buildings in northern climates. The performance of the installations could be improved by implementing a solar shading system and a more precise control strategy.

INTRODUCTION

The global energy use has been increasing drastically in the past decades, mainly due to the population growth and the industrial and technological progress. In order to address this issue, the European Union (EU) launched several directives to decrease energy use, increase energy efficiency and increase the use of renewable energy sources (EP, 2009, 2010). The aim is that by 2020 all new buildings constructed in the EU must be nearly zero-energy buildings. A solution that could contribute achieving this goal is coupling photovoltaic panels for the production of electricity and phase change material (PCM) for the reduction of peak cooling demand.

PCMs are organic (e.g. paraffin) or inorganic (e.g. salts) substances which absorb latent heat when they melt and release it when they solidify. During the melting and solidifying process their thermal capacity increases considerably. The advantages of PCMs compared to conventional construction materials are the reduction of peak cooling load, the increase of the thermal inertia of the building, the shift of portion of the cooling demand to night-time where electricity prices are lower in several countries, the reduction of the room air temperature fluctuation and the reduction of the size of the heating and cooling system (Koschenz & Lehmann, 2004; Cabeza et al., 2007; Pavlov,

E. Bourdakis is a Ph.D. candidate in the ICIEE, Technical University of Denmark, Denmark. O.B. Kazanci is a Ph.D. candidate in the ICIEE, Technical University of Denmark, Denmark. F. Grossule is Area Manager at Sierra S.p.A., Verona, Italy. B.W. Olesen is a Professor in the ICIEE, Technical University of Denmark, Denmark.

2014; Grossule, 2015).

One passive method that could be utilized for discharging the PCM is the night-time radiative cooling. During night-time the solar collectors have a higher temperauter than the sky; therefore they release heat towards the sky in form of radiation. There are several ways with which night-time radiative cooling can be exploited (Grossule, 2015); in this study a closed water based system will be simulated. The main advantages of such a system are the reduction of energy use, since the only electrical energy required is that for the operation of a recirculation water pump and a higher utilization factor for solar thermal panels since they are exploited also during the night. Cooling demand and cold water production through night-time radiative cooling are in phase since clear sky occurs more often during summer and it can be coupled with thermal storage materials such as PCM (Eicker & Dalibard, 2011; Hosseinzadeh & Taherian, 2012; Meir, Rekstad, & Løvvik, 2002).

The purpose of this simulation study was to examine the coupling of suspended ceiling panels including PCM for conditioning an office room with solar collectors, exploited for discharging the PCM passively through night-time radiative cooling. The combination of these two technologies was tested in three different locations, namely Copenhagen (Denmark), Milan (Italy) and Athens (Greece). The system was evaluated in terms of the resulting indoor thermal conditions, the electricity production and the cooling output of the PV/T panels.

METHOD

A software based model was created to simulate a two persons' office room in three different locations, namely Copenhagen (CPH), Milan (MIL) and Athens (ATH). The floor area was 22.7 m², 244.3 ft² (5.4 m X 4.2 m, 17.7 ft X 13.8 ft) while the height was 3 m, 9.8 ft. At 2.5 m (8.2 ft) above the floor the radiant system with the PCM was installed as a suspended ceiling. The plenum that was formed between the suspended ceiling and the office's roof was used to supply fresh air inside the room. A vertical section of the office room is shown in Figure 1. The external wall of the office faced south and the office was assumed to be in an intermediate floor of an office building. Therefore, three walls, the roof and the floor were adjacent to office rooms with identical thermal conditions and only the south wall was exposed to ambient weather conditions. The U-value of the external wall was 0.3 W/(m²K), 0.1 Btu/ft²·h·°F while the internal surfaces had a U-value of 4.9 W/(m²K), 0.9 Btu/ft²·h·°F. On the external wall there was a 3 m², 32.3 ft² window with a U-value of 1.4 W/(m²K), 0.2 Btu/ft²·h·°F and a g-value of 0.59. The heat gains of the office consisted of two occupants at sedentary activity level (1.2 Met), the corresponding office equipment and the ceiling lighting which in total was 540 W, 1843 Btu/h (23.8 W/m², 7.5 Btu/h·ft²). The heat gains were activated during typical office hours, namely from 9:00 to 17:00.

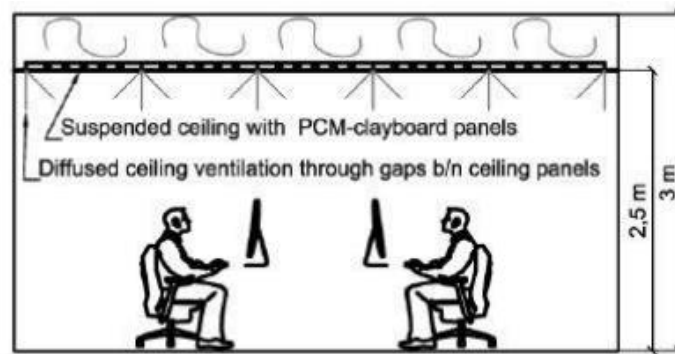**Figure 1. Vertical section of the simulated office room (Pavlov, 2014)**

The external diameter of the pipes supplying cold water to the suspended ceiling was 8 mm, 0.026 ft, the thickness 1 mm, 0.003 ft and the pipe spacing 85 mm, 0.279 ft, while the water flow rate was 150 kg/h, 331 lb/h. The ventilation air flow rate was set to 30 L/s, 63.6 ft³/min (1.9 ACH), sized according to EN 15251 (DS/EN 2007) for

providing fresh air and removing pollutants. The air supply temperature was 18.5°C, 65.3°F and the ventilation was operated from 9:00 until 17:00 every day.

For providing electricity, hot water and cold water for the radiant system, three PhotoVoltaic/Thermal (PV/T) panels and an unglazed solar thermal collector were used. The emissivity of the absorber plate of the unglazed solar collector was 0.91 while for the PV/Ts was 0.89. The plate absorptance of the collectors was 0.95. The PV/T panels had 15 water tubes with an inner diameter of 18 mm (0.06 ft) and a thickness of 1 mm (0.003 ft). The panels were facing south with a tilt angle of 45°. The total surface of the PV/Ts was 3.9 m², 42 ft² and for the unglazed collector 2.4 m², 25.8 ft². The water flow rate in the solar panels was 100 kg/h, 220 lb/h and was split in 62 kg/h, 136 lb/h for the PV/Ts and 38 kg/h, 84 lb/h for the unglazed collector in order to ensure the same flow per m² for the two types of solar collectors. Two tanks were used to store hot water (HWT) and cold water (CWT). Between the solar collectors and the tanks a plate heat exchanger was installed. The direction of the water after the heat exchanger toward the HWT or the CWT was determined automatically based on the two following conditions:

- If $\quad T_{PV/T} - T_{HWT} > 3\,K \quad$ then water directed towards HWT $\hfill (1)$

- If $\quad T_{CWT} - T_{PV/T} > 3\,K \quad$ then water directed towards CWT $\hfill (2)$

where $T_{(PV/T)}$ is the water temperature exiting the PV/T panels, T_{HWT} is the temperature in the middle of the HWT and T_{CWT} is the temperature in the middle of the CWT. If neither of the two conditions was met, then the pump between the heat exchanger and the tanks was switched off. The CWT had two internal spiral heat exchangers. The upper one was connected to the heat exchanger, while the lower one was connected to a chiller (air-to-water heat pump) as shown in Figure 2. The chiller was used as an auxiliary system for providing cold water when the production from night-time radiative cooling was not sufficient. The heat pump had a seasonal COP of 5.4 (18.4 EER). The chiller could be activated from 00:00 until 09:00 provided that the temperature in the middle of the CWT was above 18°C, 64.4°F. The temperature of the water leaving the chiller was 12°C, 53.6°F. The water from the lower part of the CWT was circulated to the PCM panels and from there it was returned to the top of the CWT. The water flow rate was 150 kg/h and the circulation of the water was started at 20:00 and continued until 09:00, provided that the following conditions were met:

- The average lower surface temperature of the PCM panels was above 21°C, 69.8°F
- The operative temperature of the room was above 21°C, 69.8°F
- The temperature of the water in the middle of the CWT was below 20°C, 68°F

The hot water was not utilized, e.g. through a tapping schedule and the tank was used only to store hot water in order to reduce the surface temperature of the PV/T panels. In this way the efficiency of the PV/T panels in terms of electricity production would be increased.

The simulation period for all cases was from the 1st of May until the 30th of September which is considered the cooling period in Denmark. For the simulations, the International Weather for Energy Calculations (IWEC) files for Copenhagen, Milan and Athens were used. In Figure 2 the schematic drawing of the system is shown.
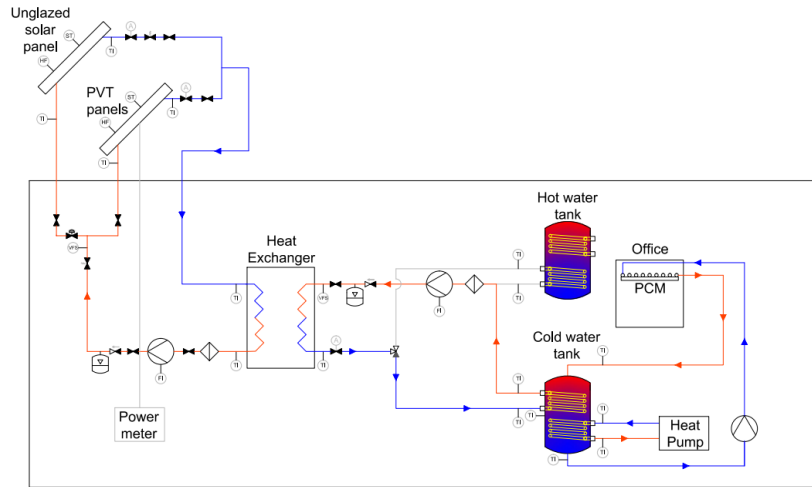
Figure 2. Schematic drawing of the system

RESULTS

In Table 1 the percentages of the occupancy period where the operative temperature was within the limits of each category of EN 15251 (DS/EN, 2007b) are presented. The temperature should be within the ranges 23.5 – 25.5°C, 23 – 26°C and 22 – 27°C (74.3 – 77.9°F, 73.4 – 78.8°F and 71.6°F – 80.6°F) for Category I, II and III, respectively.

Table 1. Percentages of Occupancy Period in Categories of Standard EN 15251

City	Category I, %	Category II, %	Category III, %
Copenhagen	27	40	63
Milan	30	44	81
Athens	26	53	82

It can be seen that Athens had the highest percentage of occupancy time with an operative temperature within the range of Category III. For Milan, the portion of time with thermal conditions within Category III was 1% less than in Athens. Copenhagen had significantly lower percentage of occupancy period within the range of Category III compared to the other two cities.

In Table 2 the average power per m² of the PV/T panels in terms of production of electricity, hot and cold water in the three simulated cities is presented. The highest average electrical power was obtained in Athens, while the average hot and cold water production power was measured in Milan and Copenhagen, respectively.

Table 2. Average Power of the PV/T Panels

City	Average electrical power, W/m² (Btu/h.ft²)	Average hot water production power, W/m² (Btu/h.ft²)	Average cold water production power, W/m² (Btu/h.ft²)
Copenhagen	26.6 (8.4)	76.1 (24.1)	42.8 (13.6)
Milan	27.5 (8.7)	108.2 (34.3)	35.9 (11.4)
Athens	32.6 (10.3)	95.0 (30.1)	33.4 (10.6)

In Table 3 the average power per m² of the unglazed solar collector in terms of hot and cold water production in the three cities is presented. The negative values of power for the production of the cold water mean the water was warmed up instead of cooled down.

Table 3. Average Power of the Unglazed Solar Collector

City	Average hot water production power, W/m² (Btu/h.ft²)	Average cold water production power, W/m² (Btu/h.ft²)
Copenhagen	55.4 (17.6)	-9.4 (-3)
Milan	63.1 (20)	-2.3 (-0.8)
Athens	66.7 (21.1)	8.0 (2.5)

In Figure 3 the percentage of cooling energy provided by night-time radiative cooling and the chiller is shown. Night-time radiative cooling had the highest potential in Copenhagen, while the lowest cooling energy was achieved in Athens.
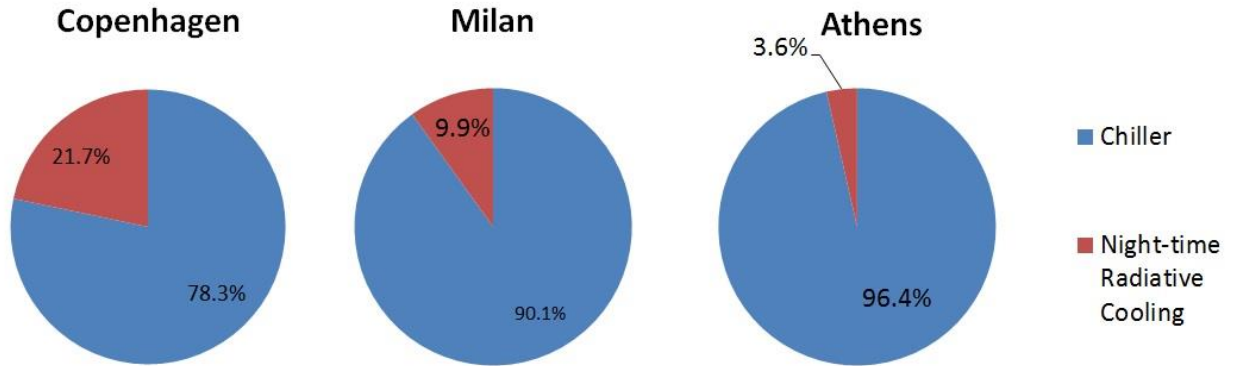
Figure 3. Percentage of cooling energy provided by night-time radiative cooling and the chiller

In Figure 4 the comparison between the electrical energy production and electrical energy usage of the three cities is presented. The latter is tabulated separately for the office equipment, the pumps, the ventilation and the chiller. The energy usage of the office equipment was always 279.1 kWh, 952000 Btu. The pumps bar represents the energy usage of all three pumps shown in Figure 2. The solar loop pump was operated continuously, while the operation of the other two pumps differed based on the weather conditions of each city. The total energy usage of the three pumps varied slightly from 52.8 kWh 180000 Btu for Milan and Athens to 53.2 kWh 181000 Btu for Copenhagen. The ventilation bar includes the energy usage of the fan and the cooling coil. For the fan, a specific fan power (SFP) of 1000 W/(m³/s), 96.6 Btu(ft³/s) was assumed, which corresponds to Category SFP 3 of DS/EN

13779 (DS/EN, 2007a). The energy usage of the ventilation system was 49.1 kWh, 168000 Btu for all three cities. The electricity usage of the chiller was 178 kWh (607000 Btu) in Copenhagen, 268 kWh (914000 Btu) in Milan and 388 kWh (1324000 Btu) in Athens. The electrical energy production from the PV/Ts for the simulated period was 371 kWh or 94.4 kWh/m² of PV/T area (1266000 Btu or 29900 Btu/ft²) for Copenhagen, 380 kWh or 96.7 kWh/m² (1297000 Btu or 30700 Btu/ft²) for Milan and 439 kWh or 111.7 kWh/m² (1498000 Btu or 35400 Btu/ft²) for Athens. The percentage of electricity usage covered from PV/Ts was 66% in Copenhagen, 58% in Milan and 57% in Athens.
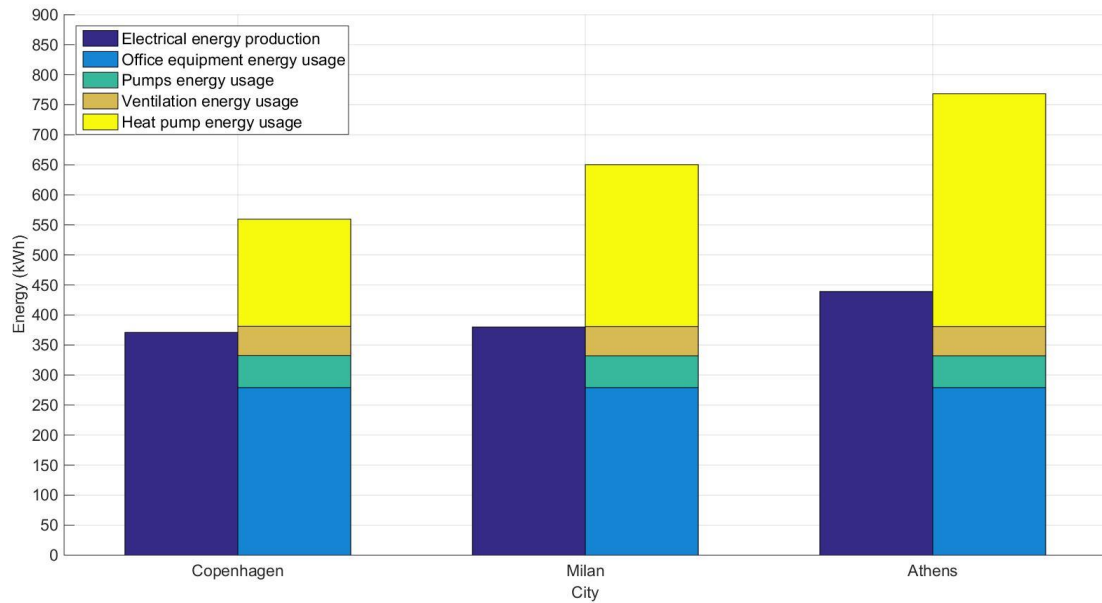
Figure 4. Energy Production and Usage Comparison

DISCUSSION

Analyzing the results shown in Table 1, it may be seen that Copenhagen had the lowest percentage of occupancy time within the range of Category III out of the three examined cities. This is because of the high solar heat gains in Copenhagen due to the low average elevation angle of the sun at this latitude. This can be seen in Figure 5, where the peak value per day of solar heat gains for the three cities is presented. It can be seen that the values simulated in Copenhagen, for most of the simulated days are considerably higher than the values measured in Milan and Athens. In these simulations no solar shading system for the windows was used, since it was not attempted to minimize the cooling demand by means of improving the envelope but intended to examine the performance of the systems as the building was given. If a solar shading system was used, the thermal conditions in all three cities would improve.
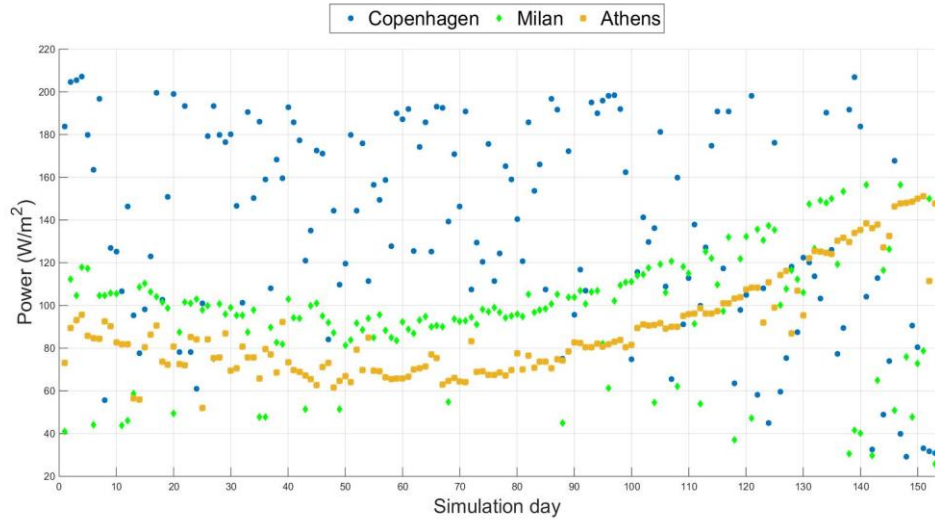
Figure 5. Solar Heat Gains Daily Peak Value

The properties of the PV/T panels and the unglazed solar collector (water flow rate, tilt angle and orientation) remained the same for the three cities. Therefore, the considerable differences observed in the values shown in Table 2 and Table 3, were caused by the different weather conditions the panels were exposed to in the three cities. The results of the unglazed solar collector in Copenhagen and Milan, shown in Table 3, indicate that the temperature of the water was increasing during the night. A better performance of the night-time radiative cooling would thus be achieved if in these two cities only PV/T panels were used.

In Figure 3 it can be seen that Copenhagen has the highest percentage of cooling energy provided by night-time radiative cooling, while Athens has the lowest percentage, almost negligible. The heat exchange of the solar collectors is a combination of radiation towards the sky and convection between the air and the surface of the collectors. Radiation towards the sky resulted in heat losses in all three cities. The air temperature was lower than the collectors' surface temperature only in Copenhagen resulting in heat loss in Copenhagen and heat gain in Milan and Athens. That resulted in the limited performance of the night-time radiative cooling in Milan and Athens. That was the reason why the performance of the unglazed solar collectors in terms of producing cold water through night-time radiative cooling was negligible.

The simulation model was designed in a way to examine mainly the performance of the night-time radiative cooling principle for solar collectors, so the hot water stored in the HWT was not utilized, as it was mention in the "Method" chapter. During a sunny day the temperature in the HWT was increasing considerably. Since the hot water was not utilized, the only temperature drop in the HWT was caused by heat losses. Therefore, the following day the pump placed after the heat exchanger would hardly be activated since Condition (1) would not be fulfilled, even if the weather conditions were suitable for producing hot water. This resulted in underestimating the performance of the solar collectors in terms of domestic hot water production.

In Figure 4 it can be seen that Athens is the city with the highest electricity production from the PV/T, as expected. In spite that, due to the negligible production of cooling energy from the night-time radiative cooling, the use of the chiller was significantly higher compared to the other two cities, resulting in the lowest percentage of electrical energy usage covered by the production from the PV/T panels. On the other hand, in Copenhagen the use of the chiller was considerably lower; resulting in a higher fraction of electrical energy usage covered by the production from the PV/T panels. Although in all the three simulated cities the electricity production from the PV/Ts did not cover completely the electrical energy demand, it should be taken into consideration that the production of hot and cold water from the PV/Ts would reduce the operation time of the heat pump. If a water-to-

water heat pump or a ground source heat exchanger was used instead of an air-to-water heat pump a higher COP would be achieved and the use of the heat pump would be reduced. The considerable differences in terms of electrical energy production and chiller energy usage observed between the three cities can be explained by the different climates to which the panels were exposed in the different locations.

As it was mentioned in the "Method" chapter, the circulation of the water in the PCM panels was activated from 20:00 until 09:00 while the heat pump was activated from 00:00 until 09:00. This gave only a limited amount of time for the exploitation of night-time radiative cooling before the heat pump was activated. A time schedule that may improve the performance of the solar collectors in terms of cooling energy production would be to activate the PCM and the heat pump later during the night, e.g. at 05:00 until 9:00. In this way the night-time radiative cooling could be exploited for a longer period, and the use of the heat pump could be reduced. This control method will be addressed in a later study.

CONCLUSIONS

1) The PCM ceiling panels provided better thermal conditions in Athens and Milan than Copenhagen due to the position of the sun during daytime. 2) The cooling power of the unglazed solar collector was negligible and in Milan and Copenhagen a better performance would have been achieved if only PV/T had been used. 3) Night-time radiative cooling covered a higher percentage of the cooling demand at higher latitudes in spite of the lower percentage of clear sky. 4) Higher fraction of energy usage was covered by the production from the PV/Ts in Copenhagen than Milan and Athens. 5) The performance of the installations could be improved by implementing a solar shading system on the window and an improved control strategy, as described at the end of the "Discussion" chapter.

REFERENCES

Cabeza, L. F., Castellón, C., Nogués, M., Medrano, M., Leppers, R., & Zubillaga, O. (2007). Use of microencapsulated PCM in concrete walls for energy savings. *Energy and Buildings*, *39*(2), 113–119. doi:10.1016/j.enbuild.2006.03.030

DS/EN. (2007a). 13779: Ventilation for non-residential buildings. Performance requirements for ventilation and room-conditioning systems, (2).

DS/EN. (2007b). DS/EN 15251:2007 Indoor environment input parameters for design and assessment of energy performance of buildings adressing indoor air quality, thermal environment, lighting and acoustics.

Eicker, U., & Dalibard, A. (2011). Photovoltaic-thermal collectors for night radiative cooling of buildings. *Solar Energy*, *85*(7), 1322–1335. doi:10.1016/j.solener.2011.03.015

EP. (2009). Directive 2009/28/EC of the European Parliament and of the Council of 23 April 2009 on the promotion of the use of energy from renewable sources and amending and subsequently repealing Directives 2001/77/EC and 2003/30/EC. *Official Journal of the European Union*, *140*(16), 16–62. doi:10.3000/17252555.L_2009.140.eng

EP. (2010). Directive 2010/31/EU of the European Parliament and of the Council of 19 May 2010 on the energy performance of buildings (recast). *Official Journal of the European Union*, 13–35. doi:doi:10.3000/17252555.L_2010.153.eng

Grossule, F. (2015). *The use of phase changing materials for cooling of buildings combined with night sky radiant cooling -*.

Hosseinzadeh, E., & Taherian, H. (2012). An Experimental and Analytical Study of a Radiative Cooling System with Unglazed Flat Plate Collectors. *International Journal of Green Energy*, *9*(October), 766–779. doi:10.1080/15435075.2011.641189

Koschenz, M., & Lehmann, B. (2004). Development of a thermally activated ceiling panel with PCM for application in lightweight and retrofitted buildings. *Energy and Buildings*, *36*(6), 567–578. doi:10.1016/j.enbuild.2004.01.029

Meir, M. G., Rekstad, J. B., & Løvvik, O. M. (2002). A study of a polymer-based radiative cooling system. *Solar Energy*, *73*(6), 403–417. doi:10.1016/S0038-092X(03)00019-7

Pavlov, G. K. (2014). Building Thermal Energy Storage, (April), 313.

Paper 7: Bourdakis E., Peán Q. T., Gennari L., & Olesen B. W. (2016). Experimental study of discharging PCM ceiling panels through nocturnal radiative cooling. Presented at IACVEQ 2016

Experimental study of discharging PCM ceiling panels through nocturnal radiative cooling

Eleftherios Bourdakis[1,*], Thibault Q. Péan[2] and Luca Gennari[3], Bjarne W. Olesen[1]

[1]Technical University of Denmark - ICIEE, Kgs Lyngby, Denmark
[2]Polytechnic University of Catalonia - IREC, Barcelona, Spain
[3]Except Integrated Sustainability, Rotterdam, Netherlands

[*]*elefbur@byg.dtu.dk*

ABSTRACT
PhotoVoltaic/Thermal (PV/T) panels were used for cooling water through the principle of nocturnal radiative cooling. This water was utilised for discharging Phase Change Material (PCM) which was embedded in ceiling panels in a climate chamber. Three different sets of flow rates were examined for the solar and the PCM loops, for five days each. The highest examined water flow rate (210 l/h) in the PCM loop provided the best thermal environment in the climate chamber, namely 92% of the occupancy time was within the range of Category III of Standard EN 15251. Although the lowest examined water flow rate (96 l/h) in the solar loop provided the highest average cooling power, due to the significant variations in the weather conditions during the three experimental cases, made it impossible to determine to which extent the difference in the cooling power is due to the different water flow rate. The percentage of electrical energy use that could be covered from the PV/Ts on site was 71.5% for Case 1, 68.3% for Case 2 and 86.8% for Case 3. In any case, the PV/T panels proved to be an efficient solution for the production of electrical energy, heated and chilled water.

KEYWORDS
Ceiling cooling panels, Phase change material, nocturnal radiative cooling, Photovoltaic/thermal panels, High temperature cooling

INTRODUCTION
Following the outcome of the recent United Nations Conference on Climate Change 2015 (UNFCCC 2015) and the recently adopted policies from the European Union (EP 2009; EP 2010) vast changes have to be implemented in the buildings sector, such as installing photovoltaic panels on existing building or increasing the efficiency of the heating, ventilation and air conditioning (HVAC) equipment. According to UNEP (2009) the majority of the buildings that will exist by the year 2050 in the developed countries have already been built. Therefore, the interest should be focused on renovating existing buildings.
A solution that could contribute in energy retrofitting existing buildings and at the same time improving the interior thermal conditions could be the installation of ceiling panels with phase change material (PCM). PCMs are either organic or inorganic substances that store large amounts of energy when they melt and release it when they solidify. During the phase change the temperature of the PCM remains constant resulting in a lower surface temperature compared to a conventional material that would absorb the same amount of heat (Kuznik et al. 2011). The most important advantages of installing ceiling panels with PCM are the reduction of the peak cooling load, the shift of fraction of the cooling demand to night-time, the reduced temperature span and the reduction of the size of the HVAC system (Koschenz & Lehmann 2004; Cabeza et al. 2007; Pavlov 2014).

A possible method to discharge the PCM passively consists in exploiting solar panels during the night through the process of radiative cooling. Night sky can be used as a natural heat sink, since its effective temperature, depending on the weather conditions, can be significantly lower than the ambient temperature. Therefore, water circulated during night-time in solar panels can be cooled down passively and utilised for discharging the PCM panels. The benefits of exploiting night-time radiative cooling are the higher utilization factor of solar panels, the possible coupling with thermal storage systems(e.g. PCM), and the fact that cold water production and cooling demand are in phase. Indeed, clear sky occurs more often during summer time when the cooling demand is higher (Meir et al. 2002; Eicker & Dalibard 2011; Hosseinzadeh & Taherian 2012; Péan et al. 2015).

The purpose of the present experiment was to realize the coupling of solar panels with PCM ceiling panels and examine different water flow rates circulating in the two loops to identify the optimum combination.

METHODS

The experiment took place at the facilities of the International Centre for Indoor Environment and Energy at the Technical University of Denmark, during June 2015. For simulating a two persons' office, a climatic chamber that is inside a greater building was used, therefore this chamber was not affected from changes in the ambient weather conditions. The floor area of the chamber was 22.7 m² while the height of the chamber was 3 m. The floor, the roof and the four walls of the chamber were made of two aluminium plates and 100 mm of mineral wool between them.

At 2.5 m above the floor, 24 ceiling panels containing the PCM were installed, forming a 0.5 m plenum above the office room. The surface of each panel was 0.78 m² and the thickness was 25 mm. Each panel contained 6 kg of PCM, corresponding to 26% of the total weight of each panel. The fusion temperature of the PCM used was 23°C. Alu-PEX pipes were installed inside the panels in order to discharge the PCM by recirculating cold water.

Heat dummies were used for simulating the two occupants and the office equipment, and they were activated from 09:00 until 17:00 which are considered typical office hours. The total internal heat gains from the occupants, the equipment, the desk lamps and the ceiling lamps were 540W (23.8 W/m²). Since the chamber was not exposed directly to solar heat gains, an electrical heating panel was used to simulate the solar heat gains of a window facing south. The setup of the climatic chamber is shown in Figure 1; the electrical heating panel is located in the background.

Figure 1: The interior of the climatic chamber

Air was supplied to the office from the plenum above the suspended ceiling. The air flow rate was 30 l/s (1.9 ACH), sized according to Standard EN 15251 (DS/EN 2007) for removing

latent heat gains and pollutants. The air supply temperature was varying between 18°C and 20°C.

On the roof of the building where the chamber was installed, three PV/T panels were installed in series. The panels were facing south with an angle of 45° and the surface of each panel was 1.3 m². The PV/T panels were connected with two storage tanks through a plate surface heat exchanger, as it is shown in Figure 2. In the first tank hot water was stored (HWT), while in the other one cold water (CWT) was stored. The direction of the water after the heat exchanger was determined automatically based on the two following equations:

- If $T_{PV/T} - T_{HWT} > 1\,K$ then the water was directed towards the HWT

- If $T_{CWT} - T_{(PV/T)} > 1\,K$ then the water was directed towards the CWT

where $T_{(PV/T)}$ is the temperature exiting the PV/T panels, T_{HWT} is the temperature in the middle of the HWT and T_{CWT} is the temperature in the middle of the CWT. If neither of the two conditions was met, then the pump located between the plate surface heat exchanger and the tanks was deactivated. The locations of these three sensors are shown in Figure 2.
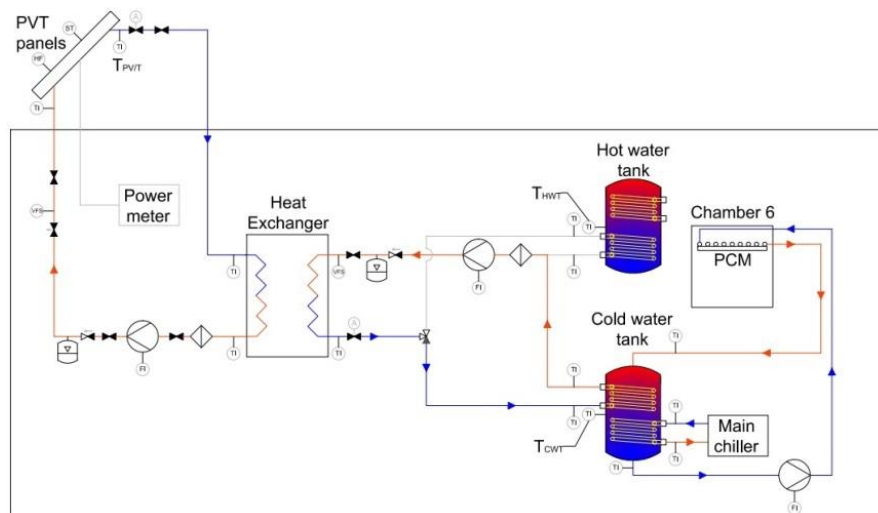

Figure 2: Schematic drawing of the hydraulic system

As it is shown in Figure 2, the CWT had two internal spiral heat exchangers. The upper one was connected with the plate surface heat exchanger, while the lower one was connected with the main chiller of the facilities. The main chiller was used as a backup system for providing cold water in case the production from the night-time radiative cooling was not sufficient to reduce the temperature in the CWT. If it was required, the chiller would operate during the period 05:00 – 09:00. The water supply temperature of the main chiller was 7°C. The water stored in the CWT was circulated to the ceiling panels to discharge the PCM, provided that all three following conditions were met:
- The average lower surface temperature of the ceiling panels was above 21°C
- The operative temperature of the office room was above 21°C
- The temperature of the water in the middle of the CWT was below 20°C

During the occupancy period (09:00 – 17:00) water from the CWT would be circulated in the ceiling panels in case the operative temperature in the office was exceeding 25.5°C and the temperature in the middle of the CWT was below 20°C.

The three different cases that were examined are presented in Table 1. The duration for each case was five consecutive days. During the whole experimental period, the electrical power of the PV/T panels was also monitored.

Table 1. Cases examined

Case number	Solar loop water flow rate, l/h	PCM loop water flow rate, l/h
1	216	150
2	166	180
3	94	210

RESULTS

In Figure 3 the operative temperature of the three examined cases is presented. The horizontal pairs of dashed lines are the lower and upper limits of the three categories of Standard 15251 (DS/EN 2007). The temperature ranges for each category are 23.5 – 25.5°C for Category I, 23 – 26°C Category II and 22 – 27°C for Category III. The gray shaded areas are the occupancy period, namely from 09:00 to 17:00, each day. The sudden drop that is observed after 05:00 during the nights was by the activation of the chiller, causing the temperature in the CWT to drop drastically.
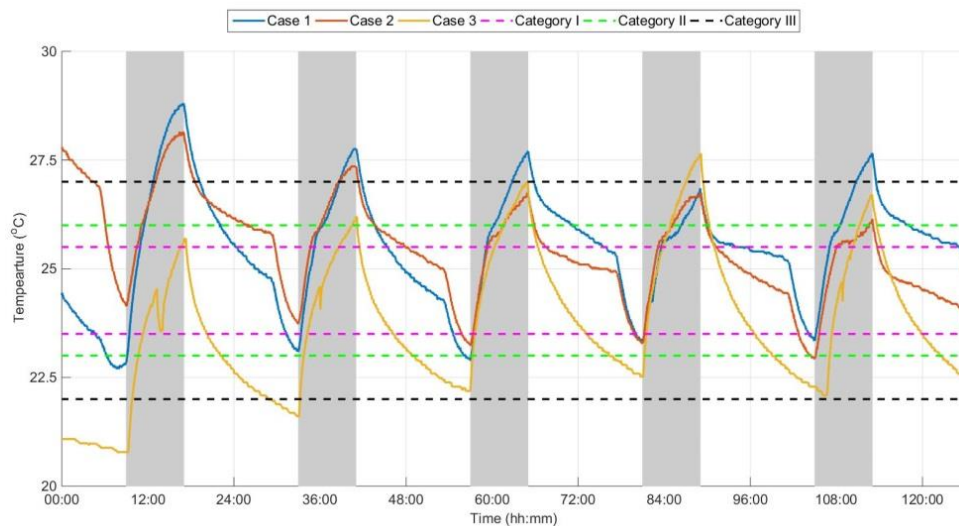

Figure 3. Operative temperature over time

The percentage of occupancy time when the temperature was within the range of each category of Standard 15251 (DS/EN 2007) is presented in Table 2.

Table 2. Percentage of occupancy time in each category of Standard 15251 (DS/EN 2007)

Case number	Percentage of occupancy time in Category I, %	Percentage of occupancy time in Category II, %	Percentage of occupancy time in Category III, %
1	23	45	72
2	24	53	84
3	45	63	92

The average power output of the PV/T panels in terms of electrical, hot water and cold water production are presented in Table 3.

Table 3. Average power outputs of the PV/T panels

Case number	Average electrical power, W/m^2	Average heating power, W/m^2	Average cooling power, W/m^2
1	53.8	41.5	61.9
2	49.3	33.9	65.8
3	51.0	35.0	70.8

A comparison between the electrical energy produced by the PV/Ts and the electrical energy use for each experiment is presented is presented in Figure 4. The electrical energy production was 18.8 kWh, 16.8 kWh and 16.9 kWh for Case 1, 2 and 3, respectively. The electrical energy use is separated into electrical energy use for the office equipment, the pumps, the ventilation and the chiller. The office equipment consisted of two laptops with one screen each, four ceiling lamps and two office lamps and the total energy use was 9.1 kWh for each case. The pumps tab shows the energy usage of the three pumps shown in Figure 2, and it varied between 1.6 kWh in Case 3 and 2.7 kWh in Case 1. The ventilation tab includes the energy use of the fan and the cooling coil and it was 1.2 kWh for all three cases. Because the specific fan power (SFP) of the fan was unknown, an SFP of 1000 W/(m^3/s) was assumed based on the required flow rate. The electrical energy use of the chiller was 7.5 kWh for Case 3, 12.1 for Case 2 and 13.3 for Case 1. In order to calculate the energy use of the cooling coil and the chiller, it was assumed that the HVAC was connected to an air to water heat pump. The specifications of a heat pump available on the market were used, based on which a seasonal COP of 4.5 was calculated. The total energy was 26.3 kWh, 24.6 and 19.5 kWh for Cases 1, 2 and 3 respectively. The percentage of electrical energy use that could be covered from the PV/Ts on site was 71.5% for Case 1, 68.3% for Case 2 and 86.8% for Case 3.
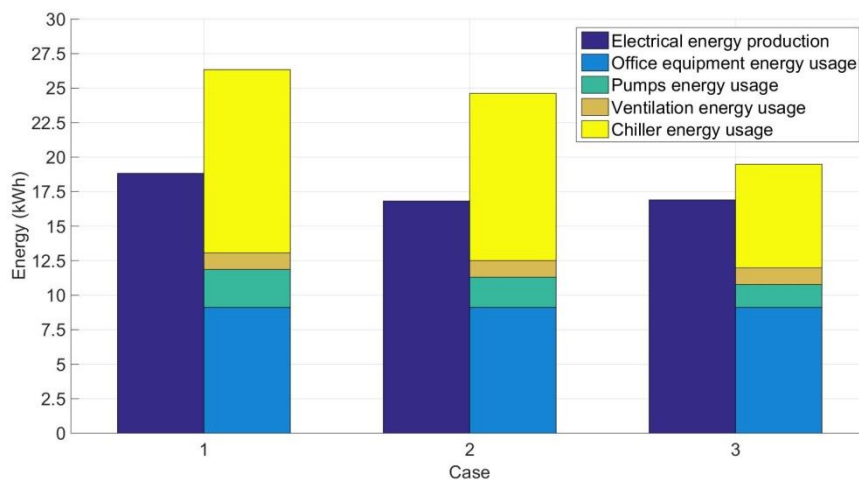

Figure 4. Electrical energy production vs energy use comparison

DISCUSSIONS

From the results presented in Figure 3 and Table 2 it can be seen that the case where the best thermal environment was provided in the chamber was Case 3. The air temperature in the building where the climate chamber was located is presented in Figure 5. The average air temperature measured outside the chamber for each case was 25.2°C for Case 1, 24.5°C for Case 2 and 25.4°C for Case 3. Since the building's average air temperature difference among the three cases is not significant and the chamber was not exposed to direct solar radiation, it can be concluded that the differences observed in the thermal performance of the chamber

were attributed to the change of the flow rate of the pump circulating water to the PCM panels.
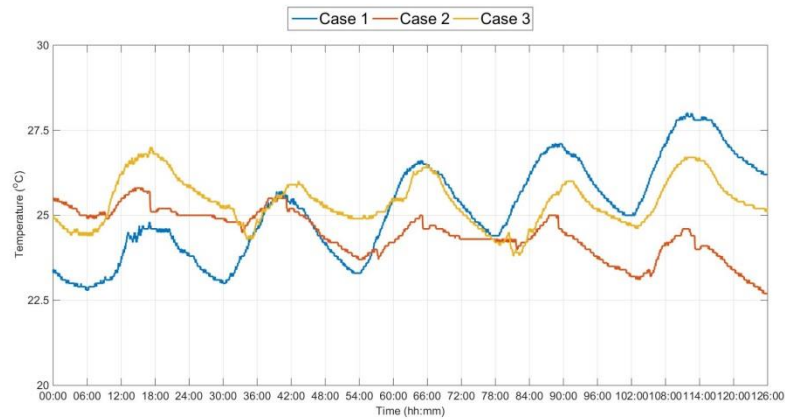

Figure 5. Air temperature outside the chamber

The higher average electrical power of Case 1 reported in Table 3 and consequently the higher electrical energy production shown in Figure 4 are attributed to the higher solar radiation on the panels during that Case, as it is shown in Table 4. These weather data were recorded by a weather station installed next to the PV/T panels.

Table 4. Weather conditions during the experiment

Case Number	Minimum ambient air temperature, °C	Maximum ambient air temperature, °C	Average ambient air temperature, °C	Solar energy on the panels, kWh/m²	Max. wind speed, m/s	Aver. wind speed, m/s
1	12.0	27.8	18.9	2220	4.5	1.5
2	12.3	21.4	17.4	1795	7.2	1.9
3	11.1	24.7	18.1	1656	5.4	1.2

The variation of the solar radiation and the ambient air temperature between the three cases shown in Table 4 and Figure 6, affected the heating power output of the PV/Ts and therefore it cannot be concluded which flow rate in the solar loop is the most effective for water heating.
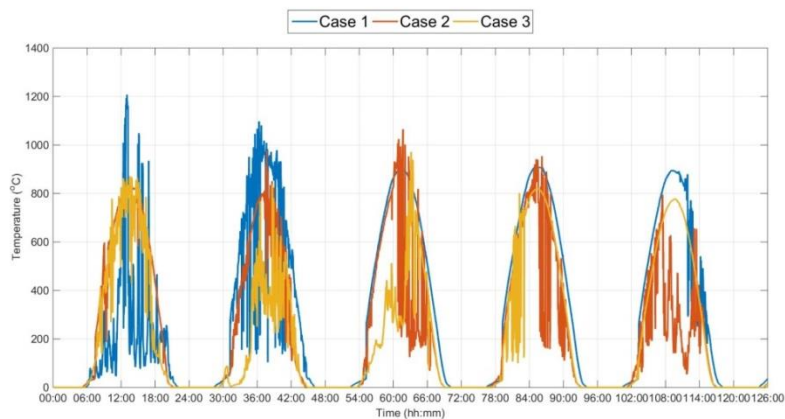

Figure 6. Solar radiation over time

The cooling power of the PV/Ts is determined by the convection on the surface of the panels and the radiation towards the sky. The installed weather station did not have the possibility of recording the percentage of cloud cover, therefore the only indication of the effect of the weather conditions on the cooling power is through the ambient air temperature and the wind speed, both affecting the convection on the panels' surface. As can be seen from Table 4 and Figure 7 considerable variations were observed in both weather parameters among the three experimental cases. Therefore, as before it cannot be concluded which flow rate in the solar loop was the most beneficial for cooling the water.
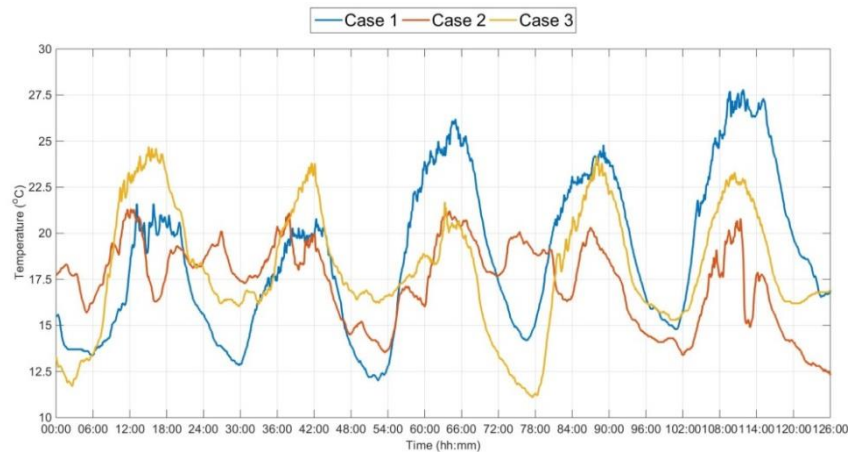

Figure 7. Ambient air temperature over time

The PV/T panels did not provide all the electrical energy required for the chamber, but it should be taken into consideration that the electrical energy demand would be higher if regular photovoltaic panels were used due to the demand for heating and cooling covered by the PV/T panels. As mentioned before, it was assumed that an air to water heat pump was used. If a water to water heat pump or a ground source heat exchanger were used instead, a higher COP would have been estimated and therefore the energy use of the chiller and the cooling coil would be lower. The difference in the electrical energy production among the three cases was not significant, but in Case 3 the chiller operated for considerably lower amount of time, resulting in lower energy use compared to the previous two cases. That resulted in the higher percentage of electrical energy use covered by the PV/Ts for the 3rd case.

CONCLUSIONS
1. It was concluded that out of the three examined flow rates in the PCM loop, the highest one provided the best thermal environment in the chamber. 2. The variations in the weather conditions between the three cases cannot lead to a safe conclusion whether the measured differences in the heating and cooling power of the PV/Ts can be attributed to the different flow rate in the solar loop or the weather conditions. 3. PV/T panels proved to be an efficient solution for the production of electrical energy and heating and cooling water for domestic hot water and space cooling respectively.

REFERENCES

Cabeza, L. F., Castellón, C., Nogués, M., Medrano, M., Leppers, R., & Zubillaga, O. (2007). Use of microencapsulated PCM in concrete walls for energy savings. *Energy and Buildings*, *39*(2), 113–119.

DS/EN. (2007). DS/EN 15251:2007 Indoor environment input parameters for design and assessment of energy performance of buildings adressing indoor air quality, thermal environment, lighting and acoustics.

Eicker, U., & Dalibard, A. (2011). Photovoltaic-thermal collectors for night radiative cooling of buildings. *Solar Energy*, *85*(7), 1322–1335.

EP. (2009). Directive 2009/28/EC of the European Parliament and of the Council of 23 April 2009 on the promotion of the use of energy from renewable sources and amending and subsequently repealing Directives 2001/77/EC and 2003/30/EC. *Official Journal of the European Union*, *140*(16), 16–62.

EP. (2010). Directive 2010/31/EU of the European Parliament and of the Council of 19 May 2010 on the energy performance of buildings (recast). *Official Journal of the European Union*, *153*(13), 13–35.

Hosseinzadeh, E., & Taherian, H. (2012). An Experimental and Analytical Study of a Radiative Cooling System with Unglazed Flat Plate Collectors. *International Journal of Green Energy*, *9*(8), 766–779.

Koschenz, M., & Lehmann, B. (2004). Development of a thermally activated ceiling panel with PCM for application in lightweight and retrofitted buildings. *Energy and Buildings*, *36*(6), 567–578.

Kuznik, F., David, D., Johannes, K., & Roux, J. J. (2011). A review on phase change materials integrated in building walls. *Renewable and Sustainable Energy Reviews*, *15*(1), 379–391.

Meir, M. G., Rekstad, J. B., & Løvvik, O. M. (2002). A study of a polymer-based radiative cooling system. *Solar Energy*, *73*(6), 403–417.

Pavlov, G. K. (2014). *Building Thermal Energy Storage*. Copenhagen, Denmark: DTU-Tryk.

Péan, T., Gennari, L., Olesen, B. W., & Kazanci, O. B. (2015). Nighttime radiative cooling potential of unglazed and PV / T solar collectors : parametric and experimental analyses. *Proceedings of the 8th Mediterranean Congress of Heating, Ventilation and Air-Conditioning (Climamed 2015)*.

UNEP. (2009). *Buildings and Climate Change - Summary for Decision-Makers. Sustainable Buildings & Climate Initiative*.

UNFCCC. (2015). COP 21 Climate Agreement, *21932*(December), 32.

Paper 8: Bourdakis E., Kazanci O. B., Peán Q. T., & Olesen B. W. (2016). Parametric analysis of the control of solar panels for nocturnal radiative cooling coupled with in room PCM ceiling panels. Presented at ASHRAE Winter Conference 2017

Parametric Analysis of the Operation of Nocturnal Radiative Cooling Panels Coupled with in Room PCM Ceiling Panels

E. Bourdakis
Student member ASHRAE

O.B. Kazanci
Student Member ASHRAE

T.Q. Péan

B. W. Olesen, PhD
Fellow ASHRAE

ABSTRACT

The scope of this parametric simulation study was to identify the optimal combination of set-points for different parameters of a radiant PCM ceiling panels cooling system that will result in the best indoor thermal environment with the least possible energy use. The results showed that for each parameter examined, a different set-point value was optimal for the thermal environment than the value that was optimal for the reduction of energy use. Therefore, two additional simulations were run, one with the combination of set-point values that resulted in the improvement of the thermal environment and one with the set-point values resulting in the reduction of energy use. In the first case, the temperature was within the range of Category III of EN 15251 (23 – 26°C, 73.4 – 78.8°F) for 83.5% of the occupancy time, while in the second case it was within Category III for 39.4%. In the first simulation, the energy usage of the pumps and the heat pump was 178 kWh, 608 kBtu, while for the second one it was 36 kWh, 121 kBtu. It was concluded that the optimal combination of set-point values to provide the most comfortable thermal environment was to activate the pump circulating water to the PCM no earlier than 03:00 and get activated when the temperature in the storage tank was below 21°C, 69.8°F, activate the heat pump no earlier than 05:00 and get activated when the temperature in the storage tank was below 15°C, 59°F, and lastly have a temperature difference between the output of the solar panels and the temperature in the middle of the storage tanks of 5 K, 9°F.

INTRODUCTION

As HVAC systems advance, their operation and control system becomes increasingly complicated, consisting of multiple conditions and parameters, which interact with each other. In order to optimize the operation of a control system, the ideal combination of set-points for these parameters needs to be realized, aiming at providing an acceptable indoor environment, as this is defined by the standards, and at the same time reducing the energy use as much as possible. The operation optimization of the controller of radiant heating and cooling systems has been the subject of several studies, both simulations and experimental.

Sourbron and Helsen (2013) studied the impact of using different temperature (air, operative, surface and core temperature) for controlling a Thermo Active Building System (TABS) and different setpoint values for these parameters. They concluded that the controller settings, apart from the indoor thermal environment and the energy use, affect considerably also the required power of the heating and cooling source. In addition to that, inappropriate control settings resulted in switching between heating and cooling mode during the same day, resulting in a significant increase of the energy used by the radiant system.

Tödtli et al. (2007) and Gwerder et al. (2008) studied the coupling of TABS control with building automation and developed a tool for dimensioning the TABS using the "Unknown-But-Bounded" method. With this method they were able to verify the system's applicability for a given situation, determine the maximum heating/cooling

E. Bourdakis is a Ph.D. candidate in the ICIEE, Technical University of Denmark, Denmark. O.B. Kazanci is a PhD candidate. in the ICIEE, Technical University of Denmark, Denmark. T.Q. Péan is a PhD student at the Polytechnic University of Catalonia, Spain. B.W. Olesen is a Professor in the ICIEE, Technical University of Denmark, Denmark

capacity and maintain the thermal comfort, provided that the heat gains were within the predefined range.

Lim et al. (2006) studied radiant floor cooling systems in Korean residential buildings regarding the possibility of condensation occurrence and thermal comfort due to the Korean tradition of sitting on the floor. They concluded that controling the room air temperature by adjusting the supply water temperature and having a constant water flow provided better thermal environment than controlling with a variable water flow. Regarding condensation, they suggested that the water supply temperature should be adjusted based on the room dew point temperature.

In a different study, Lim et al. (2014), developed an operational guideline for TABS, based on heating and cooling load charchteristics of a specific campus building in Seoul, Korea. Furthermore, they found that although the radiant system was able to deal with most of the heating load, it was able to remove less than 50% of the cooling loads due to the limitations caused by the risk of forming condensation on the radiant surface.

In the present simulation study, the coupling of solar panels with in room Phase Change Material (PCM) ceiling panels for cooling an office room was examined during the summer (cooling) period of Copenhagen, Denmark. The solar panels were utilized to produce cold water through nocturnal radiative cooling which was then used to discharge the PCM panels in the room. The purpose of this parametric study was to identify the optimal combination of set-point values that will result in providing the ideal indoor thermal environment. The simulation model that was used, has already been validated and tested under different climatic conditions (Bourdakis et al. 2015; 2016a).

METHODOLOGY

The model was created using commercially available software, to simulate an office room located in Copenhagen, Denmark. The simulation period was from the 1st of May until the 30th of September which is considered the cooling period in Denmark, using the corresponding IWEC weather file. The floor dimensions were 5.4 m X 4.2 m (17.7 ft X 13.8 ft) corresponding to 22.7 m² (244.3 ft²), while the total height was 3 m (9.8 ft). At 2.5 m (8.2 ft) above the floor PCM panels were installed forming a suspended ceiling as it can be seen in Figure 1. Outside air was supplied to the office from the plenum formed between the suspended ceiling panels and the roof of the office. The office was assumed to be in an intermediate floor of an office building and the external wall of the office was facing south. Therefore, the three internal walls, the roof and the floor were assumed to be adjacent to office rooms with identical thermal conditions, so no heat exchange occurred from these surfaces. The U-value of the external wall was 0.3 W/m²K (0.1 Btu/ft²·h·°F) while the internal surfaces had a U-value of 4.9 W/m²K (0.9 Btu/ft²·h·°F). On the external wall there was a 3 m² (32.3 ft²) window with a U-value of 1.4 W/m²K (0.2 Btu/ft²·h·°F) and a g-value of 0.59. The heat gains of the office consisted of two occupants at sedentary activity level (1.2 Met), the corresponding office equipment and lighting which in total was 540 W (1843 Btu/h) corresponding to 23.8 W/m² (7.5 Btu/h·ft²). The heat gains were activated during typical office hours, namely from 9:00 to 17:00.
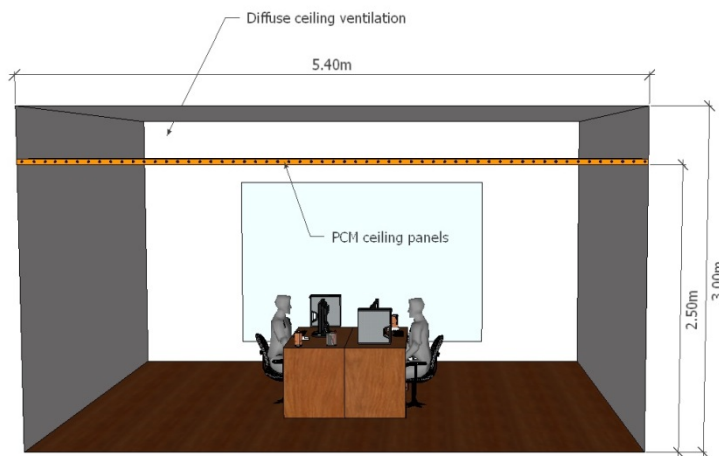

Figure 1. Vertical cross-section of the simulated office room

The PCM panels covered 18.8 m² (201.8 ft²) of the total ceiling surface and the panel thickness was 25 mm (0.082 ft). The PCM density was 1217 kg/m³ (76 lb/ft³) while the latent enthalpy was 28.7 kJ/kg (12.3 Btu/lb). The phase change temperature range of the PCM was 21 – 25°C (70°F – 77°F). The PCM ceiling panels had embedded pipes for water circulation to discharge the PCM. The external diameter of the pipes was 8 mm (0.026 ft), the pipe thickness was 1 mm, the pipe spacing was 85 mm (0.279 ft). and the water flow rate was 150 kg/h (331 lb/h). The ventilation system was sized based on EN 15251 (DS/EN 2007) for providing outside air and removing pollutants, which resulted in an air flow rate of 30 L/s (63.6 ft³/min) corresponding to 1.9 ACH. The ventilation was operating during the occupancy period, namely 09:00 – 17:00 and the air supply temperature was 18.5°C (65.3°F).

Three PhotoVoltaic/Thermal (PV/T) panels and an unglazed solar collector were installed for providing electricity, hot and cold water to the office. The cold water would be utilized to discharge the PCM. The solar collectors were facing south at a tilt angle of 45°. The total surface of the PV/T panels was 3.9 m² (42 ft²) while for the unglazed solar collector was 2.4 m² (25.8 ft²). The water flow rate in the solar panels was 100 kg/h (220 lb/h) and was split in 62 kg/h (136 lb/h) for the PV/T panels and 38 kg/h (84 lb/h) for the unglazed solar collector in order to ensure the same water flow rate per m² for the two types of solar collectors. The emissivity of the absorber plate of the unglazed solar collector was 0.91 while for the PV/Ts was 0.89. The plate absorptance of the collectors was 0.95. The PV/T panels had 15 water tubes with an inner diameter of 18 mm (0.06 ft) and a thickness of 1 mm (0.003 ft).

Two tanks were used to store the hot water (HWT) and the cold water (CWT) output of the solar collectors. Between the solar collectors and the storage tanks a plate heat exchanger was used due to the different pressure settings of the tanks and the solar collectors. A schematic drawing of the hydronic system is shown in Figure 2.
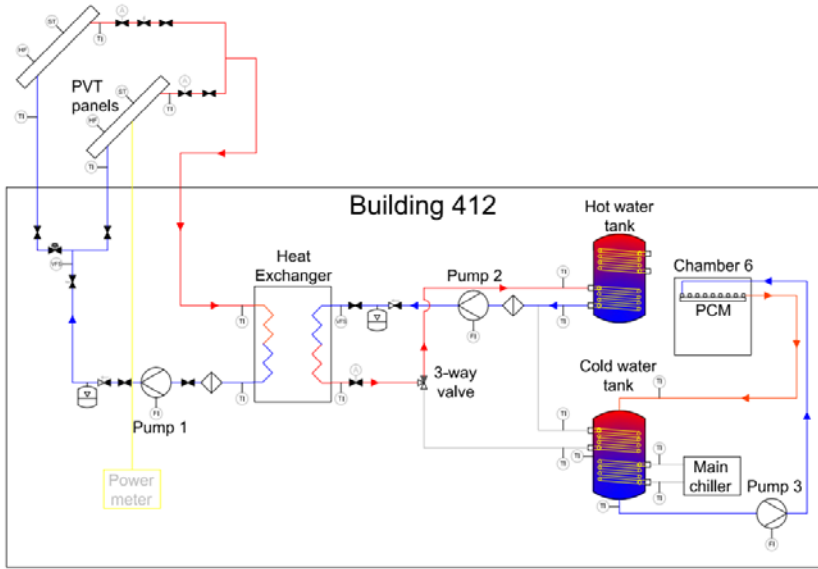
Figure 2. Schematic drawing of the hydronic system

After the heat exchanger a 3-way valve was installed to direct the water either towards the CWT or the HWT. The direction of the water was determined automatically based on the following conditions:

$$\text{If } T_{PV/T} - T_{HWT} > \Delta T \text{ then water directed towards HWT} \tag{1}$$

$$\text{If } T_{CWT} - T_{PV/T} > \Delta T \text{ then water directed towards CWT} \tag{2}$$

where $T_{PV/T}$ is the water temperature exiting the PV/T panels, T_{HWT} is the temperature in the middle of the HWT and T_{CWT} is the temperature in the middle of the CWT. If neither of the two conditions was met, then pump 2 (see Figure 2) was switched off. The ΔT was one of the examined parameters, and the values used were 1 K, 2 K, 3 K, 4 K and 5 K (1.8°F, 3.6°F, 5.4°F, 7.2°F and 9°F, respectively). The CWT had two internal spiral heat exchangers. The upper one was connected to the heat exchanger, while the lower one was connected to an air-to-water heat pump (AWHP) as shown in Figure 2. The AWHP was used as a supporting system for providing cold water when the production from nocturnal radiative cooling was not sufficient. The AWHP had a seasonal COP of 5.4 (18.4 EER).

The hot water was not utilized, e.g. through a tapping schedule and the tank was used only to store hot water in order to reduce the surface temperature of the PV/T panels. In this way the efficiency of the PV/T panels in terms of electricity production would be increased.

The examined parameters were the set-point temperature and the starting time for activating Pump 3 circulating water to PCM panels, the set-point temperature and the starting time for activating the AWHP, and, the temperature difference between the outlet temperature of the solar panels and the water temperature in the middle of the storage tanks. For both Pump 3 and the AWHP, the setpoint temperature was the temperature in the middle of the CWT. The values that were examined for each parameter are shown in Table 1, and the values that were used when examining a different parameter are highlighted in bold. Since the setpoints for activating Pump 3 and the AWHP are closely related, all the possible combinations of these two parameters were simulated.

Table 1. Setpoint values for examined parameters

AWHP starting time, hh:mm	CWT temperature to activate the AWHP, K (°F)	Pump 3 starting time, hh:mm	CWT temperature to activate Pump 3, K (°F)	Panels – Tanks ΔT, K (°F)
03:00	15 (59)	03:00	15 (59)	1 (1.8)
04:00	16 (60.8)	04:00	16 (60.8)	2 (3.6)
05:00	17 (62.6)	**05:00**	17 (62.6)	3 (5.4)
06:00	**18 (64.4)**	06:00	**18 (64.4)**	4 (7.2)
07:00	19 (66.2)	07:00	19 (66.2)	5 (9)
	20 (68)		20 (68)	
	21 (69.8)		21 (69.8)	

The examined parameters will be evaluated in terms of the indoor thermal environment of the office and the energy required for the operation of the pumps and the AWHP. The thermal environment will be assessed in terms of percentage of occupancy time that the operative temperature was within the range of Category III of EN 15251 (DS/EN 2007), which is 22 – 27°C (71.6°F – 80.6°F). The PCM panels will be assessed in terms of cooling energy removed by the PCM ceiling panels and the utilization factor of the PCM, namely the percentage of PCM quantity being discharged or charged at the beginning or the end of the occupancy period respectively.

RESULTS

In the following tables, the results from each set of simulations are presented. The optimal value for each output is highlighted in bold. The results from the simulations in which the starting time of the operation of the AWHP was examined, are shown in Table 2. The calculations of the energy use of the pumps and the AWHP is based on the calculations done previously by Bourdakis et al. (2016a, 2016b).

Table 2. Results from the AWHP starting time simulations

AWHP starting time, hh:mm	Percentage of occupancy time in Category III, %	Pumps energy usage, kWh (kBtu)	AWHP energy usage, kWh (kBtu)	Energy removed by the PCM, kWh (kBtu)	Percentage of PCM discharged at 09:00, %	Percentage of PCM charged at 17:00, %
03:00	65.6	48 (162)	74 (253)	**50 (169)**	**84.2**	82.2
04:00	65.6	48 (162)	74 (251)	**50 (169)**	**84.2**	82.1
05:00	**65.9**	48 (162)	72 (247)	49 (168)	83.7	82.1
06:00	64.4	47 (161)	66 (226)	48 (165)	82.5	82.5
07:00	62.3	**46 (160)**	**55 (187)**	46 (157)	79.4	**83.2**

In Table 3 the results from the simulations in which the starting time of the operation of Pump 3 was examined, are presented.

Table 3. Results from the Pump 3 starting time simulations

Pump 3 starting time, hh:mm	Percentage of occupancy time in Category III, %	Pumps energy usage, kWh (kBtu)	AWHP energy usage, kWh (kBtu)	Energy removed by the PCM, kWh (kBtu)	Percentage of PCM discharged at 09:00, %	Percentage of PCM charged at 17:00, %
03:00	**70.4**	52 (176)	99 (337)	**59 (200)**	**94.7**	77.9
04:00	68.5	50 (170)	88 (301)	54 (185)	90.7	80.2
05:00	65.9	48 (162)	72 (247)	49 (169)	83.7	82.1
06:00	62.3	45 (153)	52 (177)	44 (150)	74.8	83.5
07:00	59.9	**43 (146)**	**32 (110)**	39 (132)	65.1	**84.1**

The results from the simulations in which the temperature difference of the output of the solar panels and the temperature in the middle of the storage was examined, are shown in Table 4.

Table 4. Results from the Panels – Tanks ΔT simulations

Panels – Tanks ΔT, K (°F)	Percentage of occupancy time in Category III, %	Pumps energy usage, kWh (kBtu)	AWHP energy usage, kWh (kBtu)	Energy removed by the PCM, kWh (kBtu)	Percentage of PCM discharged at 09:00, %	Percentage of PCM charged at 17:00, %
1 (1.8)	**65.9**	48 (162)	**72 (246)**	**49 (169)**	**83.7**	82.1
2 (3.6)	65.8	47 (161)	73 (247)	**49 (169)**	**83.7**	**82.2**
3 (5.4)	65.8	47 (159)	73 (248)	**49 (169)**	**83.7**	82.1
4 (7.2)	65.8	46 (157)	73 (250)	48 (168)	**83.7**	**82.2**
5 (9)	65.6	**45 (156)**	74 (253)	48 (168)	83.5	**82.2**

In Figure 3 the percentage of occupancy period outside the range of Category III of Standard EN 15251 vs the energy usage of the pumps and the AWHP in terms of kWh/m² is presented, for the cases of AWHP and Pump 3 operation starting time and the temperature difference between the output of the solar panels and the temperature in the middle of the storage tanks.
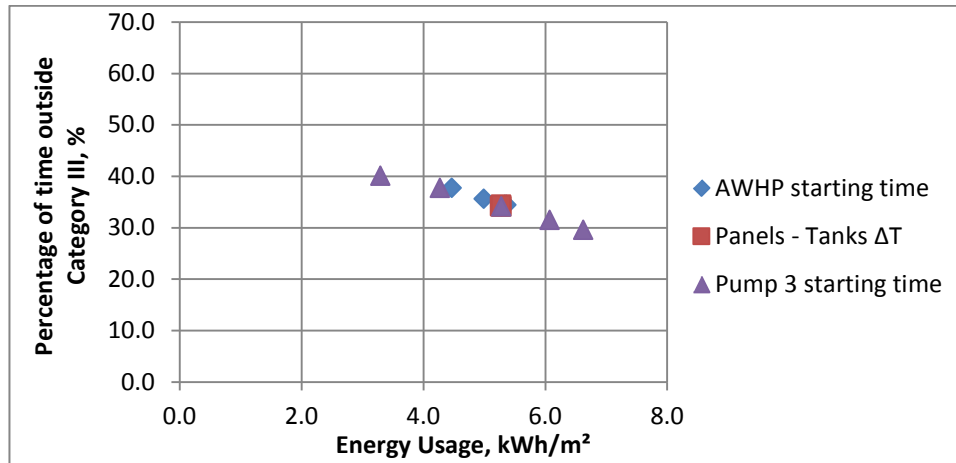
Figure 3 Percentage of time outside Category III vs energy use

In Figure 4 the percentage of occupancy period outside the range of Category III of Standard EN 15251 vs the energy usage of the pumps and the AWHP in terms of kWh/m² is presented for the cases of set-point values for the activation of the AWHP and Pump 3.
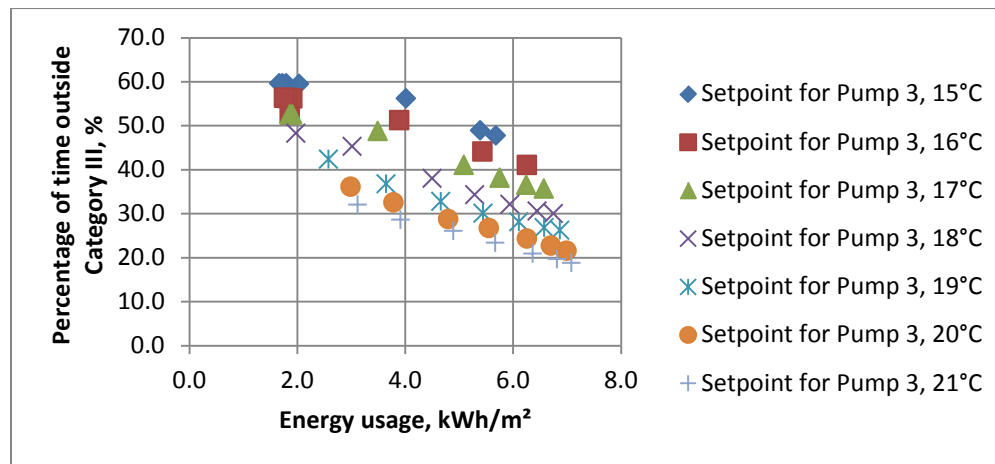

Figure 4 Percentage of time outside Category III vs energy use for AWHP and Pump 3 setpoint simulations

DISCUSSION

From Table 2 it can be seen that the starting time of the operation of the AWHP did not have a clear impact on the indoor thermal environment, since the higher percentage of occupancy time occurred when the AWHP was activated on earlier than 05:00. On the other hand, as it can be seen from Table 3, the earlier Pump 3 is starting to operate, the higher the percentage of occupancy time within Category III of EN 15251, as it was expected. For both the AWHP and Pump 3, the later the operation starts, the lower the energy usage of the pumps and the AWHP is. The impact of the starting time of Pump 3 is significantly higher for the energy usage of pumps and AWHP compared to the starting time setpoint of the AWHP itself. The reason is that if Pump 3 is activated earlier than the AWHP, the temperature in the middle of the CWT will increase and then the AWHP will be required to operate for more time once it gets activated. On the other hand, if the AWHP is activated prior to Pump 3, the temperature in the middle of the CWT will not increase until Pump 3 is activated, and the AWHP will only need to operate if nocturnal radiative cooling is not enough for cooling down the water in the CWT. That is why the energy usage of AWHP is increased only by 1.9 kWh, 6500 Btu when the start of the AWHP operation changes from 05:00 to 03:00, as it is shown in

Table 2, while for the same time change of the operation of Pump 3 the increase in the energy use is 26.4 kWh, 90000 Btu. Regarding the cooling energy removed by the PCM, the impact of the starting time set-point of the AWHP is insignificant (ranges from 46 kWh to 50 kWh) compared to the impact of the starting time setpoint of Pump 3 (ranges from 38 kWh to 59 kWh). For both cases, the earlier the operation starts, the higher percentage of PCM is discharged before the start of the occupancy period and the lower percentage is utilized at the end of it. As before, the impact is higher in the case of the activation time of Pump 3.

From the results reported in Table 4, it can be seen that no significant changes where observed in any of the examined outputs. For that reason, further analysis was required for this parameter. Therefore, it was examined in terms of activation sensitivity, namely how many times Pump 2 was activated/deactivated on average during a day. In Table 5 the average times Pump 2 was activated and deactivated per day are shown.

Table 5. Pump 2 activation sensitivity

Panels – Tanks ΔT, K (°F)	1 (1.8)	2 (3.6)	3 (5.4)	4 (7.2)	5 (9)
Activation/deactivation times per day	16	12	8	6	4

From Table 5 it can be seen that the higher the ΔT between the water temperature exiting the solar panels and the middle of the storage tanks, the lower the number the pumps is activated or deactivated during a day, ensuring a more stable operation of the pump.

As it can be seen in Figure 3 and Figure 4, there is a clear trend for all the examined parameters; the lower the percentage of occupancy period outside the range of Category III the higher the energy usage. As mentioned before, the only exception is the ΔT between the output of the solar panels and the middle of the storage tanks, for which all the points almost coincide, as it is shown in Figure 3. For that reason, two more simulations were run, with the combination of settings that contributed the most in energy savings and providing the optimal indoor thermal environment. Since the ΔT between the output of the solar panels and the middle of the storage tanks had no impact either in the energy savings of the system or the provided indoor thermal environment, the ΔT of 5°C (9°F) was chosen for both simulations since it gave the most stable operation for Pump 2. Table 6 shows the set-points used in the last two simulations.

Table 6. Setpoint values for examined parameters for optimized simulations

	AWHP starting time, hh:mm	CWT temperature to activate the AWHP, K (°F)	Pump 3 starting time, hh:mm	CWT temperature to activate Pump 3, K (°F)	Panels- Tanks ΔT, K (°F)
Energy savings simulation	07:00	21 (69.8)	07:00	15 (59)	5 (9)
Indoor thermal environment simulation	05:00	15 (59)	03:00	21 (69.8)	5 (9)

In Table 7 the results from the two optimized simulations are presented. By comparing these results with the results shown in Table 2, Table 3 and Table 4, it can be seen that the simulation focused on energy savings had significantly lower energy usage for the pumps and the AWHP, but with a considerable compromise on the indoor thermal environment. On the other hand, the last simulation provided the best indoor thermal environment, 83.5% of occupancy time within the range of Category III, but with the higher energy usage observed among all the

simulations, namely 178 kWh (198 kBtu).

Table 7. Results from the optimized simulations

	Percentage of occupancy time in Category III, %	Pumps energy usage, kWh (kBtu)	AWHP energy usage, kWh (kBtu)	Energy removed by the PCM, kWh (kBtu)	Percentage of PCM discharged at 09:00, %	Percentage of PCM charged at 17:00, %
Energy savings simulation	39.4	34 (116)	2 (5)	16 (56)	53.4	91.1
Indoor thermal environment simulation	83.5	58 (198)	120 (410)	69 (235)	97.3	43.4

CONCLUSION

All the examined parameters had inverse results in terms of energy use and indoor thermal environment, namely the better the indoor thermal environment provided, the higher the energy use of pumps and the heat pump. The only exception was the ΔT between the water temperature exiting the solar panels and the temperature in the middle of the storage tanks. For this ΔT, the highest examined value (5K, 9°F) performed the best by having the most stable operation. Based on that, it was concluded that when an output of a condition is based on a temperature difference, the set-point value should be carefully decided in order to avoid continuous activation/deactivation of the pump or the heat pump, that could possibly damage it. The ideal combinations of setpoints for providing the best indoor thermal environment and minimizing the energy use were identified. The impact of the starting time of the operation of the AWHP was less significant than the starting time of the operation of Pump 3 in terms of indoor thermal comfort and energy.

REFERENCES

Bourdakis, E., Olesen, B. W., & Grossule, F. (2015). Night time cooling by ventilation or night sky radiation combined with in - room radiant cooling panels including Phase Change Materials. In 36 Air Infiltration Ventilation Centre Conference.

Bourdakis, E., Kazanci, O. B., Grossule, F., & Olesen, B. W. (2016a). Simulation Study of Discharging PCM Ceiling Panels through Night-time Radiative Cooling. In ASHRAE Transactions.

Bourdakis, E., Péan, T., Gennari, L., & Olesen, B. W. (2016b). Daytime space cooling with Phase Change Material (PCM) ceiling panels discharged using rooftop PV / T panels and night-time ventilation. Science and Technology for the Built Environment, 1–9.

DS/EN. (2007). DS/EN 15251:2007 Indoor environment input parameters for design and assessment of energy performance of buildings adressing indoor air quality, thermal environment, lighting and acoustics.

Gwerder, M., Lehmann, B., Tödtli, J., Dorer, V., & Renggli, F. (2008). Control of thermally-activated building systems (TABS). Applied Energy, 85(7), 565–581.

Lim, J. H., Jo, J. H., Kim, Y. Y., Yeo, M. S., & Kim, K. W. (2006). Application of the control methods for radiant floor cooling system in residential buildings. Building and Environment, 41(1), 60–73.

Lim, J. H., Song, J. H., & Song, S. Y. (2014). Development of operational guidelines for thermally activated building system according to heating and cooling load characteristics. Applied Energy, 126, 123–135.

Sourbron, M., & Helsen, L. (2013). Sensitivity analysis of feedback control for concrete core activation and impact on installed thermal production power. Journal of Building Performance Simulation, 7(5), 1–17.

Tödtli, J., Gwerder, M., Lehmann, B., Renggli, F., & Dorer, V. (2007). Integrated Design Of Thermally Activated Building Systems And Of Their Control. In CLIMA 2007.

Buildings are accountable for 40% of the energy use in the EU, and 65% of this energy is used for space heating. In addition, the demand for cooling is expected to rise, due to global warming, increased comfort requirements, better insulated and airtight buildings keeping the internal loads inside, resulting in temperature increase. The EU has recently set updated targets for energy use reduction by the year 2030, while it recognises the importance of buildings in achieving these targets and especially the importance of renovating existing building stock, as this was underlined in the amended version of the Directive on Energy Performance of Buildings.

The aim of the present dissertation is to examine the potential of incorporating active ceiling panels containing Phase Change Material (PCM) in office buildings, using both numerical and experimental means. The main objectives were to examine experimentally the possibility of combining PVT panels to produce cold water with PCM ceiling panels for space cooling and to create and validate a model in TRNSYS to conduct parametric studies and optimise it without being affected by the contingency of the outdoor weather conditions.